Forest Growth and Timber Quality: Crown Models and Simulation Methods for Sustainable Forest Management

Proceedings of an International Conference

August 7–10, 2007
Portland, OR

TECHNICAL EDITORS

CREDITS

DISCLAIMERS

Forest Growth and Timber Quality: Crown Models and Simulation Methods for Sustainable Forest Management

Proceedings of an International Conference

Dennis P. Dykstra and Robert A. Monserud, Technical Editors
Portland, OR, USA, August 7–10, 2007

ABSTRACT

Dykstra, Dennis P.; Monserud, Robert A., tech. eds. 2009. Forest growth and timber quality: crown models and simulation methods for sustainable forest management. Proceedings of an international conference. Gen. Tech. Rep. PNW-GTR-791. Portland, OR: U.S. Department of Agriculture, Forest Service, Pacific Northwest Research Station. 267 p.

The purpose of the international conference from which these proceedings are drawn was to explore relationships between forest management activities and timber quality. Sessions were organized to explore models and simulation methodologies that contribute to an understanding of tree development over time and the ways that management and harvesting activities can influence the quality of timber products recovered from those trees. Five keynote addresses, 29 plenary presentations, and 16 poster presentations covered the full breadth of forest growth and timber quality issues related to forest management. These proceedings comprise 19 papers based on presentations and posters, plus 28 abstracts for presentations whose authors chose not to write full papers. In addition, the proceedings include abstracts and slides from the presentations prepared by three keynote speakers who elected not to write papers for the proceedings. The conference was attended by 75 participants from 19 countries who represented universities, private companies, and government research institutes.

KEYWORDS: forest management, forest operations, process models, hybrid models, mechanistic crown models, simulation, sustainable forest management, wood quality

ACKNOWLEDGMENTS

CONTENTS

Mechanistic Crown Models

Hybrid Modeling Approaches

Forest Operations and Timber Quality

Modeling Wood Quality

Simulation in Sustainable Forest Management

Poster Presentations

Mechanistic
Crown Models

Mechanistic Crown Models

Keynote Presentation

Why Mechanisms Should Be in the Eye of the Beholder: Notes from the Overground

Douglas A. Maguire

ABSTRACT

ECOSYSTEMS CAN BE MODELED AT MANY different hierarchical levels. The phenomenon being simulated has a context represented by the next higher level of ecosystem organization, as well as driving mechanisms represented by the next lower level of ecosystem organization. In this sense, the level at which mechanisms are represented in models of tree crowns depends on the crown attributes or processes to be simulated. Crown models are reviewed and classified by their attribute resolution and the specific mechanisms driving the crown system to future states. Ecophysiological models fix carbon through photosynthesis and typically allocate this photosynthate to branches and foliage. Allometric models grow trees in height, diameter, and often crown size, retrieving structural attributes of the crown from allometric relationships between bole dimensions, branch size and location, and foliage amount. Architectural models simulate the two- or three-dimensional structure of the crown, sometimes by proliferation of individual modules comprising the crown. Intended applications of the model dictate the appropriate resolution in time and space and, therefore, the most appropriate and efficient mechanisms. Difficulties often arise when models are developed to meet more than one objective, particularly when the objectives entail several levels of organization.
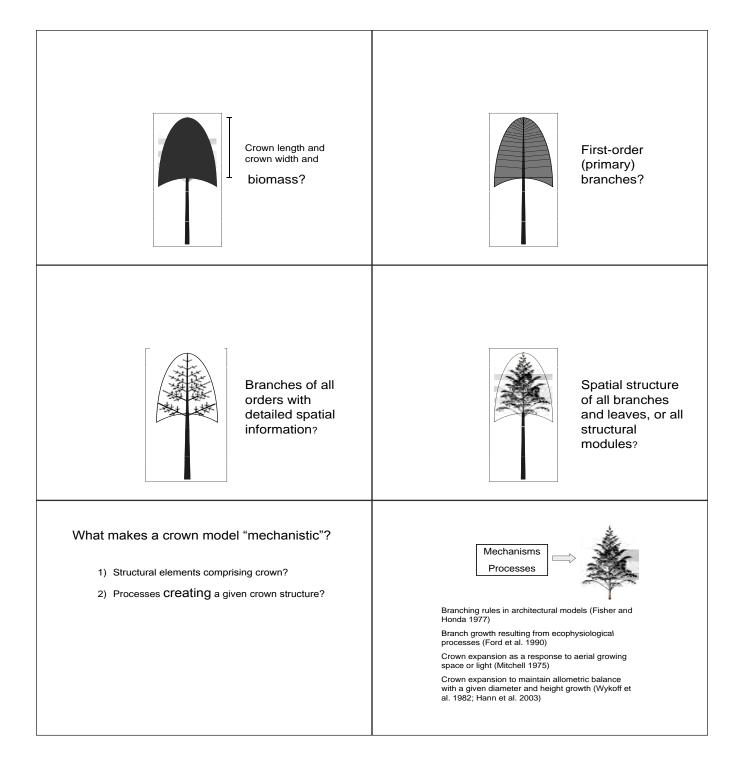
Editors' note: The author elected not to provide a full paper for these proceedings because it was being submitted to a refereed journal. As with all of the keynote addresses, this presentation was designed to provide context for the related presentations that follow. In lieu of the keynote paper, the author's slides from the presentation are reproduced on the following pages to introduce the topic for this section of the proceedings.

Douglas A. Maguire (doug.maguire@oregonstate.edu) is a professor of silviculture, Forest Science Department, Oregon State University, Corvallis, OR 97331, USA.

Forest Growth and Timber Quality:
Crown Models and Simulation Methods for
Sustainable Forest Management

Session 1: Mechanistic Crown Models

Why mechanisms should be in the eye of the beholder: Notes from the overground

Doug Maguire
Department of Forest Science
Oregon State University

Mechanistic crown models

Objectives:
(1) Provide a setting for the six papers of this session by looking somewhat comprehensively at crown models, or at the crown component of forest simulation models
(2) Suggest the aspects of crown models that best address the theme of this meeting

---

Mechanistic crown models

- The issue of mechanisms
- Model types
- Model objectives and context
- Crown models for linking environment and silviculture to wood quantity and quality
- Kludges and parsimony

What makes a crown model "mechanistic"?

1) Structural elements comprising the crown?

Crown length?

Crown length and crown width?

Crown length and crown width and

biomass?

First-order (primary) branches?

Branches of all orders with detailed spatial information?

Spatial structure of all branches and leaves, or all structural modules?

What makes a crown model "mechanistic"?

1) Structural elements comprising crown?

2) Processes creating a given crown structure?

Mechanisms Processes

Branching rules in architectural models (Fisher and Honda 1977)

Branch growth resulting from ecophysiological processes (Ford et al. 1990)

Crown expansion as a response to aerial growing space or light (Mitchell 1975)

Crown expansion to maintain allometric balance with a given diameter and height growth (Wykoff et al. 1982; Hann et al. 2003)

What makes a crown model "mechanistic"?

1) Structural elements comprising crown?

2) Processes creating a given crown structure?

3) Processes **resulting from** crown structure?

Mechanisms
Processes

Morphology/architecture
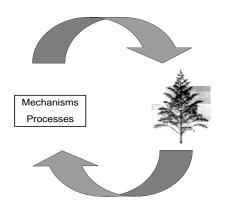
New buds, elementary units
Foliage production, senescence

Ecophysiology

Light interception
Net photosynthesis
Transpiration
Respiration
Carbon allocation

Allometric

Bole and branch growth

Mechanisms
Processes

Mechanistic crown models

- The issue of mechanisms
- Model types
- Model objectives and context
- Crown models for linking environment and silviculture to wood quantity and quality
- Kludges and parsimony

Historical models addressing crown dynamics at some level

Architectural / morphological models

Ecosystem dynamics models

Ecophysiological models ("process")

Allometric models (empirical, theoretical)

Morphological – architectural models (botanical context)

Tree = Branching structure

Sometimes main stem and branches have secondary thickening

Allometric models (timber production context)
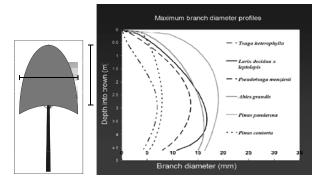
Tree = a volume of bolewood
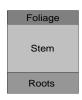
Sometimes the tree has annoying appendages like branches, foliage, and even roots

Allometric models (silvicultural context)

Maximum branch diameter profiles

- --- *Tsuga heterophylla*
- —— *Larix decidua x leptolepis*
- – – *Pseudotsuga menziesii*
- —— *Abies grandis*
- ···· *Pinus ponderosa*
- ···· *Pinus contorta*

Depth into crown (m)

Branch diameter (mm)

Ecosystem models (production ecology context)

Trees = bins of biomass

| Foliage |
| Stem |
| Roots |

1-yr	2-yr	3-yr	4+yr
Branchwood			
Bolewood			
Bark			
Coarse roots		Fine roots	

Sometimes trees are broken into components at a finer resolution

Ecophysiological models (environmental effects context)
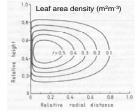
Tree = physiologically meaningful compartments

1-yr leaves	2-yr leaves	3-yr leaves	4+-yr leaves
Branch sapwood		Branch heart wood	
Bole sapwood		Bole heart wood	
Cambium		Phloem	
Coarse roots		Fine roots	

Ecophysiological models (environmental effects context)

Tree = physiologically meaningful compartments

1-yr leaves	2-yr leaves	3-yr leaves	4+-yr leaves
Branch sapwood		Branch heart wood	
Bole sapwood		Bole heart wood	
Cambium		Phloem	
Coarse roots		Fine roots	

Leaf area density ($m^2 m^{-3}$)

Relative height

Relative radial distance

$r = 0.5$ 0.4 0.3 0.2 0.1
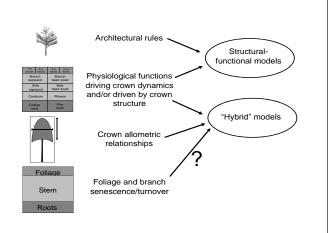
Sometimes spatial distribution of foliage is represented to improve simulation of light interception

Architectural rules → Structural-functional models

Physiological functions driving crown dynamics and/or driven by crown structure

Crown allometric relationships → "Hybrid" models

Foliage and branch senescence/turnover

?

5

Architectural model:

The normal growth program that determines the successive architectural phases of a plant derived from a seed, undisturbed by unusual or severe extrinsic forces (such as pruning, defoliation, injury), and excluding reiterations.

The visible morphological expression of the genotype at any one time is the architecture, a static concept distinguished from the dynamic concept of the architectural model

---

Crown architecture & morphology

White (1979) The plant as a metapopulation.

Review of primarily descriptive studies of plant architecture, but includes reference to:
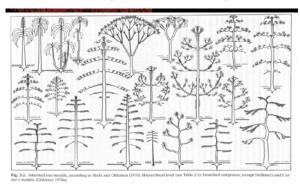
Hallé, Oldeman, Tomlinson. (1978). Tropical trees and forests – An architectural analysis:

24 architectural models defined by:

(1) The life span of meristems (determinate or indeterminate) and

(2) The differentiation of meristems (sexual or vegetative; giving rise to erect or horizontal axes; functioning episodically or continuously).

Only primary (extension) growth is considered.

Inherited tree models (Hallé and Oldeman 1970)

Fig. 3.2. Inherited tree models, according to Hallé and Oldeman (1970). Hierarchical level (see Table 2.1): branched complexes, except Holttum's and Corner's models. (Oldeman 1974a)

Crown architecture & morphology on the basis of elementary units or modules

- Braun (1853): "Our feelings aroused by the sight of the most ramified plant-stocks, especially by a tree . . . excite the presentiment that this is not one single being . . . comparable with the animal or human individual, but rather a world of united individuals which have sprung from each other in a succession of generations . . . "

Phytonism and modules

The phyton is "the segment of the axis which subtends a leaf initial and surrounds its leaf trace as it develops."

The conceptualized phyton or unit of shoot growth in the grass *Alstroemeria* and their arrangement in a stem segment (Priestley et al. 1935)

Arber (1930): "the phyton theory seems to me to belong to that group of over-ingenious, academic conceptions which are difficult to discuss because they bear so little relation to reality"

If a mathematical process or rule set produces the right morphology, does it matter if the process or rules have a physical counterpart?

branching rule set A

branching rule set B ——— : crown shape

real branching pattern

White notes that attempts at modeling branching structure have yielded unrealistic results, with some more promising and sophisticated approaches "now" being explored by :

Cannell (1974)

Combe et al. (1974)

deReffye (1976)

Fisher and Honda (1977)

Fisher (1992)

Architectural – morphological models

Approaches:

(1) Branching rules with respect to number of buds, angle of buds, longitudinal extension of buds (Fisher and Honda 1977)

(2) L-system or Lindenmayer systems (Prusinkiewicz and Lindenmayer 1990)

(3) Fractals based on parameters from real trees (Chen et al. 1991)

Architectural – morphological models

First computer simulations were:

(1) Deterministic

(2) Invariant in parameters

(3) Stationary (rules of branching remain constant throughout crown)

Kellomäki and Kurttio (1991) A model for the structural development of a Scots pine crown based on modular growth.

In the future development of the structural model, the influence of the prevailing conditions should be included in such a way that the branching principles presented in this study provide the framework for the structural process being modified by the supply of resources affecting the growth and survival of the shoot population.

Structural-Functional Models

Pursued in recognition of the possible advantages of more explicit structural representation of tree crowns in ecophysiological models

or

adding effects of environment on genetically coded architectural development

Excellent review papers by:

Kurth (1994) Morphological models of plant growth: Possibilities and ecological relevance.

Sievänen et al. (2000) Components of functional-structural tree models.

Sievänen et al. (2000) Components of functional-structural tree models.

Two types:

(1) Structural model modified to be responsive to environmental conditions through ecophysiological processes.

Examples include:

context sensitive, parametric, or open L-systems;

AMAPmod (growth rules) → AMAPpara (addition of ecophysiological processes) (de Reffye et al. 1997)

(2) Process-based model modified to represent more accurately crown structure and, hence, to allow better estimation of light interception and other processes

Examples include:

LIGNUM (Perttunen et al. 1996, 1998)
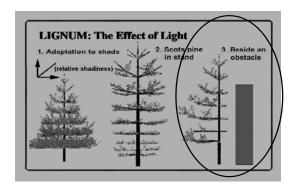
LIGNUM represents tree structure as a set of IEMs (Idealized elementary units)

Basic physiological processes are represented: gas exchange, transpiration, nutrient uptake, growth (carbon) allocation

Authors underscore:
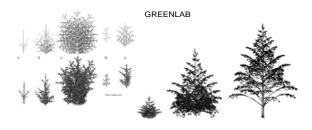
- the challenge of allocation, or distributing growth mechanistically

- the computational burden

Plant Modelling Unit at CIRAD in France

De Reffye, Fourcaud, Barthélémy, Blaise, Houllier
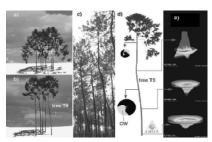
Yan et al. (2004) A Dynamic, Architectural Plant Model Simulating Resource-dependent Growth

GREENLAB
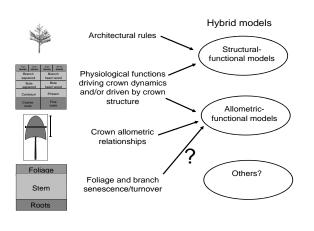
Fourcaud et al. (2003) Numerical modelling of shape regulation and growth stresses in trees. II. Implementation in the AMAPpara software and simulation of tree growth

Role of mechanical stressses in tree form and reaction wood

Hybrid models

Architectural rules → Structural-functional models

Physiological functions driving crown dynamics and/or driven by crown structure → Allometric-functional models

Crown allometric relationships

Foliage and branch senescence/turnover

?

Others?

Foliage

Stem

Roots

Hybrid of allometric-functional models
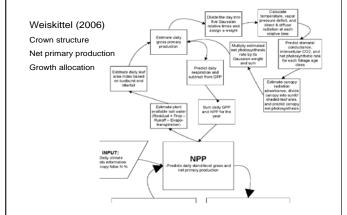
Baldwin et al. (2001) Linking growth and yield and process models to estimate impact of environmental change on growth of loblolly pine.

PTAEDA + MAESTRO

More fully integrated "hybrids"

Valentine and Mäkela (2005) Bridging process-based and empirical approaches to modeling tree growth.

Weiskittel (2006) Development of a hybrid modeling framework fo intensively managed Douglas-fir plantations in the Pacific Northwest.

Weiskittel (2006)
Crown structure
Net primary production
Growth allocation

Mäkela and Mäkinen (2003) Generating 3D sawlogs with a process-based growth model.

PipeQual

Carbon balance model based on pipe model theory to grow trees and simulate changes in crown height and surface area combined with empirical models of branch size

---

Mechanistic crown models

- The issue of mechanisms
- Model types
- Model objectives and context
- Crown models for linking environment and silviculture to wood quantity and quality
- Kludges and parsimony

Why mechanisms should be in the eye of the beholder:

- Cannot start to construct a model unless we have at the very least a fuzzy idea of the objective, i.e., what we (or someone else) might use the model for
- Model development will be infinitely more efficient if the objective is very explicit (including minimum performance standards; validation criteria)
- There will exist no perfect, comprehensive, or complete simulation model that can answer all questions that forest managers or forest scientists may want to ask

---

- Model objectives
  - Questions/hypotheses
  - Required accuracy
  - Validation criteria
- Ideally, model should be just adequate
- In reality, objectives are or will soon become multiple!

QUESTION OR
HYPOTHESIS

MODEL CONSTRUCTION

SIMULATION

Objectives often
not stated, or
they are fuzzy or
only implied

TENTATIVE
ANSWER

Mechanistic crown models

- The issue of mechanisms
- Model types
- Model objectives and context
- Crown models for linking environment and silviculture to wood quantity and quality
- Kludges and parsimony

Fundamental questions about plant development in architectural models:

What are the genetically imposed branching processes that lead to different crown forms?

Can a set of branching rules specified by a growth grammar simulate the structural/morphological development of tree crowns?

Fundamental questions about plant development:

Branching
rules

Crown
architecture

Crown
morphology

Accurate representation of real branching processes?

Genetic design vs. environmental effects?

Leaf primordia
Axillary buds
Bud differentiation
Bud survival

Environmental alteration of genetically imposed branching pattern?

Self-shading
Competition Hydraulic limitations
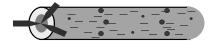
Alternative processes leading to same morphology

Alternative architecture yielding same morphology but different physiological behavior

Relevance of branching processes and resulting crown architecture to silviculture and forest management

- Implications for light interception, photosynthesis, and growth potential
- Allocation of net production to branches and foliage
- Implied number, size, and location of 1st-order (primary) branches
- Nutrient capital in branches and foliage

Wood Quality
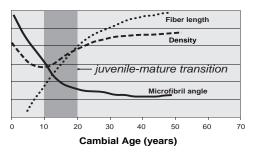
Determinants of log, lumber, veneer, composite, engineered product quality:

Knot size and number
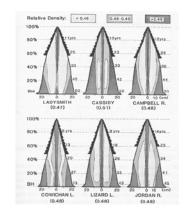
Density

Micro-anatomical properties: fiber length, density, cell wall thickness, lumen size, microfibril angle

Radial trend in microanatomical properties

Fiber length

Density

juvenile-mature transition

Microfibril angle

Cambial Age (years)
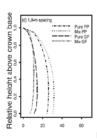
Gartner et al. 2004
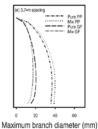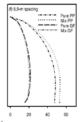
Still have only rudimentary understanding of the relationship between crown dynamics and wood properties

Average stem profiles and maps of relative wood density for Douglas-fir trees at six sites in British Columbia

Josza et al. 1989

More progress has been made on linking branch size, and to some extent branch number and location, to silvicultural regime

Maximum branch diameter (mm)

Garber and Maguire (2005)

Contributions toward integrated systems for simulating stand dynamics and wood quality

France: Francis Colin / François Houllier / Jean Michel LeBan

Finland: Harri Mäkinen / Annikki Mäkela / Seppo Kellomäki

PNW/USA: Dave Briggs / Eric Turnblom / Sean Garber / Aaron Weiskittel / Temesgen Hailemariam

New Zealand: Jenny Grace / David Pont

Canada: Jim Goudie / Ken Mitchell
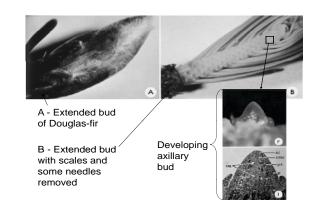
Germany: Sebastian Hein

Needle primordia within bud of Douglas-fir, set at end of growing season

(branches formed from axillary buds, but bud primordia not initiated until spring)

A - Extended bud of Douglas-fir

B - Extended bud with scales and some needles removed

Developing axillary bud
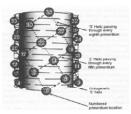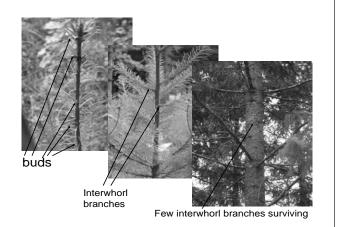
Potential for simulating the process by which are buds set in a select few leaf axils

→Branch position by height and azimuth

Particularly appealing for *Pseudotsuga*, *Abies*, *Picea* species that have interwhorl branches grading into whorl branches

Pont (2001) Use of phyllotaxis to predict arrangement and size of branches in *Pinus radiata*.

buds

Interwhorl branches

Few interwhorl branches surviving

Simulate branch occurrence as inhomogeneous Poisson process
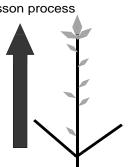
Changing Poisson mean, λ
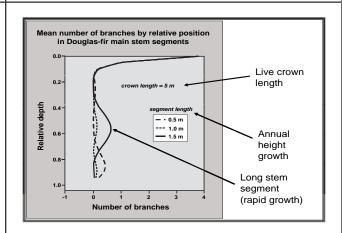
Changing probability of bud set or branch initiation

Poisson regression with log link function
(generalized linear model)

$\eta = \ln(\lambda) = \beta_0 + \beta_1 X_1 + \beta_2 X_2 + \ldots + \beta_k X_k$

where λ = mean of Poisson distribution

Mean number of branches by relative position in Douglas-fir main stem segments

Live crown length

Annual height growth

Long stem segment (rapid growth)

Mechanistic crown models

- The issue of mechanisms
- Model types
- Model objectives and context
- Crown models for linking environment and silviculture to wood quantity and quality
- Kludges and parsimony

A **kludge** (or, alternatively, **kluge**) is a clumsy or inelegant solution to a problem or difficulty.

In engineering, a kludge is a workaround, typically using unrelated parts cobbled together.

Applied by George Furnival to forest growth models (1987)

Currently have an unprecedented opportunity to borrow bits and pieces of models constructed for widely divergent objectives.

This abundance is both a asset and liability:

Validation value.

Efficiency of model building.

Specialization.

Often less than perfect fit to another application → danger of creating or enabling a "kludge".

When does a model or model system become a kludge?

Must consider:

Elegance vs. functionality

Parsimony vs. complexity

Basic vs. applied models

Cost vs. efficacy

Why mechanisms should be in the eye of the beholder:
Notes from the overground

How do we balance efficiency gains from a focus on objectives with the potential benefits of:

venture research

free-reigning modelling

serendipity

?

Comfort or angst from Dostoyevsky?

(Notes from the Underground)

" *. . . intellectual activity is a disease*"

" *. . . men of action, doers, quite genuinely give up when faced with a wall; to them a wall is not challenge as it is to us, for example, men who think and therefore don't do anything.*"

" *. . . all spontaneous people, men of action, are active because they are stupid and limited.*"

(Recall Arber's reference to "over-ingenious, academic conceptions which are difficult to discuss because they bear so little relation to reality")

Important confessions to assuage critics

All models are wrong.

There is no perfect model for answering more than one type of question.

The imperfect representation of our biological and/or operational forestry systems by models does not preclude their utility.

If we think too hard about all the weaknesses of models and all the situations in which they would not apply, we would never get started.

Predicting wood and branch properties of norway spruce as a part of a stand growth simulation system

Harri Mäkinen, Annikki Mäkelä, Jari Hynynen

ABSTRACT

The purpose of our study was to model how stem, branch and wood properties of Norway spruce (*Picea abies* (L.) Karst.) are linked to each other, and how they are distributed along the stem. The branchiness data were used to develop models for the crown ratio, the self-pruning ratio (i.e. height of the lowest dead whorl divided by the height of the crown base), number of living branches in a whorl, total number of branches in a whorl, diameter of the thickest branch in a whorl, diameters of smaller branches, and branch angle. The material on wood and fiber properties was used to develop models for wood density, early-latewood ratio, fiber length, fiber width, and cell wall thickness. A multilevel modeling approach was used to separate the variation of branch, wood and tracheid properties at region, stand and tree levels, as well as within a tree. A multivariate approach was used to simultaneously estimate the parameters of the equations. The independent variables were restricted to those collected in forest inventories or for forest management planning purposes. Such data sets are normally not very detailed.

The models were connected to the empirical growth simulation system MOTTI and to a process-based growth model PipeQual. The dynamic growth model provides a description of tree growth down to the annual ring level. This structure will be used as a skeleton for calculating branch and wood properties. The growth model will update the stand and tree attributes from year to year and, consequently, change the distribution of the branch and wood properties within the stem. The variances of branch and wood properties and their covariances estimated during model development can be used to produce more realistic predictions compared to models, which are fitted separately. When used in practice, the predictions of other models can be calibrated for a particular stand or tree if one dependent variable of the system is measured. The combined simulation system can be used for predicting the development of stem structure under environments controlled by different silvicultural management regimes. The results as such will also increase our understanding of the development of wood quality as a function of forest management, and the quality models are applicable independently of the growth models.

KEYWORDS: branchiness, cell wall thickness, modeling, *Picea abies,* tracheid length, tracheid width, wood density

INTRODUCTION

I N FINLAND, NORWAY SPRUCE IS ECONOMICALLY and ecologically one of the most important tree species. Norway spruce timber has mainly been used for mechanical pulping and for sawn goods in structural uses. Differences in the unit price of the timber grades for Norway spruce have been rather small. Therefore, controlling wood quality has been considered a secondary matter. The demand for Norway spruce timber used in high-quality products such as panels, furniture, and plywood, has increased in recent years. Accordingly, the price of Norway spruce lumber has also increased.

Harri Mäkinen (harri.makinen@metla.fi) is a researcher, Finnish Forest Research Institute, Vantaa Research Unit, P.O. Box 18, 01301 Vantaa, Finland; **Annikki Mäkelä** is professor of silviculture (forest production), Department of Forest Ecology, University of Helsinki, PO Box 27, 00014 Helsinki, Finland; **Jari Hynynen** is a researcher, Finnish Forest Research Institute, Vantaa Research Unit, P.O. Box 18, 01301 Vantaa, Finland.

The number and size of branches are major determinants of log grading in Norway spruce. For the reasons given above, detailed studies on the branch characteristics of Norway spruce and the factors controlling them are scarce in the Nordic countries. Characteristics of fibers largely determine the suitability of wood for further processing in the pulp and paper industry as well as in the sawmilling industry. Fiber morphology and cell wall structure directly influence fiber flexibility, plasticity and resistance to processing and, therefore, influence the strength and other physical and optical properties of the end products. Wood density is also an important characteristic that is related to the yield and quality of pulp and sawn products.

How the stem grows and acquires its structure—or how silvicultural management controls the development of stem structure—is one of the key considerations in the integrated optimization of the wood production and conversion chain. Models have conventionally treated stem properties separately from tree growth. A more general and flexible model can be constructed if quality characteristics are included in a growth model, allowing us to predict stem structure at each moment of time (e.g., Houllier et al. 1995). Such a model would automatically portray the effects of silvicultural treatments on stem properties, because the primary effect of the environment on tree growth would be interpreted in terms of changes in ring width, branchiness, etc.—characteristics which have been demonstrated to depend largely on stem growth.

Models describing the branch characteristics of Scots pine (*Pinus sylvestris* (L.) and silver birch (*Betula pendula* Roth.) have been developed in the Nordic countries (Mäkinen and Colin 1998, 1999, Moberg 1999, Mäkinen et al. 2003a). The models of Mäkinen and Colin (1998, 1999) were connected to the empirical growth simulation system MOTTI (Hynynen et al. 2005, Salminen et al. 2005), and to the process-based growth

model PipeQual (Mäkelä 1997, Mäkelä and Mäkinen 2003, Mäkinen and Mäkelä 2003). These tools can be used to assess the development of wood quality and to assess the possibilities of using silvicultural treatments to control timber properties (Mäkinen et al. 1999, 2004, Mäkelä et al. 2000). However, the models developed thus far have been concerned with Scots pine and silver birch, as well as the properties of logs utilized by sawmilling industries.

Our goal was to extend the previous modeling approach to branch, wood and tracheid properties of Norway spruce. The purpose was to model how stem, branch, wood and tracheid properties are linked with each other and how they are distributed along the stem from stem base to apex and from pith to bark. The models had to be applicable as a part of a stand growth simulation system that is based on growth models for individual trees. Although a large number of stand and tree characteristics would certainly improve the accuracy of the models, the information collected in forest inventories or for forest management planning purposes is not normally very detailed. Thus, the variables used in the models had to be restricted to those found in the data sets to which the models are applied.

MATERIAL AND METHODS

Data on the wood and tracheid properties

The material used for modeling the wood and tracheid properties consisted of five separate data sets: (1) two thin-

Table 1— Characteristics of the experiments sampled for modeling wood and tracheid properties.

Data set	Location	Number of sample trees	Age	DBH (cm)	H_{dom}[a] (m)	H_{100}[b] (m)
Thinning	Heinola	12	87	29.4	30.3	32.4
	Punkaharju	12	67	32.8	27.2	33.0
Thinning+ fertilization	Parikkala	45	64	24.9	22.7	28.5
	Suonenjoki	40	77	27.9	26.1	28.8
Fertilization	Heinola	10	54	24.5	23.9	32.6
	Kemijärvi	10	65	14.6	11.3	16.3
Nutrient- optimization	Flakaliden	27	40	12.1	8.9	19.3
	Asa	18	31	17.2	15.0	31.2
Clones	Nurmijärvi	3	20	8.8	n.a.[c]	34.0
	Ruotsinkylä	4	81	27.0	n.a.[c]	24.0

[a] Dominant height, height of 100 thickest trees ha-1
[b] Site index, dominant height at age 100 years
[c] not available

ning experiments in southern and central Finland, (2) two thinning-fertilization experiments in central Finland, (3) two fertilization experiments in southern and northern Finland, (4) two nutrient optimization experiments in southern and northern Sweden, and (5) fast-grown clones and their reference trees in southern Finland (Table 1). The data sets were originally sampled for different purposes and studies (Mäkinen et al. 2002a,b, Jaakkola et al. 2005a,b, 2006, 2007). In all the data sets, however, the measurements were carried out according to the same methods. The study material included 181 sample trees (Table 1).

Sample trees were felled and stem discs were sawn out at different heights on the stem avoiding whorls. Ring width and wood density of all annual rings were measured along the south radius of each disc. Tracheid lengths of every fifth annual ring were measured from bark to pith. In addition, lumen diameter and cell wall thickness were measured from selected annual rings at regular intervals from pith to bark. The sampling and measurements are described in detail in Mäkinen et al. (2007).

Branchiness data

The material used for branchiness models consisted of five separate data sets: (1) commercial forests in southern and central Finland, (2) thinning experiments in southern Finland, (3) a young naturally regenerated stand in southern Finland, (4) a nutrient optimization experiment in northern Sweden, and (5) pruning experiments in southern Finland. The data were collected from 677 trees of different age and canopy position growing on mineral soils and peatlands of different fertility (Table 2). The data sets were originally sampled for different purposes and studies. In all the data sets, however, the measurements were carried out according to the same methods.

Stem diameter at breast height, tree height, crown length, and height to the lowest dead whorl were measured on each sample tree. The sample trees were felled and the distance of whorls from the stem apex, the horizontal diameter of each branch above the butt swell, and the status of each branch (living or dead) were measured. The sampling and measurements are explained in detail in Mäkinen et al. (2003b).

Model development

Our goal was to develop generally applicable models. All of the models were based on statistical fitting of equations to the measured data. When selecting curve forms and variables for the models, we considered the potential biological significance of the selected variables to the branch, wood and tracheid properties based on the relationships presented in the literature.

Multivariate multilevel models were used because, by simultaneously estimating the parameters of the equations, they provide techniques to produce consistent and asymptotically efficient estimates for regression equation systems. Variance components were used to separate random variation at different levels, e.g., between regions, stands, plots, trees, whorls, branches or stem heights and annual rings, depending on the model in question.

For example, the multivariate multilevel model structure for two dependent variables (*a* and *b*) measured at whorl level could be as follows:

$$g(\mu^a) = f(x,\alpha) + s^a + p^a + t^a + w^a \qquad (1.1)$$

$$g(\mu^b) = f(x,\beta) + s^b + p^b + t^b + w^b \qquad (1.2)$$

where $g(\mu)$ is an appropriate link function, *x* matrix of the independent variables, *ß* vectors of fixed parameters, and *s*, *p*, *t* and *w* random variables at stand, plot, tree and whorl levels. The models can be used to decompose the raw variances and covariances into parts at the four levels. The between- and within-group covariance matrices can then be estimated:

Table 2—Characteristics of the experiments sampled for modeling branch properties.

Data set	Location	Number of sample trees	Age	DBH (cm)	H$_{dom}$ (m)	H$_{100}$ (m)
Commercial forests	Southern Finland	240	92	26.9	22.9	24.2
Thinning	Punkaharju	12	85	32.8	31.0	33.9
	Heinola	12	67	29.4	26.4	33.5
Sapling	Lapinjärvi	5	22	3.1	4.4	24.5
Nutrient optimization	Flakaliden	24	37	12.1	8.9	19.3
Pruning	Southern Finland	384	29	12.6	12.2	33.8

cov $(s^a, s^b)=C_s$, cov $(p^a, p^b)=C_p$, cov $(t^a, t^b)=C_t$, cov $(w^a, w^b)=C_w$

RESULTS

Models for wood and tracheid properties

The data on wood and tracheid properties were used to develop models for (1) proportion of latewood in individual annual rings, (2) average wood density of individual annual rings, (3) tracheid length, (4) tracheid width, and (5) cell wall thickness. The wood and tracheid properties were mainly related to cambial age of an annual ring and radial increment rate. Site index was also a significant variable in most of the models. The magnitude of changes associated with increasing increment rate differed depending on the properties of wood density and tracheid length, as demonstrated in Figure 1. However, increasing increment rate caused by thinning or fertilisation resulted in similar kinds of changes in wood and tracheid properties, irrespective of the factor promoting radial increment.

The variation that accounted for the fixed part of the models was: tracheid length 82.8 percent, tracheid width 64.9 percent, cell wall percentage 48.0 percent, latewood proportion 24.8 percent, and wood density 21.1 percent. The behaviour of the models for a randomly selected tree
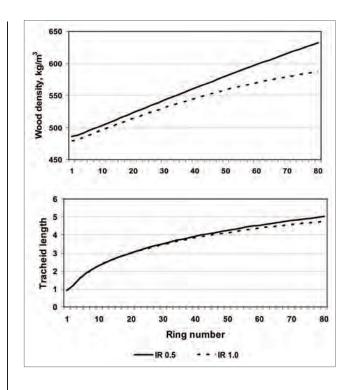
Figure 1—Predicted profiles of wood density and tracheid length for a slow and fast growing tree (radial increment 0.5 and 1.0 mm y^{-1}, respectively) plotted against ring number counted from the pith outwards. The other independent variables were the same for both trees.
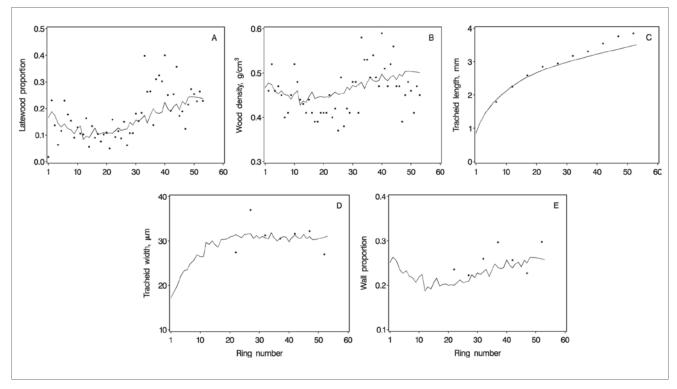
Figure 2—Measured (dots) and predicted (line) proportion of latewood (A), wood density (B), tracheid length (C), tracheid width (D) and proportion of cell wall (E) of individual annual rings at breast height plotted against ring number counted from the pith outwards for a randomly selected tree (age=77 y, dbh=27.3 cm, h=23.7 m).

is demonstrated in Figure 2. The equations and parameters of the models are given in Mäkinen *et al.* (2007).

Models for branch properties

The branchiness data were used to develop models for (1) crown ratio, (2) self-pruning ratio, i.e., height of the lowest dead whorl divided by the height of the crown base, (3) number of living branches in a whorl, (4) total number of branches in a whorl, (5) diameter of the thickest living branch in a whorl, (6) diameters of smaller branches, and (7) branch angle. The equations and parameters of the models are given in Mäkinen et al. (2003b). The behaviour of the models for the number of living branches and branch diameter is demonstrated in Figures 3 and 4, respectively.

Application

The above models do not describe dynamic development of branch, wood, and tracheid properties. The models can be combined with a dynamic growth model that provides a detailed description of tree growth down to the annual ring width level. This structure will be used as a skeleton when predicting branch, wood and tracheid properties during stand development. During simulation, information on branch, wood, and tracheid properties of each sample tree are updated annually together with the other tree and stand characteristics. Predicted variation of the latewood proportion, wood density, tracheid length, and tracheid width within a stem using PipeQual simulation system is demonstrated in Figure 5.

DISCUSSION

An integrated system of models was developed for prediction of 3D stem structure of different branch and wood properties using a wide range of stand and tree data. The main purpose

Figure 3—Predicted probabilities for 1, 2, 4, and 6 living branches in a whorl within the living crown.
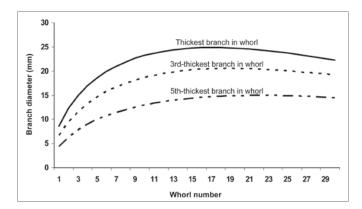
Figure 4—Predicted profiles of branch diameter for the thickest, third, and fifth thickest branch in a whorl counted from the stem apex downwards within the living crown.
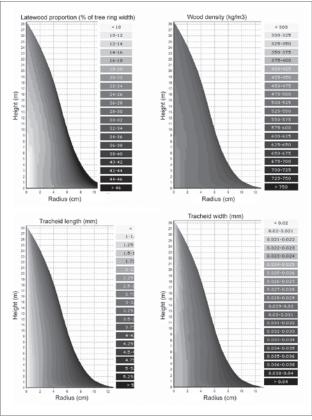
Figure 5—Predicted latewood proportion, wood density, tracheid length, and tracheid width within a stem. The figures were produced by the PuMe software (Vanninen et al. 2006).

was to develop simple and logical models based on routine stand and tree measurements. Adding stand level variables as independent variables to the models slightly improved the model performance, but stem properties were often sufficient to reliably predict branch and wood properties.

The branchiness models represent a prediction system for the primary branching structure of Norway spruce. The models predict the crown ratio and self-pruning ratio, as well as the trend in individual branch characteristics along the stem. The models must be linked with each other when recursively predicting branch characteristics.

Wood and tracheid properties were modeled as a function of the position in the stem, growth in this position, and the growth conditions of the tree. Most previous models for Norway spruce found in the literature describe wood and tracheid properties by means of the average value of a stem disc taken at a given stem height. In contrast, all the annual rings were used as individual observations in this study. This approach makes it possible to describe radial variations of wood and tracheid properties within the stem. In addition, the effects of silvicultural treatments can be predicted at the level of individual annual rings.

Even though we found bias in predicting some wood and tracheid properties, as well as wide variation of the residuals, the behaviour of the models was reasonably good. They reproduced the profiles of properties along the stem that were similar to those reported in several studies on wood and tracheid properties. The models predict the properties within the stem, but they do not describe functional relationships between wood formation and tree physiology. Annual ring width was closely related to wood and tracheid properties, but cannot be regarded as a causal driving variable.

Our main goal was to develop models that can be applied as part of a growth simulation system. The system consists of models for property distributions, which are functions of stand and tree characteristics. In application, the models can be used stochastically by generating random variation in the predictions. The variances and their covariances estimated during the simultaneous model development can be used to produce more realistic predictions compared to models fitted separately. The predictions of other models can be calibrated for a particular stand or tree if one dependent variable of the system is measured.

The results will increase our understanding of the development of wood quality as a function of forest management.

They are also applicable independent of the growth models. Incorporating wood and tracheid properties into forest management planning enables estimates for conversion of different silvicultural regimes into internal stem structure and wood quality.

LITERATURE CITED

Houllier, F.; Leban, J.M.; Colin, F. 1995. Linking growth modeling to timber quality assessment for Norway spruce. Forest Ecology and Management 74: 91-102.

Hynynen, J.; Ahtikoski, A.; Siitonen, J. [et al.]. 2005. Applying the MOTTI simulator to analyse the effects of alternative management schedules on timber and non-timber production. Forest Ecology and Management 207: 5-18.

Jaakkola, T.; Mäkinen, H.; Saranpää, P. 2005a. Wood density in Norway spruce: changes with thinning intensity and tree age. Canadian Journal of Forest Research 35: 1767-1778.

Jaakkola, T.; Mäkinen, H.; Saranpää, P. 2006. Wood density of Norway spruce: Responses to timing and intensity of first commercial thinning and fertilisation. Forest Ecology and Management 237: 513-521.

Jaakkola, T.; Mäkinen, H.; Saranpää, P. 2007. Effects of thinning and fertilisation on tracheid dimensions and lignin content of Norway spruce. Holzforschung 61: 301-310.

Jaakkola, T.; Mäkinen, H.; Sarén, M.P.; Saranpää, P. 2005b. Does thinning intensity affect the tracheid dimensions of Norway spruce? Canadian Journal of Forest Research 35: 2685-2697.

Mäkelä, A. 1997. A carbon balance model of growth and self-pruning in trees based on structural relationships. Forest Science 43: 7-23.

Mäkelä, A.; Mäkinen, H. 2003. Generating 3D sawlogs with a process-based growth model. Forest Ecology and Management 184: 337-354.

Mäkelä, A.; Mäkinen, H.; Vanninen, P. [et al.]. 2000. Predicting yield and quality of Scots pine stands.

Finnish Forest Research Institute, Research Papers 794. 89 p. (in Finnish with English summary)

Mäkinen, H.; Colin, F. 1998. Predicting branch angle and branch diameter of Scots pine from usual tree measurements and stand structural information. Canadian Journal of Forest Research 28: 1686-1696.

Mäkinen, H.; Colin, F. 1999. Predicting the number, death, and self-pruning of branches in Scots pine. Canadian Journal of Forest Research 29: 1225-1236.

Mäkinen, H.; Hynynen, J.; Colin, F.; Mäkelä, A. 1999. Predicting branch characteristics of Scots pine from usual tree measurements and stand information. In: Nepveu, G., ed. Connection between Silviculture and Wood Quality through Modeling Approaches and Simulation Software. Proceedings of the Third Workshop IUFRO WP S5.01.04, La Londe-Les-Maures, France. September 5-12, 1999, pp. 42-49.

Mäkinen, H.; Jaakkola, T.; Piispanen, R.; Saranpää, P. 2007. Predicting wood and tracheid properties of Norway spruce. Forest Ecology and Management 241: 175-188.

Mäkinen, H.; Mäkelä, A. 2003. Predicting basal area of Scots pine branches. Forest Ecology and Management 179: 351-362.

Mäkinen, H.; Ojansuu, R.; Hynynen, J.; Niemistö, P. 2004. Predicting branch properties of silver birch (*Betula pendula* Roth.) from simple stand and tree properties. In: Nepveu, G., ed. Connection between Forest Resources and Wood Quality: Modelling Approaches and Simulation Software. Proceedings of the Fourth Workshop IUFRO WP S5.01.04, Harrison Hot Springs, British Columbia, Canada, September 8-15, 2002, pp. 265-273.

Mäkinen, H.; Ojansuu, R.; Niemistö, P. 2003a. Predicting branch characteristics of planted silver birch (*Betula pendula* Roth.) on the basis of routine stand and tree measurements. Forest Science 49: 301-317.

Mäkinen, H.; Ojansuu, R.; Sairanen, P.; Yli-Kojola, H. 2003b. Predicting branch characteristics of Norway spruce (*Picea abies* (L.) Karst) from simple stand and tree measurements. Forestry 76: 525-546.

Mäkinen, H.; Saranpää, P.; Linder, S. 2002a. Effect of growth rate on fibre characteristics in Norway spruce (*Picea abies* (L.) Karst.). Holzforschung 56: 449-460.

Mäkinen, H.; Saranpää, P.; Linder, S. 2002b. Wood-density variation of Norway spruce in relation to nutrient optimization and fibre dimensions. Canadian Journal of Forest Research 32: 185-194.

Moberg, L. 1999. Models of internal knot diameter for *Pinus sylvestris*. Scandinavian Journal of Forest Research 15: 177-187.

Salminen, H.; Lehtonen, M.; Hynynen, J. 2005. Reusing legacy FORTRAN in the MOTTI growth and yield simulator. Computers and Electronics in Agriculture 49: 103-113.

Vanninen, P.; Härkönen, S.; Enkenberg, J.; Mäkelä, A. 2006. PuMe—Interactive learning environment employing the PipeQual model for forest growth and wood quality. New Zealand Journal of Forest Science 36: 280-292.

Models on Branch Characteristics of Wide-Spaced Douglas-fir

Sebastian Hein, Aaron R. Weiskittel, Ulrich Kohnle

ABSTRACT

Models of Douglas-fir branch and whorl characteristics were developed from contrasting spacing experiments in southwest Germany. The dataset was based on 100 unpruned and partially pruned trees from a 1200, 200, and 100 stems ha^{-1} spacing experiment on 24–42 year old Douglas-fir. The material was used to predict (1) the number of branches whorl^{-1}, (2) the branch angle, (3) the status (living/dead) of the branches within the living crown, (4) the maximum branch diameter whorl^{-1}, and (5) the diameter of smaller branches whorl^{-1}. For each of these models, linear generalized hierarchical mixed effects equations were developed. Overall, individual branch and tree properties were sufficient to give logical and precise predictions of the branch characteristics for the models. The models performed well across a range of stand conditions and will be further integrated into an individual tree growth and yield simulations system.

KEYWORDS: branchiness, Douglas-fir, generalized linear mixed models, timber quality, wide spacing

INTRODUCTION

ATTRIBUTES OF INDIVIDUAL BRANCHES define crown structure and have important implications at multiple levels in a forest stand. For example, crown development and structure has been related to stem growth, wood quality attributes, wildlife habitat, and key physiological processes such as interception of radiation and precipitation. Crown structure is quite sensitive to stand conditions imposed by silviculture, but these changes are generally predictable from concurrent modifications in tree and crown size.

Models of individual branch attributes exist for several commercially important species including: silver birch [*Betula pendula* Roth.] (Mäkinen et al. 2003), Scots pine [*Pinus sylvestris* L.] (Mäkinen and Colin 1999), Norway spruce [*Picea abies* (L.) Karst.] (Hein et al. 2007), radiata pine [*Pinus radiata* D. Don.] (Grace et al. 1999), Douglas-fir [*Pseudotsuga menziesii* var. *Menziesii* (Mirb.) Franco] (Maguire et al. 1994), and Sitka spruce [*Picea sitchensis* (Bong.) Carr.] (Achim and Gardiner 2006). These models have been combined with individual tree growth and yield computer simulators and have been found useful for understanding the effects of silviculture on wood quality across a wide range of stand conditions. Despite the wide array of research that has been done on individual branches, little work has been done comparing the performance of models based on datasets from contrasting thinning regimes (i.e. close spacing vs. wide spacing).

An important distinction between branch modeling done in Europe and the United States is model form. Hierarchical linear models have generally been used in Europe, while nonlinear forms have been preferred in the United States. In addition, overall modeling approaches have been different. For example, Hein et al. (2007) used a generalized mixed effects Poisson distribution probability approach to predict the number of branches per annual whorl and Maguire et al. (1994) used a nonlinear model based on the normal distribution. Further, the degree and impact of autocorrelation

Sebastian Hein (hein@hs-rottenburg.de) is professor of silviculture at the University of Applied Forest Sciences, 72108 Rottenburg, Germany and **Ulrich Kohnle** is at the Forest Research Institute of Baden, Wonnhaldestrasse 4, Freiburg i Br, Baden-Wurttemberg 7900, Germany. **Aaron R. Weiskittel** is a forest modeling assistant professor, University of Maine, Orono, ME 04471, USA.

on branch-level models has not been assessed. Weiskittel et al. (2007) found a significant degree of autocorrelation in several branch-level models, but Garber and Maguire (2005) detected no significant autocorrelation between maximum branch diameters throughout an individual crown. In this study we apply generalized linear mixed effects models. The evaluation of these types of modeling approaches will help guide future efforts.

Douglas-fir is an important species in western Europe and specifically in south-western Germany. The development of these branch-level prediction models will further our understanding of growth response at the tree-level and allow assessment of potential wood product quality in this region. This should promote more effective and efficient silvicultural practices. The overall goal of this research project was to develop branch-level models that can be integrated into an individual tree growth and yield simulation system. Specific objectives were to develop models for (1) the number of branches per annual whorl, (2) branch angle, (3) the probability of a branch being alive or dead, (4) branch diameter profiles for the thickest branch per whorl, and (5) the subsequent smaller branches. In the process, the performance of the models with respect to treatments effects and different modeling assumptions will be tested.

MATERIAL AND METHODS

Experiments and Measurements

The material was collected from three spacing experiments within the program "Solitary Trees" ("Solitärprogramm") in south-western Germany (Abetz 1987; Abetz and Lässig 1989). The principal aim of the experiments was to study the effects of weather conditions, air pollution, and biotic damage on tree growth without confounding effects of inter-tree competition.

The experiments were established in seven approximately 10–25 year-old single-species stands of Douglas-fir all located in south-western Germany between 1989 and 1991. At each location, one to three plots were set up including (1) a plot with very wide-spaced density at the establishment of the experiment where the saplings were thinned to a density of 100 stems ha-1 (4 plots); (2) a plot with an initial density of 200 stems ha-1 (8 plots); and (3) a plot with an initial density 1200 stems ha-1 (5 plots). The latter represents the common number of stems at sapling phase in Germany and is also close to recommendations for planting Douglas-fir in neighboring countries. In total, data from 17 plots from 7 locations were available. The site index defined as the dominant height at the age of 100 years ranged between 49.9 and 56.5 m with no large differences between the three treatments. All symbols for plot, tree, whorl and branch attributes used in the analysis are explained in Table 1.

In total, 100 trees were sampled from the 17 plots with 23 trees from the lowest density, 40 from the intermediate density, and 37 trees from the highest density. The sampling was targeted to dominant trees that were randomly selected under the condition of having no visible signs of damage. The trees used in this study were harvested 15 - 17 years after the beginning of the experiments. No thinnings have been carried out since the establishment of the experiments. Summary statistics of tree attributes are listed in Table 2.

The whole dataset covers a range of tree diameter between 24.1 and 54.2cm and a height of 18.0 to 30.0m measured at the time of felling.

For each plot tree, height; stem diameter at breast height; height of the crown base (defined as the height of the lowest living primary branch); and tree age were measured. After felling the sample trees, the distance of whorls

Table 1—Explaination of Symbols

Variable	Definition
brd	branch diameter, excluding the thickest branch of a whorl [mm]
brdmax	maximum branch diameter in a whorl [mm]
brs	branch status [living = 1, dead = 0]
dbh	diameter at breast height [cm]
dist	distance between the whorl and stem apex [m]
dist1	dist/(h – hcb) [-]
dist2	ln(1.1 – dist/(h – hcb) [-]
dist3	ln(dist1 + 0.1) [-]
wh	whorl height above ground
h	tree height [m]
hcb	height of the crown base (lowest living branch), measured from stem base [m]
hd	h [m]/ diameter at breast height [cm]*100 [-]
ih	annual height increment [m]
r	rank of the branch, ordered from largest to smallest diameter [-]
nbrt	total number of branches in a whorl (living and dead combined) [-]
$\alpha, \beta, \gamma, \delta, \varepsilon$	variance components of the models 4 to 8, respectively
$E, |E|, E^2$	mean error, mean absolute error, mean squared error, respectively
l, p, t, w, b, D	subscripts for location, plot, tree, whorl, branch, treatment (i.e. initial density), respectively

Table 2—Plot and tree sample description (N$_t$=100) by experiment with the initial densities of 100, 200 and 1200 trees ha^{-1}, abbreviations: see Table 1.

	100		200		1200	
	min.– max.	$\bar{x}$	min.– max.	$\bar{x}$	min.– max.	$\bar{x}$
age	24 – 42	30.1	24 – 30	26.3	24 – 31	30.0
dbh	35.9 – 54.2	44.8	29.1 – 46.7	40.6	24.1 – 40.3	33.1
h	18.0 – 30.0	23.1	20.2 – 26.5	23.1	19.4 – 27.8	23.5
hd	40.8 – 61.8	51.8	48.9 – 76.3	57.3	56.6 – 88.3	71.8
hcb	.7 – 6.7	3.0	.6 – 9.5	4.9	1.8 – 12.6	7.3
si	49.9 – 55.0	51.9	53.8 – 56.5	55.3	53.3 – 56.0	54.0

Table 3— Whorl and branch sample description (N$_b$=12855) by experiment with the initial densities of 100, 200 and 1200 trees ha^{-1}, abbreviations: see Table 1.

	100		200		1200	
	min.– max.	$\bar{x}$	min.– max.	$\bar{x}$	min.– max.	$\bar{x}$
bra	10 – 130	73.7	10 – 130	69.7	10 – 150	68.9
brdmax	.6 – 9.6	5.0	.7 – 9.4	4.2	.6 – 6.9	3.4
brd$_{lptwb}$/ brdmax$_{lptw}$	.1 – 1.0	.7	.3 – 1.0	.8	.1 – 1.0	.7
dist1	.0 – 1.0	.5	.0 – 1.0	.5	.0 – 1.0	.5
dist2	-2.3 – .1	-.7	-2.3 – .1	-.7	-2.3 – .1	-.7
dist3	-2.2 – .1	-.6	-2.1 – .1	-.6	-2.1– .1	-.6
ih	.3 – 1.8	.8	.2 – 1.6	.9	.2 – 1.7	.9
nbrt	0 – 18	7.6	0 – 17	6.2	0 – 19	7.1
r	2 – 18	5.3	2 – 16	4.9	2 – 18	5.4

from the stem apex; branch status (living or dead); the branch angle (in steps of 5 degrees); and horizontal and vertical diameter (on branch base after base swell) of all branches above 1.3m height were measured. The average branch diameter was calculated as an arithmetic mean of the horizontal and vertical diameters. Cross-sections were taken at 0.3 and 1.3m heights, then every 5.0m thereafter beginning from 5.0m height upwards. The number of annual rings was counted and compared with the number of whorls above the cross-section in order to assure the correct numbering of the whorls. In total, 12,855 branches from 2226 whorls were measured. The summary branch and whorl statistics (Table 3) cover similar ranges for the three treatments with the maximum branch diameter per whorl as an exception.

Due to our modeling approach, the number of records differs by the model. Only one observation per whorl was used in the model for the maximum branch diameter per whorl. For the model on the relative branch diameter of smaller branches in a whorl, all branches excluding the maximum branch were taken. Furthermore, modeling logic requires excluding all green pruned trees (N=57) from the model

on branch status, as we intended to model the branch status within the living crown undisturbed by artificial pruning. In addition, no branch angle was recorded on 15 trees. We thus record the number of observations available for each model separately. Lastly, since branch angle is a potential predictor for branch diameter, we excluded trees with no branches recorded from the two models on branch diameter.

Statistical Analysis

Our dataset contains discrete (e.g. counts of branches per whorl) as well as continuous data (e.g. maximum branch diameter per whorl). In addition, our dataset has a hierarchical structure with branches nested within whorls that are themselves clustered within trees and then in plots. Thus, mutual dependence of the measurements should be considered in the statistical analysis. An appropriate statistical analysis of such data should combine the concept of generalized linear or nonlinear models (Agresti 2002, Littell et al. 2006) together with the multilevel and mixed model approach (Snijders and Bosker 2003).

We therefore modeled the data using "generalized linear mixed models" (GLMM) in which the data may display any distribution of the exponential family. In addition, GLMM consists of a non-linear link function that describes how the response variable is related to the linear predictor. The link function creates linearized pseudo-data on the link scale, based on the original values (the data scale). We considered the hierarchical structure of the data and the mutual dependence of the measurements in the statistical analysis by applying the mixed model approach including random experiment, plot, tree, whorl and branch effects, varying around the fixed population mean. Our measurements of the branch and whorl characteristics can be thought of as repeated measures along the stem or along a gradient within the whorl. Since our data indicated a significant longitudinal error for the model on maximum

25

branch diameter in a whorl, we included such an effect by choosing a covariance structure for irregularly spaced repeated measures (Gregoire et al. 1995).

Models were calculated using the empirical "sandwich" estimators to adjust the standard errors and test statistics. The sandwich estimators are useful for inferences on fixed effects that are not sensitive to the choice of the covariance models (SAS 2005). For all our models we used the root-sandwich estimator of Kauermann and Carroll (2001). The models on count (number of branches) and binomial data (branch status) had an over- or under-dispersion parameter Φ added to the variance function in order to prevent misinterpretations from inflated or deflated test statistics. The error variance is thus $\Phi[\mu(1-\mu)]/n$ and $\Phi\lambda$ for binomial and count data, respectively (McCullagh and Nelder 1999), where μ and λ are the respective means for binomial and count data and n the number of observations.

In order to examine the residuals of the models at tree, whorl, or branch levels, the empirical "best linear unbiased predictors" (BLUP) were calculated for each level. The BLUPs were calculated from the solution of the random effects on the link scale, and then transformed to the data scale. All residual graphs display the values in the data scale. It should be noticed that by using this procedure, the residuals at the lower levels are conditional to the residuals of the higher levels, i.e. the average higher-level residual of each sampling unit was removed from the lower-level residuals and displayed as the mean residual over the corresponding sampling unit. For example, the whorl-level residuals for the model of the relative diameter of the smaller branches in a whorl are calculated and displayed as whorl-mean residuals over the whorl attribute.

In model-building, independent fixed variables and their different combinations describing the properties of the plots, trees, whorls, and branches were tested for potential relationship to the branch and whorl properties. Variables were included into the models at the α=0.05 level of significance.

In order to examine the performance of the fixed part of the models, we calculated the following error statistics using only the fixed part of the models:

$$E = \sum (y_i - \hat{y}_i) / n$$

(1a) mean error

$$|E| = \sum |y_i - \hat{y}_i| / n$$

(1b) mean absolute error

$$E^2 = \sum (y_i - \hat{y}_i)^2 / n$$

(1c) mean squared error

where y_i is the measured observation, $\hat{y}_i$ as the predicted value, and n the number of observations. For calculating the error statistics, all values were used in their data scale.

In the case of the model on branch status, we also evaluated the goodness of fit by calculating the share of true positive events "true positive rate = sensitivity" and the false positive rate "1–specificity" for varying cutpoints (event = living branch). The cutpoint determines the predicted probability where a branch can be considered as living for simulations. The optimal cutpoint was taken from the probability where the Youden-index reaches its maximum value: i.e. sensitivity + 1–specificity – 1 (Youden 1950). As a measure of the goodness of fit that is cutpoint independent, we constructed the receiver operating characteristic curve and calculated the area under curve (AUC).

The applicability of the models to account for the effects of stand density on branch properties was tested using the marginal residuals. The marginal residuals were calculated as a difference between the measured observation and the predicted value on the data scale. Depending on the level of the measurements (whorl or branch level), the models used to test for possibly remaining treatment effects were:

$$(y_{lptw} - \hat{y}_{lptw}) = \mu + \tau_D + u_l + u_{lp} + u_{lpt} + u_{lptw}$$

(2a)

or

$$(y_{lptwb} - \hat{y}_{lptwb}) = \mu + \tau_D + u_l + u_{lp} + u_{lpt} + u_{lptw} + u_{lptwb}$$

(2b)

where $(y_{lptw} - \hat{y}_{lptw})$ are the marginal residuals, μ is the overall mean, τ_D the treatment effect, and u_l, u_{lp}, u_{lpt}, u_{lptw} and u_{lptwb} the random effects for location l, plot p, tree t, whorl w and branch b. For comparison of the three treatments, a Bonferroni adjustment was used α=0.05. In order to analyze the performance of the models for effects of the three pruning intensities we applied the same procedure as described in the section on stand density. We therefore tested the marginal residuals as well for remaining pruning effects in a mixed model.

The predictive power r of the models was calculated as the squared correlation between the observed response and the marginal model predicted value on the data scale (Zheng and Agresti 2000):

$$r^2 = (cor(Y, \hat{Y}))^2$$

(3)

where Y is the observed dependent variable at the data scale and $\hat{Y}$ the marginal estimated value of Y given the fixed effects predictors.

The following measures were used to compare the goodness of fit of the models: sensitivity to silvicultural measures, mean error, mean absolute error, mean squared error, the analysis of the marginal residuals for residual effects, and the predictive power. As a substitute to the predictive power (Model 3) for the model on branch status we used the values for sensitivity, 1-specificity (both at a predicted probability of 0.5 and at the maximum Youden-index), and the AUC-value.

All of the linear statistical analyses were carried out by SAS software (SAS 2004, 2006).

RESULTS
Model: Number of Branches Whorl^{-1}
For the construction of the model on number of branches whorl^{-1} the combined number of living and dead branches on all the whorls available was used. The dataset contained 2,226 whorls from 100 trees. For the total number of branches per whorl (*nbrt*), a log-link function with the Poisson distribution was used:

$$\ln\left(nbrt_{lptw}\right) = a_0 + a_1 hd_{lpt} + a_2 ih_{lptw} + \alpha_{lpt} + \alpha_{lptw} \qquad (4)$$

The number of branches per whorl was related to the height-to-diameter ratio (hd-ratio) and annual height increment (ih) (Table 4). No other variables were found statistically significant. The error statistics (Equation $1a - c$) showed no large bias (Table 4) and there was no trend in the residuals when plotted against the hd-ratio, the height increment, or the predicted values of *nbrt*. The residuals in initial spacings of 100, 200 and 1200 trees ha^{-1} did differ slightly from each

other (Table 7) with the highest difference (1.4 branches whorl^{-1}) occurring between the 100 and the 1200 initial spacing plots. The model explained only a low proportion from the total variance (6.1 percent).

Model: Branch Angle
For the construction of the model on the branch angle we used all observations within the green crown whether from pruned or from unpruned trees. The dataset contained a total of 11,493 branches from 85 trees. Since branch angle (*bra*) was measured in discrete steps of 5 degrees, a log-link function with the Poisson distribution was used:

$$\ln(bra_{lptwb}) = c_0 + c_1 hd_{lpt} + c_2 dist3_{lptw} + c_2 brd_{lptwb} + \gamma_{lpt} + \gamma_{lptw} + \gamma_{lptwb} \qquad (5)$$

The predictors of the branch angle model were the hd-ratio, the branch position within the living crown (*dist3*), and the branch diameter (Table 4). No other tree level variables were statistically significant. The error statistics (Equation $1a - c$) showed no large bias but a large mean squared error (Table 4) and there was no trend in the residuals when plotted against the predictors or predicted values (Fig. 2). The residuals of the model did not differ significantly between the initial spacings (Table 7). The model explained 25.8 percent of the total variance.

Model: Branch Status (Living or Dead)
The model for the status of individual branches (*brs*) was based on all the branches in the dataset within the living crown excluding the trees with pruning to a stem height of more than 2.5m (N_b=6879, N_t=43). Status of a branch is a binary phenomenon (0, dead; 1, living). Therefore, a logit-link function with a binomial distribution was used to model the probability (*Pr*) that a branch is alive:

Table 4—Parameter estimates of the model for the number of branches in a whorl (left, Equation 4, N_t=100, N_w=2226) and of the model for branch angle (Equation 6, N_t=85, N_{branch}=11493).

Parameter	Estimate	se ($S_{\bar{x}}$)	t-value	p > t		Estimate	se ($S_{\bar{x}}$)	t-value	p > t
Fixed parameters									
a_0	1.7181	.1250	13.75	<.0001	c_0	4.6698	.0619	75.48	<.0001
a_1	.0052	.0020	-2.62	.0089	c_1	-.0038	.0009	-4.24	<.0001
a_2	.5543	.0558	9.93	<.0001	c_2	.2438	.0115	21.14	<.0001
a_3	-	-	-	-	c_3	-.0177	.0034	-5.24	<.0001
Error statistics									
E				.2189					1.3749
|E|				2.50757					8.8577
E²				10.6628					138.3430

$$\ln\left[\frac{Pr(brs_{lptwb})}{(1 - Pr(brs_{lptwb}))}\right] = b_0 + b_1 hd_{lpt} + b_2 dist2_{lptw}$$

$$+ \ b_3 \frac{brd_{ptwb}}{brd\,max_{ptw}} + \beta_{lpt} + \beta_{lptw} + \beta_{lptwb} \qquad (6)$$

The branch status was related to the hd-ratio, the branch position within the living crown (*dist2*), and the relative branch diameter within a whorl (Table 5). The other variables were not statistically significant. The error statistics (Equation *1a – c*) showed no large bias (Table 5) and there was no trend in the residuals when plotted against the hd-ratio, position within the crown, relative branch diameter, or predicted values of the branch status. The residuals of the model did not differ significantly between the initial spacings (Table 7). The area under the ROC-curve was high: AUC=0.945. At a cutpoint of 0.5 the true positive rate (living branches) was satisfyingly high (98.2 percent). However the false negative rate is also high (51.6 percent) (Table 5). With the optimal cutpoint at Pr=0.76 the sensitivity is still high: 87.6 percent and the 1-specifity is improved to 11.7 percent.

Model: Maximum Diameter Branch Whorl[1]

For building the model on maximum branch diameter, only whorls with at least one branch were taken. The parameters of this model were estimated using a dataset of 1,662 branches from 85 trees. For the model of the maximum branch diameter in a whorl (*brdmax*), a log-link function with a normal distribution of the response variable was used:

$$\ln\!\left(brd\,max_{lptw}\right) = d_0 + d_1 bhd_{lpt} + d_2 hd_{lpt} + d_3 dist1_{lptw}$$

$$+ \ d_4 dist3_{lptw} + \delta_{lpt} + \delta_{lptw} + \delta_{lptwb}$$

$$(7)$$

The diameter of the thickest branch in a whorl was related to the tree's diameter at breast height (*dbh*), the hd-ratio, and the whorl location within the living crown. The other variables were not statistically significant (Table 6). The error statistics (Equation *1a – c*) show no large bias (Table 6). In addition, no trend in the residuals was found when plotted against the predictors or the predicted variable. Furthermore, the residuals did not differ between the initial spacings (100, 200, and 1200 trees ha^{-1}, Table 7). The model explained 85.3 percent of the total variance.

Table 5—Parameter estimates of the linear model for model for branch status (1, living; 0, dead) (Equation 5) N_t=43 N_b=6879.

Parameter	Estimate	se ($S_{\bar{x}}$)	t-value	p > t
Fixed parameters				
b_0	7.6453	1.6395	4.66	<.0001
b_1	-.0578	.0260	-2.22	.0262
b_2	5.0967	.3233	15.77	<.0001
b_3	.0985	.0082	12.02	<.0001
Error statistics		E=-.0190 |E|=.0732 E²=.0495		
Cutpoint = .50		predictions "0"		predictions "1"
observations "0"		48.4% (ok)		51.6% (wrong)
observations "1"		1.8 % (wrong)		98.2% (ok)
Cutpoint = .76 (max. Youden Index)				
observations "0"		88.3% (ok)		11.7% (wrong)
observations "1"		12.4% (wrong)		87.6% (ok)

Table 6—Parameter estimates of the models for the diameter of thickest branch (left, Equation 7; N_t=85 N_w=1662) and smaller branches (right, Equation 7; N_t=85 N_b=9831) in a whorl.

Parameter	Estimate	se ($S_{\bar{x}}$)	t-value	p > t		Estimate	se ($S_{\bar{x}}$)	t-value	p > t
Fixed parameters									
d_0	3.6923	.3072	12.02	<.0001	e_0	-3.5258	1.6015	-2.20	.0464
d_1	.0152	.0035	4.32	<.0001	e_1	.1032	.0297	3.47	.0005
d_2	-.0068	.0022	-3.05	.0023	e_2	.1480	.0082	17.95	<.0001
d_3	-2.4167	.1129	-21.40	<.0001	e_3	.4000	.0156	-25.60	<.0001
d_4	2.1192	.0615	34.44	<.0001		-	-	-	-
Error statistics									
E				.0390					.0147
|E|				.5474					.1068
E²				.5313					.0206

Table 7—Residual means for the four models tested for differences between the initial densities of 100, 200, and 1200 trees ha^{-1}.

model	100		200		1200	
	mean	se ($S_{\bar{x}}$)	mean	se ($S_{\bar{x}}$)	mean	se ($S_{\bar{x}}$)
Eq.4	-.92[a]	.2958	-.77[b]	.3174	.48[ab]	.5491
Eq.5	2.16[a]	1.3654	-1.47[a]	1.1751	1.40[a]	1.2772
Eq.6	-.02[a]	.0122	-.02[a]	.0143	-.02[a]	.0128
Eq.7	.17[a]	.0882	-.04[a]	.0768	-.02[a]	.0723
Eq.8	-.01[ab]	.0132	.01[ab]	.0117	-.05[ac]	.0114

The values in the same row marked with a different superscript are significantly different (p>0.05)

Model: Smaller Branches Whorl[-1]

For the model of the smaller branches' diameters (omitting the thickest branch per whorl) 9,831 branches from 85 trees were available. Only whorls with at least 2 branches were included in the dataset. The dependent variable was the ratio between the diameter of a smaller branch and the thickest branch in each whorl, i.e. the values of the dependent variable vary between 0 and 1. If the other branches of a whorl had the same diameter as the thickest branch, their diameter was reduced by 0.1mm (1/10th of measurement accuracy) to avoid non-defined values in the log-transformation. For the model of relative branch diameter, a logit-link function with a binomial distribution was used:

$$\ln\left[\frac{brd_{ptwb}}{brd\max_{ptw}} \middle/ \left(1 - \frac{brd_{ptwb}}{brd\max_{ptw}}\right)\right] = e_0 + e_1 si_{lp}$$
$$+ e_2 nbrt_{lptw} + e_2 r_{lptwb} + \varepsilon_{lp} + \varepsilon_{lpt} + \varepsilon_{lptw} + \varepsilon_{lptwb}$$

(8)

Figure 1—(A) Predicted number of branches in a whorl for three hd-ratios plotted against the annual height increment (Equation 4). (B) Predicted branch angle within the living crown for three hd-ratios at a branch diameter of 2cm. (C) The same as (B) but branch diameter = 5cm (both Equation 5). (D) Predicted probability for a branch being alive within the living crown for two hd-ratios combined with two branch relative diameters (Equation 6). 0=apex, 1=crown base. The abbreviations refer to the explanations given in Table 1.

The diameters of the smaller branches were related to the site index, the total number of branches whorl[-1] and their rank within a whorl according to branch diameter from rank 2 on (Table 6). The relative diameters of the smaller branches were not related to whorl position within the living crown. The error statistics (Equation *1a - c*) did not show a large bias (Table 6) and there was no trend in the residuals when plotted against the predictors and the dependent variable. Furthermore, the residuals of the model did not differ systematically from low to high initial density levels (Table 7). The model explains 58.0 percent of the total variance.

Simulations

Predictions of the branchiness models as a part of the growth and yield simulation system are demonstrated in Figure 1 and 2. With increasing annual height increment, the number of branches in a whorl also increases (Fig. 1A). However, trees with higher hd-ratios have fewer branches per whorl. With increasing hd-ratio, the branches are more steeply inserted within the crown (Fig. 1B). Along the crown profile all branches tend towards a more horizontal insertion. Larger branches are more steeply inserted than smaller branches (Fig. 1B vs. C). The thickest branch in each whorl has a high probability of being alive throughout the living crown (Fig. 1D). However, smaller branches tend to die early when they are located in the lowest quarter of the living crown. With increasing stem diameter and decreasing hd-ratio, the diameter of the thickest branch per whorl increases over the total length of the living crown (Fig. 2A, B). The size of smaller branches within the crown is demonstrated (Fig. 2C-F) in varying levels and combinations of branch rank, diameter at breast height, and hd-ratio.
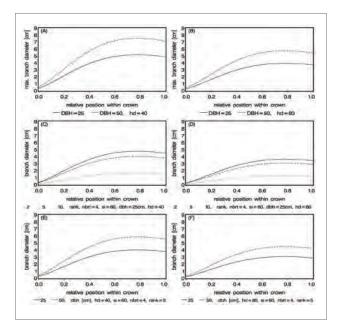
Figure 2—(A) Predicted diameter of the thickest branch in a whorl within the living crown for two dbhs and hd=40. (B) The same as (A) but hd=80 (Equation 7). (C) Predicted branch diameters within the living crown for three branches of different diameter rank within a whorl (nbrt=4, si=60m, dbh=25 cm, hd=40). (D): The same as (C) but hd=40 (Equation 7). (E) Predicted diameter for branches with rank 5 for two dbhs at a hd-ratio of 40 (nbrt=4, si=60m, dbh=25 cm) (Equation 7). (F) The same as (E) but hd=80. 0=apex, 1=crown base. The abbreviations refer to the explanations given in Table 1.

DISCUSSION

Model: Number of Branches Whorl[-1]

The hd-ratio can be used as a general indicator for the vigour of a tree. In our model the number of branches increased with decreasing hd-ratio. According to the previous studies for Scots pine and Norway spruce, the number of new branches in a whorl increases with increasing vigour of trees (e.g. Kellomäki and Tuimala 1981; Hein et al. 2007). The number of branches in a whorl is also related to annual height increment, which is again indicative of tree vigour (e.g. Mäkinen and Colin 1999; Hein et al. 2007). A possible explanation is that the number of branches in a whorl as well as height increment, is controlled by the growing conditions during two successive years. For Scots pine, Junttila and Heide (1981) and Junttila (1986) observed that temperature during bud formation has an effect on final shoot length achieved in the following year. The influence of tree social position and annual height increment on the number of branches per whorl has also been observed in Pacific Northwest Douglas-fir (Maguire et al. 1994; Weiskittel et al. 2007).

Annual height increment, which was used as an independent variable in this study, is only occasionally measured. However, in growth simulation systems, annual or periodical height increment is often estimated with the help of a height increment model. The year-to-year variation in the number of branches can then be added according to the observed large residual variation. Only a low percentage of total variance in the number of branches could be explained. One reason for this could be that the number of branches is under moderate genetic control (Velling 1988; Liesebach 1994; Vestøl et al. 1999). Another explanation may be that our analysis did assess all branches per whorl down to the threshold branch diameter for timber grading of 5mm. Previous studies on Norway spruce stopped at less than the first six branches starting from the thickest (Schmidt 2001). However, van Laar (1967), Lewark (1981), and Weiskittel et al. (2007) also found a large variability in the number of branches per whorl.

Model: Branch Angle

The angle at which branches are attached to the stem has a major influence on crown form as well as wood quality. On an individual tree, branch angle is largely determined by the effects of gravity and light availability. Hence, branch diameter and location in the crown were particularly important determinants of branch angle in this study. In addition, tree social position in the stand can be a significant factor influencing branch angle. This study supports this general observation since branch angles became flatter as the tree hd-ratio increased. In the case of Douglas-fir in the Pacific Northwest, site index has been found to exert a significant influence on branch angle, even after accounting for branch size and tree social position (Roeh and Maguire 1997; Weiskittel et al. 2007). However, site index was not found to influence branch angle in German Douglas-fir.

Model: Branch Status (Living or Dead)

Branch status was modeled within the living crown from the stem apex to crown base. The main emphasis was on modeling the progress of branch die-off within the living crown. It was assumed that branch death at a certain relative distance between the stem apex and crown base is independent of the actual length of the living crown. The probability of a branch being alive diminished towards the base of the living crown in accordance with a reverse S form. The shape of the curve was the same regardless of

initial stand density. The model accounted for a sufficient proportion of the total variation in branch status. The emergence of spike knots results in irregular development of branches and may cause additional variation in branch mortality.

Stand density is known to be a strong determinant of branch mortality and, therefore, it controls branch die-off (e.g. Valentine et al., 1994). In our model, increasing competition associated with increasing hd-ratio decreased the probability of a branch being alive. Furthermore, the large branches in a whorl had a greater probability to remain alive than the smaller ones in the same whorl (c.f. on Norway spruce Mäkinen and Colin 1999). Mutual shading by branches from upper parts of the crown and neighboring trees (Grote and Pretzsch 2002) may give a physiological explanation for the statistical model described. The experiments sampled in this study were on rather young trees, under 50 years old. Mäkinen et al.(2003) showed that for Norway spruce tree age had an effect on the number of living branches at a given depth within the crown. Thus, it can be expected that the model for the probability of a branch being alive must be adapted to older trees.

Models: Branch Diameter

Factors promoting the diameter growth of a tree increase branch diameters as well (cf. Kenk 1990). As with branch status, branch diameter is closely related to the hd-ratio and branch location within the living crown. However, differences in branch diameters between trees of different stem diameter (hd and dbh) were larger in the lower crown than in the upper crown (Mäkinen 1999). Kantola and Mäkelä (2004) also reported for Norway spruce that in the first five meters downwards from the tree top, branch size did not differ between thinning intensities. Obviously, branch growth in the upper crown is not closely related to between-tree competition.

Within the living crown, the thickest branches were located around 75 percent of the crown length from the tree top downwards. Decreasing branch diameters when moving downwards near the crown base have also been reported by Colin and Houllier (1992) for Norway spruce and by Maguire et al. (1994) for Douglas-fir in the Pacific Northwest. In a dynamic application, a decreasing branch diameter trend near the crown base may cause illogically declining branch diameter estimates under some conditions. The mutual dependence between thickest branch and smaller branches was taken into account by estimating the smaller branches relative to the size of the largest branch whorl[-1] (see also Hein et al. 2007).

CONCLUSIONS

Even though the spacing experiments on Douglas-fir were originally designed for the development of branchiness models, the plots provided interesting information for forest management practice. The results demonstrated the possibility to predict the effects of a wide range of stand densities on branch characteristics with only one model. In addition, the behaviour of the models is logical and in accordance with the earlier studies. When integrated into a stand growth simulator, the models allow simultaneous comparison of the effects of different silvicultural treatments on tree growth and branchiness.

Stem and crown properties were sufficient to predict reliable branch properties. Thus, branch properties can be predicted without detailed knowledge of the past and current stand conditions if tree- and crown-level variables that synthesize their effects are measured. Even though the models were largely unbiased in respect to initial stand density, they could not be evaluated in respect to other silvicultural treatments. For example, species admixture may affect branch profiles in the crown due to changes in resource utilization.

LITERATURE CITED

Abetz, P. 1987. Das "Solitärprogramm 1987". AFJZ 45/1987: 1172. [Original in German]

Abetz, P.; Lässig, R. 1989. Erfreuliches Echo auf das "Solitärprogramm 1987". AFJZ 27/ 1989: 714-716. [Original in German]

Achim, A.; Gardiner, B. 2006. Predicting the branching properties of Sitka spruce grown in great Britain. New Zealand Journal of Forestry Science 36: 246–264.

Agresti, A. 2002. An introduction to categorial data analysis. Wiley-Interscience. New York. 710 p.

Colin, F.; Houllier, F. 1992. Branchiness of Norway spruce in Northeastern France: Predicting the Main Crown Characteristics from Usual Tree Measurements. Annals of Forest Science 49: 511-538.

Garber, D.M.; Maguire, D.A. 2005. Vertical trends in maximum branch diameter in two mixed-species spacing trials in the central Oregon Cascades. Canadian Journal of Forest Research. 35: 295-307.

Grace, J.C.; Pont, D.; Goulding, C.J. 1999. Modeling branch development for forest management. New Zealand Journal of Forest Science 29: 391-408.

Gregoire, T.G.; Schabenberger, O.; Barret, J.B. 1995. Linear Modelling of Irregularly Spaced, Unbalanced, Longitudinal Data from Permanent-Plot Measurements. Canadian Journal of Forest Research 25: 137–156.

Grote, R.; Pretzsch, H. 2002. A model for individual tree development based on physiological processes. Plant Biology 4: 167-180.

Hein, S.; Mäkinen, H.; Yue, C.; Kohnle, U. 2007. Modelling branch characteristics of Norway spruce from wide spacings in Germany. Forest Ecology and Management 242: 155-164.

Junttila, O. 1986. Effects of temperature on shoot growth in northern Provenances of *Pinus sylvestris* L. Tree Physiology 1: 185-192.

Junttila, O.; Heide, O.M. 1981. Shoot and needle growth in *Pinus sylvestris* as related to temperature in northern Fennoscandia. Forest Science 27: 423-430.

Kantola, A.; Mäkelä, A. 2004. Crown Development in Norway Spruce (*Picea abies* (L.) Karst.). Trees 18: 408-421.

Kauermann, G.; Carroll, R.J. 2001. A Note on the Efficiency of Sandwich Covariance Estimation. Journal of the American Statistical Association 96: 1387-1396.

Kellomäki, S.; Tuimala, A. 1981. Effect of Stand Density on Branchiness of Young Scots Pine. Folia Forestalia 478: 1-27.

Kenk, G. 1990. Fichtenbestände aus Weitverbänden —Entwicklung und Folgerungen. Forstwissen-schaftliches Centralblatt 109: 86-100.

Lewark, S. 1981. Untersuchungen von Holzmerkmalen junger Fichten (*Picea abies* (L.) Karst.) Jahrringbreite, Rohdichte und Ästigkeit von Stecklingsklonen. PhD, Universität Göttingen. 193 p. [Original in German with English summary]

Liesebach, M. 1994. Untersuchungen an ausgewählten Herkünften des internationalen Fichtenprovenienzversuchs 1964/68 über den Zusammenhang zwischen Isoenzym-Merkmalen und morphologischen, phänologischen sowie Wachstumsmerkmalen. PhD, Universität Hamburg. 210 p. [Original in German with English summary]

Littell, R.C.; Milliken, G.A.; Stroup, W.W. [et al.]. 2006. SAS System for Mixed Models. Cary, North Carolina, USA. 814 p.

Maguire, D.A.; Moer, M.; Bennet, W.S. 1994. Models for Describing Basal Diameter and Vertical Distribution of Primary Branches in Young Douglas-fir. Forest Ecology and Management 63: 23-55.

Mäkinen, H. 1999. Growth, suppression, death, and self-pruning of branches of Scots pine in southern and central Finland. Canadian Journal of Forest Research 29: 585-594.

Mäkinen, H.; Colin, F. 1999. Predicting the Number, Death and Self-Pruning of Scots Pine in Finland. Canadian Journal of Forest Research 29: 1225-1236.

Mäkinen, H.; Ojansuu, R.; Niemistö, P. 2003. Predicting external branch characteristics of planted silver birch (*Betula pendula* Roth.) on the basis of routine stand and tree measurement. Forest Science 49: 301-317.

McCullagh, P.; Nelder, J. A. 1999. Generalized Linear Models. Chapman & Hall/CRC, Boca Raton. 511 p.

Roeh, R.L.; Maguire, D.A. 1997. Crown profile models based on branch attributes in coastal Douglas-fir. Forest Ecology and Management 96: 77-100.

SAS. 2004. SAS/STAT 9.1 User's Guide. SAS Publishing, Cary, NC. 5121 p.

SAS. 2006. The GLIMMIX Procedure. SAS Publishing, Cary. 256 p.

Schmidt, M. 2001. Prognosemodelle für ausgewählte Holzqualitätsmerkmale wichtiger Baumarten. PhD,

Universität Göttingen. 302 p. [Original in German with English summary]

Snijders, T.A.B.; Bosker, R.J. 1999. Multilevel Analysis. SAGE Publications Ltd, London. 266 p.

Valentine, H.T.; Ludlow, A.R.; Furnival, G.M. 1994. Modeling crown rise in even-aged stands of Sitka spruce or loblolly pine. Forest Ecology and Management 69: 189-197.

van Laar, A. 1967. Single-Tree Parameters of Norway Spruce (*Picea abies* (L.) Karst.) in Relation to Site and Environment. Forstliche Forschungsberichte München, Schriftenreihe der Forstwissenschaftlichen Fakultät der Universität München und der Bayer. Forst-u. Forschungsanstalt, 30. 88 p. [Original in German]

Velling, P. 1988. The Relationships between Yield Components in the Breeding of Scots Pine. PhD, University of Helsinki. 59 p.

Vestøl, G.I.; Colin, F.; Loubère, M. 1999. Influence of Progeny and Initial Stand Density on the Relationship between Diameter at Breast Height and Knot Diameter of *Picea abies*. Scandinavian Journal of Forest Research 14: 470-480.

Weiskittel, A.R.; Maguire, D.A.; Monserud, R.A.; 2007. Modeling crown structural responses to competing vegetation control, thinning, fertilization, and Swiss needle cast in coastal Douglas-fir of the Pacific Northwest, USA. Forest Ecology and Management 245, 96-109.

Youden, W. 1950. Index rating for Diagnostic Test. Cancer 3: 32-35.

Zheng, B.; Agresti, A. 2000. Summarizing the predictive power of a generalized linear model. Statistics in Medicine 19: 1771-1781.

Radiata Pine Crown Development: Model, Model Performance, and Incorporation into Forest Inventory

Jennifer C. Grace

EXTENDED ABSTRACT

R ADIATA PINE (*Pinus radiata* D. Don) IS THE MAIN commercial forestry species grown in New Zealand, covering 1.6 million ha within a land area of 26.9 million hectares (New Zealand Forest Owners Association, 2006). New Zealand covers a wide range of environmental conditions and early research indicated that there were significant differences in the patterns of radiata pine growth across the country (Goulding 1994). To account for this variation, separate stand and individual tree distance-independent growth models have been developed for different regions within New Zealand.

Radiata pine is also genetically variable. This variability has been exploited in a tree-breeding program that has been in place since the 1950's (www.rpbc.co.nz). Different "breeds" of radiata pine have been developed, including the "Growth and Form (GF) Breed" developed to produce trees with fast growth and excellent form and the "Long Internode Breed" developed to produce knot-free wood from unpruned trees (Jayawickrama and Carson 2000). This later breed, in particular, exploits the genetic variability in the number of branch clusters formed annually, and has fewer clusters in an annual shoot compared to the "Growth and Form Breed". In addition, trees with long internodes tend to have larger-diameter branches compared with more multinodal trees (www.rpbc.co.nz).

A model predicting crown development in radiata pine with a "Growth and Form" rating of GF14 has been developed by destructively sampling 49 trees from eight different regions within New Zealand. This has been linked with the individual-tree distance-independent growth model to create the model "TreeBLOSSIM". As with the growth model, this is a regionally based model. The branching component of TreeBLOSSIM is hierarchical in structure. At the tree level, it predicts the probability that the tree will form stem cones. At the annual shoot level, it predicts the number of branch clusters formed and their relative position within the annual shoot. At the cluster level it predicts the number of stem cones and branches formed, and their angular distribution around the stem. At the branch level, it predicts the change in branch diameter through time, the age when the branch dies (when the branch knot becomes bark encased), and whether there will be bark trapped above the live branch (Grace et al. 1998, Grace et al. 1999, Grace 2004).

As with any model, it is important to demonstrate that TreeBLOSSIM provides realistic predictions across a wide range of sites, silvicultural treatments, and improved seedlots. Model performance in predicting the number of branch clusters and the diameter of the largest branch in a cluster was examined by comparing model predictions with measurements collected from images using a non-destructive, ground-based photogrammetric method, TreeD (Brownlie et al. 2007). To date, TreeD data have been collected from 19 trials. Each trial contains a number of permanent sample plots (PSPs), and several were assessed to provide data for selected silvicultural treatments and/or seedlots. In total measurements are available for:

- 259 trees from 54 PSPs with a GF rating of 14
- 193 trees from 35 PSPs with a GF rating between 21 and 25
- 134 trees from 25 PSPs containing long internode seedlots with a long internode rating between 19 and 28

In terms of "average branch diameter", TreeBLOSSIM

Jennifer C. Grace (jenny.grace@ensisjv.com) is a senior scientist at Scion, Private Bag 3020, Rotorua, New Zealand.

predictions were good with 85 percent of the GF14 trees falling within the defined acceptable limits. The performance was similar for the GF20+ seedlots, but noticeably poorer for the long internode seedlots. In terms of "maximum branch diameter", TreeBLOSSIM predictions were good for 54 percent of the GF 14 trees. The performance was similar for the GF20+ seedlots but noticeably poorer for the long internode seedlots. Images were re-examined for trees where the "maximum branch diameter" prediction was poor. This highlighted that stem damage is a common occurrence at some sites and has a major influence on the branching characteristics of radiata pine, resulting in larger than expected branch diameters. In terms of "number of branch clusters", TreeBLOSSIM predictions were good for 48 percent of the GF14 trees, but TreeBLOSSIM tended to predict more clusters than observed. TreeBLOSSIM predictions were slightly better for the GF20+ seedlots, and indicate that the GF20+ seedlots have more branch clusters than the GF14 seedlots. TreeBLOSSIM, as expected, predicted more branch clusters than observed for the long internode seedlots. These results give confidence in the model and its use within forest inventory.

During a forest inventory, a tree stem is visually classified into lengths according to a given set of maximum branch diameters, i.e. each stem length has an associated branch diameter class. Some typical values of maximum branch diameters that may be used are 4 cm, 7 cm, 10 cm, and 15 cm. These data may be imported into a version of TreeBLOSSIM included in Atlas Cruiser (developed by Atlas Technology, www.atlastech.co.nz). Rules are in place to adjust model predictions to correspond with the inventory data. One positive aspect of inventory data is that it will identify the unusually large branches that are often underpredicted by TreeBLOSSIM.

The position of branch clusters is rarely measured in forest inventories. For situations where branch cluster positions have not been measured, the possibility of predicting the number of branch clusters from environmental variables has been investigated using the Land Environments of New Zealand (Leathwick et al., 2003). Where a field count of branch clusters is available, a method of using these data to estimate the number of branch clusters in an annual shoot has been developed.

Combining inventory data with TreeBLOSSIM allows TreeBLOSSIM to be adapted for specific sites and seedlots, and provides a realistic description of the branching pattern of the tree, including the position of unusually large branches, which may be grown forward in time to the required age to provide estimates of yield by log-types.

KEYWORDS: *Pinus radiata,* branching, forest inventory, modeling

LITERATURE CITED

Brownlie, R.K.; Carson, W.W.; Firth, J.G.; Goulding, C.J. 2007. An image-based dendrometry tool for standing trees. New Zealand Journal of Forestry Science 37 (2): 153-168.

Goulding, C.J. 1994. Development of growth models for *Pinus radiata* in New Zealand—Experience with management and process models. Forest Ecology and Management 69: 331-343.

Grace, J.C. 2004. Links between science and forest management: As illustrated by a model of branch development. In: Mencuccini, M.; Grace, J.; Moncrieff, J.; McNaughton, K.G., eds. Forests at the Land—Atmosphere Interface. CABI Publishing pp. 255-267.

Grace, J.C.; Blundell, W.; Pont, D. 1998. Branch development in radiata pine—model outline and data collection. New Zealand Journal of Forestry Science 28: 182-194.

Grace, J.C.; Pont, D.; Goulding, C.J.; Rawley, B. 1999. Modeling branch development for forest management. New Zealand Journal of Forestry Science 29: 391-408.

Jayawickrama, K.J.S.; Carson, M.J. 2000. A breeding strategy for the New Zealand Radiata Pine Breeding cooperative. Silvae Genetica 49 (2): 82-90.

Leathwick, J.; Wilson, G.; Rutledge, D. [et al.]. 2003. "Land Environments of New Zealand (LENZ)—Nga Taiao o Aotearoa". Ministry for the Environment, Wellington.

New Zealand Forest Owners Association. 2006. New Zealand Forest Industry Facts and Figures 2006/7. New Zealand Forest Owners Association, Wellington.

Modeling Crown Recession in Three Conifer Species of the Northern Rocky Mountains

Sean M. Garber, Robert A. Monserud, Douglas A. Maguire

ABSTRACT

CROWN LENGTH IS A FUNDAMENTAL TREE dimension that has important implications for growth potential, wildlife habitat, stand aesthetics, and wood quality. The relative rates of height growth and crown recession determine the progression of crown length over time. We investigated patterns in crown recession of three co-occurring species in the northern Rocky Mountains: western white pine (*Pinus monticola* Dougl. ex D. Don), ponderosa pine (*Pinus ponderosa* Dougl. ex P. & C. Laws.), and interior Douglas-fir (*Pseudotsuga menziesii* (Mirb.) Franco var. *glauca*). Past height, diameter, and crown length on 169 forest-grown trees were reconstructed by detailed stem analysis. Crown length was estimated for each year of the tree's life by dating the mortality of all whorl branches and determining the progression of height to crown base. Five-year crown recession was modeled in two parts, the first predicting the probability that a crown recedes, and the second estimating recession distance conditional on its occurrence. The probability of crown recession increased and then decreased with increasing crown ratio for Douglas-fir, but increased monotonically with crown ratio in western white pine. Both behaviors were observed in ponderosa pine, depending on alternative definitions of crown base. The conditional distance of recession increased monotonically with crown ratio for Douglas-fir and ponderosa pine, but peaked at approximately 0.7 in western white pine. The resulting models have applications for simulating stand development under various silvicultural alternatives and predicting the effect of alternative management regimes on the quality of logs and wood products, architectural aspects of wildlife habitat, fuel distribution, and crown fire hazard.

Sean M. Garber (sean.garber@oregonstate.edu) and **Douglas A. Maguire** are in the Department of Forest Science, Oregon State University, Corvallis, OR 97331, USA. **Robert A. Monserud** (retired) was a research forester and team leader at the Pacific Northwest Research Station, Portland, OR 97205, USA.

Analysis of Within- and Between-Crown Variability for mechanistic crown models

H. Temesgen, A.R. Weiskittel, D.A. Maguire, D.S. Wilson

ABSTRACT

SPECIFIC LEAF AREA (SLA) IS AN IMPORTANT ecophysiological trait variable, but its variability within- and between-crowns has rarely been examined and modeled across multiple species simultaneously. Using extensive datasets on SLA for coastal Douglas-fir [*Pseudotsuga menziesii* var. *menziesii* (Mirb.) Franco], hybrid spruce [*Picea engelmannii* Parry × *Picea glauca* (Moench) Voss × *Picea sitchensis* (Bong.) Carr], and ponderosa pine [*Pinus ponderosa* Dougl. ex P. & C. Laws.], we examined variability of SLA within a canopy and its relationship with tree- and stand-level covariates. In all species, SLA systematically increased from tree tip to crown base and decreased with foliage age class. Cardinal direction did not have a highly significant influence in either Douglas-fir or hybrid spruce, but SLA did significantly decrease from branch tip to bole in hybrid spruce. Tree- and stand-level (e.g. age, density, site index) factors had relatively little influence on SLA. Consequently, a mixed linear model was fitted to estimate SLA at various points in the canopy for each species and foliage age class using absolute height in the canopy and relative vertical height in the tree.

In this presentation, we also provide a hierarchical model that reconstructs within-stand variability of SLA for three important Pacific Northwest conifer species. Given that SLA is strongly correlated with leaf photosynthetic capacity, the model developed in this study can serve as a practical tool for assessing tree-level potential primary production in mechanistic crown models, can help to understand the photosynthetic capacity of the canopy, and refine estimates of key environmental conditions such as site water and radiation balances in mechanistic crown models.

H. Temesgen (hailemariam.temesgen@oregonstate.edu) is an assistant professor, Department of Forest Resources, Oregon State University, Corvallis, OR 97331, USA; **A.R. Weiskittel** is an assistant professor, University of Maine, Orono, ME 04471, USA; **D.A. Maguire** is a professor and **D.S. Wilson** is a research associate, Department of Forest Sciences, Oregon State University, Corvallis, OR 97331, USA.

The Effects of Including a Model of Crown Shyness for Lodgepole Pine (*Pinus contorta* var. *latifolia* [Engl.] Critch.) in a Spatially Explicit Crown Growth Model

James W. Goudie, Kenneth R. Polsson, Peter K. Ott

ABSTRACT

CROWN SHYNESS OR CANOPY DISENGAGEMENT, the phenomenon wherein gaps around trees develop from swaying, whipping, and shading, has been identified in the literature since the 1920s. Recent results by researchers at the University of Alberta have clearly described many of the processes involved for lodgepole pine (e.g. Rudnicki et al. 2001, 2003, 2004; Fish et al. 2006; Meng et al. 2006). Explicit models of crown shyness are in large part lacking in the literature. This paper describes the development of empirical models of crown shyness in lodgepole pine for British Columbia (BC). We measured crown area and neighbor locations on 60 trees growing in 13 stands in central BC. We estimated potential crown area using crown maps, Voronoi polygons, and mixed-model frontier functions; and fit several models that relate observed crown area to various individual tree variables. One of the models was programmed into the Tree and Stand Simulator (TASS, Mitchell 1975) to evaluate the effect of various management scenarios on crown cover and simulated understory light environment.

LITERATURE CITED
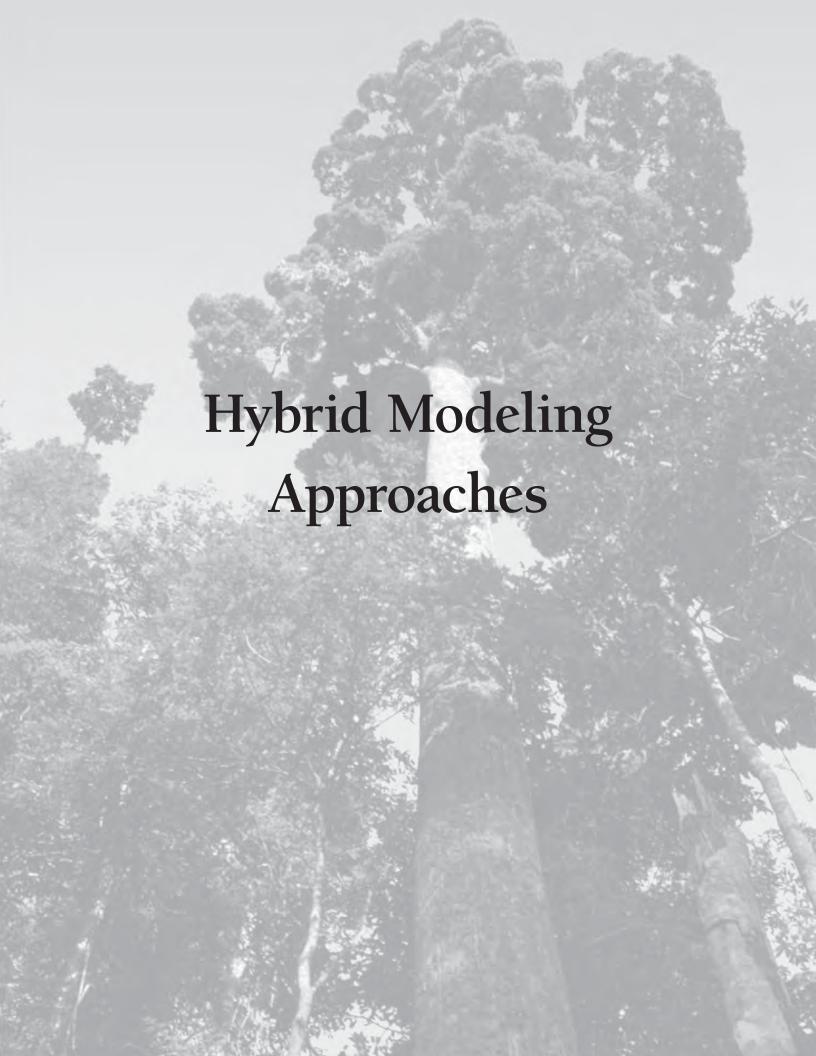
Fish, H.; Lieffers, V.J.; Silins, U.; Hall, R.J. 2006. Crown shyness in lodgepole pine stands of varying stand height, density, and site index in the upper foothills of Alberta. Canadian Journal of Forest Resources. 9:2104-2111.

Meng, S.X.; Rudnicki, M.; Lieffers, V.J. [et al.]. 2006. Preventing crown collisions increases the crown cover and leaf area of maturing lodgepole pine. Journal of Ecology. 94:681–686.

Mitchell, K.J. 1975. Dynamics and simulated yield of Douglas-fir. Forest Science Monographs 17.

Rudnicki, M.; Lieffers, V.J.; Silins, U. 2003. Stand structure governs the crown collisions of lodgepole pine. Canadian Journal of Forest Resources. 33:1238-1244.

Rudnicki, M.; Silins, U.; Lieffers, V.J. 2004. Crown cover is correlated with relative density, tree slenderness, and tree height in lodgepole pine. Forest Science 50:356-363.

Rudnicki, M.; Silins, U.; Lieffers, V.J.; Josi, G. 2001. Measure of simultaneous tree sways and estimation of crown interactions among a group of trees. Trees 15:83-90.

James W. Goudie (jim.goudie@gov.bc.ca), **Kenneth R. Polsson,** and **Peter K. Ott** are scientists in the Research Branch of the BC Ministry of Forests, PO Box 9519, Victoria, BC V8W 9C2, Canada.

Hybrid Modeling Approaches

Hybrid Modeling Approaches
Keynote Presentation

Hybrid Models of Forest Stand Growth and Production

Annikki Mäkelä

ABSTRACT

IN FOREST GROWTH MODELING, the term "hybrid model" is generally used for models that combine process-based elements with empirical elements at the same hierarchical level. Process models usually focus on the physiology of stand production and its dependence on the environment at variable time scales, while empirical models focus on predictions of the marketable product; i.e., the distributions of stems into diameter classes and stem attributes relevant for wood quality, over the stand's rotation. Hybrid models hence aim at utilizing relevant physiological knowledge while simultaneously incorporating inputs and outputs applicable to forest management. The prospect of environmental change has further emphasized the importance of the hybrid approach.

Hybrid models defined in this way may be classified as follows:

1. Models that utilize process elements as submodels to provide additional inputs to empirical growth models. The inputs are often expressed as modifiers of the growth functions developed statistically, including, e.g., intercepted radiation, gross or net photosynthetic production, soil water status, or summary functions derived from full process model simulations (e.g., CanSPBL(water), MELA-FinnFor).

2. "Genuine hybrid models" that derive potential growth from empirical data or functions, modified using a complex system of physiologically-based functions or submodels. This group includes models of the gap model family, and ecosystem models such as FORECAST.

3. Process-driven hybrid models where growth is derived explicitly from carbon acquisition and allocation. Empirical elements relate, e.g., to the allocation of carbon between and within trees, but also to the process of parameterization and calibration of the model as a whole (e.g. 3-PG, PipeStem, PipeQual, TRIPLEX).
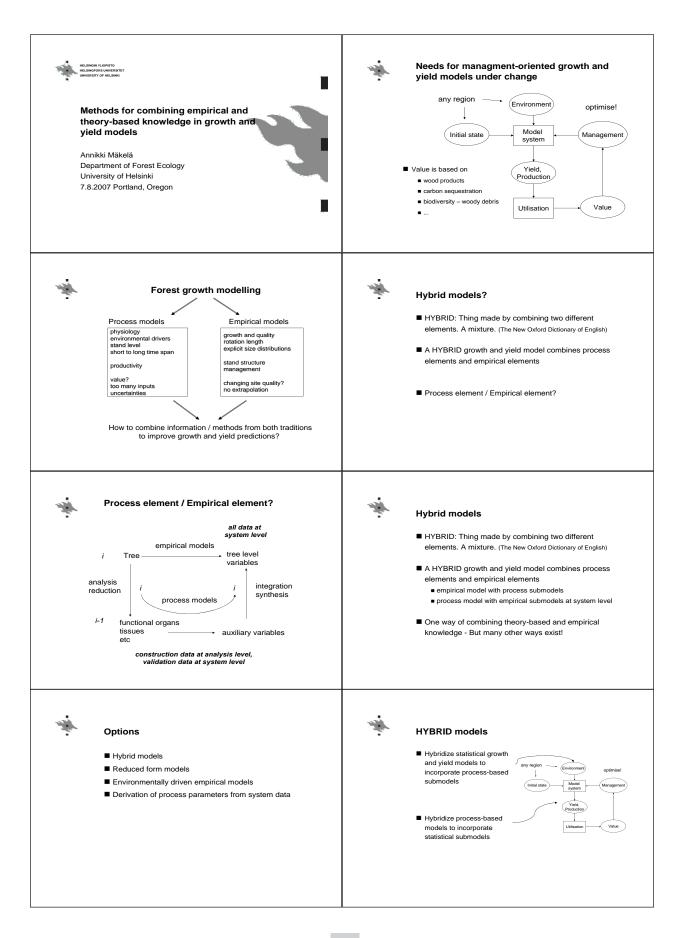
This paper first presents a brief review of hybrid models, their objectives and model building philosophies, and then describes the process-driven hybrid approach in more detail using the PipeQual model as an example. Carbon acquisition in PipeQual is based on canopy photosynthesis and respiration. Size distributions follow from carbon allocation between trees, while the development of tree and stem structure is a result of carbon allocation within trees. The allocation rules are largely based on empirical relationships. The model produces stems with 3D structure as outputs and has already been applied to forest management problems. Finally, an outlook on the challenges and future prospects of developing hybrid models is presented.

KEYWORDS: Growth model, timber products, empirical, process-based, forest management, parameter estimation

Editors' note: The author elected not to provide a full paper for these proceedings because it was being submitted to a refereed journal. As with all of the keynote addresses, this presentation was designed to provide context for the related presentations that follow. In lieu of the keynote paper, the author's slides from the presentation are reproduced on the following pages to introduce the topic for this section of the proceedings.

Annikki Mäkelä (annikki.makela@helsinki.fi) is a professor of silviculture (forest production), Department of Forest Ecology, University of Helsinki, PO Box 27 (Latokartanonkaari 7), 00014 Helsinki, Finland.

HELSINGIN YLIOPISTO
HELSINGFORS UNIVERSITET
UNIVERSITY OF HELSINKI

Methods for combining empirical and theory-based knowledge in growth and yield models

Annikki Mäkelä
Department of Forest Ecology
University of Helsinki
7.8.2007 Portland, Oregon

Needs for managment-oriented growth and yield models under change

any region → Environment   optimise!

Initial state → Model system ← Management

Yield, Production

- Value is based on
  - wood products
  - carbon sequestration
  - biodiversity – woody debris
  - ...

Utilisation → Value

Forest growth modelling

Process models
- physiology
- environmental drivers
- stand level
- short to long time span
- productivity
- value?
- too many inputs
- uncertainties

Empirical models
- growth and quality
- rotation length
- explicit size distributions
- stand structure
- management
- changing site quality?
- no extrapolation

How to combine information / methods from both traditions to improve growth and yield predictions?

Hybrid models?

- HYBRID: Thing made by combining two different elements. A mixture. (The New Oxford Dictionary of English)

- A HYBRID growth and yield model combines process elements and empirical elements

- Process element / Empirical element?

Process element / Empirical element?

all data at system level

i Tree — empirical models → tree level variables

analysis reduction

i process models *i* integration synthesis

i-1 functional organs tissues etc → auxiliary variables

construction data at analysis level, validation data at system level

---

Hybrid models

- HYBRID: Thing made by combining two different elements. A mixture. (The New Oxford Dictionary of English)

- A HYBRID growth and yield model combines process elements and empirical elements
  - empirical model with process submodels
  - process model with empirical submodels at system level

- One way of combining theory-based and empirical knowledge - But many other ways exist!

Options

- Hybrid models
- Reduced form models
- Environmentally driven empirical models
- Derivation of process parameters from system data

HYBRID models

- Hybridize statistical growth and yield models to incorporate process-based submodels

any region → Environment   optimise!
Initial state → Model system ← Management
Yield, Production
Utilisation → Value

- Hybridize process-based models to incorporate statistical submodels

Hybridized statistical growth and yield models: Examples

- METHOD 1: Additional inputs from a mechanistic submodel

- CanSPBL(water) (Pinjuv et al. 2006, For Ecol Manage 236:37-46)
- A water balance model was added as a submodel to an empirical growth model; parameters were fitted accordingly
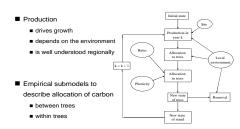
Hybridized statistical growth and yield models: Examples

- METHOD 2: Modifiers of model variables / outputs from a mechanistic submodel

- MOTTI with climate change impacts (Matala et al. 2006, Ecol Mod 199:39-52)
- Relative change in volume growth predicted using FinFor, applied as modifier functions
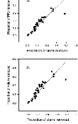
Hybridized process-based growth and yield models

- Production
  - drives growth
  - depends on the environment
  - is well understood regionally

- Empirical submodels to describe allocation of carbon
  - between trees
  - within trees

Hybridized process-based growth and yield models: Examples

- 3-PG (Landsberg and Waring 1997)
  - Assimilation of carbon from a monthly-based model for NPP
  - Mean tree approach
  - Allocation within trees:
    - Empirical submodel based on allometric relationships
  - Allocation between trees (stand structure)
    - Empirical submodel to account for size distributions and their effect on mean size of removed trees

Landsberg et al. Tree Phys 2005

Hybridized process-based growth and yield models: Examples

- PipeQual (Mäkelä and Mäkinen 2003, For Ecol Manage)
- Stand production from a summary model
- Allocation between trees based on shading and photosynthesis
- Competition affects allocation
- Allocation within trees using allometric constraints for structure
- Theoretically-based vs empirical allometries?
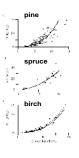
Biological constraints or Empirical submodels? Examples

- Crown allometry:

  $W_F = \xi \, L_C{}^z$
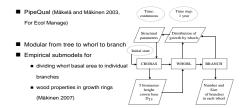
  - empirical model: best fit parameters
  - optimal allocation of wood and foliage under shading, yields $z \approx 2.5$ (Mäkelä & Sievänen 1992)
  - fractal allometry of crown, yields $2 \leq z \leq 3$ (Zeide and Pfeifer 1991)
  - volume filling fractal allometry, yields $z = 3$ (West et al. 1999)

pine

spruce

birch

)3)

Hybridized process-based growth and yield models: Examples

- PipeQual (Mäkelä and Mäkinen 2003, For Ecol Manage)

- Modular from tree to whorl to branch
- Empirical submodels for
  - dividing whorl basal area to individual branches
  - wood properties in growth rings (Mäkinen 2007)
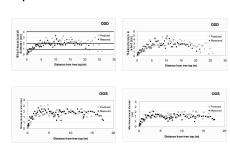
PipeQual: Results from empirical submodels

- Model yields
  - 3D stems
  - wood properties
  - variable environments
  - management options

- Cooperation:
  - Metla, VTT, STFI-Packforsk, INRA, USDA Forest Service

Mäkelä & Mäkinen 2003 For. Ecol.Manage., Mäkelä & Valentine 2006 Ecology; Kantola et al. 2007 For.Ecol.Manage.

PipeQual: Branch Size

Reduced form models

- Motivation:
  - Process models may have too many inputs for practical use
  - Often only few inputs / summarised input combinations relevant for system properties at the scale of interest
  - A reduced model contains the relevant information but is more straight-forward to use and test
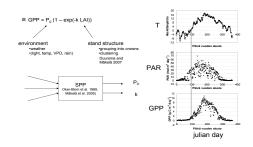
- Method:
  - Reduce model form => number of parameters & inputs
  - computer simulations
  - mathematical derivation
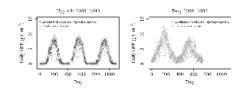
Reduced form models: Examples

- $GPP = P_0 (1 - exp(-k\ LAI))$

environment
- weather
- (light, temp, VPD, rain)

stand structure
- grouping into crowns
- clustering Duursma and Mäkelä 2007

SPP
Oker-Blom et al. 1989,
Mäkelä et al. 2005

P_0
k

T

PAR

GPP

julian day

Hybridized process-based growth and yield models
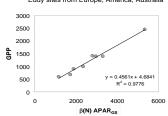
- Example (Mäkelä et al. in press, GCB): Prediction of ecosystem GPP on the basis of daily temperature, radiation, air humidity and LAI across geographic regions and vegetation zones

Reduced form models: Examples

Testing an annual level summary model (in prep.)
Eddy sites from Europe, America, Australia

$y = 0.4561x + 4.6841$
$R^2 = 0.9776$

GPP

$\beta(N)\ APAR_{GS}$

Reduced form models: Examples

- Derivation of diameter and height growth equations from a process-based growth model (PipeStem /CROBAS) (Valentine and Mäkelä 2005, Tree Phys.)

$$\frac{dH}{dt} = g_1(H\quad H_c)\left[\frac{g_2\quad (g_4\quad 1)H_c\quad H}{g_1\quad (g_3\quad 1)H_c\quad H}\right]$$

$$\frac{dH_c}{dt} = s(c)\frac{dH}{dt}\qquad G_{t_2} = G_{t_1}\quad \beta_3\left|L_{t_1,t_2}^2\quad (H_{t_1}\quad H_{2,t_2})^2\right|$$

- Parameters are combinations of metabolic and structural parameters
- Model can be identified from parameter definitions but also by fitting to data on H, H_C and D_{13}
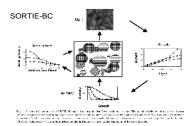
Environmentally driven empirical models

- Empirical growth models for D_{13}, H, etc, with environmental factors as explanatory variables, e.g.

$$\Delta D = \Delta D_{max}\ f_1(T)\ f_2(I)$$

(JaBoWa)

- Objective: to make models easily applicable to different regions and to different local environments

- Often used in individual-based stand models, but
  - no mass balance
  - construction data and validation data at tree level
  - => not process-based / hybrid under present definition
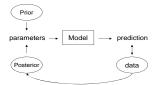
Environmentally sensitive empirical models: Example

SORTIE-BC

Pacala, S.W., Canham, C.D., Silander Jr., J.A., 1993. Can. J. For. Res. 23, 1980–1988.

Derivation of process parameters from system data
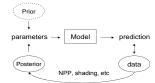
- Fudge factors
- Calibration
- "Inverse problem"
- Bayesian method, Monte Carlo simulation

Derivation of process parameters from system data: Examples

- FORECAST (Kimmins et al. 1999)
  - Objective: Utilise "historical bioassay" in a process model
  - "Hybrid approach" (Kimmins 1999) – but not a hybrid model in strict sense
  - Extreme case of utilising output data for estimating process parameters – "Inverse problem" solution part of programme

Derivation of process parameters from system data: Examples

- Monte Carlo methods to estimate parameters
  - CROBAS (Mäkelä 1988, Scand. J. For Res.)

- Bayesian synthesis to estimate parameters and their uncertainty for process-based models
  - PipeStem (Green et al. 1999. *Forest Science* 45:528-538)
  - Four forest growth models (Van Oijen et al. Tree Phys 25:915–927)

Summary 1/2

- Growth and yield models need
  - environmental inputs
  - outputs relevant for management decisions

- Hybridized empirical models
  - fitted submodels: elaborate transformation of variables
  - modifiers: requires confidence in reference PBM => the same problems as with PBMs in general

- Hybridized process models
  - Carbon balance with constrained allocation a robust alternative

- Reduced form models
  - allow us to utilise process understanding in more easily quantifiable models, more direct link to measurements

Summary 2/2

- Environmentally driven empirical models
  - seems to require more work than (1) conventional empirical or (2) process-based models, but some results may be promising esp. for modelling competition

- Use of system-level data for parameterisation
  - making this procedure systematic is a key to combining empirical data sets with process models for applications
  - could potentially unify modelling and join forces between statisticians and process modellers

- Whatever the strategy, modelling alone will not solve the problems of predicting into an uncertain future – biological experimentation is crucial

Is There a Niche for Hybrid Models?

Margarida Tomé, José Tomé, Paula Soares

ABSTRACT

THE TERM "HYBRID MODEL" HAS BEEN USED for models developed through a combination of process-based and an empirical models. Hybrid models offer practitioners advantages from both model types, including 1) the ability to simulate the effect of intensive silvicultural practices such as irrigation and/or fertilization, 2) sensitivity to climate change (as process-based models), 3) detailed output on stand structure attributes such as diameter distribution or merchantable volume to a given top diameter (as growth and yield models). The use of stand variables as link functions between the two types of models has been proposed by the authors in a previous study. (Tomé et al.2004). In this study, the methodology is further developed and tested with long-term data from permanent plots. Our goal was to combine the whole stand process-based model 3PG with the whole stand model GLOBULUS. One of the objectives of the hybridization process was to guarantee total compatibility between the outputs of the two models. For most sub-models compatibility was achieved through the fitting of new equations. During this hybridization procedure it was found that, in the end, not much was left from the original GLOBULUS model. The result of the hybridization process was actually an improved version of the 3PG model, complemented by new sub-models which guarantee simulations with the type of detailed output traditionally offered by growth and yield models.

Margarida Tomé (magatome@isa.utl.pt), **José Tomé,** and **Paula Soares** are at the Universidade Técnica de Lisboa, Instituto Superior de Agronomia, Centro de Estudos Florestais, Tapada da Ajuda, 1349-017 Lisboa, Portugal.

Development of a Hybrid Model for Intensively Managed Douglas-fir in the Pacific Northwest

Aaron R. Weiskittel, Douglas A. Maguire, Robert A. Monserud

ABSTRACT

Hybrid models offer the opportunity to improve future growth projections by combining advantages of both empirical and process-based modeling approaches. Hybrid models have been constructed in several regions and their performance, relative to a purely empirical approach, has varied. A hybrid model was constructed for intensively managed Douglas-fir plantations in the Pacific Northwest by embedding a hierarchy of components representing fundamental processes (e.g. light interception, photosynthesis, carbon allocation) into a spatially implicit individual-tree model. Simulated processes operated at a variety of scales from individual branches to trees and stands. The resulting hybrid model improved predictions of stand-level leaf area index (10–55 percent mean square error (MSE) reduction) and periodic annual increment (28–49 percent MSE reduction), and reduced the bias of individual-tree growth predictions (3–11 percent MSE reduction) when compared to existing models. These improvements were attributed to a finer resolution of crown structure and dynamics, simple yet mechanistically sound representation of key physiological processes at an appropriate spatial and temporal scale for simulating tree growth, and empirical growth equations that were modified by simulated physiological responses to annual climatic variation and site edaphic characteristics. The probability of individual-tree mortality was predicted equally well as a function of either growth efficiency (stemwood increment per unit leaf area) or conventional tree dimensions and stand density. Overall, the hybrid modeling framework showed significant potential for predicting growth of trees and stands from fundamental processes mediating tree responses to silvicultural treatments.

KEYWORDS: Douglas-fir, hybrid model, plantations growth and yield, intensive management

INTRODUCTION

THE LONG-TERM EFFECTS OF INTENSIVE MANAGEMENT on tree growth and stand yield are difficult to quantify empirically because natural variability necessitates extensive replication. In addition, a thorough understanding of long-term responses to complex treatment regimes requires continuous monitoring over a long period of time and over an entire region (Monserud 2002). Other difficulties are the constant change of intensive silvicultural practices and the relatively high degree of variability in local site conditions (e.g. soil, climate, aspect). Empirical growth and yield models can predict changes in productivity for management regimes represented in the modeling data, but their performance outside the range of data carries varying degrees of uncertainty. Even in regions with adequate data, predicted responses to management can vary dramatically due to choices made about the form of equations, predictor variables to include, and the manner in which equations are assembled into a growth simulator. Johnson (2005) recently found a very wide range (1.3–2.3 fold difference) of predicted responses to standard regimes of thinning,

Aaron R. Weiskittel (aaron.weiskittel@umit.maine.edu) is a forest modeling assistant professor, University of Maine, Orono, ME 04471, USA; **Douglas A. Maguire** is a professor of silviculture, Oregon State University, College of Forestry, Corvallis, OR 97331, USA; **Robert A. Monserud** (retired) was a research forester and team leader, USDA Forest Service PNW Research Station, Portland, OR 97208, USA.

fertilization, and the combination of these treatments among six empirical growth models that are widely available for species in the Pacific Northwest (PNW), USA.

Process-based models have recently found increasing application for decision-making in intensively managed forests (Mäkelä et al. 2000). These models offer the advantage of simulating growth responses to silvicultural treatments by representing some of the key ecophysiological mechanisms driving growth. As a result, they have a much greater capacity for predicting responses to natural and anthropogenic changes in environmental conditions, for example, annual weather fluctuations, changes in nutrient availability, and stand structural influences on environmental conditions. However, a strong theoretical basis does not currently exist for predicting all aspects of tree growth and morphology from fundamental physiology, and the number of parameters that must estimated can sometimes greatly exceed the number allowed in empirical models. The hybridization of empirical and process-based models has been proposed to retain the desirable attributes of both modeling approaches (Landsberg 2003a), while keeping parameter requirements to a minimum. Hybrid models have been successful at improving stand-level growth predictions (Pinjuv et al. 2006, Snowdon 2001, Woollons et al. 1997), but their performance in predicting individual-tree growth has been more varied. Baldwin et al. (2001) found that an individual-tree hybrid model was significantly superior to a purely empirical model for predicting growth of *Pinus taeda* trees in the southeastern USA. In contrast, Henning and Burk (2004) achieved only a moderate improvement in short-term predictions for mixed conifer and deciduous stands in north central USA. This type of modeling approach may be best suited for pure even-aged stands of a fast-growing species (Henning and Burk 2004), but this hypothesis has not been tested. However, it should be pointed out that these specific improvements should be expected as it is not surprising that residual variation around an empirical model can be explained by the use of actual weather information.

The goal of this research project was to compare the performance of existing hybrid models and a newly developed model across a series of several silvicultural trials throughout the PNW. The specific objectives of this study were to (1) develop a hybrid model for intensively managed Douglas-fir stands, (2) compare a variety of approaches for mechanistically simulating individual-tree growth and mortality, and (3) test performance of the model relative to 3-PG and a purely empirical model across a wide range

of intensively managed plantations. Recommendations for future work in refining hybrid models are discussed in the context of simulating Douglas-fir responses to silvicultural treatments and annual weather variation in the PNW.

METHODS

Model development

The modeling approach emphasized a hierarchical treatment of multiscale processes (Mäkelä 2003), with predictions made at the individual branch-, tree-, and stand-levels. The desired features of the model included (1) prediction of annual growth in diameter, height, and crown size of individual trees; (2) characterization of knot size, knot location, crown wood core, and sapwood width as determinants of wood quality; (3) sensitivity to annual climatic variables; (4) representation of soil water availability and its effect on tree growth; (5) representation of nutrient availability and its effect on tree growth; (6) simulation of light interception as influenced by solar geometry and stand density; and (7) prediction of responses to silvicultural regimes through treatment effects on basic ecophysiological processes controlling water and nutrient uptake, carbon assimilation, and carbon allocation. This approach ensured that the model was capable of answering the questions that motivated the modeling effort, i.e., the effect of silvicultural treatments, site conditions, and annual weather on wood yield, wood quality, and tree and stand structure. Likewise, the hybrid structure needed to take advantage of the current state of knowledge at the appropriate scale and offer the flexibility to accommodate future modifications due to improved data availability or physiological modeling. The model is comprised of three primary components: characterization of crown structure (BCACS), estimation of annual net primary production (NPP), and allocation of carbon and growth to different parts of the tree (ALOGRO) (Figure 1). The model is available online at: http://holoros.com/DF.HGS.htm.

Branch, Crown, and Canopy Simulator (BCACS)—
The number, size, and location of branches, as well as the implied size and position of the live crown, determine stem, log, and product quality through their effects on micro-anatomical properties and knottiness of the wood (Bowyer et al. 2002). Branches are also an appropriate level to sample when estimating foliage amount (e.g. Kershaw and Maguire 1995), facilitating estimation of vertical foliage distribution, particularly in coniferous and other species
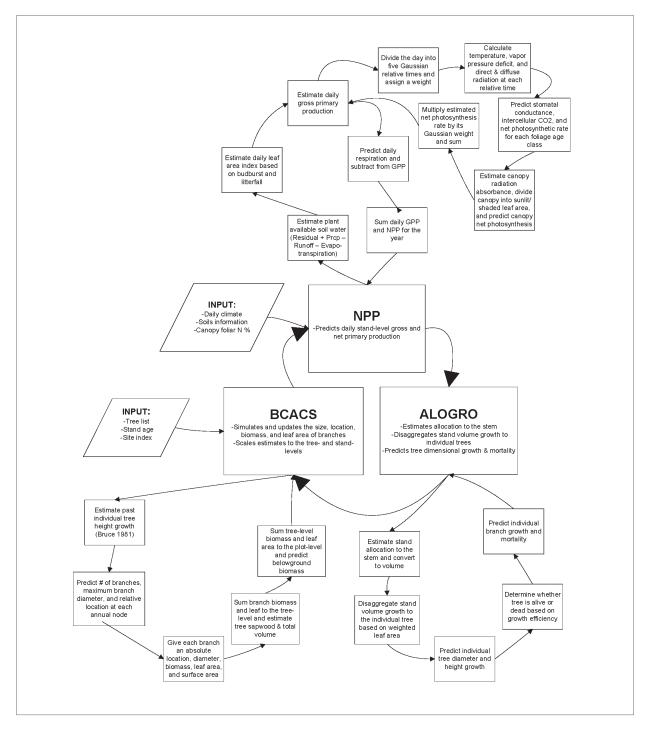
Figure 1. Components of the modeling framework used in this study.

with excurrent form (Garber and Maguire 2005, Maguire and Bennett 1996, Weiskittel et al. 2006). BCACS contains a set of empirical equations that predict the location, diameter, and biomass of every branch on each tree on the sample plot being simulated. The input is a tree list containing diameter at breast height (DBH), height (HT), height to crown base (HCB; lowest live branch), and expansion factor (EXPF, in

trees per ha) as well as estimates of total age and site index (base age 50 years). Past height growth is reconstructed from the dominant height curves developed by Bruce (1981) to determine the location of annual whorls of branches. Branch diameter, length, and angle were predicted following the approach outlined by Maguire et al. (1994), but with the equations developed by Weiskittel et al. (in review). Branch

location was assumed to follow the empirical distribution in Maguire et al. (1994). Woody biomass, woody surface area, foliage biomass, and foliage area of all branches were predicted from basal diameter and relative height in the crown (Weiskittel and Maguire 2006, Weiskittel et al. 2006). These attributes were then summed to estimate biomass and surface area at the tree- and stand-levels.

Total stem and sapwood volume were estimated at the tree-level from existing stem volume and sapwood taper equations (Maguire and Batista 1996, Walters et al. 1985). Volumes were converted to biomass by applying regional values for total and sapwood density (500 and 455 kg m^{-3}, respectively). Belowground biomass at the stand level was estimated from total aboveground biomass assuming the relationship presented by Ranger and Gelhaye (2001). Crown projection areas were calculated from estimated crown widths of individual trees and these areas were then summed to determine percent canopy cover (Crookston and Stage 1999).

Net Primary Production (NPP)—

Previous reviews of process-based models and their components (Grant et al. 2006, Landsberg 2003b, Medlyn et al. 2003, Schwalm and Ek 2001, Wang 2003) have suggested a common list of attributes that future models should possess to accurately capture the effects of silvicultural treatments, climate, and their interaction on NPP. These attributes include (1) daily time-step; (2) separation of direct and diffuse radiation; (3) light extinction coefficients dependent on solar geometry, canopy structure, and type of radiation; (4) separation of sunlit and shaded leaf area; (5) photosynthesis estimates based on the Farquhar et al. (1980) biochemical equation, (6) site slope and aspect effects on diurnal distribution of radiation and fraction of sunlit leaf area (particularly in areas with complex terrain); (7) estimates of stomatal conductance as a function of vapor pressure deficit and soil water availability; and (8) canopy gas exchange linked to soil water and nutrition availability.

All of these desired attributes were incorporated into the NPP submodel, as described below. Inputs were kept as simple as possible to capture the fundamental processes and included (1) daily climate obtained from DAYMET (http://www.daymet.org), (2) site physiographic features (elevation, slope, aspect), (3) stand structural attributes from BCACS (leaf area index (LAI), biomass, canopy cover, etc.), (4) basic soils information (rooting depth, texture, rock content), (5) foliar nitrogen concentration, and (6) physiological parameters obtained from the literature (Ap-

pendix 1). The model runs on daily time-step and estimates gross primary production (GPP) five times daily based on Gaussian integration (e.g. Leuning et al. 1995). The development of the current-year foliage was assumed to occur linearly for 30 days following bud burst, with date of bud burst predicted from a model developed by Thomson and Moncrieff (1982). Annual foliage litterfall and its seasonal distribution were predicted from an empirical equation (Weiskittel and Maguire 2007).

Light interception—

Although highly detailed light interception models exist (e.g. Brunner 1998), they still remain quite computer intensive and too complex for application in management-oriented hybrid models. Further, estimating light interception for an individual-tree crown based on canopy-level principles (e.g. Schwalm and Ek 2004) does not fully account for the competitive position of the tree. Light interception was, therefore, estimated by applying the Beer-Lambert law after accounting for the effects of incomplete canopy closure on the sunlit and shaded portions of the canopy. Mean daily radiation was separated into direct and diffuse components following the approach outlined by Bristow and Campbell (1985), which is based on the ratio of total incoming shortwave radiation to potential shortwave radiation. The amount of direct and diffuse radiation at a given time of the day was estimated from cosine-diurnal distribution following the procedure outlined by Wang et al. (2002), in contrast to the more common approach of assuming a sinusoidal pattern to diurnal radiation. Light extinction coefficients for direct and diffuse radiation were based on the relationships described by Smith (1993) and Campbell and Norman (1998), respectively. The direct radiation extinction coefficient was a function of solar zenith angle, LAI, and stand relative density (Curtis 1982), while the diffuse radiation extinction coefficient was simply a linear function of LAI. Clumpiness was accounted for by an equation presented in Campbell and Norman (1998) that included the ratio of stand mean crown depth to diameter and the solar zenith angle. A penumbra effect was not simulated because any resulting bias from ignoring this effect was expected to be relatively small when the diffuse fraction is high (e.g. Bernier et al. 2001), as is typical in forest canopies of this region.

Photosynthesis—

Net photosynthetic rates were estimated with the Farquhar et al. (1980) model for both sunlit and shaded current-year

foliage. Maximum Rubisco activity (V_{cmax}), electron transport capacity (J_{max}), and dark respiration rate (R_{dark}) were estimated from their relationship to mean canopy concentrations of foliar nitrogen (Manter et al. 2005, Ripullone et al. 2003). These rates were assumed to be the same for both sunlit and shaded foliage. An alternative approach was found to perform better. First, V_{cmax}, J_{max}, and R_{dark} were estimated at an optimum foliar nitrogen concentration from the equations of Manter et al. (2005), net photosynthesis was estimated, and then this rate was multiplied by a modifier that ranged from 0 to 1 and was a nonlinear function of actual foliar nitrogen concentration (Brix 1993). Temperature modifiers for V_{cmax} and J_{max} were obtained from Manter et al. (2003). Other Farquhar et al. (1980) parameters such as CO_2 compensation point in the absence of mitochondrial respiration and the Michaelis-Menten constant of Rubisco were estimated from standard equations. To account for the effects of complex terrain on canopy photosynthesis, sunlit and shaded leaf area were calculated with equation [11] presented by Wang et al. (2002). Foliage age structure is known to influence total photosynthesis in conifer canopies (e.g. Bernier et al. 2001), but actual V_{cmax}, J_{max}, and R_{dark} measurements for age classes older than the current year were not available. Therefore, the net photosynthetic rates for the 1-, 2-, 3-, and ≥4-year-old foliage age classes were assumed to be 75, 50, 30, and 10 percent of the net photosynthetic rates of current year foliage calculated from the Farquhar et al. (1980) equation based on information available in the literature (Ethier et al. 2006, Manter et al. 2003, Woodman 1971).

Water stress effects on canopy photosynthesis are particularly important in the PNW because of high evaporative demand during the warm, dry summer (Waring and Franklin 1979). In a recent review of models for simulating the effect of water stress on canopy photosynthesis, Grant et al. (2006) found approaches ranging from simple scaling factors (Garcia-Quijano and Barros 2005, Kirschbaum 1999) to complex iterative solutions (Williams et al. 1996). Although the impact of stomatal conductance on CO_2 fixation is poorly understood, proper behavior requires interactive effects of soil and atmospheric water deficits on CO_2 fixation (Grant et al. 2006). The simplest approach was to predict stomatal conductance from both soil and atmospheric water deficits. However, the equation developed by Bond and Kavanagh (1999) predicts only mean daily values of stomatal conductance. To estimate conductance throughout the day, the mean daily values were modified by the amount of intercepted radiation and time since sunrise (Livingston and Black 1987). Intercellular CO_2 concentration was then estimated from a theoretical relationship to CO_2 compensation point, atmospheric CO_2 concentration, and root water potential (Katul et al. 2003). One limitation of this approach is the assumption that water deficit effects on CO_2 fixation are entirely stomatal, which is not entirely true (Warren et al. 2004). A better understanding of the relationship between stomatal conductance and leaf internal transfer conductance, and the response of both to environmental conditions, is required before they can be better integrated into models (Warren and Adams 2006).

Respiration—

One key simplification in 3-PG is the assumption that NPP is a constant fraction of GPP (~0.5). This assumption has generated considerable debate in the literature (Lai et al. 2002, Mäkelä and Valentine 2000), but results of several studies have supported the generality of this NPP/GPP fraction across a wide range of forest types (Gifford 2003, Siqueira et al. 2006). Three alternatives to this simplification were tested, including (1) daily respiration as a function of biomass and temperature (Schwalm and Ek 2004), (2) daily respiration as a function of nitrogen content and both a short- and long-term response to temperature (Kirschbaum 1999), and (3) annual respiration as a function of nitrogen content and temperature (Battaglia et al. 2004). Preliminary analysis indicated that estimating NPP as a constant fraction of GPP yielded the strongest correlation with observed stem volume growth.

Soil water and nutrients—

Daily soil water balance was calculated in a manner similar to Schwalm and Ek (2004). Soil water-holding capacity was estimated from rooting depth, texture, and rock content using standard equations (Cosby et al. 1984, Rawls et al. 1992). Daily canopy transpiration and soil evaporation were simulated with modified Penman-Monteith equations as presented in Waring and Schlesinger (1985) and Kirschbaum (1999), respectively. In the canopy transpiration equation, mean daily stomatal conductance was estimated from leaf and soil water potential, leaf to air vapor pressure gradient, and leaf specific conductance (Bond and Kavanagh 1999). Based on the data presented by Tan and Black (1976), canopy conductance was estimated by reducing this mean daily stomatal conductance by 88 percent. In a manner similar to Schwalm and Ek (2004), daily soil water balance was determined by subtracting canopy transpira-

tion and soil evaporation from soil water, and adding daily net precipitation after subtracting interception by canopy leaf and branch surface area. The amount of intercepted precipitation was based on empirical rainfall attenuation in Douglas-fir stands (Keim 2004).

For simplicity, daily nitrogen mineralization was the only aspect of nutrient availability that was simulated in the model. Driving variables included temperature, water content, texture, bulk density, and water-holding capacity of the soil, as well as daily air temperature, rainfall, and solar radiation (Paul et al. 2002). In addition, the mass and height of the litter layer must be known or estimated, as well as the leaf area index and slope. Simulation of daily nitrogen mineralization was achieved by considering the influence of all these factors on the optimum nitrogen mineralization rate estimated from published data (Chappell et al. 1999). Daily soil temperature was calculated from air temperature as modified by the effects of the tree canopy, understory vegetation, litter mass, and depth of the soil layer (Paul et al. 2004). Daily nitrogen uptake was estimated as a function of root nitrogen concentration, soil temperature, and the amount of available soil nitrogen (Thornley 1991).

Allocation and Growth (ALOGRO)

Allocation—
Several reviews on carbon allocation have outlined the myriad of approaches to quantifying the sources of its variability; however, no single solution is yet widely accepted (Barton 2001, Lacointe 2000, Litton et al. 2007). The 3-PG approach of maintaining a fixed NPP/GPP ratio and assuming empirical allometric ratios (Lansberg and Waring, 1997) is robust and provides realistic values; however, the ratio of NPP to GPP is obviously very influential on estimated dry matter productivity, and the allometric ratios available for many, if not most, species are based on empirical relationships in unmanaged stands. Similarly, Mäkelä (1997) maintained a constant ratio of foliage to fine root biomass to reflect an expected functional balance between the two, regardless of growing conditions. Carbon allocation, however, is highly sensitive to intensive management, as well as to inherent site resource availability, particularly belowground (e.g. Keyes and Grier 1981). Allocation conditional on site resource availability was, therefore, initially built into the model. A variety of approaches were examined, including those of Running and Gower (1991), Johnson and Thornely (1987), Kirschbaum (1999), and Landsberg and Waring (1997).

Preliminary analysis, however, suggested that a modified 3-PG approach resulted in the highest correlation between simulated above-ground NPP and observed stem volume growth. The modifications to the 3-PG allocation approach involved estimation of the site fertility rating from canopy N percentage (Swenson et al. 2005) and applying Duursma's and Robinson's (2003) correction for inherent bias when estimating stand-level biomass (or its allocation in this case) from stand-level mean tree size. The site fertility rating estimated the amount of belowground allocation and was predicted with equation [2] of Swenson et al (2005).

Disaggregating stand growth to individual trees—
Disaggregating stand-level projections of growth to individual trees has been widely debated in the empirical growth and yield model literature (e.g. Qin and Cao 2006). Process-based models have generally concentrated at the whole-stand level, so little work has been done on mechanistically disaggregating stand NPP to individual trees. Models such as BALANCE (Grote and Pretzsch 2002) and MAESTRO (Wang 1990) make highly detailed physiological calculations at the individual-tree level, but a simpler approach was desired for this model. Confronted with the same dilemma, Korol et al. (1995) developed an algorithm to disaggregate stand NPP and allocate it to individual trees. Their approach was to divide the canopy into layers of equal leaf area index. Within each layer, individual-tree radiation absorbance was estimated as a function of tree leaf area (Korol et al. 1995). Allocation to each tree was based on the amount of radiation absorbed by that particular tree as well as an adjustment for hydraulic architecture (Korol et al. 1995). Brunner and Nigh (2003) ran extensive simulations with a highly detailed light interception model to simulate individual-tree growth. A regression model was fitted to the data presented in Brunner and Nigh (2003). The final model predicted the mean proportion of incoming light absorbed by an individual crown as a function of its size, relative social position, and stand density. This proportion was then multiplied by the tree leaf area, similar to the weighted leaf areas estimated by Brunner and Nigh (2003). Finally, whole-stand NPP was allocated to each tree based on its proportion of the total stand weighted leaf area. For comparison, disaggregation rules based on each tree's unweighted proportion of stand leaf area and on the purely empirical approach of Zhang et al. (1993) were also tested.

Individual tree dimensions—
Several methods were used to estimate individual tree diameter and height growth based on the portion of net primary production allocated to a tree. These methods included differentiated allometric equations (Kirschbaum 1999, Korol et al. 1996, Zhang and Deying 2003), pipe-model theory (Valentine and Mäkelä 2005), and a transport resistance model (Thornley 1999). Vertical distribution of annual increment along the bole of an individual tree was predicted with an empirical equation similar in form to Ikonen et al. (2006) but re-parameterized for Douglas-fir. For comparison, predictions were also made with purely empirical equations (Weiskittel et al. 2007a) and the following hybridized form of these equations:

[1]

$$\Delta Y_{adj} = \Delta Y_{EMP} * (\beta_{ij} + \beta_{ij} * NPP + \beta_{ij}*ln(NPP)) + \varepsilon_i$$

where ΔY_{adj} is the adjusted growth rate (diameter or height), ΔY_{EMP} is the predicted growth from the empirical equation, the β_{ij}'s are annualized parameters to be estimated from an independent dataset for the jth equation (diameter vs. height). The modifier was not constrained between 0 and 1 because the original empirical equations of Weiskittel et al. (2007a) were developed for plantations that had not received any thinning or fertilization treatments. In this study, they were being applied to plots with a variety of intensive management activities. The modifier was, therefore, expected to be above one for several plots. While Henning and Burk (2004) found no difference in predictions made by an additive versus a multiplicative equation form in their hybrid model, the multiplicative form performed better for Douglas-fir. Presumably this modifier represents the environmental effects and fundamental processes that impact site quality not captured in site index. In addition,

it is a more parsimonious approach because predicting site index as a function of NPP (e.g. Baldwin et al. 2001) required adjustments for stand density and age to ensure proper behavior.

Previous hybrid models have estimated crown recession as a function of crown coverage (e.g. Mäkelä 1997), light availability (Nikinmaa and Hari 1990), or a combination of the two (Valentine and Mäkelä 2005). In this model, crown recession was predicted as the consequence of simulated individual branch dynamics (Weiskittel et al. in review). This approach was shown to perform better than a static height to crown base equation.

Figure 2. Location of Stand Management Cooperative installations in Oregon and Washington used for model verification.

Table 1. Physiographic and soils features of the nine Stand Management Cooperative installations yielding verification data for the Douglas-fir hybrid model.

Stand	Elevation (m)	% Slope	Aspect	Rootable soil depth (m)	% silt in soil	% clay in soil	% rock content in soil
704	182.8	20	270	0.76	35	35	25
705	250.8	30	180	0.76	25	10	30
708	300	5	0	0.64	25	10	35
713	73.4	5	180	0.76	40	20	50
718	102.1	10	180	1.01	55	35	10
722	204.2	10	270	0.66	40	20	20
725	50.9	0	180	0.64	25	10	0
726	27.3	10	225	0.89	55	20	0
736	54.8	40	270	0.61	40	20	35

Mortality—

The literature review by Hawkes (2000) underscored the wide variety of approaches to simulating individual tree mortality. Mortality in ALOGRO was assumed to occur when individual tree growth efficiency (stem biomass increment/tree leaf area) fell below 0.10 kg m^{-2} yr^{-1}. Performance of this approach was compared to that of an empirical model for estimating annual probability of individual tree mortality (Flewelling and Monserud 2002).

Model verification

Study area—

Data from nine Stand Management Cooperative (SMC; University of Washington) installations in Oregon and Washington, USA, comprised the verification and testing dataset (Figure 2). These installations covered a wide range of growing conditions that are typical for the region (Table 1). The overall climate is humid oceanic, with a distinct dry summer and a cool, wet winter. Twenty-year mean annual rainfall for these locations ranged from 150 to 315 cm and January mean minimum temperature and July mean maximum temperature ranged from -2.2 to 3.5°C and 21.3 to 26.3°C, respectively. Variation in precipitation and temperature were strongly related to elevation and distance from the coast. Elevation ranged from 25 to 300 m above sea level and all aspects were represented. Soils varied from a moderately deep sandy loam to a very deep clay loam. The plantations were established between 1971 and 1982 at varying densities (905–1,575 stems per ha) and levels of vegetation control.

Silvicultural regimes—

Several sets of 0.2-ha permanent plots were established by the SMC at each installation between 1986 and 1992.

Since establishment, the 56 plots have received a variety of silvicultural regimes that have involved thinning, pruning, and nitrogen fertilization. Canopy mean plot foliage N concentration ranged from 1.26 to 2.98.

Plot measurements—

All trees on each plot were remeasured for DBH every 4 years. At each remeasurement, a subsample of at least 40 Douglas-fir trees was also measured for total height and height to crown base. Four to eight years after plot establishment, current-year foliage was sampled from the upper crown of 12 trees in each plot, and analyzed for nutrient content.

Model simulations—

The model assembled from BCACS, NPP, and ALOGRO was evaluated by simulating one-sided LAI and growth on each of the 56 SMC plots and comparing the predicted stem volume growth to observed periodic annual increment (PAI; m^3 ha^{-1} yr^{-1}). Since observed LAI was not available, initial LAI of the plots was derived from BCACS and the three following approaches examined by Turner et al. (2000): (1) allometric function of DBH; (2) ratio of leaf area to sapwood area at breast height; and (3) ratio of leaf area to sapwood area at crown base. Although this assumes that PAI is a good proxy of LAI, this is a valid assumption in Douglas-fir as a previous analysis has found a highly linear relationship between LAI and PAI across a range of LAI values (Schroeder et al. 1982). Given the uncertainty in carbon allocation patterns, the correlation between predicted NPP and PAI was also examined to indicate the relative magnitude of estimation error that may be attributable to inaccuracy in estimating NPP vs. allocation of NPP to stemwood production. The same plots were also simulated in 3-PG (Landsberg and Waring 1997) and SECRETS-3PG (Sampson et al. 2006)

Table 2. Mean bias, mean square error (MSE), and r-square (r^2) for observed and predicted stand-level periodic annual increment (PAI; m^3 ha^{-1}) on 67 intensively managed Douglas-fir Stand Management Cooperative plots in Oregon and Washington. Predicted PAI was obtained using 4 foliage biomass imputation methods and 3 net primary production models (NPP).

| | Method used for estimating foliage biomass | | | | | | | | | | | |
| | Gholz et al. (1979) | | | BHSAP[1] | | | CBSAP[2] | | | BCACS[3] | | |
NPP Model	Mean Bias	MSE	R^2	Mean Bias	MSE	R^2	Mean Bias	MSE	R^2	Mean Bias	MSE	R^2
This study	6.2544	6.5197	0.60	3.4189	4.5839	0.50	1.7941	3.2703	0.76	0.8078	2.9405	0.67
3-PG[4]	3.1803	4.2468	0.70	2.4066	4.0809	0.71	1.8146	4.1833	0.38	-1.5117	4.1166	0.24
SECRETS 3-PG[5]	-	-	-	-	-	-	-	-	-	1.03475	5.7273	0.32

1. constant amount of leaf area per unit of predicted sapwood area at breast height (Turner et al., 2000)
2. constant amount of leaf area per unit of predicted sapwood area at crown base (Turner et al., 2000)
3. Branch, Crown, And Canopy Simulator (this study)
4. Landsberg and Waring (1997)
5. Sampson et al. (2006)

after parameterizing for Douglas-fir with information presented by Waring and McDowell (2002). To estimate soil fertility index for 3-PG and SECRETS-3PG, the measured soil nitrogen percentage was converted to nitrogen content based on soil depth and estimated bulk density (Kaur et al. 2002). This value for total nitrogen was then converted to the soil fertility index with the equation developed by Swenson et al. (2005). Climate information for the growth periods represented on the SMC plots was obtained from DAYMET (http://www.daymet.org).
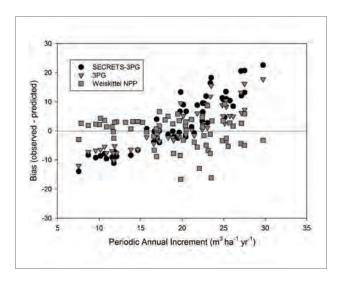
Figure 3. Plot of model bias (observed – predicted) over observed periodic annual increment.
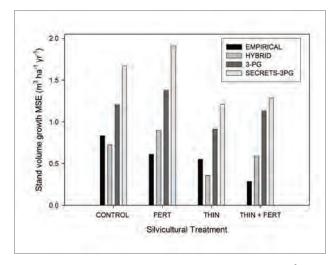
Figure 4. Mean square error of predicted 4-year volume growth (m^3 ha yr^{-1}) by silvicultural treatment. The four models used were an empirical one (Weiskittel et al., 2007), the hybrid model developed in this study, 3-PG (Landsberg and Waring, 1997), and SECRETS-3PG (Sampson et al., 2006).

RESULTS

Stand-level growth—

All four methods for estimating LAI led to simulated stem volume increments that were significantly correlated with observed PAI (p<0.0001). The relative strengths of these correlations, in descending order, were associated with LAI from the following (1) sapwood area at crown base (r=0.81; CBSAP), (2) regional allometric equation based on diameter at breast height (r=0.79, Gholz et al. 1979), (3) sapwood area at breast height (r=0.78; BHSAP), and (4) summed branch predictions from BCACS (r=0.75).

Comparison of observed PAI and simulated stem volume increments indicated that LAI predicted from BCACS resulted in the lowest mean bias and lowest mean square error, followed closely by CBSAP (Table 2). The NPP algorithm described in this study performed significantly better than 3-PG when LAI was estimated by BCACS and CBSAP, but the reverse was true when LAI was estimated by either BHSAP or the regional allometric equation (Figure 3).

Across the silvicultural treatments, the hybrid model developed in this study improved predictions of volume growth in the control and thinned stands, but led to poorer predictions in both the fertilized and the fertilized and thinned stands (Figure 4). The predictions were significantly better than those obtained using 3-PG and SECRETS-3PG across all treatments.

Tree-level growth—

Observed volume growth was significantly correlated with predicted volume growth under all four disaggregation methods. The relative strengths of these correlations, in descending order, were associated with disaggregation by (1) weighted tree leaf area (p<0.0001; r=0.73), (2) tree leaf area (p<0.0001; r=0.62), (3) competition index (Korol et al. 1995) (p<0.0001; r=0.49), and (4) empirical allocation (Zhang et al. 1993) (p<0.0001; r=0.46). The level of bias from predicting diameter and height growth by the first three approaches was higher than that from a purely empirical approach. However, the hybrid approach developed in this study produced a level of bias comparable to the empirical approach, in large part due to its empirical basis (Table 3). The hybrid model predictions modified empirical estimates as follows:

[2]

$$\Delta DBH_{adj} = \Delta DBH_{EMP} * (0.4078 + 0.1846*\ln(NPP))$$
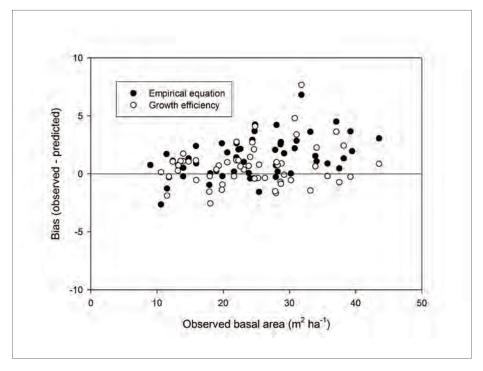
Figure 5. Bias (observed – predicted) in stand basal area (m² ha⁻¹) on 56 Stand Management Cooperative plots with varying levels of silvicultural treatments located throughout the Pacific Northwest, USA after 4 years of simulation using an empirical mortality equation and the growth efficiency concept.

[3]

$$\Delta HT_{adj} = \Delta HT_{EMP} * (0.5192 + 0.2133*NPP$$

$$- 0.0200*ln(NPP))$$

where ΔDBH_{EMP} and ΔHT_{EMP} are predicted diameter and height growth using the equations of Weiskittel et al. (2007a). The equations suggest that the diameter growth modifier linearly increased with NPP and ranged from 0.41 to 1.05. The height growth modifier linearly in-

creased up to a NPP of 10 t ha⁻¹ and then slowly decreased. These modifiers decreased the mean square error of diameter and height growth prediction by 3 and 12 percent, respectively. Tree mortality, imposed when growth efficiency fell below the threshold, produced final stand basal areas that were comparable to predictions produced with an empirical mortality equation (Figure 5). However, both approaches underpredicted mortality in stands with higher densities.

DISCUSSION

The goal of this project was to develop the framework for a hybrid model by incorporating features from both empirical and process-based models. These features were selected based on their potential to enhance the capacity of the model to simulate responses to both intensive silvicultural treatments and variations in environmental conditions. Most of the parameters were gleaned from the literature, and the framework was intended to be useful to both researchers and forest managers. The framework also needed to be flexible enough to accommodate improvements in modeling techniques and the increasing availability of physiological data. Although 3-PG is a simple and very effective model for simulating

Table 3. Mean bias, mean square error (MSE), and percent (%) bias for individual tree predictions of diameter and height growth on 56 Stand Management Cooperative plots with varying levels of silvicultural treatments located throughout the Pacific Northwest, USA.

Approach	DBH (n = 8860)			HT (n = 2805)		
	Mean bias	MSE	% bias	Mean bias	MSE	% bias
1. Empirical (Weiskittel et al., 2007)	-0.01	1.22	-0.61	-0.56	0.96	-3.76
2. Allometric (Kirschbaum, 1999)	1.24	1.63	4.97	-0.42	1.30	-3.87
3. Pipe-model (Valentine and Mäkelä, 2005)	3.07	3.25	13.04	-2.52	3.43	-19.78
4. Thornley (1999)	-3.75	3.91	-20.63	-0.06	1.28	-1.41
5. Hybrid	0.53	1.18	1.99	0.15	0.85	1.04

stand-level growth (e.g. Pinjuv et al. 2006), its reliance on the radiation-use efficiency concept and environmental 0-1 modifiers limit the model's capacity to clarify the role of important processes (e.g. nutrient uptake, interaction of water availability and photosynthesis). A more explicit treatment of those processes facilitates future refinements and assessment. The framework developed here for Douglas-fir resembles many first-generation process-based models (reviewed by Ryan et al. 1996), but with some important refinements, including (1) hierarchical treatment of growth at branch, tree and stand levels, (2) explicit representation of crown structure and function to drive growth processes, (3) incorporation of slope and aspect effects on canopy processes, (4) clear connection between water stress and reductions in photosynthesis, (5) patterns in light extinction that depend on stand structure, (6) net photosynthesis rates specific to foliage age classes, (7) prediction of tree mortality based on a threshold of growth efficiency, and (8) initiation from readily available information rather than from subjective but very influential parameters or detailed and expensive physiological measurements.

The simulation results from the Douglas-fir hybrid model illustrated three important points regarding mechanistic hybrid models, namely (1) their performance is sensitive and quite dependent on initial LAI estimates, (2) models with more detail and finer resolution can significantly increase the precision of growth predictions, and (3) a generic modeling approach that works in a variety of geographic regions is difficult to develop satisfactorily. Process-based models usually require information on tree and stand biomass components other than the main stem, but estimating these components is usually not straightforward. Different methods for estimating LAI in Douglas-fir stands gave generally similar results for younger stands, but differed significantly in the older stands (Turner et al. 2000). However, neither actual LAI nor the effects of intensive management were known or considered in the analysis of these methods. Allometric equations based only on DBH were significantly biased in young fertilized Douglas-fir plantations (Grier et al. 1984). Actual LAI was unknown in our study also, but the degree of bias in the growth projections suggested that LAI estimated from crown size and location was superior to LAI estimated solely from DBH. This conclusion was not surprising given that most silvicultural treatments directly affect crown attributes (Weiskittel et al. 2007b).

With accurate estimates of LAI, the NPP model used in the Douglas-fir hybrid model had a much lower level of bias

in its growth predictions than 3-PG and SECRETS-3PG. Given the range of stand structures and silvicultural treatments simulated in this study, 3-PG performed remarkably well, although it was slightly biased. Since the carbon allocation algorithms were quite similar in both models, the differences appear to be driven by the estimates of NPP. The Douglas-fir hybrid model of this study also benefited from the mean tree correction factor developed by Duursma and Robinson (2003). NPP predicted with 3-PG covered a very narrow range compared to the hybrid Douglas-fir model. When LAI is relatively high (greater than 5) nearly 95 percent of all incoming radiation is intercepted and the radiation use efficiency (RUE) concept becomes harder to apply. Moreover, the relationship between intercepted radiation and NPP becomes less clear when stands have significant water stress (e.g. Raison and Myers 1992), a condition routinely experienced by most Pacific Northwest plantations during the summer months. This prevalence of water limitation underscores the need to properly simulate the effects of soil and atmospheric water deficits on CO_2 fixation. Scalars that vary from zero to one in 3-PG and SECRETS-3PG are insufficiently flexible to capture net effect of daily water relations (Grant et al. 2006). Finally, RUE treats direct and diffuse radiation in the same way, despite the fact that canopy processes behave differently under direct versus diffuse conditions. Schwalm et al. (2006) suggested that the ratio of diffuse to total photosynthetically active radiation (PAR) was a key predictor of the daily RUE across a variety of climate zones and vegetation types.

Unfortunately, many of the shortcomings of this Douglas-fir hybrid model are similar to those found by Ryan et al. (1996) in his assessment of several first-generation process-based models. Missing or poorly represented components include long-term controls on nitrogen mineralization, the uptake and allocation of nitrogen by plants, and the response of belowground allocation and respiration to changes in resource availability. Both CenW (Kirschbaum 1999) and C&N-CLASS (Arain et al. 2006) address many of the difficulties in modeling soil nutrient dynamics, but the level of input on soil nitrogen and carbon stores required by these models significantly limits their wide application by forest managers. Predictions of nitrogen mineralization and uptake in the hybrid model were simple and mechanistically sound, but its performance against observed responses could not be tested. Future refinements to this nutrient availability component and better representation of belowground processes in general will be needed in order to develop a

hybrid model capable of simulating responses to intensive nutrient management.

Adding detail and complexity to improve accuracy when modeling key physiological processes is not always a justified solution. Respiration calculated under the Waring et al. (1998) assumption that NPP is a constant fraction of GPP produced the strongest correlation between NPP and observed stem volume growth. This simplification remains controversial (e.g. Litton et al. in review, e.g. Mäkelä and Valentine 2000). However, it is difficult to separate the effect of NPP/GPP assumptions from their interaction with the many other model components. Another important simplification in this hybrid model was estimation of the soil water balance, which was simulated with a single-layer tipping bucket approach (Schwalm and Ek 2004). More complex approaches have been developed (Kirschbaum 1999, Paul et al. 2003) but their performance compared to simpler approaches has rarely been assessed. A relatively simple soil water balance model developed by Rötzer (2004) was compared to the performance of a more complex model presented by Grote and Pretzsch (2002), and the simpler model was found to be equally effective at predicting observed daily soil water balance (T. Rötzer, per. comm.). This result suggests that the simpler approach is adequate for most practical applications, particularly when detailed information on soil water dynamics is not needed. A major function of future hybrid modeling efforts will be to find the right balance between complexity and simplicity that meets the objectives of the simulation model.

Current understanding of the key factors driving carbon allocation, dynamics of tree morphology, and mortality of individual trees is lacking. The carbon allocation approaches of many process-based models are built on the assumption that priorities exist for the products of photosynthesis (Kirschbaum 1999, McMurtrie and Landsberg 1992, Running and Gower 1991). However, recent empirical evidence does not support the existence of such priorities (Litton et al. in review). Further, it is commonly assumed that allocation to fine roots is driven by resource availability (Keyes and Grier 1981). However, several studies have concluded that site fertility and fertilization have no effect on carbon allocation to fine roots (e.g. Carter et al. 2004), and sometimes even the opposite effect of what is generally reported; namely, greater allocation under conditions of lower fertility (Majdi and Andersson 2005). Dean (2001) suggested that stand structure and its apparent influence on stem bending stress may drive belowground allocation

processes, but the data to test this in Douglas-fir do not exist. New non-destructive research techniques may allow belowground allocation processes to be better quantified in the future (e.g. Johnsen et al. 2007).

Very few studies have linked the dynamics of tree morphology with individual tree net primary production. In this study, diameter growth was much more difficult to accurately predict than height growth. The increment in cross-sectional area of the tree bole has commonly been assumed to be proportional to the leaf area above a given height, implying that increment is constant below crown base (Mäkelä 2002). However, empirical evidence has suggested a much more complex pattern along the bole (e.g. Kershaw and Maguire 2000). Thornley (1999) linked diameter and height growth to carbon and nitrogen fluxes based on theoretical principles, but this approach performed poorly when predicting diameter growth for Douglas-fir. However, the relatively simple treatment of carbon and nitrogen dynamics in the model of this study may have been inadequate to accommodate Thornley's (1999) approach. The Douglas-fir hybrid model circumvents this with empirically derived modifier functions that may not extrapolate well to new conditions. This approach does, however, increase the flexibility of the empirical equations by allowing them to be modified by factors such as climate, soil, and edaphic characteristics, which all directly influence NPP. The modifiers suggest that individual tree diameter growth logarithmically increases with NPP, while height growth peaks at a relatively low NPP and then decreases. This pattern is consistent with the general observations that diameter growth allocation is increased when conditions are favorable (e.g. fertilization, thinning) and height growth allocation is increased when conditions are less favorable (e.g. high competition). The decrease in the height growth modifier is unexpected, but may suggest that the empirical equation overestimates growth at more productive sites.

The performance of hybrid models relative to purely empirical models has varied. Pinjuv et al. (2006), moving to a hybrid model, reduced mean square error of predicting stand basal area by approximately 4 percent. Dzierzon and Mason (2006), using hybrid models, achieved reductions of 14 and 8 percent, respectively, for stand basal area and top height growth across *Pinus radiata* plantations in New Zealand. At the individual tree level, using a hybrid model, Schwalm and Ek (2004) had a level of bias comparable to an empirical model when predicting diameter growth over a 25-yr. However, the hybrid model significantly improved

mean prediction error for height growth. Henning and Burk (2004) showed that a hybrid model did not improve mean square error of predicted diameter growth when compared to an empirical model, but it did significantly decrease the mean bias by nearly 50 percent. Although they did not compare performance directly to an empirical model, Rötzer et al. (2005) simulated diameter growth with the hybrid model BALANCE and obtained discrepancies of 1 to 23 percent from actual diameters after 7–8 years of simulation. The Douglas-fir hybrid model gave results similar to Schwalm and Ek (2004), with a level of bias in diameter growth comparable to the empirical model, but with significantly improved height growth predictions. Again, it is important to mention that these reported improvements with the use of hybrid models should be expected given that they utilized information (i.e. observed weather records) not used by their empirical counterparts. A real test of a hybrid model should be how well it performs over key variables such as precipitation, soil properties, and foliar N levels.

Neither empirical nor process-based models have found a totally satisfying approach to predicting individual tree mortality with the desired level of accuracy (Hawkes 2000). In hybrid models, mortality has been predicted using (1) a minimum crown ratio (Valentine and Mäkelä 2005), (2) an increasing function of crown coverage (Mäkelä 1997), (3) empirical functions of tree size (Schwalm and Ek 2004), and (4) carbon-based algorithms. Despite their appealing mechanistic basis, carbon-based algorithms have not performed well (Hawkes 2000). Mäkelä and Hari (1986) found that their mechanistic approach to mortality generated a decline in accuracy when compared to empirical approaches. Running (1994) indicated that FOREST-BGC should not be run longer than 100 years because mortality predictions became too unrealistic. The major obstacles to a carbon balance approach are probably the difficulty in accurately estimating respiration and uncertainty about the tree's ability to store reserves. In the Douglas-fir hybrid model, a growth efficiency threshold performed comparably to an empirical model for predicting probability of mortality, at least in the short-term. The growth efficiency threshold has several advantages: (1) thresholds may be less site- or species-specific than other approaches, (2) low growth efficiency is a sign of a stressed tree, (3) growth efficiency inherently reflects climatic variation, and (4) growth efficiency declines with age so size and age do not have to be explicitly included as predictors (Hawkes 2000). The growth efficiency approach showed promise in the Douglas-fir hybrid model, but as

with the empirical equation, it underpredicted mortality at the higher stand densities. The increased availability of intensively managed Douglas-fir plantation growth and yield data with estimates of individual tree leaf area from Light Detection and Ranging (LiDAR) in the upcoming years will allow further assessment of this approach for predicting long-term trends in mortality.

Although growth projections are similar to those of a purely empirical model, the hybrid model developed in this study provides information on stand attributes beyond just growth and mortality. For example, the major aspects of wood quality such as branch number, size, and location as well as bole sapwood and heartwood content are readily available. Future improvements for this model at the individual tree level will be the result of (1) developing growth modifiers from annual growth measurements on destructively sampled stems rather than by annualizing growth from periodic plot remeasurements; (2) better representing the effects of climate and site edaphic characteristics on tree ring characteristics (e.g. Deckmyn et al. 2006), particularly density, thereby refining the conversion of stem biomass increment to volume increment; and (3) further quantifying the relationship between tree growth efficiency and its probability of mortality.

CONCLUSIONS

Hybrid models, which combine the features of empirical and process-based models, have been suggested as the next step forward for improving growth projections for managed stands (e.g. Landsberg 2003b). The hybrid modeling framework combines the strengths of both empirical and process-based models. The hybrid model constructed here for intensively managed Douglas-fir plantations in the Pacific Northwest significantly improved predictions of LAI and PAI compared to other modeling approaches. At the individual tree-level, disaggregation of NPP and prediction of stem diameter and height growth were improved. In addition, imposing mortality when growth efficiency fell below a threshold value predicted mortality at a level of accuracy comparable to empirical approaches. These improvements resulted directly from (1) more detailed representation of crown structure and dynamics, (2) inclusion of key physiological mechanisms at an appropriate spatial and temporal resolution, and (3) application of empirical equations modified by simulated NPP to predict diameter and height growth of individual trees rather than relying on allometric or theoretical equations. Areas of future improvement for

these types of models include (1) components that simulate the effects of soil water and nutrients on physiological processes, particularly respiration and carbon allocation, in a simple yet mechanistic manner; (2) components that account for the effects of silvicultural treatment and environmental conditions on foliage age class dynamics, so that seasonal variation in LAI and net photosynthesis can be simulated more accurately; and (3) rigorous assessment of the relationship between growth efficiency and probability of individual tree mortality.

ACKNOWLEDGEMENTS

LITERATURE CITED

Arain M.A.; Yuan F.; Black T.A. 2006. Soil-plant nitrogen cycling modulated carbon exchanges in a western temperate conifer forest in Canada. Agricultural and Forest Meteorology 140: 171-192.

Baldwin V.C.; Burkhart H.E.; Westfall J.A.; Peterson K.D. 2001. Linking growth and yield and process models to estimate impact of environmental changes on growth of loblolly pine. Forest Science 47: 77-82.

Barton C. 2001. The role of allocation in modelling NEE. In: Kirschbaum MUF, Mueller R, editors; 2001; Canberra. Cooperative Research Centre for Greenhouse Accounting p43-49.

Battaglia M.; Sands P.; White D.; Mummery D. 2004. CABALA: a linked carbon, water and nitrogen model of forest growth for silvicultural decision support. Forest Ecology and Management 193: 251-282.

Bernier P.Y.; Raulier F.; Stenberg P.; Ung C.H. 2001. Importance of needle age and shoot structure on canopy net photosynthesis of balsam fir (*Abies balsamea*): a spatially inexplicit modeling analysis. Tree Physiology 21: 815-830.

Bond B.J.; Kavanagh K.L. 1999. Stomatal behavior of four woody species in relation to leaf-specific hydraulic conductance and threshold water potential. Tree Physiology 19: 503-510.

Bowyer J.L.; Shmulsky R.; Haygreen J.G. 2002. Forest products and wood science: an introduction, 4th edition. Ames, IA: Iowa State Press.

Bristow K.L.; Campbell G.S. 1985. An equation for separating daily solar irradiation into direct and diffuse components. Agricultural and Forest Meteorology 35: 123-131.

Brix H. 1993. Fertilization and thinning effect on a Douglas-fir ecosystem at Shawnigan Lake: a synthesis of project results. Victoria, British Columbia: Ministry of Forests. FRDA Report 196. 64 p.

Bruce D. 1981. Consistent height-growth and growth-rate estimates for remeasured plots. Forest Science 4: 711-725.

Brunner A. 1998. A light model for spatially explicit forest stand models. Forest Ecology and Management 107: 19-46.

Brunner A.; Nigh G. 2003. Light absorption and bole volume growth of individual Douglas-fir trees. Tree Physiology 20: 323-332.

Campbell G.S.; Norman J.M. 1998. An introduction to environmental biophysics. New York, NY: Springer.

Carter D.C.; Hendricks J.J.; Mitchell R.J.; Pecot S.D. 2004. Fine root carbon allocation and fates in longleaf pine forests. Forest Science 50: 177-187.

Chappell H.N.; Prescott C.E.; Vesterdal L. 1999. Long-term effects of nitrogen fertilization on nitrogen availability in coastal Douglas-fir forest floors. Soil Science Society of America Journal 63: 1448-1454.

Cosby B.J.; Hornberger G.M.; Clapp R.B.; Ginn T.R. 1984. A statistical exploration of the relationships of soil moisture characteristics to the physical properties of soils. Water Resources Management 20: 682-690.

Crookston N.L.; Stage A.R. 1999. Percent canopy cover and stand structure statistics from the Forest Vegetation Simulator. Ogden, UT: USDA Forest Service, Rocky Mountain Research Station. 11 p.

Curtis R.O. 1982. A simple index of stand density for Douglas-fir. Forest Science 28: 92-94.

Dean T.J. 2001. Potential effect of stand structure on belowground allocation. Forest Science 47(1): 69-76.

Deckmyn G.; Evans S.P.; Randle T.J. 2006. Refined pipe theory for mechanistic modeling of wood development. Tree Physiology 26: 703-717.

Duursma R.A.; Robinson A.P. 2003. Bias in the mean tree model as a consequence of Jensens' inequality. Forest Ecology and Management 186: 373-380.

Dzierzon H.; Mason E.G. 2006. Towards a nationwide growth and yield model for radiata pine plantations in New Zealand. Canadian Journal of Forest Research 2533-2543.

Ethier G.J.; Livingston N.J.; Harrison D.L. [et al.]. 2006. Low stomatal and internal conductance to CO_2 versus Rubisco deactivation as determinants of the photosynthetic decline of ageing evergreen leaves. Plant, Cell and Environment 29: 2168-2184.

Farquhar G.D.; von Caemmerer S.; Berry J.A. 1980. A biochemical model of photosynthetic CO_2 assimilation in leaves of C_3 leaves. Planta 149: 78-90.

Flewelling J.W.; Monserud R.A. 2002. Comparing methods for modeling tree mortality. Fort Collins, CO: USDA Forest Service Rocky Mountain Research Station. 169-177 p.

Garber S.M.; Maguire D.A. 2005. The response of vertical foliage distribution to spacing and species composition in mixed conifer stands in central Oregon. Forest Ecology and Management 211: 341-355.

Garcia-Quijano J.F.; Barros A.P. 2005. Incorporating canopy physiology into a hydrological model: photosynthesis, dynamic respiration, and stomatal sensitivity. Ecological Modelling 185: 29-49.

Gholz H.L.; Grier C.C.; Campbell A.G.; Brown A.T. 1979. Equations for estimating biomass and leaf area of plants in the Pacific Northwest. Corvallis, OR: Oregon State University Forest Research Laboratory. Research paper 41.

Gifford R.M. 2003. Plant respiration in productivity models: conceptualisation, representation and issues for global terrestrial carbon-cycle research. Functional Plant Biology 30: 171-186.

Grant R.F.; Zhang Y.; Yuan F. [et al.]. 2006. Intercomparison of techniques to model water stress effects on CO_2 and energy exchange in temperate and boreal deciduous forests. Ecological Modelling 196: 289-312.

Grier C.C.; Lee K.M.; Archibald R.M. 1984. Effects of urea fertilization on allometric relations in young Douglas-fir trees. Canadian Journal of Forest Research 14: 900-904.

Grote R.; Pretzsch H. 2002. A model for individual tree development based on physiological processes. Plant Biology 4: 167-180.

Hawkes C. 2000. Woody plant algorithms: description, problems, and progress. Ecological Modelling 126: 225-248.

Henning J.G.; Burk T.E. 2004. Improving growth and yield estimates with a process model derived growth index. Canadian Journal of Forest Research 34: 1274-1282.

Ikonen V.P.; Kellomäki P.; Väisänen H.; Peltola H. 2006. Modelling the distribution of diameter growth along the stem in Scots pine. Trees 20: 391-402.

Johnsen K.; Maier C.A.; Sanchez P. [et al.]. 2007. Physiological girdling of pine trees via phloem chilling: proof of concept. Plant, Cell and Environment 30: 128-134.

Johnson G.P. 2005. Growth model runoff II. Portland, OR: Growth Model Users Group. 61 p. Available online: www.growthmodel.org.

Johnson I.R.; Thornley J.H.M. 1987. A model of shoot: root partitioning with optimum growth. Annals of Botany 60: 133-142.

Katul G.; Leuning R.; Oren R. 2003. Relationship between plant hydraulic and biochemical properties from a steady-state coupled water and transport model. Plant, Cell and Environment 26: 339-350.

Kaur R.; Kumar S.; Gurung H.P. 2002. A pedo-transfer function (PTF) for estimating soil bulk density from basic soil data and its comparison with existing PTFs. Australian Journal of Soils Research 40: 847-857.

Keim R.F. 2004. Attenuation of rainfall by forest

canopies. Corvallis, OR: College of Forestry, Oregon State University. 150 p.

Kershaw J.A.; Maguire D.A. 1995. Crown structure in western hemlock, Douglas-fir, and grand fir in western Washington: trends in branch-level mass and leaf area. Canadian Journal of Forest Research 25: 1897-1912.

Kershaw J.A.; Maguire D.A. 2000. Influence of vertical foliage structure on the distribution of stem cross-sectional area increment in western hemlock and balsam fir. Forest Science 46: 86-94.

Keyes M.R.; Grier C.C. 1981. Above- and below-ground net primary production in 40-year old Douglas-fir stands on low and high productivity sites. Canadian Journal of Forest Research 11: 599-605.

Kirschbaum M.U.F. 1999. CenW, a forest growth model with linked carbon, energy, nutrient and water cycles. Ecological Modelling 181: 17-59.

Korol R.L.; Milner K.S.; Running S.W. 1996. Testing a mechanistic model for predicting stand and tree growth. Forest Science 42: 139-153.

Korol R.L.; Running S.W.; Milner K.S. 1995. Incorporating intertree competition into an ecosystem model. Canadian Journal of Forest Research 25: 413-424.

Lacointe A. 2000. Carbon allocation among tree organs: A review of basis processes and representation in functional-structural tree models. Annals of Forest Science 57: 521-533.

Lai C.T.; Katul G.; Butnor J. [et al.]. 2002. Modelling the limits on the response of net carbon exchange to fertilization in a south-eastern pine forest. Plant, Cell and Environment 25: 1095-1119.

Landsberg J. 2003a. Modelling forest ecosystems: state of the art, challenges, and future directions. Canadian Journal of Forest Research 33: 385-397.

Landsberg J. 2003b. Physiology in forest models: history and the future. Forest Biometry, Modelling and Information Sciences 1: 49-63.

Landsberg J.J.; Waring R.H. 1997. A generalized model of forest productivity using simplified concepts

of radiation use efficiency, carbon balance and partitioning. Forest Ecology and Management 95: 209-228.

Leuning R.; Kelliher F.M.; DePury D.G.G.; Schulze E.D. 1995. Leaf nitrogen, photosynthesis, conductance, and transpiration: scaling from leaves to canopies. Plant, Cell and Environment 18: 1183-1200.

Litton C.M.; Ryan M.G.; Raich J.W. 2007. Carbon allocation in forest ecosystems. Global Change Biology: in press.

Litton C.M.; Ryan M.G.; Raich J.W. in review. Carbon allocation in forest ecosystems. submitted to Global Change Biology.

Livingston N.J.; Black T.A. 1987. Stomatal characteristics and transpiration of three species of conifer seedlings planted on a high elevation south-facing clear-cut. Canadian Journal of Forest Research 17: 1273-1282.

Maguire D.A.; Batista J.L.F. 1996. Sapwood taper models and implied sapwood volume and foliage profiles for Coastal Douglas-fir. Canadian Journal Forest Research 26: 849-863.

Maguire D.A.; Bennett W.S. 1996. Patterns in the vertical distribution of foliage in young coastal Douglas-fir. Canadian Journal of Forest Research 26: 1991-2005.

Maguire D.A.; Moeur M.; Bennett W.S. 1994. Models for describing basal diameter and vertical distribution of primary branches in young Douglas-fir. Forest Ecology and Management 63: 23-55.

Majdi H.; Andersson P. 2005. Fine root production and turnover in a Norway spruce stand in northern Sweden: effects of nitrogen and water manipulation. Ecosystems 8: 191-199.

Mäkelä A. 1997. A carbon balance model of growth and self-pruning in trees based on structural relationships. Forest Science 42: 7-24.

Mäkelä A. 2002. Derivation of stem taper from the pipe theory in a carbon balance framework. Tree Physiology 22: 891-905.

Mäkelä A. 2003. Process-based modelling of tree and

stand growth: towards a hierarchical treatment of multiscale processes. Canadian Journal of Forest Research 33: 398-409.

Mäkelä A.; Hari P. 1986. Stand growth model based on carbon uptake and allocation in individual trees. Ecological Modelling 33: 205-229.

Mäkelä A.; Landsberg J.; Ek A.R. [et al.]. 2000. Process-based models for forest ecosystem management: current state of the art and challenges for practical implementation. Tree Physiology 20: 289-298.

Mäkelä A.; Valentine H.T. 2000. The ratio of NPP to GPP: evidence of change over the course of stand development. Tree Physiology 21: 1015-1030.

Manter D.K.; Bond B.J.; Kavanagh K.L. [et al.]. 2003. Modelling the impacts of the foliar pathogen, *Phaeocryptopus gaeumannii*, on Douglas-fir physiology: net canopy carbon assimilation, needle abscission, and growth. Ecological Modelling 164: 211-226.

Manter D.K.; Kavanagh K.; Rose C.L. 2005. Growth response of Douglas-fir seedlings to nitrogen fertilization: importance of Rubisco activation state and respiration rates. Tree Physiology 25: 1015-1021.

McMurtrie R.E.; Landsberg J.J. 1992. Using a simulation model to evaluate the effects of water and nutrients on the growth and carbon partitioning of *Pinus radiata*. Forest Ecology and Management 52: 243-260.

Medlyn B.; Barrett D.; Landsberg J. [et al.]. 2003. Conversion of canopy intercepted radiation to photosynthate: a review of modelling approaches for regional scales. Functional Plant Biology 30(2): 153-169.

Monserud R.A. 2002. Large-scale management experiments in the moist maritime forests of the Pacific Northwest. Landscape and Urban Planning 59: 159-180.

Nikinmaa E.; Hari P. 1990. A simplified carbon partitioning model for Scots pine to address the effects of altered needle longevity and nutrient uptake on stand development. In: Dixon RK, Meldahl GA, Ruark GA, Warren WG, editors. Process modeling of forest

growth responses to environmental stresses. Portland, OR: Timber Press. p 263-270.

Paul K.I.; Polglase P.J.; O'Connell A.M. [et al.]. 2002. Soil nitrogen availability predictor (SNAP): a simple model for predicting mineralisation of nitrogen in forest soils. Australian Journal of Soil Research 40: 1011-1026.

Paul K.I.; Polglase P.J.; O'Connell A.M. [et al.]. 2003. Soil water under forests (SWUF): a model of water flow and soil water content under a range of forest types. Forest Ecology and Management 182: 195-211.

Paul K.I.; Polglase P.J.; Smethurst P.J. [et al.]. 2004. Soil temperature under forests: a simple model for predicting soil temperature under a range of forest types. Agricultural and Forest Meteorology 121: 167-182.

Pinjuv G.; Mason E.G.; Watt M. 2006. Quantitative validation and comparison of a range of forest growth model types. Forest Ecology and Management 236: 37-46.

Qin J.; Cao Q.V. 2006. Using disaggregation to link individual-tree and whole-stand growth models. Canadian Journal of Forest Research 36: 953-960.

Raison R.J.; Myers B.J. 1992. The Biology of Forest Growth experiment: linking water and nitrogen availability to the growth of *Pinus radiata*. Forest Ecology and Management 52: 279-308.

Ranger J.; Gelhaye D. 2001. Belowground biomass and nutrient content in a 47-year-old Douglas-fir plantation. Annals of Forest Science 58: 423-430.

Rawls W.J.; Alhuja L.R.; Brakensiek D.L. 1992. Estimating soil hydraulic properties from soil data. In: van Genucthen M, Leij FJ, Lund LJ, editors. Indirect methods for estimating hydraulic properties of unsaturated soils. Riverside, CA: University of California Riverside Press. p 329-340.

Ripullone F.; Grassi G.; Lauteri M.; Borghetti M. 2003. Photosynthesis-nitrogen relationships: interpretations of different patterns between *Pseudotsuga menziesii* and *Populus x euroamericana* in a mini-stand experiment. Tree Physiology 23: 137-144.

Rötzer T.; Dittmar C.; Elling W. 2004. A model for site specific estimation of the available soil water content and the evapotranspiration in forest ecosystems. Journal of Environmental Hydrology 12: 1-14.

Rötzer T.; Grote R.; Pretzsch H. 2005. Effects of environmental changes on the vitality of forest stands. European Journal of Forest Research 124: 349-362.

Running S.W. 1994. Testing FOREST-BGC ecosystem process simulations across a climatic gradient in Oregon. Ecological Applications 4: 238-247.

Running S.W.; Gower S.T. 1991. FOREST-BGC, a general model of forest ecosystem processes for regional applications. II. Dynamic carbon allocation and nitrogen budgets. Tree Physiology 9: 147-160.

Ryan M.G.; Hunt E.R.; McMurtrie R.E. [et al.]. 1996. Comparing models of ecosystem function for temperate conifer forests. I. Model description and validation. In: Breymeyer AI, Hall DO, Melillo JM, Agren GI, editors. Global change: Effects on coniferous forests and grasslands. New York, NY: John Wiley & Sons. p 313-362.

Sampson D.A.; Waring R.H.; Maier C.A. [et al.]. 2006. Fertilization effects on forest carbon storage and exchange, and net primary production: A new hybrid process model for stand management. Forest Ecology and Management 221: 91-109.

Schroeder P.E.; McCandlish B.; Waring R.H.; Perry D.A. 1982. The relationship of maximum canopy leaf area to forest growth in eastern Washington. Northwest Science 56: 121-130.

Schwalm C.R.; Black T.A.; Amiro B.D. [et al.]. 2006. Photosynthetic light use efficiency of three biomes across an east-west continental-scale transect in Canada. Agricultural and Forest Meteorology 140: 269-286.

Schwalm C.R.; Ek A.R. 2001. Climate change and site: relevant mechanisms and modeling techniques. Forest Ecology and Management 150: 241-257.

Schwalm C.R.; Ek A.R. 2004. A process-based model of forest ecosystems driven by meteorology. Ecological Modelling 179: 317-348.

Siqueira M.B.; Katul G.G.; Sampson D.A. [et al.]. 2006. Multiscale model intercomparisons of CO_2 and H_2O exchange rates in a maturing southeastern US pine forest. Global Change Biology 12: 1189-1207.

Smith N.J. 1993. Estimating leaf area index and light extinction coefficients in stands of Douglas-fir (*Pseudotsuga menziesii*). Canadian Journal Forest Research 23: 317-321.

Snowdon P. 2001. Short-term prediction of growth of *Pinus radiata* with models incorporating indexes of annual climatic variation. Forest Ecology and Management 152: 1-11.

Swenson J.J.; Waring R.H.; Fan W.; Coops N.C. 2005. Predicting site index with a physiologically based growth model across Oregon, USA. Canadian Journal of Forest Research 35: 1697-1707.

Tan C.S.; Black T.A. 1976. Factors affecting the canopy resistance of a Douglas-fir forest. Boundary-Layer Meteorology 10: 475-488.

Thomson A.J.; Moncrieff S.M. 1982. Prediction of bud burst in Douglas-fir by degree-day accumulation. Canadian Journal of Forest Research 12: 448-452.

Thornley J.H.M. 1991. A transport-resistance model of forest growth and partitioning. Annals of Botany 68: 211-226.

Thornley J.H.M. 1999. Modelling stem height and diameter growth in plants. Annals of Botany 84: 195-205.

Turner D.P.; Acker S.A.; Means J.E.; Garman S.L. 2000. Assessing alternative allometric algorithms for estimating leaf area of Douglas-fir trees and stands. Forest Ecology and Management 126: 61-76.

Valentine H.T.; Mäkelä A. 2005. Bridging process-based and empirical approaches to modeling tree growth. Tree Physiology 25: 769-779.

Walters D.K.; Hann D.W.; Clyde M.A. 1985. Equations and tables predicting gross total stem volumes in cubic feet for six major conifers of southwest Oregon. Corvallis, OR: Oregon State University, Forest Research Laboratory. 36 p.

Wang S.; Chen W.; Cihlar J. 2002. New calculation methods of diurnal distribution of solar radiation

and its interception by canopy over complex terrain. Ecological Modelling 155: 191-204.

Wang Y.P. 1990. Description and validation of an array model—MAESTRO. Agricultural and Forest Meteorology 51: 257-280.

Wang Y.P. 2003. A comparison of three different canopy radiation models commonly used in plant modelling. Functional Plant Biology 30: 143-152.

Waring R.H.; Franklin J.F. 1979. Evergreen coniferous forests of the Pacific Northwest. Science 204: 1380-1386.

Waring R.H.; Landsberg J.; Williams M. 1998. Net primary production of forests: a constant fraction of gross primary production? Tree Physiology 18: 120-134.

Waring R.H.; McDowell N. 2002. Use of a physiological process model with forestry yield tables to set limits on annual carbon balances. Tree Physiology 22: 179-188.

Waring R.H.; Schlesinger W.H. 1985. Forest ecosystems: concepts and management. Orlando, FL: Academic Press.

Warren C.R.; Adams M.A. 2006. Internal conductance does not scale with photosynthetic capacity: implications for carbon isotope discrimination and the economics of water and nitrogen use in photosynthesis. Plant, Cell and Environment 29: 192-201.

Warren C.R.; Livingston N.J.; Turpin D.H. 2004. Water stress decreases the transfer conductance of Douglas-fir (*Pseudotsuga menziesii*) seedlings. Tree Physiology 24: 971-979.

Weiskittel A.R.; Garber S.M.; Johnson G.P. [et al.]. 2007a. Annualized diameter and height growth equations for Pacific Northwest plantation-grown Douglas-fir, western hemlock, and red alder. Forest Ecology and Management: in press.

Weiskittel A.R.; Maguire D.A. 2006. Branch surface area and its vertical distribution in coastal Douglas-fir Trees 20: 657-667.

Weiskittel A.R.; Maguire D.A. 2007. Response of Douglas-fir leaf area index and litterfall dynamics to Swiss needle cast in north coastal Oregon, USA. Annals of Forest Science 64: in press.

Weiskittel A.R.; Maguire D.A.; Garber S.M.; Kanaskie A. 2006. Influence of Swiss needle cast on foliage age class structure and vertical distribution in Douglas-fir plantations of north coastal Oregon. Canadian Journal of Forest Research 36: 1497-1508.

Weiskittel A.R.; Maguire D.A.; Garber S.M. [et al.]. in review. Influence of intensive management and stand health on Douglas-fir stem taper. submitted to Forest Ecology and Management.

Weiskittel A.R.; Maguire D.A.; Monserud R.A. 2007b. Modeling crown structural responses to competing vegetation control, thinning, fertilization, and Swiss needle cast in coastal Douglas-fir of the Pacific Northwest, USA. Forest Ecology and Management 245: 96-109.

Williams M.; Rastetter E.B.; Fernandes D.N. [et al.]. 1996. Modelling the soil-plant-atmosphere continuum in a *Quercus-Acer* stand at Harvard Forest: the regulation of stomatal conductance by light, nitrogen and soil/plant hydraulic properties. Plant, Cell and Environment 19: 911-927.

Woodman J.N. 1971. Variation of net photosynthesis within the crown of a large forest-grown conifer. Photosynthetica 5: 50-54.

Woollons R.C.; Snowdon P.; Mitchell N.D. 1997. Augmenting empirical stand projection equations with edaphic and climate variables. Forest Ecology and Management 98: 267-274.

Zhang L.; Moore J.A.; Newberry J.D. 1993. Disaggregating stand volume growth to individual trees. Forest Science 39: 295-308.

Zhang X.; Deying X. 2003. Eco-physiological modelling of canopy photosynthesis and growth of a Chinese fir plantation. Forest Ecology and Management 173: 201-211.

Estimating Natural Regeneration in Stands Following Attack by Mountain Pine Beetle Using a Linked-Model Approach

Derek F. Sattler, Valerie LeMay, Peter Marshall

ABSTRACT

A LINKED-MODELING APPROACH, USING Prognosis[BC] and SORTIE-ND, was tested for predicting natural regeneration and forecasting future stand conditions in stands attacked by mountain pine beetle (*Dendroctonus ponderosae* Hopkins-MPB). The models used data collected from the Interior Douglas-fir (IDF), Sub-Boreal Pine Spruce (SBPS), Sub-Boreal Spruce (SBS) and Montane Spruce (MS) biogeoclimatic zones of central and southeastern British Columbia. Prognosis[BC] is a growth model calibrated for use in complex stands and is capable of providing accurate estimates of small and large tree growth when used over projection periods of less than 50 years. The lack of an effective sub-model capable of predicting the abundance and species composition of natural regeneration for MPB-attacked stands is a major limitation of Prognosis[BC]. Obtaining regeneration estimates from the light mediated growth model SORTIE-ND, was identified as a possible alternative to the Most Similar Neighbor regeneration imputation techniques used by Prognosis[BC]. A method to link estimated tree-lists for trees less than 7.5 cm dbh from SORTIE-ND to Prognosis[BC] was developed. Using a 25-year projection period, the timing of the tree-list hand-off from SORTIE to Prognosis was tested at five and ten years post-MPB attack and compared to simulations using Prognosis[BC] only and SORTIE-ND only for the entire projection period. For spruce and aspen trees less than 7.5 cm dbh, the 10-year hand-off simulation provided the best estimate of trees per hectare when compared to actual observations. For lodgepole pine trees less than 7.5 cm dbh, the 5-year hand-off simulation provided the best results. Although use of the linked-model approach provided slight improvements over using Prognosis[BC] only or SORTIE-ND only, overall results were generally poor. In particular, densities of lodgepole pine were largely underestimated for smaller trees. Further testing using an extensive dataset and further parameterization of the SORTIE-ND model is likely required if improvements are to be seen.

KEYWORDS: natural regeneration, individual tree growth model, Prognosis[BC] and SORTIE-ND, mountain pine beetle

INTRODUCTION

Accurate growth and yield estimates are an important component in the development and implementation of sustainable forest management practices (Boisvenue et al. 2004). Mid- to long-term timber supply estimates rely heavily on growth and yield models (Hyytiainen et al. 2006). In the absence of reliable growth estimates, current allowable annual cut volumes could be inadvertently set too high or too low (Pedersen 2003). In complex forest systems, where

Derek F. Sattler (dsattler@ualberta.ca) is a doctoral student, University of Alberta, Department of Renewable Resources, 751 General Services Building, Edmonton, AB, T6G 2H1, Canada. When this paper was written he was a graduate student at the University of British Columbia. **Valerie LeMay** is a professor, Forest Resource Management Department, Faculty of Forestry, University of British Columbia, 2424 Main Mall, Vancouver, BC, V6T IZ4, Canada; **Peter Marshall**, is a professor and associate dean, Faculty of Forestry, University of British Columbia, 2424 Main Mall, Vancouver, BC, V6T IZ4, Canada.

multi-species and multi-cohort stands form a mosaic pattern across the landscape, model projections of growth and yield for periods greater 50 years can become increasingly unreliable (Zumrawi et al. 2005a). This may, in large part, be attributed to the high variability in stand structure and species composition, which is a result of frequent small scale gap disturbances and less frequent but more extensive disturbances such as fires and insect outbreaks (Oliver and Larson 1996). Added to the mix are the various silvicultural practices (e.g., partial cutting and variable retention) that are currently being employed in these complex stands. Given these conditions few, if any, growth and yield models have been able to excel in both managed and unmanaged stands (Robinson and Monserud 2003). Finding the best management strategies for complex stands continues to be an evolving process (Coates et al. 2004).

Given this complexity, it is not surprising that the province of British Columbia (BC) currently supports eight growth and yield models. This allows foresters to match their specific requirements to an appropriate growth model. One such growth model that is currently being used in complex stands of central and southeastern BC is Prognosis[BC] (Snowdon 1997, Zumrawi et al. 2002, Hassani et al. 2004). Adapted from the U.S. Forest Service Forest Vegetation Simulator (FVS) that was originally developed by Stage (1973), Prognosis[BC] is best suited for projecting existing stands and can simulate a wide range of silvicultural treatments. Although the small tree and large tree growth components of Prognosis[BC] were calibrated to the Interior Douglas-fir (IDF) and Interior Cedar Hemlock (ICH) biogeoclimatic zones, efforts to calibrate the regeneration sub-model did not fare well (Boisvenue 1999, Zumrawi et al. 2005a). Nevertheless, Prognosis[BC] has been able to provide reliable landscape-level estimates of growth for projection periods of 50 years or less; a result of the many permanent sample plots (PSP) that were used to calibrate the model.

In place of the regeneration sub-model, model users currently have two options: 1) specify the amount and composition of natural and/or planted regeneration, or 2) use the most similar neighbour (MSN) regeneration sub-component. The former option limits the use of Prognosis[BC] to short-term projections unless new regeneration lists are added at the end of each growth cycle. The latter approach was designed to impute natural regeneration by predicting several regeneration variables at once (Hassani et al. 2004). To be successful, the MSN approach requires a large amount of data collected from stands with natural regeneration and which have developed under a wide range of ecological conditions (LeMay et al. 2006). Its ability to accurately predict regeneration in under-represented ecological conditions is therefore limited (Moeur and Stage 1995, Hassani et al. 2004). The prevailing ecological conditions of lodgepole pine dominated stands, which have been (and are being) created in BC's interior in the wake of the current outbreak of mountain pine beetle (*Dendroctonus ponderosae* Hopkins-MPB), give one example of where the applicability of the MSN approach is currently limited. The immense magnitude of the current outbreak has created ecological conditions that, until now, were less common and therefore under-represented in most PSP datasets (Hawkes et al. 2004).

Our search for an alternative means of estimating natural regeneration post-MPB attack led us to an existing forest simulation model, SORTIE-ND (Kobe and Coates 1997). This model is an adaptation of the original SORTIE model (Pacala et al. 1993) developed for use in the deciduous forests of northeastern United States (Canham and Burbank 1994). The current SORTIE-ND model (Version 6.07) has been calibrated for use in BC's ICH and Sub-boreal Spruce (SBS) forests using long-term PSP data (Kobe and Coates 1997, Astrup et al. 2007). More recently, efforts to calibrate SORTIE-ND using data from managed stands have made it useful for application in silvicultural planning (Coates et al. 2004). However, our use of SORTIE-ND for this study is motivated by the need for a method to accurately estimate a tree-list comprised of new seedling recruits and advanced regeneration that can be transferred into Prognosis[BC].

In our search for alternative methods we had two main criteria, namely that the method be able to predict multiple dependent variables and be feasible given the plot data available and the data requirements of Prognosis[BC]. SORTIE-ND satisfied both of these conditions (LeMay et al. 2006). A method was then developed to link regeneration estimates from SORTIE-ND to Prognosis[BC]. It was envisaged that using these two models as a linked set would allow us to take advantage of the strengths of each model. In the case of SORTIE-ND, the advantage was related to the model's flexibility and the ability to adjust model parameters related to regeneration establishment, while in the case of Prognosis[BC] we could make use of the well developed, empirically-based small and large tree growth models.

In this paper, we describe the model flow of the linked-model approach and present the results of an initial test

using tree measurements collected from stands that experienced a MPB attack roughly 25 years ago.

METHODS

Study Area

Potential stands for sampling were selected from an area attacked by MPB between the late 1970s and the late 1990s, within approximately 200 km of Williams Lake, BC. Many of the sampled stands were located on the Fraser Plateau, within the former Cariboo Forest Region. This area contains gentle slopes and has an elevation between 900 and 1500 m. There are four major biogeoclimatic ecosystem classification zones in this area: Sub-Boreal Pine-Spruce (SBPS), Sub-Boreal Spruce (SBS), Interior Douglas-fir (IDF), and Mountain Spruce (MS).

Plots were located mainly in stands dominated by lodgepole pine (*Pinus contorta* Dougl. ex Loud. var. *latifolia* Engelm). Overall, species composition in selected stands included lodgepole pine (about 80 percent), Douglas-fir (*Pseudotsuga menziesii* var. *glauca* (Beissn.) Franco) (7 percent), and hybrid spruce (*Picea engelmannii* x *glauca* (Moench) Voss) (5 percent). Trembling aspen (*Populus tremuloides* Michx.) and subalpine-fir (*Abies lasiocarpa* (Hook.) Nutt.) were present, but in small numbers overall.

Historically, outbreaks of MPB have been common within the study area and have served to shape the forested landscape (Aukema et al. 2006). In the absence of stand-replacing fires, regional outbreaks of MPB have served to create gaps in the forest canopy. Depending on stocking levels and the composition of the understory, previous MPB attacks have resulted in either the release of an existing understory or the recruitment of new seedlings (Campbell et al. 2007). In either situation, such events resulted in the creation of uneven-aged, mixed-species stands (Hawkes et al. 2004).

Field Sampling and Data Collection

Candidate stands for sampling were selected following reconnaissance of stands selected from forest inventory maps and anecdotal information provided by local foresters and researchers. Two to six plots were established in each selected stand, depending on the size. Systematic sampling with a random start was used. The distance between each plot center ranged between 50 m and 150 m, with a minimum distance of 50 m from a road or any other significant opening. The plot edges were at least 20 m from any logging areas or skid trails.

A total of 175 plots from 55 stands were sampled. Each plot consisted of seven circular sub-plots: one for large trees (11.28 m radius), another for small trees (5.64 m radius), and five for regeneration (2.07 m radius). In the large tree plot (overstory trees), all trees greater than or equal to 7.5 cm diameter at breast height (dbh) were measured. Each dead standing or downed tree was assigned a decay class based on a nine class scale, created by combining class one to four from the wildlife tree classification (Backhouse and Lousier 1991) and class five to nine from the coarse woody debris classification for downed trees (Stevens 1997). Height to live crown (m) was measured for all live trees. Species, dbh (cm), and height (m) of each standing tree, live or dead, were recorded. For downed trees in decay class seven or greater, species, dbh, and height were recorded. For trees with broken tops, the height to the broken top (m) was measured, and the total height of the tree was estimated. Crown width was measured along two axes at right angles for two trees selected randomly for each species. In the small tree plot, all trees from 2.0 cm to less than 7.5 cm dbh were included and species, dbh, status (live or dead), visual estimate of live crown ratio (live only), and height were recorded for each tree. In the regeneration subplots, the number of live seedlings less than 2.0 cm dbh and over 15 cm in height were recorded by species into four height classes: 1) >0.15 to ≤ 0.50 m; 2) >0.50 to ≤1.0 m; 3) >1.0 to ≤1.5 m; and 4) >1.5 m in height and < 2.0 cm dbh.

Data Preparation

The overstory conditions at each plot shortly after the time of attack were reconstructed using the measures of live and dead trees in the large tree plot. Two time of MPB-attack cohorts were present in the collected data: (1) attack approximately 25 years ago and (2) attack approximately eight years ago. Each live tree was grown back in time by subtracting the estimated 10-year diameter growth (DG), using functions previously fitted by Zumrawi et al. (2005b). For plots that were 25 years post-MPB attack, this process was repeated for three intervals, with the third period prorated at half of the estimated growth rate. Since measures of competition are used in the DG functions, these were summarized for each 10-year interval and used in estimating the DG. For plots that were eight years post-MPB attack, the 10-year DG was prorated for eight years. Once dbh shortly after the attack was estimated for each live tree, heights were estimated from dbh using existing regression equations developed in the process of calibrating Prognosis[BC]. These

were localized for each tree by multiplying by the ratio of measured height to estimated height for the 2006 measures. For standing dead or fallen trees, the decay class was used to decide whether the tree was live or dead shortly after attack. For all trees that were alive at some point after the MPB attack, the crown ratio was estimated using crown ratio functions developed for this area. Ten-year DG was then estimated using the estimated crown ratio. The same process was followed for trees that were alive at the time of sampling. Following these approaches, an estimated tree-list of all live and dead trees greater than or equal to 7.5 cm dbh was obtained for each plot shortly after attack. The tree-list was coupled with the regeneration (less than 7.5 cm dbh) measured in 2006, either eight or 25 years following MPB attack.

Linked Model Approach

The process of linking SORTIE-ND and Prognosis[BC] began by importing tree-lists representing individual stands into each model. The tree-lists imported into the models were from the reconstructed dataset and thus represented stand conditions for the years immediately following MPB attack. Since each model has its own data input specifications, some additional data preparation was required. In the case of SORTIE-ND, for example, imported tree-lists must contain spatial coordinates for each tree. As this type of information was not collected during field sampling, a random number generator algorithm was used to assign coordinates to each tree within a simulated 9 ha plot. Additionally, SORTIE-ND requires the user to provide parameter estimates for the specific model behaviours that have been selected. For this study, we used the collected data to obtain parameter estimates for allometric relationships, including height-diameter relationships and crown dimension relationships. Parameter estimates were also obtained for the SORTIE-ND snag fall-down model, which is used to define the rate at which dead standing trees become downed trees. Lastly, the fraction of the forest floor occupied by different substrates was defined. All other parameters within SORTIE-ND, including light and growth parameters, were obtained from Astrup et al. (2007). Prognosis[BC] did not require any parameterization as it has been calibrated to the study area using permanent sample plots.

For the analyses presented in this report, we restricted our list of potential stands to those stands that were attacked 25 years ago. Thus, the total length of each model projection period was 25 years. Once loaded, the stand-level tree-lists were projected forward in time in each model. For SORTIE-ND, each growth cycle was defined as a single year; while in Prognosis[BC], the initial growth cycle was five years with subsequent cycles operating on a ten year basis. The transfer of tree-list projections from SORTIE-ND to Prognosis[BC] was restricted to five years and ten years following MPB attack, referred to as the five-year hand-off simulation and ten-year hand-off simulation. For the five-year off simulation, a list of trees less than 7.5 cm dbh was obtained from SORTIE at the end of the fifth growth cycle. Since this list represented the number of trees over a simulated 9 ha plot, a value of 0.11 stems per hectare was given to each tree in this list so that it would be compatible with the tree-list requirements of Prognosis[BC]. Trees selected from SORTIE-ND were appended to the tree-list from Prognosis[BC] following the initial five-year growth cycle, replacing any trees less than 7.5 cm dbh that were in the Prognosis[BC] tree-list but retaining all trees greater than 7.5 cm dbh. The new composite tree-list was then projected forward for 20 years using Prognosis[BC]. A similar approach was used for the ten-year hand-off simulation, except that tree-lists following the tenth growth cycle were joined and projected forward in Prognosis[BC] for 15 years.

The results of the five and ten year hand-off simulations were compared to actual values as well as estimated values obtained by using Prognosis[BC] and SORTIE-ND separately over the 25 year projection period. To evaluate the four model simulations, we compared the estimated number of trees per hectare (tph) across the six stands that were tested. Bias, defined here as predicted value minus observed value, was calculated by species group (Pine, Spruce-Aspen) and by dbh size class. Two individual stands, one a low density stand (425 tph) at the time of MPB attack and the other a high density stand (1184 tph), were examined to gauge the effectiveness of the models under different stand densities.

Results

Plot data were summarized to provide initial stand conditions following reconstruction (1981 data), as well as observed 2006 conditions (Table 1). All stands, with the exception of stand 25, had at least a minor component of spruce and/or aspen in the understory. All stands were dominated by lodgepole pine in the overstory. Understory densities at the time immediately following attack ranged from 92 tph to 183 tph, while overstory densities ranged from 267 tph to 883 tph. Compared with recorded obser-
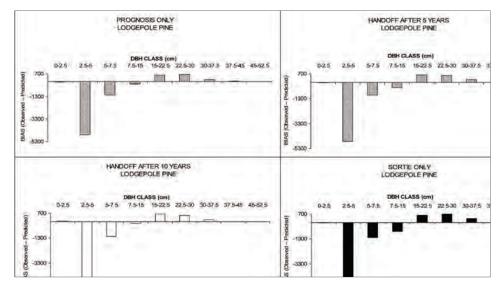
Figure 1—Average biases (predicted-observed) of estimating the number of trees per ha of lodgepole pine across all dbh classes for the four different simulations following a 25-year projection.
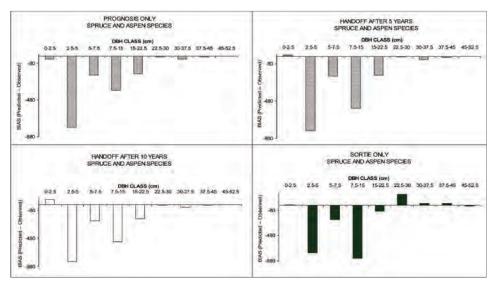
Figure 2—Average biases (predicted-observed) of estimating the number of trees per ha for spruce-aspen across all dbh classes for the four different simulations following a 25-year projection.

Table 1—Reconstructed (1981) and recorded (2006) stand level densities (tph=trees per hectare) by species group and dbh size class for the six tested stands

Year	Stand	No. of plots	Pine < 7.5cm dbh	Pine > 7.5cm dbh	Spruce and Aspen < 7.5cm dbh	Spruce and Aspen > 7.5cm dbh	Total
			(tph)	(tph)	(tph)	(tph)	(tph)
	4	3	58	308	100	83	550
	15	3	150	242	8	25	425
1981	18	3	50	742	150	141	1084
	24	3	91	384	92	167	734
	25	3	167	350	0	83	600
	28	3	67	751	25	42	884
	4	3	567	225	467	158	1416
	15	3	2167	284	67	33	2550
2006	18	3	233	317	233	292	1075
	24	3	1800	183	433	259	2675
	25	3	750	317	0	58	1125
	28	3	400	409	100	58	967

vations from 2006, all stands with the exception of stand 18, showed an increase in the total tph following MPB attack. Understory densities in 2006 ranged from 433 tph to 2234 tph, while overstory densities ranged from 375 tph to 609 tph.

Bias values related to tph across all six stands were much larger for lodgepole pine than for spruce-aspen. The density of lodgepole pine less than 7.5 cm dbh was underestimated in all four simulations, with the 2.5 to 5.0 cm dbh class showing the poorest results for all simulations (Figure 1). For lodgepole pine trees with a dbh greater than 7.5 cm, the 10-year hand-off simulation had the best results, although all four simulations had similar results and provided reasonably good estimates of tph. Overall, estimates of tph for spruce and aspen were much lower than actual values (Figure 2). Estimates for the spruce-aspen species group were poorest in the 2.5 to 5.0 cm dbh class, with densities being under estimated by as much as 850 tph in the 10-year hand-off simulation. The lone exception was in the simulation that used SORTIE-ND for the entire 25 year projection period. Here, the 7.5 to 15 cm dbh class had the poorest results, under-estimating densities by 870 tph. The best approximation of stand-level densities for spruce and aspen trees larger than 7.5 cm dbh was provided by the simulation that used Prognosis[BC] only.

In order to gain some insight into how each simulation performed given a different stand density immediately following MPB attack, we compared the results of two stands. The first stand we looked at had a total density of 425 tph in 1981, while the second stand had a density of 1184 tph in 1981. The stand with the lower density in 1981 showed poor results for all tree species less than 7.5

cm dbh in both of the hand-off simulations (Figure 3). This is not surprising given the tendency for all simulations to drastically underestimate densities of small trees and the fact that this stand turned out to have one of the highest densities of small trees 25 years after MPB attack. For the stand with the higher density in 1981, the 10-year hand-off simulation provided the best estimate of tph for trees less than 7.5 cm dbh (Figure 3). In fact, this simulation actually overestimated tree densities in the 0 to 2.5 cm dbh class. However, it is important to note that actual small tree densities recorded in 2006 were low relative to the other six stands, although stand densities were high in 1981. It appears that the general tendency of the four simulations was to dramatically underestimate tph. However, the magnitude of this discrepancy may be lower in stands where low tph values for trees less than 7.5 cm dbh were recorded in 2006.

DISCUSSION

Both the 5-year hand-off and 10-year hand-off simulations for stands following MPB attack produced minor improvements in density projections for trees less than 7.5 cm dbh over the simulation that used Prognosis[BC] or SORTIE-ND only. The most noticeable improvement, although still minor, was in the 10-year hand-off simulation when estimating densities for spruce and aspen. This may be due in part to low densities of spruce and aspen trees less than 7.5 cm dbh relative to the densities of small lodgepole pine trees. Testing the simulations on stands where the densities of small spruce and aspen trees are on the same order as lodgepole pine might reveal different results among the
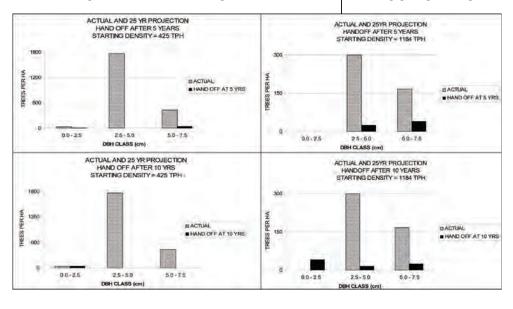
Figure 3—Estimated and actual trees per ha from a low density and a high density stand for all trees less than 7.5 cm dbh following a 25 year projection using the handoff at year 5 simulation and the handoff at year 10 simulation.

different simulations. The tendency for all simulations to underestimate densities of large spruce and aspen trees, although not as pronounced as was the case with smaller trees, was somewhat discouraging. Likewise, the tendency for all simulations to overestimate overstory densities of lodgepole pine seems to indicate that conditions in MPB-affected stands may have been under-represented in the PSPs used in the calibration of Prognosis[BC] and SORTIE-ND.

Poor estimates of stand densities following MPB attack for trees less than 7.5 cm dbh in the two simulations that used the linked-model approach and the simulation that used SORTIE-ND only may be indicative of several factors. First, the results presented here are based on results obtained from only six stands. These stands were chosen for the initial tests of the linked-model approach because they were representative of the diverse range of stand conditions observed during sampling. However, increasing the number of stands tested may improve the overall results of the hand-off simulations. The results obtained from the low density stand and the high density stand would suggest that averaging the results over more stands may reduce the biases of estimating densities.

Second, while the data collected in 2006 was used to provide parameter estimates for allometric relationships, substrate composition, and snag fall down rates in SORTIE-ND, other parameters used by the model may not reflect the exact conditions of the stands used in the simulations. For example, the growth parameters provided to SORTIE from Astrup et al. (2007) were for the SBS biogeoclimatic ecological classification zone. Although some of our plots were collected within this zone, the majority of our plots were collected from the SBPS and IDF zones where annual rainfall levels are considerably lower and tree growth is generally slower (Mah and Nigh 2003). Using growth parameters that overestimate tree growth can cause SORTIE-ND to increase competition-induced mortality rates, thus killing off more understory trees than would be expected. Since measurements collected for this study do not allow us to directly estimate many of the parameters used by SORTIE-ND, additional data may be required to improve the overall performance of SORTIE-ND.

Lastly, it is possible that the poor results obtained from the simulations are in large part due to the high variability of regeneration densities following MPB attack. This condition is cited as a likely culprit for the poor results obtained when using the MSN approach to estimate natural regeneration following partial cutting (Hassani et al. 2004). Since one of the sampling objectives was to collect data from a wide range of stand types affected by MPB, increasing the number of stands used in the simulations may improve the results since there would be a better representation of the variability in overstory and understory densities.

CONCLUSION

In addition to an overstory tree-list, PrognosisBC requires the input of a natural regeneration tree-list to provide accurate mid- to long-term estimates of growth and yield in unmanaged complex stands. Our goal in linking regeneration tree-lists estimated by SORTIE-ND to Prognosis[BC] was to improve upon the MSN approach of estimating natural regeneration following MPB attack. Compared to the MSN approach, using SORTIE-ND to estimate natural regeneration, including species composition and density, allows for greater flexibility since the SORTIE-ND model parameters can be easily adjusted to fit a specific dataset. This method is potentially advantageous when estimates of natural regeneration are required for stands that are unusual or under-represented, as is the case for stands affected by MPB in central and southeastern BC.

Between the two different hand-off times studied, the hand-off of the SORTIE-ND regeneration tree list to Prognosis[BC] after 10 years showed the best results for small spruce and aspen trees when compared to the results obtained when using SORTIE-ND or Prognosis[BC] alone. Only marginal improvements in the estimates of small lodgepole pine were noted for both the five-year hand-off and the ten-year hand-off simulations. The overall poor results obtained by using the linked-model approach would likely be improved with further parameterization of SORTIE-ND behaviors. Also, using a more extensive dataset with measurements collected from a larger number of stands should bring the estimates of small tree densities closer in-line with actual observations.

LITERATURE CITED

Astrup, R.; Coates, K.D; Hall, E.; Trowbridge, A. 2007. Documentation for the SORTIE-ND SAS Research Parameter File Version 1.0. February, 2007, Smithers, British Columbia, Canada: Bulkley Valley Centre. 50 p.

Aukema, B.H.; Carroll, A.L.; Zhu, J. [et al.]. 2006. Landscape level analysis of mountain pine beetle

in British Columbia, Canada: spatiotemporal development and spatial synchrony within the present outbreak. Ecography 29: 427-441

Backhouse, F; Louisier, J.D. 1991. Silvicultural Systems Research: Wildlife Tree Problem Analysis. Ministry of Forests, Nelson, B.C. Research Summary RS-003.

Boisvenue, C. 1999. Early height growth and regeneration: Applicability of Prognosis components to the Southern Interior of British Columbia. M.Sc. Thesis, Univ. of B.C., Vancouver, BC. 193 p.

Boisvenue, C; Temesgen, H; Marshall, P.M. 2004. Selecting a small tree height growth model for mixed-species stands in the southern interior of British Columbia, Canada. Forest Ecology and Management 202: 301-312.

Campbell, E.M.; Alfaro, R.I.; Hawkes, B. 2007. Spatial distribution of mountain pine beetle outbreaks in relation to climate and stand characteristics: a dendroecological analysis. Journal of Integrative Plant Biology 49: 168-178

Canham, C. D.; Burbank D.H. 1994. Causes and consequences of resource heterogeneity in forests—interspecific variation in light transmission by canopy trees. Canadian Journal of Forest Research 24: 337-349.

Coates, D.K.; Canham, C.D.; Beaudet, M. [et al.]. 2004. Use of a spatially explicit individual-tree model (SORTIE/BC) to explore the implications of patchiness in structurally complex forests. Forest Ecology and Management 186: 297-310.

Hassani, B.; LeMay, V.M.; Marshall, P.L. [et al.]. 2004. Regeneration imputation models for complex stands of Southeastern British Columbia. The Forestry Chronicle 80:271-278.

Hawkes, B.; Taylor, S.; Stockdale, C. [et al.]. 2004. Impacts of mountain pine beetle on stand dynamics in British Columbia. Pages 175–195. In: T.L. Shore, J.E. Brooks, and J.E. Stone, editors. Mountain Pine Beetle Symposium: Challenges and Solutions. Kelowna, British Columbia October 30-31, 2003, Natural Resources Canada, Canadian Forest Service, Pacific Forestry Centre, Information Report BC-X-399, Victoria, BC. 298p.

Hyytiainen, K.; Ilomaki, S.; Makela, A.; Kinnunen, K. 2006. Economic analysis of stand establishment for Scots pine. Canadian Journal of Forest Research 36: 1179-1189.

Kobe, R.K.; Coates, D. 1997. Models of sapling mortality as a function of growth to characterize interspecific variation in shade tolerance of eight tree species of northwestern British Columbia. Canadian Journal of Forest Research 27: 227-236

LeMay, V.M.; Lee, T.; Scott, R.E. [et al.]. 2006. Modeling Natural Regeneration Following Mountain Pine Beetle Attacks in the Southern and Central Interior of British Columbia: Results for Year 1. Internal report for Natural Resources Canada, MPB Standard Contribution Agreement, PO # 8.35. 70 pp. http://www.forestry.ubc.ca/prognosis/extension.html

Mah, S; Nigh G.D. 2003. SIBEC site index estimates in support of forest management in British Columbia. Research Branch, B.C. Ministry of Forests, Victoria, B.C. Technical Report 004. www.for.gov.bc.ca/hfd/pubs/docs/tr/tr004.htm

Moeur, M. and A.R. Stage. 1995. Most similar neighbor: an improved sampling inference procedure for natural resource planning. Forest Science 41, 337-359.

Oliver, C.D.; Larson, B.C. 1996. Forest Stand Dynamics. John Wiley and Sons, Inc., New York, 520 p.

Pacala, S.W.; Canham, C.D.; Silander, J.A. 1993. Forest models defined by field measurements: The design of a northeastern forest simulator. Canadian Journal of Forest Research 23: 1980-1988

Pedersen, L. 2003. Allowable Annual Cuts in British Columbia: The Agony and the Ecstasy. UBC Faculty of Forestry Special Presentation. Vancouver, BC, Canada: Faculty of Forestry, University of British Columbia. 24 p. http://www.for.gov.bc.ca/hts/pubs/jubilee_ubc.pdf

Robinson, A.P; Monserud, R.A. 2003. Criteria for comparing the adaptability of forest growth models. Forest Ecology and Management 172: 53-67.

Snowdon, B. 1997. British Columbia's Forest Vegetation Simulator application software. In: Proceedings of Forest Vegetation Simulator Conference. Teck, R.;

Moeur, M.; Adams, J., technical editors. Feb. 3-7, 1997, Fort Collins, CO. Gen. Tech. Rep. INT- 373. Ogden, UT: U.S. Department of Agriculture, Forest Service, Intermountain Forest and Range Experiment Station.

Stage, A.R. 1973. Prognosis model for stand development. USDA, Forest Service, Res. Pap. Intermountain Forest and Range Exp. Station. INT-137. Ogden, UT.

Stevens, V. 1997. The ecological role of coarse woody debris: an overview of the ecological importance of CWD in B.C forests. Research Branch, B.C. Ministry of Forests, Victoria, B.C. Working Paper 30/1997.

Zumrawi, A.; Stage A.; Snowdon, B. 2002. Stand level scaling of a single tree distance independent diameter growth model: Interim calibration of Prognosis in the south-eastern interior of British Columbia. In: Proceedings of Second Forest Vegetation Simulator (FVS) Conference. Crookston, N.L; Havis, R.N., compilers. February 12-14, 2002, Fort Collins,

CO. RMRS-P-25. Ogden, UT: U.S. Department of Agriculture, Forest Service, Rocky Mountain Research Station. p. 151-157.

Zumrawi, A.A.; LeMay, V.; Marshall, P.M. [et al.]. 2005a. Implementing a Prognosis[BC] Regeneration Sub-model for Complex Stands of Southeastern and Central British Columbia. Collaborative Project between Research Branch, Ministry of Forests; Forest Resources Management Department, University of British Columbia, and ESSA Technologies, Inc. Vancouver, British Columbia, Canada. Report submitted to: Forest Science Program, Project No: Y051355, 157 p. http://www.for.gov.bc.ca/hre/pubs/azumrawi.htm

Zumrawi A.A.; Marshall, P.M.; Akindele, S.O. [et al.]. 2005b. Calibrating Prognosis[BC] in the Sub-Boreal Spruce and the Sub-Boreal Pine-Spruce Biogeoclimatic Zones: Development of growth and mortality models for major tree species. Internal report for Forest Science Program, Project No: Y051356.

Effects of Silvicultural Treatments on Wood and Tracheid Properties, and Economic Returns of Norway Spruce

Tianjian Cao, Lauri Valsta, Sanna Härkönen, Annikki Mäkelä

ABSTRACT

EFFECTS OF THINNING AND FERTILIZATION on wood and tracheid properties, and economic returns of Norway spruce (*Picea abies* (L.) Karst.) were investigated in two young stands, in southeastern Finland and northern Sweden. Models for predicting wood and tracheid properties of Norway spruce were integrated into a distance-independent process-based growth model. Increasing thinning intensity resulted in lower mean wood density, tracheid length, and latewood proportion in harvest wood. Pulpwood fiber quality slightly decreased when the proportion of sawlog yield over the rotation increased. Thinning regimes with high early growing stock and decreasing later growing stock were most profitable. Fertilization accelerated volume growth and increased value growth. Decreased wood density and tracheid length due to fertilization resulted in minor effects on economic returns. Increased volume growth more than offset the economic influence of fiber quality.

KEYWORDS: fiber quality, forest fertilization, process-based growth model, Norway spruce, thinning intensity

Tianjian Cao (tianjian.cao@helsinki.fi) is a doctoral student and **Lauri Valsta** is a professor, Department of Forest Economics, P.O. Box 27, FIN-00014 University of Helsinki, Finland; **Sanna Härkönen** is at the Faculty of Forestry, P.O. Box 111, FIN-80101 University of Joensuu, Finland; **Annikki Mäkelä** is a professor, Department of Forest Ecology, P.O. Box 27, FIN-00014 University of Helsinki, Finland.

Simulating Daily Xylem Development in Eucalypts Using Outputs from the Process-Based Model CABALA

David M. Drew, Geoffrey M. Downes, Jenny Read, Michael Battaglia

ABSTRACT

THE NEED FOR ACCURATE WOOD QUALITY prediction in hardwoods has increased with the growing importance of these species to the global forest industry, in particular *Eucalyptus* species. Several process-based models of xylem development have been produced (Wilson 1964; Deleuze and Houlier 1998; Fritts et al. 2005) but have considered woody tissue development in softwoods only. The situation is more complex in hardwoods, which produce a greater variety of cell types in the xylem.

The model described here, which we have called "CAMBIUM", simulates the growth and development of a hypothetical, simulated population of cells in variable numbered cell files, bounded within sets of rays. Although models for softwood xylem effectively work in a single dimension (modeling a single radial file of cells), it is necessary to consider hardwood xylem in at least two dimensions in the transverse plane (modeling multiple, neighboring files of cells) because of the highly significant interactions between cell types and the importance of their spatial arrangement. These interactions are constantly invoked in the hypothetical cell population during the model run to modify environmentally determined "potential" cell growth and development.

The model predicts cell fate, cell division and production, cell growth, and cell secondary wall development in individual cells in the simulated population. It uses outputs of whole-tree physiological parameters generated on a daily time-step from the CABALA process-based model (Battaglia et al. 2004) which has been widely tested and validated for various *Eucalyptus* spp. Outputs of particular importance from CABALA are daily derived estimates of pre-dawn and midday water potential, stem and foliage allocation, minimum and maximum temperature, and vapour pressure deficit.

CAMBIUM relies heavily on conceptual morphogenic fields of growth-regulating substances, particularly auxin, which have been found to affect cambial activity and cyto-differentiation in the cambial zone and developing xylem. The model considers different approaches to determining cell fate as either a function of cell position with these morphogenic fields or as a function of the flow of chemical signals, or as a function of both. It currently determines between fibers or vessels in the developing xylem from a homogenous population of cambial initials. The model also provides more than one approach to calculating the potential daily growth of developing cells. Following the additional consideration of cell-cell interactions, the model is thus capable of generating high-resolution estimates of fiber and vessel transverse dimensions. The process of secondary wall thickening is currently very simple, similar to that proposed by Deleuze and Houllier (1998) and generates estimates of fiber and vessel wall thickness. Wood density is derived empirically from cell transverse and wall dimensions as well as potentially from vessel frequencies.

Model parameterization and validation is currently underway using data from four Eucalyptus species from three separate research trials in South Africa and Australia. Early results indicate that the model is able to accurately detect changes in wood properties in a radial profile in response to changing environmental conditions in a forest stand.

David M. Drew (david.drew@sci.monash.edu.au) is at the School of Biological Sciences, Building 18, Monash University, Victoria 3800 and CSIRO Ensis, Private Bag 12, Hobart 7001, Tasmania, Australia; **Jenny Read** is at the School of Biological Sciences, Building 18, Monash University, Victoria 3800, Australia; **Geoffrey M. Downes** and **Michael Battaglia** are at CSIRO Ensis, Private Bag 12, Hobart 7001, Tasmania, Australia.

Incorporating an Index of Root Zone Water Balance Into an Existing Growth and Yield Model CanSPBL(1.2)

Guy Pinjuv, Euan G. Mason, Michael Watt

ABSTRACT

The hybrid model, CanSPBL(water) was developed to predict the growth of plantation grown *Pinus radiata* in New Zealand's Canterbury Region. The hybrid model is an updated version of an existing model CanSPBL(1.2) (Pinjuv 2006), and includes an index of water balance over the simulation period. Water balance estimates were made using a sub-model for root zone water balance included in the hybrid physiological model 3-PG (Landsberg and Waring 1997). The hybrid was validated with an independent data set of growth measurements used for model fitting and was compared to the statistical version, CanSPBL(1.2) (Pinjuv 2006). The validation was run using both monthly inputs of climate (that displayed yearly variation) and monthly inputs of climate (that were ten-year averages). Using climatic inputs that included yearly variation, the hybrid model showed an increase in precision of 1–4 percent over the statistical version of the model at a stand level (with the exception of the model for maximum diameter, which showed a decrease in precision of 0.78 percent). However, using ten-year averages of monthly climatic inputs, the hybrid model showed increases of precision from 0.5 to 8 percent (with the exception of maximum diameter again, showing a decrease in precision of 0.13 percent). The components of the stand model also included mean top height, basal area per hectare, stems per hectare, and diameter distribution.

KEYWORDS: Forest growth model, hybrid model, water balance, forest productivity, model validation

INTRODUCTION

WATER BALANCE IS A WELL-ESTABLISHED INDICATOR of growing potential and has been found to be a main constraint for tree development on dry forested sites. Reduction in the availability of water decreases stem growth by restricting physiological processes such as leaf area development, photosynthesis, and stomatal conductance (Boomsma and Hunter 1990). An index for water stress (the water stress integral) has been shown by Myers (1998) to account for almost all of the variation in basal area increment of *Pinus radiata* subjected to a range of irrigation and fertilization treatments. Given the importance of water availability in regulating productivity and basal area growth on dry sites, a model of root zone water balance may provide a useful process-based approach that can be incorporated into a classical growth and yield model.

Incorporating a model of root zone water balance into a classical growth and yield model may increase accuracy of tree growth prediction, and make the model more robust under changing climatic conditions. This paper will discuss a root zone water balance model that was used to estimate water balance for all forests in the Selwyn Plantation Board Estate located in New Zealand's Canterbury Region. An index for available water at the each site will be used as a variable to predict future forest growth. This index was incorporated into the equations that comprise the existing growth model CanSPBL(1.2) described in detail by Pinjuv (2006). This paper will first examine the modeling strategy used to predict root zone water balance, discuss the input data for the model, parameterization of the model,

Guy L. Pinjuv (guy.pinjuv@gmail.com) is a doctoral student and **Euan G. Mason** is an associate professor of forestry at the University of Canterbury, Private Bag 4800, Christchurch, New Zealand; **Michael Watt** is a research scientist at ENSIS (formerly New Zealand Forest Research), P.O. Box 29237, Christchurch, New Zealand.

validation of the model used to predict root zone water balance, and then the results of incorporating that index into CanSPBL(1.2).

WATER BALANCE MODELING

3PG Water Balance Model Adapted from (Landsberg and Waring 1997) and (Sands and Landsberg 2002)

The water balance model used to calculate an index of water use over the measurement interval was the model sub-model for water balance used in 3-PG (Landsberg and Waring 1997). This model is a single layer soil-water-balance model that operates on a monthly time step. Monthly rainfall (plus irrigation) is balanced against monthly evapotranspiration computed using the Penman-Monteith equation (Landsberg and Gower 1997, p. 76.) The general equation can be written as:

$$\theta_T = \theta_{T-1} + P - I - E - D \qquad (1)$$

Where: θ_T is the root zone water balance at time T (mm), θ_{T-1} is the root zone water balance at time (T-1) in the previous month (mm), P is precipitation (mm), I is the canopy interception (mm), E is evapotranspiration (calculated using the Penman-Monteith equation,) and D is the drainage of water from the soil (mm).

The model is initialized with soil water content = maximum available water in the rooting zone (θ mm). This is dependent on the water-holding characteristics of the soil and the rooting depth of the trees (see Landsberg and Gower 1997). Available water is set to appropriate starting values for each site. The moisture ratio (r_θ) for the stand is calculated as:

$$r_\theta = \frac{\text{Current soil water content + water balance}}{\text{Available Water}} \qquad (2)$$

The moisture ratio r_θ is used in the calculation of a soil water modifier (f_{sw}), which is used to modify estimates of canopy conductance (g_c) that will be discussed later. The water balance in any month will be reduced if transpiration exceeds precipitation, and vice versa. If the numerator of the expression for r_θ exceeds θ, the excess water is assumed to have run off or drained out of the system. If it is negative $r_\theta = 0$.

Canopy interception is a fixed percentage of rainfall

when the canopy exceeds a threshold leaf area index (LAI) in the 3-PG model. When P > 2mm, and LAI ≥ 3, then I = 0.15*P. If P< 2 mm, then I = P. And if P > 2mm and 0 < LAI < 3, then I = 0.05*LAI*P.

Vapor pressure deficit, available soil water and stand age are assumed to affect stomatal conductance. Canopy conductance (g_c (m s^{-1})) is determined from a nominal stomatal conductance scaled by f_{age} and by the lesser of the environmental modifiers f_{sw} and f_{VPD}, and increases with increasing canopy LAI up to a maximum canopy conductance ($g_{c_{max}}$ (m s^{-1})).

The equation for canopy conductance is given by:

$$g_c = g_{c_{max}} \cdot e^{(-k \cdot VPD)} \qquad (3)$$

where k is a factor based on the relationship between stomatal conductance and vapor pressure deficit = 2.5 (value taken from Landsberg and Waring 1997) and *VPD* is the saturation vapor pressure (kPa).

The age modifier f_{age}, is calculated from:

$$f_{age} = \frac{1}{1 + \left(\dfrac{F_a}{0.95}\right)^{n_{age}}} \qquad (4)$$

where F_a is the relative age of a forest or plantation denoted by the ratio of actual age (in years) to the maximum age likely to be attained, n_{age} is a parameter to control the rate of change of the function and the default value from the 3-PG model is n_{age}=4.

The vapor pressure deficit modifier, f_{VPD} is calculated from:

$$f_{VPD} = e^{(-k \cdot VPD)} \qquad (5)$$

where k is a factor based on the relationship between stomatal conductance and vapor pressure deficit = 2.5 (value taken from Landsberg and Waring 1997) and *VPD* is the saturation vapor pressure (kPa).

The soil water modifier, f_{sw} is calculated from:

$$f_{sw} = \frac{1}{1 + \left[\dfrac{(1 - r_\theta)}{c_\theta}\right]^{n_\theta}} \qquad (6)$$

where c_θ and the power n_θ take different values for different soil types Landsberg and Waring (1997) suggest

c_θ =0.7, 0.6, 0.5, and 0.4 for sand, sandy-loam, clay-loam, and clay soils, respectively, and n_θ =9, 7, 5, and 3 for the same soil types.

WATER BALANCE VALIDATION

The 3PG, and sub-model for water balance was tested against a validation dataset that contained measurements taken within the study area. The validation dataset came from a study done by Arneth et al., (1998), which contained 49 measurements of volumetric root-zone water content taken at Balmoral Forest, located 100-km Northwest of Christchurch New Zealand, (42°52'S, 172°45'E at an elevation 198 m above sea level) between 1994 and 1996. A residual analysis of the model was run across the validation dataset. This residual analysis was conducted on an accumulated deficit basis over a given measurement interval. This was done to mirror the model's final use in a growth and yield modeling context where the accumulated water deficit over a measurement interval is expected to describe variations in stand growth and diameter distribution. Table 1 shows the actual and estimated accumulated water deficit for the 3PG and sub-model for water balance. An analysis of mean square error (MSE Eq. 7) was used as the final selecting criterion to determine the water balance model used in further analysis.

$$MSE = \frac{1}{n} \sum_{i=1}^{n} \left(Y - Y' \right)^2 \tag{7}$$

where Y is the measured accumulated root zone water deficit (mm), and Y′ is the modeled accumulated root zone water deficit.

METHODS
Climatic Inputs for Water Balance Modeling

The climatic inputs of solar radiation, minimum air temperature, maximum air temperature, and rainfall were estimated for each site using the method of correcting 10-year average values for each site by local met station measurements. Actual water balance climate inputs are based on a system of corrected estimates from BIOCLIM (Leathwick and Stevens 1998) climate surfaces. BIOCLIM is a set of surface equations for New Zealand that estimate climatic variables on a 10-year average based on interpolation between climate station measurements (Leathwick and Stevens 1998). BIOCLIM outputs monthly averages of temperature, wind, rainfall, radiation, and average humidity extremes across New Zealand based on location. To simulate the monthly variation in actual climate readings, as opposed to mean monthly values over a 10-year period, the long-term mean monthly climate values derived from BIOCLIM were rescaled using monthly climate measurements from a nearby weather station. These estimates were corrected by reference point measurements made at Christchurch Airport (S43.5°, E172.55°, elevation 37m). Differences between climatic estimates from BIOCLIM and measurements at Christchurch Airport were calculated for each month included in the study from 1984–2004. Corrections were added to long term monthly estimates at each permanent sample plot. So instead of using the same monthly averages every year, a new value was calculated every month based on actual climate at Christchurch Airport to reflect years of extreme climatic events such as droughts. Similar approaches to correcting long term averages with local measurements have been used by Tickle et al. (2001), and Snowdon et al. (1999).

Growth and Yield Fitting and Validation Data

The model fitting and validation dataset comprised 4416 growth observations taken within 1020 unique permanent sample plots. All measurements were recorded between December 1982 and January of 2004 on the Selwyn Plantation Board Estate located in the Canterbury region of southeastern New Zealand. Sites on the Selwyn estate vary with elevation covering the three forest types of plains, hills, and coastal sands with elevations ranging from 2–600 metres above sea level. Distinctions between these forest types are due to both elevation and soil type. With increasing distance from the sea, soils underlying forests in Canterbury change from coastal sands, shallow and dry floodplains soils, to deep wet loess hill soils (Barringer et al. 1998). Average temperatures are 10.9 °C for plains

Table 1—Measured and estimated accumulated water deficit (mm) from 3PG and water balance models.

Interval (month/year)	Measured accumulated water deficit (mm)	3PG estimate (mm)
10/1987–5/1988	273.51	273.57
6/1988–5/1989	417.11	379.52
6/1989–3/1990	164.72	128.79

and coastal forests, and 11.6 °C for forests growing on the hills. Annual rainfall increases from 600 to 1100 mm for coastal-plains and hills forest, respectively (Leathwick and Stephens 1998). The mean re-measurement interval is 6.6 years for all measurements, while the mean re-measurement interval per plot was 5.7 years. All validation data were independent of any information used for fitting or calibrating any of the included models in this study. The database was partitioned for model building and model validation. In all, there were 4416 plot measurements in the entire data set: 3667 were randomly chosen for model building, while 969 plot measurements were randomly set aside for model validation. A detailed summary of plot variable estimates with a breakdown for plains and foothills plots is listed in Pinjuv (2006).

Growth Modeling: Incorporating and Index of Root Zone Water Balance Into the Existing Model CanSPBL(1.2)

Equations used to model growth in CanSPBL(1.2) were updated to incorporate an index of root zone water balance. The water balance index used described the average available soil water deficit over the simulation period, as calculated with the model for water balance used in 3PG (Landsberg and Waring 1997). The water balance model was represented in the Java programming language by Dr E.G. Mason, and the Java program accessed weather data for each plot within a Microsoft Access database table and arranged for output to be placed alongside growth and yield data in a separate Access table. Table 2 shows the descriptive statistics of average monthly available soil water deficit (ASW) values for the model fitting data set.

The method used for incorporating the effect of average ASW deficit into the equations used in CanSBPL(1.2) was to plot the residuals of the models against ASW deficit and observe the pattern of residual bias. This bias was then accounted for by adding curvilinear forms of ASW deficit to the

models. An example of this is shown in Figure 1 where the bias of mean top height residuals plotted against ASW deficit can be corrected in part by a curvilinear model including a form of ASW deficit and ASW deficit squared.

Residuals of all of the models in CanSPBL(1.2) were first plotted against average ASW deficit. All of these plots indicated the bias could be corrected for by adding ASW deficit and ASW deficit squared to each model. The 4 best initial fit sigmoid growth equations where the effects of elevation were initially tested in Pinjuv (2006) were fitted again with ASW deficit and ASW deficit squared added to them. These final models were then tested further to see if different forms of elevation and ASW deficit could be added to them in a way that would minimize error and simplify the final model.

To fit equations, methods used by Zhao (1999), and Pinjuv (2006), of non-linear least-square procedures with SAS software (SAS Institute Inc., 2001) were employed. The Mean Square Error (MSE) and graphical residual patterns were used as the selection criteria to judge model performance. Skewness and kurtosis were often checked for final models to determine the magnitude of residual distributions of normality. Plots of residuals versus predictions and all possible explanatory variables were inspected to check for trends but only the five most important graphs are displayed in this study for each selected equation. The five graphs are residuals versus prediction, age, elevation, time increment, and ASW deficit.

No statistical tests are given in this analysis because repeated measurements have been taken from the basic experimental units (PSP). The consequences of this are (1) estimators of the regression coefficients may no longer have minimum variance but will still be unbiased and consistent, (2) standard errors of coefficients in the regression will be underestimated, and (3) any significance tests or confidence limits constructed using t or F distributions are likely to be wrong since assumed independence of errors is

Table 2: Descriptive statistics of the average ASW deficit in modeling data set.

3PG Average Water Deficit	
Mean (mm)	32.21
Minimum (mm)	0.00
Maximum (mm)	142.38
Standard Deviation (mm)	24.95
Count	3660.00

Table 3—Basal area model fitting results, after the effect of average water deficit and elevation are included in the asymptotic parameter.

Equation with elevation and average 3PG water deficit in asymptote	Basal Area MSE
Polymorphic Weibull I	failed to converge
Polymorphic Gompertz II	16.49
Polymorphic Weibull II	failed to converge
Polymorphic Schumacher II	16.81
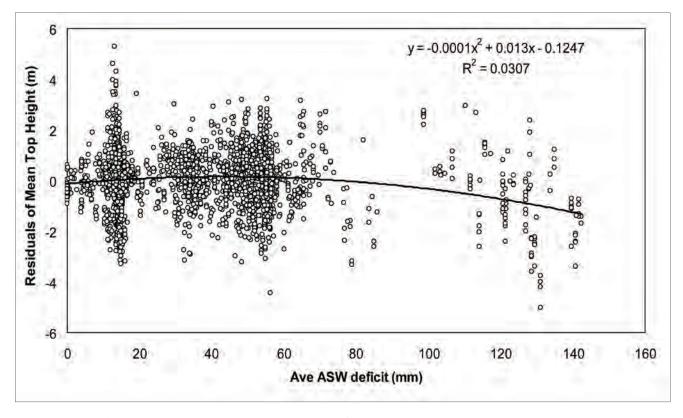
Figure 1: Residuals of mean top height vs. average 3PG available soil water deficit.

violated (West et al. 1984). The MSE for the regression is also likely to be underestimated if the correlation is positive and inflated if the correlations are negative (Snowdon et al. 1999). Some statistically valid tests are provided in this analysis as a check of the final results by preparing an auto correlation free data set. An auto correlation free data set was used to test the significance of explanatory variables being different from zero for all models and to check the normality of residuals with the Kolmogorov-Smirnov test. The Kolmogorov-Smirnov test was chosen to test normality because of the large size of the data set.

To validate the newly established model and test its performance at a plot level, a validation data set was prepared. The main model components of MTH, basal area per hectare, stems per hectare, maximum diameter, and standard deviation of diameter were examined using data at a plot level. One source of data was selected consisting of independent plot measurements chosen randomly before model fitting. The average model bias (AMB), efficiency factor (EF), skewness and kurtosis were calculated for each model component. Graphs of residual patterns were examined to detect bias. Normality of residual plots was also tested using the Kolmogorov-Smirnov test.

RESULTS

Basal Area

The four models with the best initial fit for basal area in chapter 4 were of Pinjuv (2006); Polymorphic Gompertz II, Polymorphic Schumacher II, Polymorphic Weibull I, and Polymorphic Weibull II. The effects of water balance deficit and elevation were added into these models by altering the asymptotic parameter for each equation. These equations were initially fitted with the form of elevation that was used for the final model of basal area in CanSPBL(1.2) and the effects of water deficit added in as a linear and curvilinear term. The results of initial model fits in terms of MSE are shown in Table 3.

The model with the lowest MSE after the addition of the effect of average water deficit and elevation was altered further to see if different correction forms for these effects would improve model fits. These included a linear correction for elevation for PSP's above 250 m, as was used by Zhao (1999), elevation, the square of elevation, a probit correction for the effect of elevation, ASW deficit, ASW deficit squared, and the interaction of elevation and ASW deficit.

The best model fit was found by adjusting the asymptotic parameter of the Polymorphic Gompertz II equation using

Table 4—Parameters for basal area model (Equation 8), standard errors, and approximate 95-percent confidence limits calculated with 3,659 degrees of freedom.

Parameter	Estimate	Std. Error	Approximate 95% Confidence Limits	
β	0.153	0.00219	0.1487	0.1573
γ	0.00249	0.000038	0.00242	0.00257
α_0	44311.5000	229.0	43862.6	44760.4
α_1	0.0358	0.000708	0.0344	0.0372
α_2	-31.7278	2.1729	-35.9881	-27.4675
α_3	35.2148	4.363	26.6604	43.7691
α_4	-0.3759	0.0368	-0.4481	-0.3038

elevation squared, a dummy variable for elevations above 450m, mean ASW deficit, and mean ASW deficit squared. The final model for basal area has a MSE of 16.53, which is slightly higher than the initial fitting of the Polymorphic Gompertz II model listed in Table 3. The reason for this result is that this final model does not have the term of elevation alone in the asymptotic parameter as it was insignificant. The final model was fitted without this term and is written as:

$$G_2 = e^{\left(\ln(G_1) \cdot e^{\left(-\beta \cdot (T_2 - T_1) + \gamma \cdot \left(T_2^2 - T_1^2\right)\right)} + \frac{\left(\alpha_0 + \alpha_1 \cdot elev^2 + \alpha_2 \cdot \left((elev - 450)X\right) + \alpha_3 \cdot ASW + \alpha_4 \cdot ASW^2\right)}{10000} \cdot \left(1 - e^{\left(-\beta \cdot (T_2 - T_1) + \gamma \cdot \left(T_2^2 - T_1^2\right)\right)}\right) \right)}. \tag{8}$$

where G_2 is the future basal area (m^2 / ha), G_1 is the initial basal area (m^2 / ha), T_1 is the initial stand age (years), T_2 is the final stand age (years), $elev$ is the stand elevation (m), X is a binary indicator variable, $X = 0$ if elevation < 450, and $X = 1$ if elevation $\geq$ 450, ASW is the average water deficit over the simulation period calculated with the 3PG water balance model (mm), and β, γ, α_0, α_1, α_2, α_3, α_4 are

Table 5—Mean top height model fitting results, including the effect of average water deficit and elevation in the asymptotic parameter.

Equation with elevation and average 3PG water deficit in asymptote	Mean Top Height MSE
Polymorphic Gompertz II	1.01
Polymorphic Von Bertalanffy-Richards II	1.02
Polymorphic Schumachar II	0.97
Polymorphic Hossfeld	1.80

parameters whose values are listed in Table 7.

The parameter estimates of the final model of basal area are listed in Table 4. The model showed no signs of bias for basal area / ha when plotted against prediction, age, elevation, and time increment (Figure 2).

Mean Top Height

The four models with the best initial fit for mean top height (Pinjuv 2006) were Polymorphic Gompertz II, Polymorphic Von Bertalanffy-Richards II, Polymorphic Schumacher II, and the Polymorphic Hossfeld. The effects of water balance deficit and elevation was added into these models by altering the asymptotic parameter for each equation. These equations were initially fitted with the form of elevation that was used for the final model of mean top height in CanSPBL(1.2) and the effects of water deficit added in as a linear and curvilinear term. The results of initial model fits in terms of MSE are shown in Table 5.

The model with the lowest MSE after the addition of the effect of average water deficit and elevation was altered further to see if different correction forms for these effects would improve model fits. These included a linear correction for elevation for PSP's above 250 m, as was used by Zhao (1999), elevation, the square of elevation, a probit correction for the effect of elevation, ASW deficit, ASW deficit squared, and the interaction of elevation and ASW deficit.

The best model fit was found by adjusting the asymptotic parameter of the Polymorphic Schumacher II equation using elevation squared, a dummy variable for elevations above 450m, mean ASW deficit, and mean ASW deficit squared. The final model for mean top height had a MSE of 0.97 and is written as:

$$MTH_2 = e^{\ln(MTH_1)\left(\frac{T_1 + \gamma}{T_2 + \gamma}\right)^{\beta} + \frac{\left(\alpha_0 + \alpha_1 \cdot elev^2 + \alpha_2 \cdot (elev - 450)X + \alpha_3 \cdot ASW + \alpha_4 \cdot ASW^2\right)}{10000} \cdot \left(1 - \left(\frac{T_1 + \gamma}{T_2 + \gamma}\right)^{\beta}\right)}. \tag{9}$$

where MTH_2 is the future mean top height (m), MTH_1 is the initial mean top height (m), T_1 is the initial stand age (years),
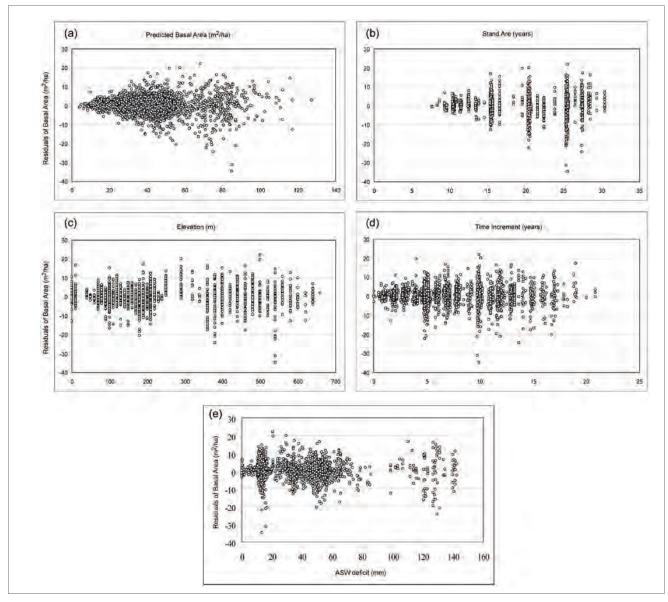
Figure 2: Fitting residual patterns of the final model for basal area: (a) residuals versus predicted, (b) residuals versus stand age, (c) residuals versus elevation, (d) residuals versus time increment, and (e) residuals versus ASW deficit.

Table 6: Parameters for mean top height model (Equation 9), standard errors, and approximate 95-percent confidence limits calculated with 3,659 degrees of freedom.

Parameter	Estimate	Std. Error	Approximate 95% Confidence Limits	
β	0.6832	0.0425	0.5998	0.7666
γ	4.1388	0.4782	3.2012	5.0764
α_0	44652.2	642.1	43393.3	45911.2
α_1	0.0238	0.000103	0.0218	0.0258
α_2	-32.8019	2.5632	-37.8276	-27.7763
α_3	40.0566	4.1723	31.8761	48.2371
α_4	-0.4519	0.039	-0.5285	-0.3754

T_2 is the final stand age (years), *elev* is the stand elevation (m), X is a binary indicator variable, where $X = 0$ if elevation < 450, and $X = 1$ if elevation ≥ 450, ASW is the average water deficit over the simulation period calculated with the 3PG water balance model (mm), and β, γ, α_0, α_1, α_2, α_3, α_4 are parameters whose values are listed in Table 6.

The parameter estimates of the final model of mean top height
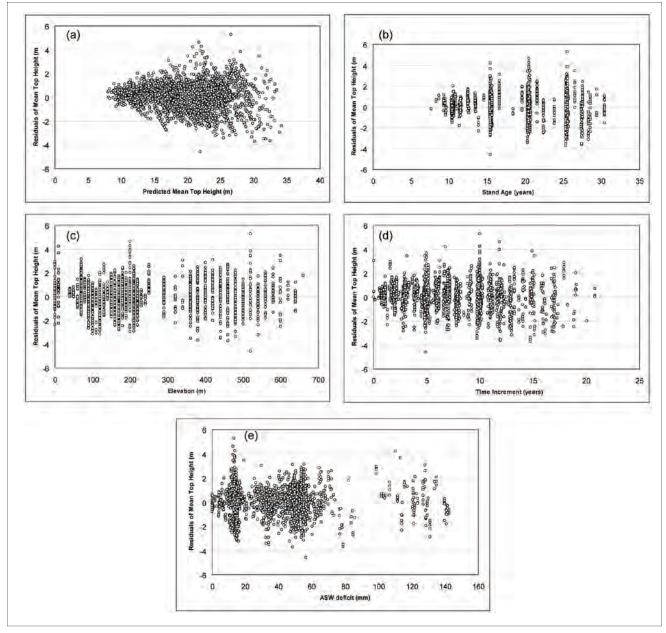
Figure 3: Fitting residuals patterns of final model for mean top height: (a) residuals versus predicted, (b) residuals versus stand age, (c) residuals versus elevation, and (d) residuals versus time increment, and (e) residuals versus ASW deficit.

are listed in Table 9. The model showed no signs of bias for mean top height when plotted against prediction, age, elevation, and time increment (Figure 3).

Maximum Diameter and Standard Deviation of Diameter

Models for maximum diameter and standard deviation of diameter were fitted by selecting the 4 model forms that had the best initial fit for basal area. These forms were also fitted to the data, incorporating the effects of average water deficit and altitude within the asymptotic parameter where

appropriate. Results for the initial fitting of these models for maximum diameter and standard deviation of diameter are shown in Table 7.

The best model fit for maximum diameter was found by adjusting the asymptotic parameter of the Polymorphic Weibull I equation using elevation squared, a dummy variable for elevations above 450m, the inverse of initial stocking, and ASW deficit squared (Eq. 10). The best model fit for the standard deviation of diameter was similarly found by adjusting the asymptotic parameter for the Polymorphic Gompertz II equation using elevation squared, a dummy

Table 7—Mean square error for initial models of maximum diameter and standard deviation of diameter including the effect of average water deficit and elevation.

Equation with elevation and average 3PG water deficit in asymptote	Maximum Diameter	Standard Deviation of Diameter
Polymorphic Weibull I	4.89	0.39
Polymorphic Gompertz II	5.09	0.38
Polymorphic Weibull II	failed to converge	failed to converge
Polymorphic Schumacher II	5.06	0.43

Table 8— Parameter values for maximum diameter model (Equation 10). Also shown are standard errors, and approximate 95-percent confidence limits for each parameter. Statistical values are calculated with 3,659 degrees of freedom.

Parameter	Estimate	Std. Error	Approximate 95% Confidence Limits	
β	0.3657	0.0421	0.2832	0.4483
γ	0.3973	0.0333	0.332	0.4626
α_0	64.8266	3.1145	58.7203	70.933
α_1	0.000159	0.00001	0.000139	0.000179
α_2	-0.1755	0.0176	-0.21	-0.141
α_3	8772.2	732.1	7336.8	10207.6
α_4	0.000463	0.000091	0.00284	0.000642

Table 9— Parameter values for standard deviation of diameter model (Equation 11). Also shown are standard errors, and approximate 95-percent confidence limits for each parameter. Statistical values are calculated with 3,659 degrees of freedom.

Parameter	Estimate	Std. Error	Approximate 95% Confidence Limits	
β	0.0715	0.00182	0.068	0.0751
γ	0.000443	0.000061	0.000323	0.000562
α_0	24777.1	358.5	24074.2	25480.0
α_1	0.0213	0.00109	0.0192	0.0235
α_2	-39.633	3.5957	-46.6829	-32.5831
α_3	-20.4624	6.0352	-32.2953	-8.6296
α_4	0.0935	0.0463	0.00276	0.1843

$$DSTD_2 = e^{\left[\ln(DSTD_1)\cdot e^{\left(-\beta\cdot(T_2-T_1)+\gamma\cdot\left(T_2^2-T_1^2\right)\right)}\right]}\cdot$$

$$e^{\left[\frac{\left(\alpha_0+\alpha_1\ elev^2+\alpha_2\cdot(elev-450)\cdot X+\alpha_3\cdot ASW+\alpha_4\cdot ASW^2\right)}{10000}\cdot\left[1-e^{\left(-\beta\cdot(T_2-T_1)+\gamma\cdot\left(T_2^2-T_1^2\right)\right)}\right]\right]} \tag{11}$$

where $DMAX_2$ is the future maximum diameter (m), $DMAX_1$ is the initial maximum diameter (m), $DSTD_2$ is the future standard deviation of diameter (m), $DSTD_1$ is the initial standard deviation of diameter (m), T_1 is the initial stand age (years), T_2 is the final stand age (years), $elev$ is the stand elevation (m), X is a binary indicator variable, $X = 0$ if elevation < 450, and $X = 1$ if elevation ≥ 450, ASW is the average water deficit over the simulation period calculated with the 3PG water balance model (mm), N1 is the initial stocking (stems / ha), and β, γ, α_0, α_1, α_2, α_3, α_4, and α_5 are parameters whose values are listed in Table 8 (for maximum diameter eq. 10) and Table 9 (for standard deviation of diameter eq. 11).

Tables 8 and 9 show parameter estimates. Figures 4 and 5 show residual patterns with little apparent bias against main modeling variables. For projection lengths of up to 20 years 95 percent of residuals for maximum diameter projections were within ± 4.3 cm, while 95 percent of the residuals for standard deviation of diameter were within ± 1.2 cm.

variable for elevations above 450m, ASW deficit, and ASW deficit squared (Eq. 11). The final models for maximum diameter and standard deviation of diameter had MSE values of 4.59 and 0.38, respectively, and are written as:

$$DMAX_2 = DMAX_1\cdot e^{\left(-\beta\cdot\left(T_2^\gamma-T_1^\gamma\right)\right)}+$$
$$\left(\alpha_0+\alpha_1\cdot elev^2+\alpha_2\cdot(elev-450)\cdot X+\alpha_3\cdot\frac{1}{N_1}+\alpha_4\cdot ASW^2\right)\cdot$$
$$\left(1-e^{\left(-\beta\cdot\left(T_2^\gamma-T_1^\gamma\right)\right)}\right) \tag{10}$$

Mortality

A set of six equations, which are variants of those, listed by Clutter et al. (1983), those used by Zhao (1999), and those used to fit CanSPBL(1.2) were used as the basic equation forms for projecting stocking (Pinjuv 2006). These equations were initially fitted using a modeling data set filtered in the same way as that used to fit CanSPBL(1.2) (Pinjuv 2006). A mortality severity index based on the -3/2 power law was used as a basis to filter the modeling data set for
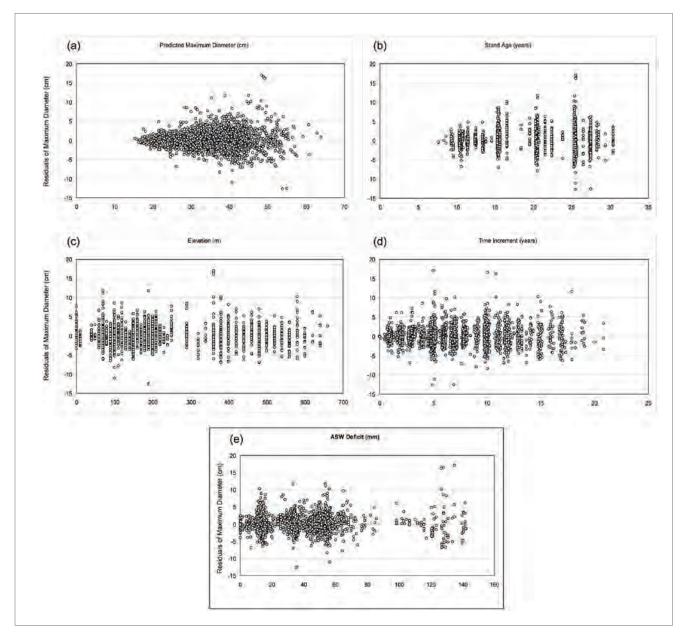
*Figure 4: Residual patterns of final model for maximum diameter: (a) residuals versus predicted, (b) residuals versus stand age, (c) residuals versus elevation, (d) residuals versus time increment, and (e) residuals versus ASW Deficit.*

mortality and a final model was built with 80 percent of the original mortality records under the recommendation of managers at SPBL. Equations were fitted incorporating the effects of ASW deficit and ASW deficit squared and the results of the initial fitting are listed in Table 13. As equation 3 (Table 10) had the smallest MSE it was chosen as the basic form of difference equation for further analysis. This model was altered further to see if different correction forms for these effects would improve model fits. These included a linear correction for elevation for PSP's above 250 m, as was used by Zhao (1999), elevation, the square

of elevation, a probit correction for the effect of elevation, ASW deficit, ASW deficit squared, and the interaction of elevation and ASW deficit.

The final model selected (Eq. 12) was fitted using Equation 3 (Table 13) and produced a MSE of 3282. Parameters for the final mortality model (Eq. 12) are listed in Table 11. Little bias was apparent in residual patterns shown in Figure 6. Ninety-five percent (greater than 2.5 percent and less than 97.5 percent) of residuals were within ± 116 stems / ha for projection lengths of up to 21 years.
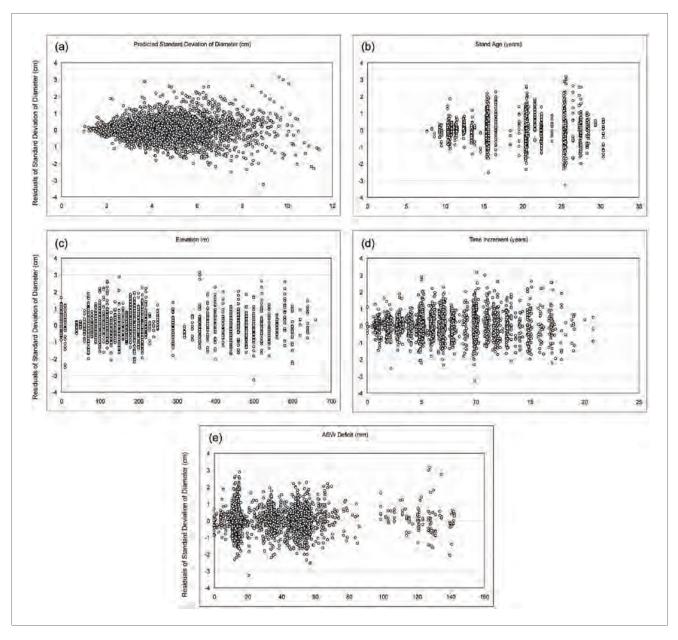
Figure 5: Residuals patterns of final model for standard deviation of diameter: (a) residuals versus predicted, (b) residuals versus stand age, (c) residuals versus elevation, (d) residuals versus time increment, and (e) residuals versus ASW deficit.

$$N_2 = \left(\frac{1}{\sqrt{N_1}} + \left(\alpha_0 + \alpha_1 \cdot ASW + \alpha_2 \cdot ASW^2 \right) \cdot \right.$$
$$\left. \left(\left(\frac{T_2}{100}\right)^2 - \left(\frac{T_1}{100}\right)^2 \right) \right)^{-2} \qquad (12)$$

where N_2 is the future stocking (stems / ha), N_1 is the initial stocking (stems / ha), T_1 is the initial stand age (years), T_2 is the final stand age (years), ASW is the average water deficit over the simulation period calculated with the 3PG water balance model (mm), and α_0, α_1, α_2 are parameters whose values are listed in Table 11 (for stocking Eq. 12).

Testing Model Parameters

Final model parameters were tested against an autocorrelation-free dataset to see if they were significantly different from zero. An autocorrelation-free dataset was prepared from the original modeling data by randomly selecting one observation from each of the 746 plots. Parameters for the models of mean top height, basal area, maximum diameter, standard deviation of diameter, and stocking were all found to be significant at the 95-percent confidence level (Tables

Table 10—Difference equation forms for projection of stocking. Initial fitted models including ASW deficit and ASW deficit squared in asymptotic parameter. Original equation forms are listed in Pinjuv (2006).

Difference Equation Forms	Parameter		
	Estimates	MSE	Model
1. $N_2 = \left(N_1^{\,c} + \dfrac{a_0 + a_1 \cdot ASW + a_2 \cdot ASW^2}{10^6} \cdot \left(T_2^{\,b} - T_1^{\,b}\right) \right)^{\left(1/c\right)}$	a_0 a_1 a_2 b c	6.2223 -0.0488 0.000802 1.8863 -0.5192	3285
2. $N_2 = \left(\dfrac{1}{\sqrt{N_1}} + \dfrac{a_0 + a_1 \cdot ASW + a_2 \cdot ASW^2}{10^8} \cdot \left(T_2^{\,b} - T_1^{\,b}\right) \right)^{-2}$	a_0 a_1 a_2 b	652.7 -5.6079 0.0844 1.8991	3283
3. $N_2 = \left(\dfrac{1}{\sqrt{N_1}} + \left(a_0 + a_1 \cdot ASW + a_2 \cdot ASW^2\right) \cdot \left(\left(\dfrac{T_2}{100}\right)^2 - \left(\dfrac{T_1}{100}\right)^2 \right) \right)^{-2}$	a_0 a_1 a_2	0.0462 -0.00035 5.828×10^{-6}	3282
4. $N_2 = N_1 \cdot e^{\left(a_0 + a_1 \cdot ASW + a_2 \cdot ASW^2\right) \cdot (T_2 - T_1)}$	a_0 a_1 a_2	-868.5 10.4256 -0.2191	3488
5. $N_2 = N_1 \cdot \left(\dfrac{T_2}{T_1}\right)^{\left(a_0 + a_1 \cdot ASW + a_2 \cdot ASW^2\right)} \cdot e^{b \cdot (T_2 - T_1)}$	a_0 a_1 a_2 b	0.1773 0.00283 -0.00004 -0.0217	3328
6. $N_2 = N_1 \cdot e^{\left(a_0 + a_1 \cdot ASW + a_2 \cdot ASW^2\right) \cdot \left(T_2^{\,b} - T_1^{\,b}\right)}$	a_0 a_1 a_2 b	-18.2851 0.1299 -0.00310 2.0982	3391

Table 11—Stocking model parameters for equation 12, standard errors, and approximate 95-percent confidence limits calculated with 2,226 degrees of freedom.

Parameter	Estimate	Std. Error	Approximate 95% Confidence Limits	
α_0	0.0462	0.00313	0.0401	0.0524
α_1	-0.00035	0.000119	-0.00058	-0.00012
α_2	5.83E-06	8.13E-07	4.23E-06	7.42E-06

12, 13, 14, 15, and 16).

Model Validation and Comparison with CanSPBL(1.2)

Validation of CanSPBL(water) and CanSPBL(1.2) with a subset of the validation data set presented in chapter 4 of Pinjuv (2006), produced model fitting statistics and residual distribution statistics listed in Tables (17) and Table (18), respectively. CanSPBL(water) showed improvements for most model components of 1.07 percent to 3.77 percent after being updated with an index of root zone water balance. However, CanSPBL(water) showed a -0.78 percent decrease in precision for the component of maximum diameter. CanSPBL(water) also showed less bias in prediction of stocking, and basal area (Table 17). Residual distributions for CanSPBL(water) showed a worse fit overall for skewness and kurtosis, while the hypothesis of normality of residuals was not rejected for both models with the Kolmogorov-Smirnov test (Table 18).

A separate validation was also completed with the same models using long term average climate as inputs into the water balance model. This was done to test how model accuracy might be affected if managers were to estimate future climate using average values. This separate validation of CanSPBL(1.2), and CanSPBL(water_using average climate) produced model fitting statistics and residual distribution statistics listed in Tables (19 and 20), respectively. CanSPBL(water_using average climate) showed improvements for most model components of 0.47 percent to 7.81 percent after being updated with an index of root zone water balance that uses average climate inputs. However, CanSPBL(water_using average climate) showed a -0.13 decrease in precision for the component of maximum diameter. These results indicate that model accuracy for the prediction of stocking, basal area, and maximum diameter would actually increase precision using
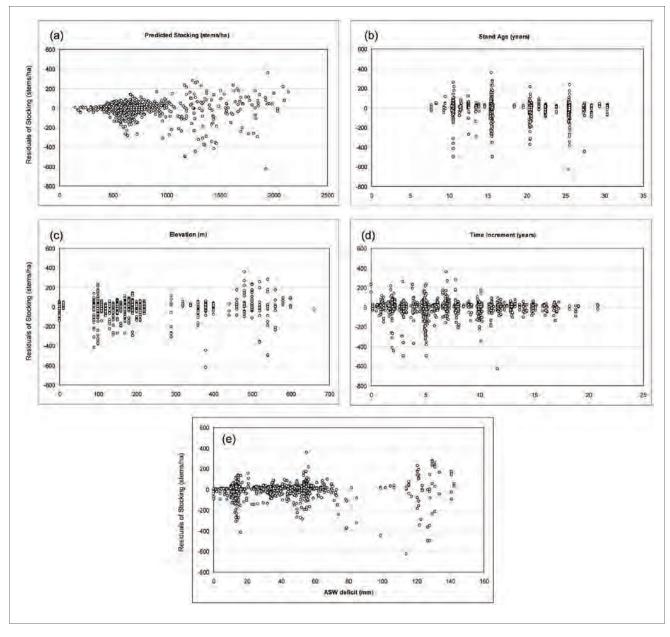
*Figure 6: Residuals patterns of final model for stocking: (a) residuals versus predicted, (b) residuals versus stand age, (c) residuals versus elevation, (d) residuals versus time increment, and (e) residuals versus ASW deficit.*

average climate inputs as opposed to those that describe yearly variations. CanSPBL(water_using average climate) showed less bias in prediction of stocking, basal area, and maximum diameter than did CanSPBL(water) (Table 17 and Table 19). Residual distributions for CanSPBL(water_using average climate) showed a worse fit overall for skewness and kurtosis in comparison to CanSPBL(1.2), with the exceptions of skewness for basal area and mean top height. The hypothesis of normality of residuals was not rejected for CanSPBL(water_using average climate) with the Kolmogo-

rov-Smirnov test (Table 20). Although the distributions of residuals for CanSPBL(water_using average climate) are better on average than CanSPBL(water).

DISCUSSION

Incorporating ASW deficit into equations that predict basal area, mean top height, standard deviation of diameter, and stocking in the growth and yield model CanSPBL(1.2) showed a small, improvement in model accuracy (Table 17). There was somewhat of an increased precision for

Table 12— Basal area model parameters for equation 8, standard errors, and approximate 95-percent confidence limits tested with an autocorrelation-free dataset with 745 degrees of freedom.

Parameter	Estimate	Std. Error	Approximate 95% Confidence Limits	
β	0.153	0.00419	0.1448	0.1612
γ	0.00241	0.00008	0.00226	0.00257
α_0	43663.9	451.9	42776.7	44551.0
α_1	0.0355	0.00147	0.0326	0.0383
α_2	-36.2397	4.3294	-44.7393	-27.7401
α_3	56.5576	10.2484	36.4378	76.6774
α_4	-0.5827	0.0901	-0.7596	-0.4058

Table 13—Mean top height model parameters for equation 9, standard errors, and approximate 95-percent confidence limits tested with an autocorrelation-free dataset with 745 degrees of freedom.

Parameter	Estimate	Std. Error	Approximate 95% Confidence Limits	
β	8.1675	1.6642	4.9002	11.4347
γ	1.0427	0.1488	0.7506	1.3349
α_0	4181.0	965.0	39586.6	43375.4
α_1	0.0214	0.00177	0.018	0.0249
α_2	-39.6227	4.5143	-48.4852	-30.7601
α_3	22.6608	8.0674	6.8228	38.4989
α_4	-0.2664	0.0723	-0.4083	-0.1246

Table 14—Maximum diameter model parameters for equation 10, standard errors, and approximate 95-percent confidence limits tested with an autocorrelation-free dataset with 745 degrees of freedom.

Parameter	Estimate	Std. Error	Approximate 95% Confidence Limits	
β	0.7474	0.2499	0.2568	1.2381
γ	0.2681	0.0761	0.1187	0.4175
α_0	77.1989	9.9047	57.7539	96.644
α_1	0.000192	0.000031	0.00013	0.000253
α_2	-0.2677	0.0515	-0.3688	-0.1665
α_3	0.00127	0.000349	0.000587	0.00196

This result was surprising in the context of varying climate over the study area. With yield modeling the results could have been markedly more significant, as the growing condition of the site is not implicit in initial stem size (as is used in the difference approach). This result highlights the power of the different modeling approaches within and between regions with varying climatic and site conditions.

Validation with average climatic inputs surprisingly increased precision of the models that predict stocking, basal area, and maximum diameter. Predicted stocking showed the largest reduction of residual mean square error, at 7.81 percent using average climate. This result is positive for forest managers who may only have average climate available to run such models. As regions vary in climate, taking this into account can result in small gains in accuracy.

The updated version of the model included both ASW deficit and a simplified form of elevation. This result indicates that the effect of elevation in the Canterbury region describes more than water relations on the site and may be a proxy for other site factors such as nutrient availability, or possibly average temperature.

The data required to run the water balance model are monthly values of maximum temperature, minimum temperature, solar radiation, vapor pressure deficit, leaf area index, rainfall, soil type, initial estimates of available soil water, maximum available soil water, and minimum available soil water. Obtaining these inputs for a given forest can be time-consuming and expensive and may not warrant the 1 –8 percent improvement in accuracy that these models offer. There is also the issue of even lower precision for the models of mean top height and standard deviation of diameter using average values of

longer intervals shown in residual plots (Figures 2, 3, 4, and particularly Figure 6). This effect may have been due to the leveling of the water balance models' precision, increasing with time of simulation. If initial water balance estimates are different from measurements, they become more precise over time for months following initialization, and this may affect growth and yield model precision for shorter measurement intervals. The results of this study show a relatively small improvement in model accuracy and growth pattern including ASW deficit into the models.

Table 15—Standard deviation of diameter model parameters for equation 11, standard errors, and approximate 95-percent confidence limits tested with an autocorrelation-free dataset with 745 degrees of freedom.

Parameter	Estimate	Std. Error	Approximate 95% Confidence Limits	
β	0.0649	0.00372	0.0576	0.0722
γ	0.000382	0.000122	0.000143	0.000622
α_0	26173.8	988.9	24232.3	28115.2
α_1	0.0232	0.00247	0.0183	0.028
α_2	-59.269	8.4106	-75.7807	-42.7573
α_3	-40.3089	15.4589	-70.6581	-9.9598
α_4	0.2613	0.1126	0.0402	0.4823

Table 16—Mortality model parameters for equation 12, standard errors, and approximate 95-percent confidence limits tested with an autocorrelation-free dataset with 745 degrees of freedom.

Parameter	Estimate	Std. Error	Approximate 95% Confidence Limits	
α_0	0.047	0.00567	0.0359	0.0582
α_1	-0.00048	0.000214	-0.0009	-0.00006
α_2	9.87E-06	1.58E-06	6.77E-06	1.30E-05

climatic inputs to describe future conditions where monthly and yearly variation may not be available. The increase in model accuracy for the models of mean top height and standard deviation of diameter using inputs that including monthly and yearly variation are 2.95 percent and 1.07 percent, respectively. There is a decrease in precision for the models of mean top height and standard deviation of diameter to 2.57 percent and 0.47 percent, respectively, using average monthly climatic inputs. These results suggest model accuracy may be maximized by using average monthly inputs for some models and including monthly and yearly variation for the inputs of the models of mean top height and standard deviation of diameter. Model precision could be increased further by considering the effect of drought only in months where growth is likely to occur. Drought in the winter months may not have the same effect on growth as drought that occurred during the growing season. Future research in this area could focus on trying to add a weight to ASW deficits according to the month in which they occur.

CONCLUSIONS

Model components of mean top height, basal area per hectare, stems per hectare, and diameter distribution were developed by using non linear least squares regression techniques to select appropriate equation forms. Explanatory variables to improve model prediction were tested and incorporated into models where appropriate. The effect of elevation, and ASW deficit was added to models of mean top height, basal area, and diameter distribution, only the effect of ASW deficit was added to the model of mortality. A polymorphic Gompertz equation displayed the best fit for basal area, while a polymorphic Schumacher equation displayed the best fit for mean top height. The diameter distribution model of maximum diameter displayed the best fit with a polymorphic Weibull equation, while the standard deviation of diameter model fit best with a polymorphic Gompertz equation.

A mortality severity index based on the -3/2 power law was used as a basis to filter the modeling data set for mortality and a final model was built with 80 percent of the original mortality records under the recommendation of managers at SPBL. Residual mean square error for the model of stocking was decreased by 2.84 percent by incorporating ASW deficit calculated by the equation (13). Residual mean square error was reduced further by 7.8 percent by using average climatic inputs. Ninety-five percent (greater than 2.5 percent and less than 97.5 percent) of residuals were within ± 116 stems / ha for projection lengths of up to 21 years using monthly climatic inputs that show yearly variation, and within ± 92 stems / ha using average climatic inputs. Future stocking is dependent on the current stocking (stems / ha), initial stand age (years), final stand age (years), elevation squared (m^2), ASW deficit (mm), and ASW deficit squared (mm^2).

$$N_2 = \left(\frac{1}{\sqrt{N_1}} + \left(\alpha_0 + \alpha_1 \cdot ASW + \alpha_2 \cdot ASW^2 \right) \cdot \left(\left(\frac{T_2}{100} \right)^2 - \left(\frac{T_1}{100} \right)^2 \right) \right)^{-2} \qquad (13)$$

All model parameters were tested against an autocorrelation free dataset for significance. Tests showed that all parameters were significant at a 95-percent confidence level. The entire updated version of the model CanSPBL(water)

Table 17— Comparison of model statistics between CanSPBL(1.2), and CanSPBL2(water). Statistics shown include Mean Square Error (MSE), Average Model Bias (AMB), Model Efficiency Factor (EF), and percent difference of MSE (% Difference of MSE) n = 967.

Model		Model Fitting Statistics			
		MSE	AMB	EF	MSE % Difference
CanSPBL(1.2)	Stocking	2154.92	6.51	0.95	2.84
	Basal Area	17.93	0.55	0..96	3.77
	Mean Top Height	1.10	0.08	0.96	2.95
	Maximum Diameter	5.60	0.27	0..93	-0.78
	Standard Deviation of Diameter	0.53	0.04	0.86	1.07
CanSPBL2 (water)	Stocking	2094.63	1.96	0.96	-2.84
	Basal Area	17.27	0.45	0.96	-3.77
	Mean Top Height	1.07	0.05	0.96	-2.95
	Maximum Diameter	5.64	0.27	0.93	0.78
	Standard Deviation of Diameter	0.52	0.04	0.86	-1.07

Table 18—Model normality distribution statistics for CanSPBL(1.2), and CanSPBL2(water) in terms of skewness, kurtosis, and p-value from the Kolmogorov-Smirnov test for normality n = 967.

Model		Residual Distribution Statistics		
		Skewness	Kurtosis	P-value
CanSPBL(1.2)	Stocking	-1.01	11.05	0.01
	Basal Area	0.42	3.74	0.01
	Mean Top Height	0.13	0.96	0.01
	Maximum Diameter	1.15	4.73	0.01
	Standard Deviation of Diameter	1.22	7.33	0.01
CanSPBL2 (water)	Stocking	-2.80	14.02	0.01
	Basal Area	0.22	4.05	0.01
	Mean Top Height	-0.02	1.10	0.01
	Maximum Diameter	1.19	4.84	0.01
	Standard Deviation of Diameter	1.20	7.35	0.01

was validated against an independent data set and compared to the original CanSPBL(1.2). CanSPBL(water) showed improvements in MSE of 1 percent to 3 percent after the effects of ASW deficit were incorporated into the model,

however the model of maximum diameter showed a worse fit by 0.78 percent.

Residual distributions for CanSPBL(water) showed a worse fit overall for skewness and kurtosis. The hypothesis of normality was not rejected for both models using the Kolmogorov-Smirnov test.

Residual mean square error for the model of basal area was reduced by 3.77 percent by incorporating ASW deficit calculated by the equation (14). Ninety-five percent (greater than 2.5 percent and less than 97.5 percent) of residuals were within $\pm$ 8.7 m^2 / ha for projection lengths of up to 21 years using monthly climatic inputs that show yearly variation, and within $\pm$ 8.8 m^2 / ha using average climatic inputs. Future basal area is dependent on the current stand basal area (m^2 / ha), initial stand age (years), final stand age (years), elevation squared (m^2), a binary indicator variable X (X = 0 if elevation < 450, and X = 1 if elevation $\geq$ 450), ASW deficit (mm), and ASW deficit squared (mm^2).

$$G_2 = e^{\left(\ln(G_1)e^{\left(-\beta \cdot (T_2 - T_1) + \gamma \cdot \left(T_2^2 - T_1^2\right)\right)} + \frac{\left(\alpha_0 + \alpha_1 \cdot elev^2 + \alpha_2 \cdot \left((elev - 450)X\right) + \alpha_3 \cdot ASW + \alpha_4 \cdot ASW^2\right)}{10000} \left(1 - e^{\left(-\beta \cdot (T_2 - T_1) + \gamma \cdot \left(T_2^2 - T_1^2\right)\right)}\right) \right)} \tag{14}$$

Residual mean square error for the model of mean top height was reduced by 2.95 percent by incorporating ASW deficit calculated by the equation (15). Ninety-five percent (greater than 2.5 percent and less than 97.5 percent) of residuals were within $\pm$ 2.1 m for projection lengths of up to 21 years using monthly climatic inputs that show yearly variation, and within $\pm$ 2.2 m using average climatic inputs. Future mean top height is dependent on the current mean top height (m), initial stand age (years), final stand age (years), elevation (m), elevation squared (m^2), a binary indicator variable X (X = 0 if elevation < 450, and X = 1 if elevation $\geq$ 450), ASW deficit (mm), and ASW deficit squared (mm^2).

Table 19—Comparison of model statistics between CanSPBL(1.2), and CanSPBL2(water) (using average climate inputs). Statistics shown include Mean Square Error (MSE), Average Model Bias (AMB), Model Efficiency Factor (EF), and percent difference of MSE (% Difference of MSE) n = 967.

Model		Model Fitting Statistics			
		MSE	AMB	EF	MSE % Difference
CanSPBL(1.2)	Stocking	2154.92	6.51	0.95	7.81
	Basal Area	17.93	0.55	0..96	3.82
	Mean Top Height	1.10	0.08	0.96	2.57
	Maximum Diameter	5.60	0.27	0..93	-0.13
	Standard Deviation of Diameter	0.53	0.04	0.86	0.47
CanSPBL2 (water) using average climate inputs	Stocking	1992.87	3.11	0.96	-7.81
	Basal Area	17.26	0.51	0.96	-3.82
	Mean Top Height	1.07	0.08	0.96	-2.57
	Maximum Diameter	5.60	0.24	0.93	0.13
	Standard Deviation of Diameter	0.52	0.05	0.86	-0.47

Table 20—Normality distribution statistics for CanSPBL(1.2) and CanSPBL2 (water; average climate inputs): skewness, kurtosis, and p-value from the Kolmogorov-Smirnov test for normality n = 967.

Model		Residual Distribution Statistics		
		Skewness	Kurtosis	P-value
CanSPBL (1.2)	Stocking	-1.01	11.05	0.01
	Basal Area	0.42	3.74	0.01
	Mean Top Height	0.13	0.96	0.01
	Maximum Diameter	1.15	4.73	0.01
	Standard Deviation of Diameter	1.22	7.33	0.01
CanSPBL2 (water) using average climate inputs	Stocking	-2.57	12.53	0.01
	Basal Area	0.27	4.12	0.01
	Mean Top Height	0.02	1.04	0.01
	Maximum Diameter	1.16	4.73	0.01
	Standard Deviation of Diameter	1.25	7.62	0.01

$$MTH_2 = e^{\ln(MTH_1)\left(\frac{T_1+\gamma}{T_2+\gamma}\right)^{\beta}+} $$
$$\frac{\left(\alpha_0+\alpha_1\cdot elev^2+\alpha_2\cdot(elev-450)\cdot X+\alpha_3\cdot ASW+\alpha_4\cdot ASW^2\right)}{10000} \cdot$$
$$\left(1-\left(\frac{T_1+\gamma}{T_2+\gamma}\right)^{\beta}\right) \tag{15}$$

Residual mean square error for the model of maximum diameter was increased by 0.78 percent by incorporating ASW deficit calculated by the equation (16). Ninety-five percent (greater than 2.5 percent and less than 97.5 percent) of residuals were within ± 5 cm for projection lengths of up to 21 years using monthly climatic inputs that show yearly variation, and within ± 5 cm using average climatic inputs. Future maximum diameter is dependent on the current maximum diameter (cm), initial stand age (years), final stand age (years), elevation squared (m^2), a binary indicator variable X (X = 0 if elevation < 450, and X = 1 if elevation ≥ 450), the inverse of initial stocking (ha / stems), and ASW deficit squared (mm^2).

$$DMAX_2 = DMAX_1 \cdot e^{\left(-\beta\cdot\left(T_2^\gamma - T_1^\gamma\right)\right)} +$$
$$\left(\alpha_0 + \alpha_1\cdot elev^2 + \alpha_2\cdot(elev-450)\cdot\right.$$
$$\left. X + \alpha_3\cdot\frac{1}{N_1} + \alpha_4\cdot ASW^2\right)\cdot \tag{16}$$
$$\left(1-e^{\left(-\beta\cdot\left(T_2^\gamma - T_1^\gamma\right)\right)}\right)$$

Residual mean square error for the model of standard deviation of diameter was decreased by 1.07 percent by incorporating ASW deficit calculated by the equation (17). Ninety-five percent (greater than 2.5 percent and less than 97.5 percent) of residuals were within ± 1.5 cm for projection lengths of up to 21 years using monthly climatic inputs that show yearly variation, and within ± 1.5 cm using average climatic inputs. Future standard deviation of diameter is dependent on the current standard deviation of diameter (cm), initial stand age (years), final stand age (years), elevation squared (m^2), a binary indicator variable X (X = 0 if elevation < 450, and X = 1 if elevation ≥ 450), ASW deficit (mm), and ASW deficit squared (mm^2).

$$DSTD_2 = e^{\left[\ln(DSTD_1)\cdot e^{\left(-\beta\cdot(T_2-T_1)+\gamma\cdot\left(T_2^2-T_1^2\right)\right)}\right]}\cdot$$
$$e^{\left[\frac{\left(\alpha_0+\alpha_1\cdot elev^2+\alpha_2\cdot(elev-450)\cdot X+\alpha_3\cdot ASW+\alpha_4\cdot ASW^2\right)}{10000}\right.}$$
$$\left.\left(1-e^{\left(-\beta\cdot(T_2-T_1)+\gamma\left(T_2^2-T_1^2\right)\right)}\right)\right] \tag{17}$$

LITERATURE CITED

Arneth, A.; Kelliher, F.M.; McSeveny, T.M.; Byers, J.N. 1998. Carbon and water fluxes in a *Pinus radiata* forest subject to soil water deficit. Australian Journal of Plant Physiology 25: 557-570.

Barringer, J.; Wilde, H.; Willoughby, J.; [et al.].1998. Restructuring the New Zealand land resource inventory to meet the changing needs for spatial information in environmental research and management. Presented at the 10'th colloquium of the spatial information research centre, University of Otago, New Zealand. 16 – 19 November, 1998.

Boomsma, D.B.; Hunter, I.R. 1990. Effects of water, nutrients and their interactions on tree growth, and plantation forest management practices in Australasia: a review. Forest Ecology and Management 3: 455–476.

Clutter, J.L.; Fortson, J.C.; Pienaar, L.V.; [et al.]. 1983. Timber management: a quantitative approach, New York, John Wiley and Sons. 333 pages.

Landsberg, J.J.; Gower, S.T. 1997. Applications of physiological ecology to forest management. Academic Press, San Diego, CA. p. 354.

Landsberg, J.J.; Waring, R.H. 1997. A generalized model of forest productivity using simplified concepts of radiation use efficiency, carbon balance and partitioning. Forest Ecology and Management 95: 209–228.

Leathwick, J.R; Stephens, R.T.T. 1998. Climate surfaces for New Zealand. Landcare Res. Contract Report LC9798/126. Landcare Research, Lincoln, New Zealand. 19pp.

Pinjuv, G.L. 2006. Hybrid forest modelling of *Pinus radiata* D. Don in Canterbury, New Zealand. Forestry thesis for Ph.D. School of Forestry, University of Canterbury, 198 pp.

Sands, P.J.; Landsberg, J.J. 2002. Parameterisation of 3-PG or plantation-grown Eucalyptus globulus. Forest Ecology and Management 163: 273–292.

SAS Institute Inc., 2001, SAS/STAT user's guide, version 8, Cary, NC.

Snowdon, P.; Jovanovic, T.; Booth, T.H. 1999. Incorporation of indices of annual climatic variation into growth models for *Pinus radiata*. Forest Ecology and Management 117: 187-197.

Tickle, P.K.; Coops, N.C.; Hafner, S,D. 2001. Comparison of a forest process model (3-PG) with growth and yield models to predict productivity at Bago State Forest, NSW. Australian Forestry 64(2): 111-122.

West, P.W.; Ratkowsky, D.A.; Davis, A.W. 1984. Problems of hypothesis testing of regressions with multiple measurements from individual sampling units. Forest Ecology and Management 7(3): 207-224.

Zhao, W. 1999. Growth and yield modelling of *Pinus radiata* in Canterbury. New Zealand. Forestry thesis for PhD, School of Forestry, University of Canterbury. 192 pages.

Increased Self-Shading with Tree Size and Increased Wood Density with Diameter Explain Some of the Observed Size-Related Decline in Forest Productivity

Remko A. Duursma and Annikki Mäkelä

ABSTRACT

THE DECLINE IN NET PRIMARY PRODUCTION (NPP) of forests with stand age is a ubiquitous phenomenon, and many hypotheses have been set out to explain this decline. The most popular hypotheses; increased fraction of respiration with tree size, and increased hydraulic constraints on stomatal conductance; have been shown to explain a varying portion, but usually not all of this decline. Here, we quantify the contributions of two additional hypotheses: 1) self-shading of foliage in tree crowns increases with the size of tree crowns and 2) increased wood density with increasing diameter increases the apparent decline in productivity.

Based on simulation experiments (Duursma and Mäkelä 2007), our previous work has shown that the ratio of tree leaf area to the surface of the crown envelope (LA/SA) determines self-shading and efficiency of foliage. Higher values of the LA/SA ratio mean more densely packed crowns, with a decreasing average light intensity on leaves and therefore lower photosynthetic production. Total leaf area and crown surface area are interrelated as $LA \propto SA^{z/2}$, where z is the fractal dimension of leaf area, and z is larger than 2 for a wide range of forest tree species, leading to a gradually increasing LA/SA with tree development.
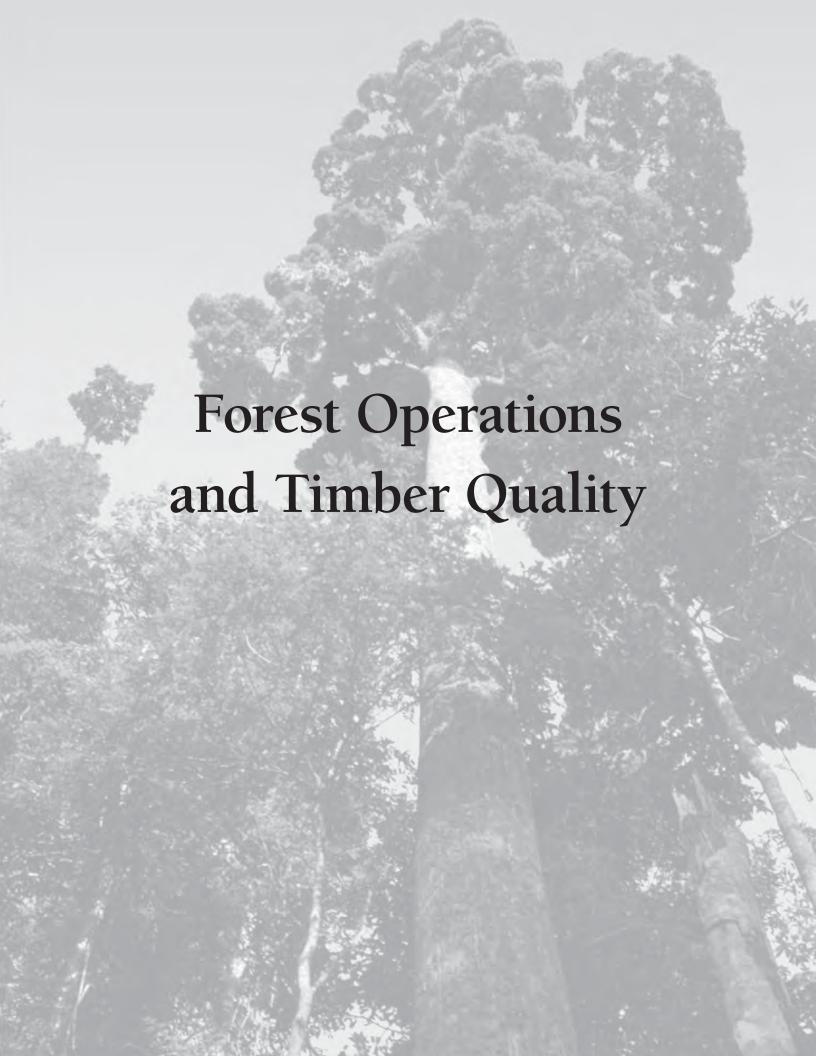
In conifers, wood basic density typically increases with increasing distance from the pith. If this pattern is not accounted for, apparent decline in productivity based on measurements of wood volume would be exaggerated. For Scots pine and Norway spruce in Finland, these relationships are well established.

We incorporate both these relationships in a forest growth model (CROBAS, Mäkelä 1997) and quantify the decline in NPP and wood volume growth as a result of increased self-shading over stand development, and increased wood density. The results indicate that this decline is significant, but does not by itself explain the commonly observed decline in NPP.

Remko Duursma (remkoduursma@gmail.com) was a postdoctoral research fellow and **Annikki Mäkelä** is professor of silviculture (forest production) in the Department of Forest Ecology, University of Helsinki, PO Box 27 (Latokartanonkaari 7), 00014 Helsinki, Finland.

Forest Operations and Timber Quality

Forest Operations and Timber Quality

Keynote Presentation

INFLUENCE OF FOREST OPERATIONS ON TIMBER QUALITY

Dennis P. Dykstra

ABSTRACT

The emphasis in many forested regions has shifted from large, older trees to young trees that are not only smaller but also much different in character. Both mills and forest operations have had to adjust to this shift. This adjustment has perhaps been more effective in the mills, where conditions can be controlled and it is possible to take full advantage of new developments in computer and scanner technologies. Increased mechanization has also occurred in forest operations, although the evolution has been less dramatic due to limitations imposed by the many timber and terrain conditions operators must accommodate. In the context of thinning operations, timber quality issues of particular importance include damage to the logs being harvested and damage to the residual trees that will make up the stand being managed as a future timber crop. Both of these issues are influenced by the equipment and logging methods used and by a range of other factors that are only partly under the operator's control.

KEYWORDS: Small logs, mechanized harvesting, logging damage, thinning operations

INTRODUCTION

OVER THE PAST SEVERAL DECADES, UTILIZATION of timber in many parts of the world has shifted from an emphasis on large, older trees to much younger, quickly grown trees. The trees now being harvested are often grown from planted stock rather than from natural regeneration. In order to increase the growth rates of selected trees, thinnings are often conducted at various stages during the development of the stand. In drier forest areas, such as the inland regions of the western United States, wildfire hazard has become a major issue as human populations living in and near forests have increased. In these forests, small-diameter trees are often removed in an effort to reduce fire hazard, particularly around populated areas. To the extent possible, it is desirable to utilize some of the wood from trees harvested during thinnings in order to offset some of the costs of the thinning operations. This is true regardless of whether the purpose of the thinning is to increase growth rates on residual trees or to reduce fire hazard. In either case, the immature trees being removed pose significant problems for handling and utilization.

The timber industry has quickly adapted to reduced log sizes in spite of the fact that small logs create substantial problems for handling and transport as well as for conversion into solid-wood products such as lumber. Highly automated sawmills introduced within the past few years are capable of rapidly processing small-diameter logs into lumber and other products. Sawing machinery is able to compensate for sweep by sawing along the curve and by turning the log to best advantage. Sensors read the diameter and a variety of other measurements along the length of

Dennis P. Dykstra (ddykstra@fs.fed.us) is a research forest products technologist, Pacific Northwest Research Station, P.O. Box 3890, Portland, OR 97208-3890, USA.

the log as it enters the saw box, while computers determine the best orientation of the log and the best settings for the multiple saws and chipping heads that convert the log into lumber and pulp chips. These settings can be adjusted as market conditions change in order to maximize the potential revenue from each log.

Harvesting equipment and methodologies have also changed in order to accommodate smaller logs, although the problems encountered in harvesting are somewhat more difficult than those in a mill because of remote location, variable topography and timber conditions, and factors such as weather that cannot be controlled. Harvesting systems are increasingly becoming mechanized in order to deal with the large number of small logs that must be handled and processed. Where terrain permits, mechanized harvesters that fell and delimb trees and cut the stems into logs are commonly used. The processor head on the harvesting machine is able to measure the length and diameter of the stem at any point, and computers are used to help determine the log lengths that will meet mill requirements or maximize revenues to the landowner. On steeper terrain, cable or helicopter yarding systems are typically required but these can be coupled with harvesting machines (Drews et al. 2001) or with processors stationed at the landing to process the stems into logs. Like the saw settings in a mill, the logic related to bucking decisions on harvesting machines and processors can be adjusted to accommodate changing market conditions so that each log provides the maximum revenue to the landowner and the harvesting operator.

Two timber-quality issues related to small logs are particularly important from the perspective of forest operations. First, small logs tend to break or suffer significant damage more easily than larger logs. Second, thinning operations may result in damage to residual trees caused by the harvesting equipment or by contact between harvested stems and residual trees. Each of these issues has implications for forest operations and for utilization of the harvested timber.

DAMAGE TO LOGS

Although small logs are generally more flexible than large logs, they are also more easily broken by heavy equipment or improper handling during harvesting and transport operations or at the mill. In the forest, broken logs may simply have to be left behind because their reduced value will not justify the cost of removing them from the site.

If a broken log is long enough it may be possible to buck it into shorter pieces while removing the broken section. This may reduce the value because each log then has a suboptimal length, and will result in handling two logs rather than one so the handling and transportation costs will increase. It also adds the cost of an additional bucking operation, which often must be done manually.

When logs are broken at the mill, some value can usually be recovered by whole-log chipping if the broken pieces are shorter than the mill's minimum processing length. However, chip prices are often far below lumber prices so the value of the chipped log may be less than the harvesting and transportation costs that have already been incurred. In addition, some species have dark heartwood that is undesirable for pulp, so chip buyers may reject whole-log chips from those species or restrict them to a percentage of the total chip volume (Zhu et al. 2007).

Surprisingly, even though virtually all logging operations involve some breakage or damage to logs (Figure 1), very few studies have quantified these effects. Surveys done over large areas, such as the Forest Service's periodic Resource Planning Act assessment reports (e.g., Smith et al. 2004), often provide regional-level estimates of logging residues. However, this information is seldom disaggregated into the

Figure 1. A Bolivian forester inspects a mahogany tree (Swietenia macrophylla) *that was destroyed by improper felling. In spite of the fact that mahogany wood is exceptionally valuable as a source of appearance-grade lumber and veneer, after being split during felling this tree did not retain sufficient value to justify taking it out of the forest.*

component parts so it is not possible to determine what portion may be due to breakage or log damage.

One of the few studies to have quantified damage to logs during logging operations is Wang et al. (2004), which assessed log damage associated with four hardwood logging operations in north-central West Virginia. About 6 percent of logs were reportedly damaged on the operations. Types of damage included gouging, splitting, slabbing, and abrasion (scraping) as well as breakage. Crushing caused by grapples or chain chokers was also observed, although it was relatively minor. Altogether, the volume loss from log damage was four times greater on the two operations utilizing chainsaw felling and skidders than on the other two operations utilizing felling machines and skidders. For the chainsaw operations the greatest share of the damage occurred during felling, with smaller amounts recorded during skidding, decking, and loading operations. On the felling-machine operations the damage was split more evenly among felling, skidding, decking, and loading. Both felling machines were fitted with saw heads rather than shears, which is probably significant. Other studies (e.g., Greene and McNeel 1989) have shown that felling damage associated with the use of shears can result in substantial losses when the butt log is later sawn into lumber.

Some of the log damage in the study by Wang et al. (2004) was species-related, with more brittle species tending to exhibit larger volume losses. There were also significant differences among log size classes, with smaller logs suffering much higher volume losses than large logs. This is due to the fact that a split or gouge of a fixed size represents a larger portion of a small log than it would on a large log. Small logs are also more likely to be crushed if run over by heavy machinery.

DAMAGE TO RESIDUAL TREES

Another important timber-quality issue related to forest operations is damage to residual trees caused by harvesting equipment or by contact between harvested stems and residual trees. In contrast to the scarcity of published information on damage to logs during logging operations, a great many studies have quantified logging damage to residual trees. This is because such damage can influence the quality of timber in the final crop trees and also can impact resources other than timber. In this paper the focus is on damage to residual trees resulting from thinning operations.

Types of damage to residual trees that are typically identified in logging studies include bark damage, deep bole wounds, crown damage, stem breakage, and root damage. In some hardwood species, abrasion of bark when a felled tree rubs along the bole of a residual tree may lead to widespread epicormic branching and consequently to a proliferation of pinhole knots (Meadows and Skojac 2006). This can significantly devalue appearance-grade lumber or veneer.

Bark damage (Figure 2) is often a relatively minor type of injury unless the wound is large, but even small injuries can permit the introduction of insects or decay fungi (Aho et al. 1983). Thin-barked or loose-barked species are particularly prone to bark injuries and non-resinous species are especially susceptible to infection by fungi. Depending on the length of time that elapses from when the damage occurs until the residual tree is harvested, volume and value losses due to discoloration or decay may occur when the tree is converted into lumber or veneer.

Deep bole wounds are usually regarded as more serious than bark damage because they are often associated with permanent scarring, gouging, or other defects that will

Figure 2. Bark damage on a young Douglas-fir (Pseudotsuga menziesii). If the tree survives it is likely to sustain a substantial volume or value loss in the butt log due to discoloration, pitch seams, and decay.

degrade lumber or have to be trimmed out entirely. They are also more likely to permit the introduction of decay fungi and insects, followed by loss of vigor or even the death of the tree.

Trees can usually survive crown damage except in extreme cases. However, significant crown damage may lead to loss of vigor and thus prevent the tree from achieving the desired growth rate after thinning.

Stem breakage usually results in the death of the tree or deforms it so that it is no longer useful as a crop tree. In hardwood species stem breakage may induce sprouting, and this can be regarded as either good or bad depending on the type of thinning and the management objectives for the stand.

Root damage may structurally weaken the tree so that it is more susceptible to windthrow, and damaged roots are likely to serve as conduits for the introduction of root rot. This type of damage is almost always caused by heavy machinery, especially when crawler tractors are used for skidding.

Stage when Damage Occurs

Damage to residual trees can occur at any stage of a logging operation. Unfortunately, studies in temperate forests typically report only overall results without disaggregating them to the stage when damage occurred. This is regrettable because research in tropical forests strongly suggests that, in those forests, by far the most severe damage occurs during felling (e.g., see Pinard and Putz 1996). This is probably because tropical tree crowns are large and frequently interwoven with vines that connect them to adjacent trees. The situation in temperate forests is usually different but

even so, observation suggests that felling damage can be substantial. Unfortunately, where felling damage has been studied separately (for instance, Sirén 2001), the studies do not report yarding or forwarding damage so comparisons are not possible.

Avoiding Damage during Felling Operations

Felling damage is caused by contact between the crown or stem of the tree being felled and the crowns or stems of nearby residual trees. Comparisons between manual and mechanized felling (e.g., see Spinelli 2004) suggest that mechanized felling is far more effective at avoiding damage because felling machines have better control over the direction a tree falls, even if chainsaw operators use the best directional felling techniques. Mechanized felling is not always feasible, however, when trees are large or the operation is located in steep terrain. Felling also influences subsequent yarding damage because proper alignment of felled trees with respect to the extraction route can reduce damage to trees near the extraction corridor. Postponing operations during bad weather and during periods when sap is flowing heavily can often reduce felling damage.

Damage in Cut-to-Length Harvesting

Cut-to-length harvesting typically involves two machines working together in a coordinated operation. A harvesting machine fells the trees, delimbs the stems, processes them into accurately measured logs, and bunches them at the stump. Then a forwarder collects the logs and transports them to a landing where they are decked and loaded onto trucks for delivery to the mill (Figure 3). Forwarders are

Figure 3. Left image: *Harvesting machine processing a tree into logs in a thinning operation.* Right image: *Forwarder at the landing with a load of logs.*

built like off-road trucks onto which the logs are loaded by a crane mounted on the forwarder itself. Skidders, unlike forwarders, drag the logs along the ground behind them. Forwarders are limited in that they can only be used with shortwood systems; skidders are required when whole trees or full stems are being yarded. Studies of cut-to-length harvesting suggest that the frequency of damage to residual trees is relatively high, with up to half the residual trees being injured, but that the damage is generally limited to minor bark injuries (Han and Kellogg 2000, Sirén 2001, Drews et al. 2001). Other studies have found that fewer than15 percent of residual trees are damaged in cut-to-length operations (e.g., Sauter and Gengle 1995). The difference in these findings may be explained by the way damage is assessed, coupled with differences in the level of operator skill as well as local timber and terrain conditions. In any case, most of the damage in cut-to-length harvesting probably occurs during the felling and processing phase, although few studies disaggregate overall damage so it is not possible to know for certain. Sirén (2001) reported that 90 percent of the damage associated with cut-to-length harvesting occurred while felled stems were being delimbed and processed into logs and only 10 percent occurred during felling itself. His study did not include damage associated with the forwarding phase of the operation.

Avoiding Extraction Damage

In addition to the forwarders used with cut-to-length harvesting, common yarding systems include skidders (both rubber-tired, articulated skidders and crawler tractors), which drag logs behind them, and cable yarding systems that utilize suspended cables to convey logs from the felling site to a landing. Helicopter yarding is less commonly used in thinnings but is an additional possibility where special considerations require the use of a yarding system that must fly over obstacles or produce essentially no ground disturbance.

Comparative studies suggest that, other things being equal, ground-skidding systems can be expected to produce more damage to residual trees than skyline or helicopter systems (e.g., Han and Kellogg 2000). The damage is also generally lower on the bole and includes a higher incidence of root damage. Damage to residual trees on cable yarding operations tends to be concentrated along cableways, and some trees adjacent to the corridor may suffer severe gouging due to multiple incidents of contact with stems being removed. Fan-shaped cable settings typically result in a

higher degree of damage to trees located near the landing as compared to settings where the cableways are laid out in parallel strips. Cable yarding is more likely to produce crown damage than ground-based yarding. Helicopter yarding generally results in very little damage to residual trees, although some crown and bark damage (primarily to the upper bole) have been reported.

The following guidelines have been suggested for avoiding damage to residual trees during extraction:

- Emphasize the importance of minimizing damage to residual trees to loggers. Otherwise, they may not realize that this is an important consideration.
- Do not allow logging during periods of the year when sap is flowing and bark is loose. At these times trees are easier to wound and injuries tend to be larger.
- Mark residual trees where feasible so that the logging crews can easily see them.
- Clearly flag skidtrails, forwarder routes, and skyline corridors in advance of felling so that the felling crew can directionally fall trees toward the extraction routes. Reflagging may be required after the trees have been felled so that the extraction routes are clearly visible to the yarding crew.
- Ensure that no crop trees are left inside extraction routes.
- Cut stumps low to the ground in order to prevent hang-ups in cable yarding or damage to nearby trees in ground skidding as the skidder drives over the stump. Contact with a high stump may cause the skidder to lurch sideways into a crop tree.
- Minimize blading of skidtrails in order to avoid root damage.
- Space skidtrails or harvester trails close enough that it is feasible for the machines to stay on the trail.
- In cable yarding, use parallel rather than fan-shaped settings where possible.
- Keep skidtrails as straight as possible and avoid sharp turns.
- In situations where damage to a crop tree seems almost inevitable (for instance, near a skidtrail), leave several nearby trees standing as protection. These buffer trees can be cut and removed as a last step.
- In ground-based yarding operations, short-log removal will almost always reduce damage to residual trees compared to whole-tree or tree-length removal. Timber purchasers may prefer longer pieces so that bucking decisions can be made in the mill rather than

in the woods. There is thus a tension between what is best for the forest and what might be best for the mill.

CONCLUDING REMARKS

Few thinning operations are totally free of damage to the logs being removed or to the future crop trees left standing. Yet this should be the goal. High-quality timber can maximize revenues to landowners and provide optimal resources to the timber industry.

Published research on damage to logs removed from thinnings is very limited. This is information that should be useful to both landowners and mill operators. Although considerable research on damage to residual trees has been published, very few studies segregate felling damage from yarding damage. Additional work in this area would provide information on the relative contributions of each phase of the operation and help identify priorities in the effort to limit damage from thinning operations.

LITERATURE CITED

Aho, P.E.; Fiddler, G.; Srago, M. 1983. Logging damage in thinned, young-growth true fir stands in California and recommendations for prevention. Research Paper PNW-RP-304. Portland, OR: U.S. Department of Agriculture, Forest Service, Pacific Northwest Research Station. 12 p.

Drews, E.S.; Hartsough, B.R.; Doyal, J.A.; Kellogg, L.D. 2001. Harvester-forwarder and harvester-yarder systems for fuel reduction treatments. Journal of Forest Engineering 12(1): 81-91.

Greene, W.D.; McNeel, J.F. 1989. Potential costs of shear damage in a southern pine chip-n-saw mill. Forest Products Journal 39(5): 12-18.

Han, H-S; Kellogg, L.D. 2000. Damage characteristics in young Douglas-fir stands from commercial thinning with four timber harvesting systems. Western Journal of Applied Forestry 15(1): 27-33

Meadows, J.S.; Skojac, D.A., Jr. 2006. Third-year growth and bole-quality responses to thinning in a late-rotation red oak-sweetgum stand in East Texas. In: Connor, Kristina F., ed. 2006. Proceedings of the 13th biennial southern silvicultural research conference. General Technical Report SRS-GTR-92.

Asheville, NC: U.S. Department of Agriculture, Forest Service, Southern Research Station. 640 p.

Pinard, M.A.; Putz, F.E. 1996. Retaining forest biomass by reducing logging damage. Biotropica 28(3): 278-295.

Sauter, U.H.; Gengle, C. 1995. Felling and logging damages by highly mechanized and short timber harvest in conifer stands. Poster presented at the XX World Congress of the International Union of Forestry Research Organizations, Aug. 6-12, 1995, Tampere, Finland. http://www.metla.fi/iufro/iufro95abs/d3pos32.htm (accessed Aug. 1, 2007).

Sirén, M. 2001. Tree damage in single-grip harvester thinning operations. Journal of Forest Engineering 12(1): 29-38.

Smith, W. B.; Miles, P.D.; Vissage, J.S.; Pugh, S.A. 2004. Forest Resources of the United States, 2002. General Technical Report NC-GTR-241. St. Paul, MN: U.S. Dept. of Agriculture, Forest Service, North Central Research Station. 137 p.

Spinelli, R. 2004. Harvesting of thinnings. In: Burley, J.; Evans, J.; Youngquist, J.A. (eds.) Encyclopedia of Forest Sciences. Elsevier Academic Press, Oxford, U.K. Volume 1, p. 252-259.

Wang, J.; LeDoux, C.B.; Vanderberg, M.; McNeel. J. 2004. Log damage and value loss associated with two ground-based harvesting systems in Central Appalachia. International Journal of Forest Engineering 15(1): 61-69.

Zhu, J.Y.; Scott, C.T.; Gleisner, R. [et al.]. 2007. Mill demonstration of TMP production from forest thinnings: Pulp quality, refining energy, and handsheet properties. BioResources 2(4): 544-559.

Predicting Branch Diameter of Thinned and Fertilized Coastal US Douglas-fir Plantations at the Mean and Individual Tree Levels

David Briggs, Rapeepan Kantavichai, Eric Turnblom

ABSTRACT

TREE BRANCHES BECOME VALUE-REDUCING knots in wood products and since branch size can be affected by the silvicultural regimes employed in growing stands, improved understanding of the linkage between silviculture, branch size, and knots in products is needed. The Stand Management Cooperative routinely measures the diameter of the largest limb in the breast height (LLBH) region of trees on its field installations. This paper focuses on nine Douglas-fir (*Pseudostsuga menziesii* [Mirb.] Franco) installations in which plots were established at ages 6–13 years with 100 percent, 50 percent, and 25 percent of the initial planting density; each of these stocking conditions has a plot that was unfertilized as well as one that was fertilized at establishment and every four years since with 224kg ha^{-1} of N as urea. The data set, consisting of 6 plots from 9 installations (54 plots and 2257 trees total), was analyzed when the installations ranged in age from 22–32 years old. The paper presents models for predicting LLBH at two levels. First, we present models predicting the mean LLBH of trees in a stand using treatments, site index, stand density, and mean tree descriptors as predictive variables. Second, we present models predicting individual tree LLBH using treatments, site index, stand density, and individual tree descriptors as predictive variables. Of special interest is the question of whether or not prediction of LLBH is improved when treatment and stand variables are used in addition to tree variables.

KEYWORDS: Thinning, fertilization, branch size, knot diameter, wood quality, stem quality

David Briggs (dbriggs@u.washington.edu) is professor and director, **Rapeepan Kantavichai** is a doctoral Student, and **Eric Turnblom** is associate professor and silviculture project leader, Stand Management Cooperative, College of Forest Resources, Box 352100, University of Washington, Seattle, WA 98195, USA.

Automatic Timber Quality Determination Using Wood Property Models and Harvester Measurements

John D. Arlinger, Lennart Moberg, Johan J. Möller, Lars Wilhelmsson

ABSTRACT

In order to create a system for automatic determination of sawlog quality, a study was carried out using the measurements from cut-to-length harvesters to feed wood property models. The primary goal was to establish a basis for payment to forest owners which not only was related to species and harvested volume, but also to wood quality equivalent to standard national grading rules. If successful, other applications could also include automatic bucking, allocation of timber to mills with specific requirements, or early detection of deviations in log deliveries. Norm values, representing a quality-index value of 100, were obtained for maximum knot size per whorl and basic density in two different regions, for Norway spruce and Scots pine, respectively. Deviations from these norms were given weights in accordance with their effect on graded sawlog quality. Data was collected in Sweden from 96 harvesting sites and 15 different harvesters. This data was accumulated in the on-board computers of the harvesters, and used to simulate wood properties. By using the calculated property values for each harvested stem, comparing these to the norm, and weighing the deviations accordingly, a relative quality-index was determined. The wood from each site was then sent to impartial grading stations at sawmills, and the species, volume, grade and value was determined for each log (as is customary in Sweden). Finally, the volume and value of the wood from each site, as obtained through the harvester and grading station measurements, could be compared. The standard deviations in value were 2–3 percent for both species in the two regions—down from about 3–4 percent without corrections; reductions were most evident at sites with extreme values. Basic density was the dominant quality-determining factor for spruce, whereas knot size had most influence for pine.

John D. Arlinger, Lennart Moberg (presenter; lennart.mobert@skogforsk.se), **Johan J. Möller**, and **Lars Wilhelmsson** are researchers at Skogforsk, the Forestry Research Institute of Sweden, Uppsala Science Park, SE-751 83 Uppsala, Sweden.

Capturing Additional Value Through In-Forest Measurement of Internal Log Properties

Glen Murphy

ABSTRACT

I N SOME PARTS OF THE WORLD, LOG BUYERS are now considering wood properties such as stiffness and density. Assessing these properties in-forest and in real-time will be a challenge for log supply managers. The utility of two sensor technologies for sorting based on internal quality characteristics were examined in Douglas-fir; near infrared (NIR) for measuring wood density, and acoustic velocity for measuring stiffness. Wood samples and measurements were collected from more than 1500 stems located at 24 sites around Oregon.

To evaluate NIR technology, spectra were first gathered from saw chip samples produced by a saw chain of a pitch similar to that used on mechanized harvesters/processors. Multivariate techniques were then used to correlate wood density with the NIR spectra. The research showed that NIR could be used to predict density with a reasonable degree of accuracy and should allow logs to be segregated into several density classes.

To evaluate acoustic velocity technology, velocity measurements were gathered at four points along the supply chain: in standing trees, in felled stems gripped by a processor, in logs on the ground, and in green veneer. Velocity measurements were correlated with log and veneer stiffness and product yields. Preliminary results will be presented for this work.

The research provides insight into how these technologies could be incorporated into the design of mechanized harvesters and processors to enhance bucking and sorting for optimal matching of wood properties to markets.

Glen Murphy (glen.murphy@oregonstate.edu) is a professor in the Department of Forest Engineering, Oregon State University, Corvallis, OR 97331, USA.

Using the Results from Thinning and Fertilizer Interaction Models In Combination with Wood-Quality Studies To Maximize Commercial Benefit in South Australia Radiata Pine Plantations

Jim O'Hehir and Jan Rombouts

ABSTRACT

THE SOUTH AUSTRALIAN RADIATA PINE estate produces approximately 2.5 million m^3 of wood products annually. South Australian radiata pine plantations typically undergo multiple thinnings and the practice of post-thinning fertilizer application is becoming increasingly widespread.

Two decades ago, a series of trials designated EP190 were established. The data from these trials allowed the development of models used to predict the volume growth response of radiata pine plantations to the interaction of two silvicultural tools, thinning and post-thinning fertilizer. The experimental plan also prescribed the collection of wood property and stem shape data. These data were used to investigate the effect of thinning and post-thinning fertilizer on wood quality as a by-product of changes in tree growth rate. The availability of SILVISCAN® meant that a range of important wood properties could be assessed at the resolution of individual growth rings at different heights in the stem profile, and at an acceptable cost.

Based on EP190 mensurational data a system of models was developed to predict annual volume growth responses as a function of natural site productivity, thinning intensity, and nitrogen fertilizer dosage, at stand and sub-stand level (next thinning crop versus final crop). These models were incorporated into the ForestrySA yield regulation system enabling prediction of the financial, economic, and log-availability effects of implementing alternative thinning and fertilizer practices at a stand and estate level. Coupled with wood property information gained from the SILVISCAN data it was possible to recommend changes to thinning regimes (intensity and frequency) and fertilizer practice (timing and dosage) which could be demonstrated—to executive decision makers and customers alike—to produce an acceptable level of wood quality. The recommended changes to management practices resulted in a 3.5 percent increase in log product sales, generating additional log-sale revenue for the forest owner of some A$1.5M/year.

Jim O'Hehir (ohehir.jim@forestrysa.sa.gov.au) and **Jan Rombouts** are at ForestrySA, the South Australian Forestry Corporation, at PO Box 162, Mount Gambier, SA 5290, Australia.

Further Progress in the Development of Prediction Models for Growth and Wood Quality of Plantation-Grown *Pinus patula* Sawtimber in South Africa

Heyns Kotze and Francois Malan

ABSTRACT

THE OBJECTIVE OF THIS PAPER IS TO FURTHER discuss and demonstrate the progress made (after an initial report by Kotze and Malan 2005), in the understanding, modeling, and simulation of tree growth and wood quality of South African-grown *Pinus patula* sawtimber as it responds to the effects of site quality, planting density, thinning and pruning. Research to date has focused on the development of stand-level growth and yield models. Model components for dominant height, survival, and basal area are used to estimate growth of unthinned stands in relation to planting density. A basal area/thinning ratio model estimates the ratio of basal area removed in a thinning in relation to the ratio of stems removed. Thinnings are done selectively from below. A basal area thinning response model estimates basal area growth after a thinning. At any point in time, the diameter distribution can be recovered by using a Weibull distribution and a method of moments approach. Height-by-diameter and live crown height models estimate tree height and live crown height for each dbh class in the distribution. Taper models were developed for the estimation of product volumes. Data for the growth and yield models were gleaned from long-term spacing trials, thinning response trials, permanent sample plots, thinning control inventories, and destructive sampling. Current research focuses on the development of models to estimate within-tree basic wood density and branch characteristics determining the knottiness of lumber such as number of branch clusters per annual shoot, maximum branch diameter, distribution of branch diameters within a branch cluster, branch angle, and branch development over time. Data for the wood quality models were gleaned from trees destructively sampled over the site-quality range. The inclusion of prediction models for tracheid length, spiral grain, and microfibril angle is envisaged at a later stage. To demonstrate our progress, the growth and wood quality models were combined in a simulation program, the Forestry Scenario Analysis Tool. This program quantifies the effect of site quality and silviculture (planting density, thinning, pruning, and rotation) on stand growth, tree dimensions, log product yields, and economics. It also includes a bucking algorithm capable of bucking each tree in the stand table to provide an estimate of the total log harvest and their qualities in terms of position in the tree, log length, and thin-end diameter. Algorithms determine the effect of pruning on the defect core size and quantify the effect of the live crown height on the live knot stem section. A sawmill conversion simulator predicts lumber yield and size distribution, using a preset sawing pattern for each log type and diameter class. Currently, the output also contains information on the expected wood density and absence or presence of knots (clear, semi-clear, or knotty). This enables the system to provide an estimate of the value of each individual lumber piece produced in terms of current lumber prices. Finally, the cash-flow for the whole stand is generated, economics criteria are applied and the influence of forest practices on wood quality evaluated in forest economic terms on a stand-level basis.

KEYWORDS: *Pinus patula*, growth and yield, pruning, thinning, wood density, branching

Heyns Kotze (hkotze@klf.co.za) is in the Research Division, Komatiland Forests, Private Bag X11201, Nelspruit, 1200, South Africa and **Francois Malan** is in the Research Division, Komatiland Forests, P.O. Box 574, Sabie, 1260, South Africa.

INTRODUCTION

Pinus patula Schiede ex Schlect. & Cham. occurs naturally in Mexico where it extends from Tamaulipas right down to the mountains of north-eastern and north-western Oaxaca, and from there as far west as Guerrero. It is commonly known as Weeping Mexican pine.

Poynton (1979) notes that *P. patula* was first introduced to South Africa in 1907, which started the wide scale use of this species in South Africa. Today, plantation forestry in South Africa occupies 1.33 million ha, predominantly in the summer rainfall region along the eastern coastal areas and interior. Pine plantations occupy 707 205 ha of this area, approximately 48 percent of which is planted with *P. patula*. It is mostly planted in the cooler, mist-belt regions of eastern and south-eastern Mpumalanga province. It is also planted in the KwaZulu-Natal midlands, southern KwaZulu-Natal, Eastern Cape, and Northern Limpopo provinces. Komatiland Forests (Pty) Ltd (KLF) has a total forest area of 125 000 ha of which 48 percent is planted with *P. patula*. In KLF, *P. patula* is established in the elevation range between 700 and 2100 m above sea level, at mean annual temperature of between 14 and 20°C, and a mean annual precipitation of between 850 and 1500 mm. KLF is predominantly a pine sawtimber grower in the Mpumalanga and Limpopo provinces and is situated between the 30th and 34th laterals and predominantly in the 31st longitude band.

The genetic improvement of *P. patula* started in the early seventies, with the main focus on improved growth rate, adaptability, good branching and stem characteristics. Today KLF manages a total of 20 first- and second-generation seed orchards (165 ha in total) of pines and eucalypts for the production of improved seed. The *P. patula* seed are harvested from the top ten families in the second-generation seed orchards. These are used to establish hedge plants for production of commercial cuttings, and seedlings for field planting. The majority of seed used for local afforestation with *P. patula* are produced by the company's own seed orchards.

South African forestry scientists are continually trying to improve the productivity and economic out-turn of the country's commercial forests. This includes choosing the right species and seed source, improving site conditions through cultivation, drainage and fertilizer application, and manipulating the crop through genetics and silvicultural practices. Increased site productivity is one of the primary objectives of forestry research, in order to promote forest sustainability. However, it is increasingly recognized that the ultimate success of the forest industry is strongly linked to the quality of the wood produced and the industry's ability to maximise effective and wise utilisation of the resource. This is of increasing importance since a synergy must be found between the economic reality of harvesting at a younger age without sacrificing on volume production per unit area (fast growth makes this possible), and a wood product market that is becoming increasingly sophisticated and demanding in terms of end-product performance. It has therefore become of utmost importance to understand the timber resource and its changing qualities, to develop mechanisms capable of accurately predicting its wood and fiber quality, and to transfer this knowledge into industrial business processes.

Existing growth and yield prediction models serve as valuable tools to planners and harvesting managers, as they provide useful information on the likely production of a forest in terms of volume and raw material product outputs. Until now, the development of models and procedures capable of predicting wood quality in terms of species, genotype, silviculture, age, and site have not been attempted at a significant scale for the South African timber resource. This is considered a serious shortcoming, as improved predictability is becoming increasingly important to ensure the sustainable utilization of a variable forest resource such as ours, and to effectively accommodate changes in resource characteristics due to the impacts of improved silviculture, tree breeding, and the introduction of hybrids and new species.

This paper describes the initial phases of a project launched by KLF designed to eventually model a number of wood quality factors for *P. patula,* as well as the expected product output of a sawmill in terms of sawn volume and lumber quality, using the existing growth and yield models as a framework.

SITE TYPE AND SITE QUALITY

In KLF a detailed 1:10 000 site classification was conducted based on soil type, soil depth, depth of limiting material, mean annual temperature, mean annual precipitation and geology. Each stand has a dominant site type, which is used to recommend a preferred (most suitable) species for each stand. Site quality is expressed in terms of site index at age 20 years (denoted as SI_{20}), which is the average height of the 20 percent largest-diameter trees in a stand (Bredenkamp

1993). For each site type/species combination, an average SI_{20} value can be estimated. Depending on the site type, *P. patula* achieves SI_{20}-values between 15 m and 35 m in KLF with an average of 25 m. SI_{20} is used to quantify site quality effects on tree and stand growth and subsequently on wood quality. The effect of site quality on utilizable mean annual increment at age 20 years ($UMAI_{20}$) can be seen in Figure 1.

SILVICULTURE

Stands are mostly established with seedlings placed into manually prepared planting pits. Pine stands are thinned and pruned intensively to improve quality and value. In KLF the planned rotation age is 30 years and the goal is to produce a target stand with an average diameter at breast height (dbh) of 42 cm over-bark pruned to 9.5 m.

Results from numerous spacing trials in South Africa have proven that planting density has a pronounced influence on basal area development of a stand, but a very small effect on dominant height. Therefore, stand density management is required to enable stands to achieve the dimensions of the target tree. Current practice within the company is a standard planting density of 1111 stems per hectare (3 m x 3 m). With this planting density, canopy closure occurs at approximately three years. It allows for 11 percent mortality during establishment and provides sufficient room for selection at first thinning. Thinnings are mostly done selectively from below. On flat terrain, a 7th row thinning is sometimes conducted in combination with selective thinning.
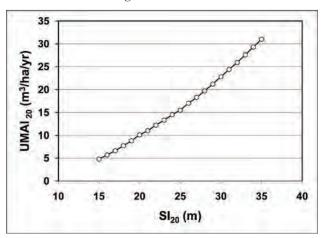
Figure 1: The relationship between site quality and mean annual volume increment of P. patula.

Table 1: Thinning regimes currently applied for *P. patula* in Komatiland Forest.

TPH remaining after thinning	Age of thinning (years)					
	SI_{20} class (m)					
	<21	21-23	23-25	25-27	27-29	>29
500	10	10	9	8	8	8
300		15	14	13	12	12

Abbreviations: SI_{20} = Site Index at the reference age of 20 years
TPH = Trees per hectare

Table 2: Pruning regimes currently applied for *P. patula* in Komatiland Forest.

Pruning lift (m)	Age of pruning (years)					
	SI_{20} class (m)					
	<21	21-23	23-25	25-27	27-29	>29
2.0	4.5	4.0	3.9	3.8	3.7	3.5
4.0	6.2	5.4	5.0	4.7	4.6	4.4
6.0	8.0	6.7	6.1	5.7	5.5	5.3
7.5		8.3	7.4	6.9	6.6	6.3
8.5			8.5	7.9	7.4	7.0
9.5			9.4	8.7	8.3	7.6

The purpose of thinning is to boost diameter growth, to encourage uniform annual incremental growth, to keep the stand in a stable and healthy growing condition and to provide room for selection at thinning so that a good final crop is ensured while providing for an interim income at the same time. Table 1 shows how the current thinning regimes are applied over the site quality range.

The purpose of live crown pruning is to confine the defect core to a cylinder smaller than 20 cm in diameter, ensuring that the knots in the defect core cylinder are tight and defect free, and that all wood formed outside this cylinder is knot free and of good quality until the final harvest. Pruning is conducted in such a manner that live crown always constitutes at least one third of the tree height. This ensures that growth loss due to pruning is minimized. To achieve this, pruning schedules were designed for the range of SI_{20}-classes.

GROWTH AND YIELD RESEARCH

Data

Structured growth and yield research started in 1936 when O'Connor established the first series of four spacing and thinning response trials for *P. patula*, the so-called Correlated Curve Trend trials (CCT) (O'Connor 1935, O'Connor 1960). Following through with the CCT trials, Craib (1939, 1947), Marsh (1957, 1978), Burgers (1976) and Marsh and Burgers (1973) continued with the pioneering work in stand density management. Bredenkamp (1984) summarized their work extensively and designed a new series of more

cost effective spacing trials in terms of area requirements (Bredenkamp 1990), the so-called Standardized Sample Size spacing trials (SSS-CCT). With this he addressed the shortcomings of the first series of trials and provided a base data set for the next generation of growing stock. To date three of these SSS-CCTs have been established for *P. patula* by KLF. Over time, data from other sources, like thinning control inventories, management inventories, Permanent Sample Plots (PSPs), and destructive sampling were collected so that the full range of model components required in a growth and yield simulator could be developed and tested.

Results from the Spacing and Thinning Research

Results from the spacing and thinning trials on *P. patula* indicate that dominant height is not affected significantly by planting density and thinning from below, within the commercial range of planting densities. Mortality occurs at a faster pace when the density is higher. After a thinning from below, mortality in a thinned stand is lower than in an unthinned stand of the same density. Tree diameter or basal area per hectare is greatly affected by planting density. Basal area growth in a thinned stand can be expressed with a response function to an unthinned counterpart.

Models for Simulating Growth and Yield

Pienaar (1964) and Pienaar et al. (1985, 1988) interpreted the data from the CCT trials and developed modeling approaches to describe unthinned stand growth and stand growth in response to thinning. The modeling strategy currently employed for *P. patula* was presented by Kotze (2003) and is summarized below.

KLF adopted a stand-level modeling approach because all our forests are planted, even-aged, and single-species stands. Stand-level growth is defined by three variables, namely dominant height, basal area, and stems per hectare. Dominant height is modeled by a Chapman-Richards-type function (Kotze 1999). Unthinned basal area is also modeled with a Chapman-Richards-type function and its parameters are dependent on planting density (Kotze 1999). Survival is modeled with the Clutter-Jones survival function (Clutter and Jones 1980).

When a thinning is applied to a stand, a number of changes occur. It is assumed that dominant height growth is not affected by thinning, only the mean height is affected. The thinning regime dictates the number of stems

per hectare to remain after the thinning. It is assumed that no mortality occurs after the first thinning, because of the intensive thinning regime. Basal area removed in a thinning is estimated with Field's thinning ratio function (Field et al. 1978). Basal area responds to thinning and the response is modeled with the index of suppression methodology, as proposed by Pienaar and Shiver (1984).

Whole-stand volume is estimated by constructing a stock table, where the tree volumes are estimated for each dbh class. The stand structure, i.e., a stand table is independent of the growth model. The dbh distribution is reconstructed by using the Weibull function with Kassier's implementation method (Kassier 1993). Garcia's method of moment's technique is used to recover the Weibull parameters (Garcia 1981). Consistency between distributions before and after thinning is obtained with the methodology developed by Murray and von Gadow (1991). Pienaar's average height by dbh function (Pienaar et al. 1988) is used to estimate the average height for each dbh class. Dyer and Burkhart's (1987) live crown height model is used to predict the progression of live crown height over time. This model is useful in estimating the development of the dead-knot zone above the pruned section of the bole. Product volumes are estimated by applying a greedy bucking algorithm to each dbh-class in the stand table (Vonck 1997). The Max and Burkhart taper function is used to estimate product volumes (Max and Burkhart 1976).

Stand growth and yield is normally projected from a calibration point where inventory data provide the calibration age (Age_1), dominant height (Hd_1), basal area per hectare (BA_1), and stems per hectare (TPH_1). If such inventory data do not exist, then a calibration point is created before the first thinning age. Each stand has an allocated SI_{20}-value and this is used to estimate height at Age_1. TPH_1 is estimated by multiplying planting density (TPH_0) with a default survival percentage (Surv%). BA_1 is estimated with a stand-level basal area yield prediction function from Age_1, TPH_1, and Hd_1.

WOOD QUALITY RESEARCH

Impacts of Site and Silviculture on Wood Density

Wood density is the property most commonly considered in wood quality studies as it has a strong bearing on lumber strength, machining, drying rate, pulp and paper proper-

ties, and permeability. Wood density is extremely variable and the variation patterns are very important. Among- and within-tree differences within a stand are mostly caused by genetic influences and relate strongly to the size of the juvenile wood zone and its variability (Zobel 1997, Zobel and Jett 1995). However, site factors especially those influenced by elevation, latitude, and soil fertility may also affect this property (Cown 1999, Malan 2001).

The basic density of the wood produced by South African *P. patula* increases from approximately 375 to 400 kg/m^3 near the pith to approximately 525 to 575 kg/m^3 in the mature wood zone. The period of increase normally lasts for approximately 20 years before leveling-off starts to occur. The height effect is relatively small as density normally decreases only by 40-50 kg/m^3 from breast height to 20 m from the ground for the same growth ring from the pith.

Studies by Boden (1982) and Malan (2001) indicated that density of the wood produced by *P. elliottii, P. taeda, P. patula,* and *P. radiata* decreases with elevation and latitude. *P. patula* seemed to be less affected by these variables, however. The interaction terms (elevation x latitude) were statistically significant for all species, suggesting that the effects of latitude and elevation are complex and should not be considered separately. Compared to results of findings

in Columbia at high elevations, findings in Swaziland suggested that the relationship with elevation at lower elevations might be much weaker. In Zimbabwe little genotype x environment interaction was found for density (several papers as reported by Dvorak et al. 2000). Clarke et al. (2003) found almost no difference in density in *P. patula* trees grown at elevations of 1200 and 1450 m above sea level at Usutu (Swaziland), but at 800 m elevation the wood was only about 15 kg/m^3 denser on average.

As early as 1939 Craib concluded that rate of growth did not affect timber strength in *P. patula*. This was later confirmed by Banks and Schwegmann (ca.1957) who found no significant effect of differences in growth rate on moisture content, green and dry density, or shrinkage. The radial increases in density were largely similar irrespective of growth rate, except that the fast-growers produced wood slightly less dense over comparable years of growth. However, the weighted mean density of the fast-grown trees was the same and sometimes even higher than that of the slow-grown trees due to the greater percentage of denser wood in the outer layers of the stem.

Results obtained from a CCT spacing trial at Weza (Malan et al. 1997) revealed that slow-grown trees exhibited higher density than fast-grown trees when comparing wood formed at the same age. The wood formed by slow-grown trees also seemed to have reached maturity at an earlier age. However, the differences observed were only applicable to extreme differences in growth rate (Figure 2). Within the range of normal spacing applied in practice, it was obvious that the effect of growth rate differences due to spacing differences on wood density and pulp and paper properties was negligible. Since this study also revealed that thinning had no recognizable effect on wood density, it was concluded that thinning

Figure 2: Differences in the radial patterns of variation in wood density at breast height in P. patula *trees as affected by age and planting density treatments.*

Figure 3: Differences in the radial patterns of variation in wood density at breast height in P. patula *trees with linear distance from the pith as affected by planting density treatments.*

basic density model as proposed by Tian et al. (1995) was selected for parametrization with the *P. patula* data.

Stem Form and Branching Characteristics

The combined effects of tree breeding towards improvement of branching characteristics and stem form and the development of thinning and pruning regimes were without doubt highly successful in promoting the quality of the wood produced by the current forest resource. As a result, problems associated with irregular growth; reaction wood; eccentricity; wandering pith; localized excessive grain deviation; and knots that exceed the limits for size, soundness, and clustering have been minimized. In the pruned sections of the stems of properly managed trees the knots and associated defects are restricted to a core of pre-planned diameter, while the proportion of clear wood in the outer more mature part of the stem is maximized. However, there is a definite need to develop models to predict branch characteristics as a function of site quality and silviculture.

Currently, Kotze (2007) is busy with a pilot study on branch modeling of *P. patula* sawtimber in KLF. The purpose of the study is to develop a set of models to describe the development of branchiness within a tree over time. The methodology described by Grace et al. (1999) was used as a starting point to define the branch modeling strategy. To reconstruct the branch growth in a single tree, the dbh and height growth will be reconstructed with the growth model. Therefore, the annual shoot lengths and stem profiles, both over-bark and inside-bark, will be available. There is of course a nodal swelling which is additional to the overbark stem profile. Once a branch is formed, it will maintain its position and azimuth for its entire life. Within each annual shoot, the number of branch clusters and their relative positions within the shoot are predicted. Within each cluster, the number of branches is allocated as a random value from

could be used to successfully control any effect different spacings might have on wood density and related properties, by carefully controlling competition.

It was clear from this study that the enhancement of growth rate of this species by the manipulation of the growing space or thinning had no adverse effect on wood density, and by implication, on any of the factors related to this property. In fact, the advantages of fast growth by far outweigh the "advantage" of higher density produced by slower growing trees (Figure 3). It implies not only higher volume production, but goes hand-in-hand with improved uniformity across the radius as well, without compromising the suitability of the wood for structural purposes to any serious level.

More recently, a study was conducted by Kotze and Malan (2005) to establish variation patterns in wood density within trees of this species and how it is affected by elevation. Approximately 90 trees were sampled over three sites at elevations of 1000, 1300, and 1700 m above sea level, respectively. This study showed that the effect of elevation on wood density is not clearly defined. Ring number from the pith and height above ground level accounted for 63 percent and 10 percent of the total variability, respectively. This study provided a suitable dataset for the development of a within-tree wood density model. The within-tree wood

an observed distribution. The azimuth of the first branch is set as a random value from a circular distribution. The azimuth of the second branch is allocated by advancing the azimuth clockwise by 137.5 degrees. This sequence simply continues to the next cluster. Branch size increases from the first to the last branch in each cluster. The last branch is considered to be the branch with maximum diameter in that cluster. The size of the other branches is allocated as a function of maximum branch diameter and branch order in the cluster. Each branch is grown over time, with the associated branch angle reconstructed. Each branch is grown until it dies, thereafter the diameter remains constant and the dead branch is encased.

Potential for Modeling Other Wood Quality Factors

A number of other properties that are known to have a strong impact on some end-uses will have to be dealt with systematically in the future and ultimately be included in existing software packages to improve predictability.

Juvenile wood is particularly marked in South African-grown soft- and hardwoods and is an important quality factor since its inherent properties are considerably more variable and different than those of mature wood. As increased volume growth is continuously and vigorously pursued to improve plantation productivity, if rotation ages are reduced to reap the benefits of fast growth and result in increased proportions of juvenile wood in the final harvest, the effect on the quality mix of the wood produced in the future could be quite significant.

Fortunately, wood densities, as well as the properties discussed below, are all important production variables of which age is by far the main controlling factor, especially in the juvenile wood zone where rapid changes with age prevail. There can thus be little doubt that the age effect will feature strongly in models designed to predict these properties and the quality of the juvenile zone in particular.

Microfibrillar Angle

Wood density and microfibril angle are considered to be the most important wood properties controlling the technical performance of wood. The latter is of particular importance because of its marked role in determining the strength, stiffness, shrinkage, and stability of wood, especially in juvenile wood, where it varies considerably across the radius, with the largest angles near the pith. There can be no doubt that modeling the variation of this feature for South

African commercial species will make a major contribution towards predicting the behavioural properties of the wood produced, assisting in its effective utilization, and increasing options for wood quality improvement.

Tracheid Length

Information on the patterns and sources of variation of this feature is extremely limited for South African pines. Average breast height tracheid length of *P. patula* increases rapidly from about 2 mm at ring 2 to 5 mm at ring 20, where after it remains relatively constant (Kromhout 1962). This means that this species produces 0.5 to 1 mm longer tracheids across the entire radius than other local commercial pines. Turner et al. (2000) found that the cell diameter, lumen diameter, and length of *P. patula* tracheids increase with site quality (growth rate) increases but wall thickness is not affected. As a result, collapsibility, which is a ratio involving cell diameter and wall thickness and which determines the ability of the fiber to defibrillate and flatten during sheet formation, improves with site quality. Thus the wood from better sites yields pulp fibers that have better fiber-to-fiber bonding.

Spiral Grain

In South African pines, spiral grain is foremost a problem of juvenile wood. Grain angles are greatest near the pith but normally drop rapidly over approximately the first ten annual rings, reaching more acceptable values as more mature wood is formed. The patterns of variation in spiral grain are not very consistent, neither between trees nor within trees (Banks 1969, Gerischer and Kromhout 1964). *P. patula* tends to be more spiral-grained than both *P. elliottii* and *P. taeda*, averaging from approximately 3.5 degrees near the pith to approximately 2.5 degrees at the 30th year of growth. Contrary to the other two pines, there is a definite tendency toward left-hand spiral grain in *P. patula*. In the latter species the average angle of spiral grain often tends to remain larger than in other pines for longer distances across the radius, with the result that its influence sometimes extends to lumber cut at quite some distance from the pith. *P. patula* growing in the cooler temperate regions tend to be less spiral-grained than those growing in the warmer areas (Kromhout and Toon 1977). Otherwise, little is known about the variation patterns in spiral grain in South African pines, and in *P. patula* in particular, and how it is affected by environmental factors.

The Forestry Scenario Analysis Tool (FORSAT)

FORSAT is a stand-alone simulation program operating on a stand-level basis (Kotze 2006). This program quantifies the effect of silviculture (planting density, thinning, pruning, and rotation) on stand growth, tree dimensions, log product yields, and economics.

The stand-level growth model estimates values for dominant height, stems per hectare, and basal area over time. At each thinning event it quantifies the number of stems removed and estimates the basal area removed. For any age, the diameter distribution is generated and a stand table is constructed. For each dbh class midpoint, the number of stems per hectare, an average tree height, and the live crown height are estimated. A bucking algorithm is then employed to buck each tree in the stand table according to a log specification and to provide an estimate of the total log harvest and their qualities in terms of position in the tree, log length and thin-end diameter, whether it is pruned or not, the clear-wood radius or the live knot radius, the density profile, and the associated log value. Finally, the cash flow for the whole stand is generated and economics criteria are estimated. Typical economic criteria like Land Expectation Value (LEV), Net Present Value (NPV), Equivalent Annual Income (EAI), Internal Rate of Return (IRR), Standing Value (SV), and Cost Value (CV) are estimated. In this way, the influence of silviculture can be evaluated in forest economic terms on a stand-level basis. This is useful from the forester's point of view.

FORSAT represents a useful framework to include models predicting wood property variation in terms of site, silviculture, and age. The within-tree wood density model described above, and models predicting growth and tree stem composition with regard to the size of the defect core, clear-wood zone, and juvenile wood (in terms of density), were included. The models describing branch characteristics have not been incorporated yet.

FORSAT also includes a sawmill processing simulator which estimates the potential yield of lumber products and their value from a specific stand. The software predicts lumber yield and size distribution, using a preset sawing pattern specification for each log type and diameter class. It also classifies each lumber piece produced into an expected product type (structural and/or any of the industrial grades) as dictated by its air-dry dimensions and expected spatial position within the stem. The latter enables the program to estimate the quality of each piece in terms of its expected mean density and status regarding the absence or presence of knots. With this information available, the system can classify the pieces into products and grades and estimate the value of each individual lumber piece in terms of current lumber prices as well as the sawn output of a stand as a whole.

CONCLUSIONS AND RECOMMENDATIONS FOR FUTURE RESEARCH

Progress to date has proven that the quality of the wood produced by *P. patula* can be modeled and effectively incorporated into existing growth and yield software and used on a stand-level basis. It has been shown that a considerable amount of information can be generated regarding the quality of the wood of round timber, as well as the quality of sawn products, by utilizing existing wood quality information on the species as basis for prediction. Although the latter is limited (in scope as well as in accuracy) it comprises three of the most important factors controlling the quality of the wood: degree of wood density variation, defect core size in the pruned section, and known patterns of branch dieback beyond the final pruning height.

While pruning has proven to be one of the most powerful techniques to improve the quality of the wood produced in the pruned section of the stem (and the predictability thereof), results of spacing and thinning trials have shown that tree volume growth can be maximized without any detriment to the wood produced. In fact, accelerated incremental growth results in increased volume of wood of improved uniformity across the radius, without compromising wood strength to any great extent.

Although studies conducted to date indicated clear site differences in within-tree wood density variation patterns, the exact site factors controlling these patterns could not yet be determined. Thus, there is a strong need for more studies to better understand the effects of site conditions on tree growth and its wood properties and their variation patterns. This will also indicate to what extent the predictive power of existing models would improve by incorporating some form of model calibration on an individual stand basis.

There is a need to improve the components and coefficient sets of the stand-level modeling approach as new data becomes available. The stand-level modeling approach is

not the most suitable approach for tracking wood properties in final crop trees and it is possible that individual tree models would be more appropriate.

Finally, there is a need to study the variation patterns of a number of quality factors that are of technological importance and the factors controlling them in order to expand the versatility and accuracy of current software. These include the whole branch model component, and models to describe spiral grain, tracheid length, and microfibril angle.

ACKNOWLEDGMENTS

LITERATURE CITED

Banks, C.H. 1969. Spiral grain and its effect on the quality of South African timber. Forestry in South Africa 10: 27-33.

Banks, C.H.; Schwegmann, L.M. 1957. The physical properties of fast- and slow-grown *Pinus patula* and *P. taeda* from South African sources. Journal of the South African Forestry Association 30: 44-59.

Boden, D.I. 1982. The relationship between timber density of the three major pine species in the Natal Midlands and various site and tree parameters. Report 1981-1982, Wattle Research Institute, University of Natal. pp. 120-126.

Bredenkamp, B.V. 1984. The C.C.T. concept in spacing research - a review. Proceedings : Symposium on site and productivity of fast growing plantations. Vol. 1: 313-332.

Bredenkamp, B.V. 1990. The Triple-S CCT design. In: von Gadow, K. and Bredenkamp, B.V., eds. Proceedings: "Management of *Eucalyptus grandis* in South Africa". Forest Mensuration and Modelling Working Group in collaboration with the Southern African Institute of Forestry and the *Eucalyptus grandis* Research Network, Stellenbosch. pp: 198-205.

Bredenkamp, B.V. 1993. Top height: A definition for use in South Africa. Southern African Forestry Journal 167: 55.

Burgers, T.F. 1976. Management graphs derived from the correlated curve trend (CCT) projects. Bulletin 54. Department of Forestry, Pretoria. 58 p.

Clarke, C.R.E.; Morris, A.R.; Palmer, E.R. [et al.]. 2003. Effect of environment on wood density and pulp quality of five pine species grown in Southern Africa. Tropical Forestry Papers 43. OFI, Department of Plant Sciences, University of Oxford, UK. 162 p.

Clutter, J.L.; Jones, E.P. (Jr). 1980. Prediction of growth after thinning in old-field slash pine plantations. U.S. Department of Agriculture, Forest Service Research Paper SE-217. pp: 1-8.

Cown, D.J. 1999. New Zealand pine and Douglas-fir. Suitability for processing. Forest Research Bulletin 216. 72 p.

Craib, I.J. 1939. Thinning, pruning and management studies on the main exotic conifers grown in South Africa. Science Bulletin 169, Department of Agriculture and Forestry, South Africa. 179 p.

Craib, I.J. 1947. The silviculture of exotic conifers in South Africa. Journal of the South African Forestry Association 15: 11-45.

Dvorak, W.S.; Hodge, G.R.; Kietzka, J. E. [et al.]. 2000. *Pinus patula*. In: Conservation and testing of tropical and subtropical forest tree species by the CAMCORE cooperative, College of Natural Resources, NCSU, Raleigh, NC, USA. pp. 140-173.

Dyer, M.E.; Burkhart, H.E. 1987. Compatible crown ratio and crown height models. Canadian Journal of Forestry Research 17: 572-574.

Field, R.C.; Clutter, J.L.; Jones, E.P. (JR). 1978. Predicting thinning volumes for pine plantations. Southern Journal of Applied Forestry 2(2): 59-61.

Garcia, O. 1981. Simplified method-of-moments estimation for the Weibull distribution. New Zealand Journal of Forest Science 11: 304-306.

Gerischer, G.F.R.; Kromhout, C.P. 1964. Notes on breast height spirality in dominant trees of *Pinus patula*, *Pinus taeda* and *Pinus elliottii*, with special reference to tree breeding. Forestry in South Africa 5: 81-97.

Grace, J.C.; Pont, D.; Goulding, C.J.; Rawley, B. **1999**. Modelling branch development for forest management. New Zealand Journal of Forestry Science 29(3): 391-308.

Kassier, H.W. 1993. Dynamics of diameter and height distributions in even-aged pine plantations. Unpublished PhD-thesis, University of Stellenbosch. 167 p.

Kotze, H. 1999. The Mac Mac CCT growth model for Pinus patula. A comparison with PCPROJ. Unpublished Research Report, South African Forestry Company Ltd. 19 p.

Kotze, H. 2003. A strategy for growth and yield research in Komatiland Forests in South Africa. In: Amaro, A.; Reed, D. and Soares, P. Modelling Forest Systems. CABI Publishing. pp. 75-84.

Kotze, H. **2006**. FORSAT – User's Manual – Version 2.3. Unpublished Research Report, Komatiland Forests. 79 p.

Kotze, H. **2007**. Branch modelling of Pinus patula sawtimber in Komatiland Forests. Preliminary results for Plot 1. Unpublished Research Report, Komatiland Forests. 12 p.

Kotze, H. and Malan, F. **2005**. Progress in the development of prediction models for growth and wood quality of plantation-grown *Pinus patula* sawtimber in South Africa. Proceedings: 'Connection between Forest Resources and Wood Quality: Modelling Approaches and Simulation Software'. IUFRO WP 5.01.04, Waiheke, New Zealand.

Kromhout, C.P. 1962. Notes on the tracheid lengths in *Pinus patula, Pinus taeda* and *Pinus elliottii*. Forestry in South Africa 2: 93-98.

Kromhout, C.P. and Toon, R.E. 1977. Variation in wood properties of some tropical species grown in plantations in southern Africa. Proceedings: 'Progress and problems of genetic improvement of tropical forest trees', IUFRO W.P. S2.02-08 and S2.03-01, Brisbane, Australia. Vol. 1: 8-45.

Malan, F.S. 2001. Wood density variation patterns in South African pine with special reference to the effect of abnormal wood in *P. taeda*. Internal Company Report, 02/2001, South African Forestry Company Ltd. 20 p.

Malan, F.S.; Retief, R.J.; Male, J.R. 1997. The influence of planting espacement on the wood density and pulping properties of *Pinus patula*. Southern African Forestry Journal 180: 23-32.

Marsh, E.K. 1957. Some preliminary results from O'Connor's correlated curve trend (C.C.T.) experiments on thinnings and espacements and their practical significance. Commonwealth Forestry Conference, Australia and New Zealand. 21 p.

Marsh, E.K. 1978. The cultivation and management of commercial pine plantations in South Africa. Bulletin 56, Department of Forestry, Pretoria. 140 p.

Marsh, E.K. and Burgers, T.F. 1973. The response of even-aged pine stands to thinning. Forestry in South Africa 14: 103-110.

Max, T.A. and Burkhart, H.E. 1976. Segmented polynomial regression applied to taper equations. Forest Science 22(3): 283-289.

Murray, D.M. and von Gadow, K. 1991. Relationships between the diameter distributions before and after thinning. Forest Science 37(2): 552-559.

O'Connor, A.J. 1935. Forest Research with special reference to planting distances and thinning. British Empire Forestry Conference, South Africa. 30 p.

O'Connor, A.J. 1960. Thinning research. Journal of the South African Forestry Association: 66-88.

Pienaar, L.V. 1964. Quantitative theory of forest growth. Ph.D. Dissertation. Seattle: University of Washington. 176 p.

Pienaar, L.V. and Shiver, B.D. 1984. An analysis and models of basal area growth in 45-year-old unthinned and thinned slash pine plantation plots. Forest Science 30(4): 933-942.

Pienaar, L.V.; Shiver, B.D.; Grider, G.E. 1985. Predicting basal area growth in thinned slash pine plantations. Forest Science 31(3): 731-741.

Pienaar, L.V.; Harrison, W.M.; Bredenkamp, B.V. 1988. Yield prediction methodology for *E*.grandis based on

Langepan CCT data. Unpublished Report, University of Georgia. 36 p.

Poynton, R.J. 1979. Tree planting in Southern Africa. Vol. 1. The Pines. Report to SARCCUS, Department of Forestry, Pretoria. 576 p.

Tian, X.; Cown, D.J.; MCConchie, D.L. 1995. Modelling of *Pinus radiata* wood properties. Part 2: Basic density. New Zealand Journal of Forestry Science 25(2): 214-230.

Turner, P.; Megown, K.A.; Grzeskowiak, V. [et al.]. 2000. An industrial evaluation of a stand-level grading system for *P. patula*. Proceedings: "Forest genetics for the next millennium", IUFRO working party 2.08.01, Durban, South Africa. pp. 228-235.

Vonck, D.I. 1997. WINCUTUP User's Manual. Unpublished report, South African Forestry Company Ltd. 6 p.

Zobel, B.J. 1997. Genetics of wood – An overview. Proceedings: 'Timber Management toward Wood Quality and End-product Value', CTIA/IUFRO International Wood Quality Workshop, Québec City, Canada. Vol. IV: 3-9.

Zobel, B.J. and Jett, J.B. 1995. Genetics of Wood Production. Springer-Verlag, Berlin. 337 p.

Developments to the Sylvan Stand Structure Model to Describe Wood-Quality Changes in Southern Bottomland Hardwood Forests Because of Forest Management

David R. Larsen and Ian R. Scott

ABSTRACT

GROWTH MODELS CAN PRODUCE A WEALTH of detailed information that is often very difficult to perceive because it is frequently presented either as summary tables, stand view or landscape view visualizations. We have developed new tools for use with the Sylvan model (Larsen 1994) that allow the analysis of wood-quality changes as a consequence of forest management. Sylview is a new computer program that allows users to visualize wood-quality characteristics of stands and individual trees within a stand. These include the effects of spacing and thinning on taper, branch size, and clear wood production.

KEYWORDS: Stand structure model, crown change, wood quality, silviculture

INTRODUCTION

The Sylvan Stand Structure model (Larsen 1991a, 1991b, 1994) was developed to allow foresters to study the development of specific stands of various species mixes based on empirical data from a subject stand and from forest stand dynamics principles. This model was developed after watching foresters try to make empirical forest-growth models fit a subject stand with species not included in the growth model or fit densities and forest structures not included in original data upon which the models were built. These foresters would try to force the model to work by substituting species or simply extrapolating the results. In Sylvan, two design criteria were adapted; first, basic stand dynamics principles guide the general function of all trees; and second, to make effective forest management decisions, the relative dynamics and the range of outcomes were more important than estimated volume or size. With these ideas in mind, Sylvan uses a 3-dimensional spatial pattern defined by stem maps and tree heights plus the crown size, defined by crown length and crown width, to provide the basis for predicting future stand structure.

THE SYLVAN S-PLUS/R DISPLAY
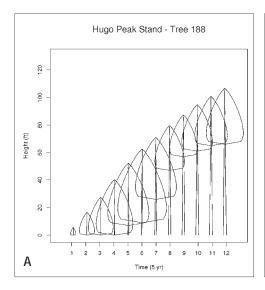
The programming for the original model was written in C programming language with a simple tree-list-in and tree-list-out approach. In the early 1990's a series of functions in S-plus language were used to provide graphical output. While these were just fine for research and publication, they were not very convenient for foresters to use.

SYLVAN DISPLAY PROGRAM

One early attempt to build a program to display the model output of the Sylvan Stand Structure model is the Sylvan Display program (Davison 1995). This program was written by a computer science masters student and had several design criteria, two of which were 1) the program should be cross platform (Unix, Window, Mac), and 2) it should have 2-dimensional and 3-dimenstional views, graphs, and tables of the model output. The student was successful in satisfying both of these criteria. One major limitation was the maturity of the windowing library used at the time.

David R. Larsen (larsendr@missouri.edu) is a professor of quantitative silviculture and chair of the Department of Forestry-203 ABNR, The School of Natural Resources, University of Missouri-Columbia, Columbia, MO 65211, USA and **Ian R. Scott** is a software engineer at Silicon Navigator, 10050 N. Wolfe Rd Suite SW2-260, Cupertino, CA 95014, USA.

A — Hugo Peak Stand - Tree 188

B — Diameter growth for tree 188
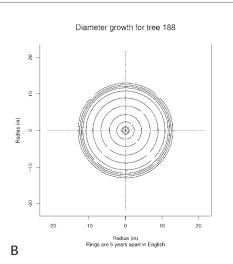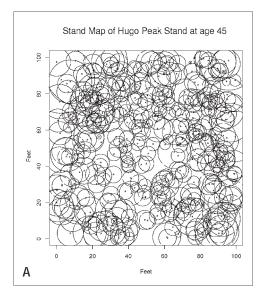
Figure 1— Typical output for a single tree from the Sylvan Stand Structure model using the Sylvan S-plus/R visualization tools. Figure 1a is an illustration of the tree profile at each time step of the model simulation. Figure 1b is a cross-section of the stem at breast height (1.37 m) rings are 5-year increments. Images from Larsen (1991a) are Douglas-fir (Pseudotsuga menziesii (Mirbel) Franco) from western Washington USA.

A — Stand Map of Hugo Peak Stand at age 45

B — Stand Profile of Hugo Peak Stand at age 45
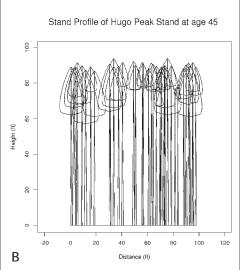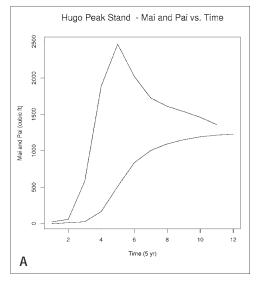
Figure 2— Typical output for a single tree from the Sylvan Stand Structure model using the Sylvan S-plus/R visualization tools. Figure 2a is a stand crown map at time step 9. Figure 2b is a stand profile at time step 9. Images from Larsen (1991) are Douglas-fir (Pseudotsuga menziesii (Mirbel) Franco) from western Washington USA.

A — Hugo Peak Stand - Mai and Pai vs. Time

B — Hugo Peak Stand - Density Management Diagram
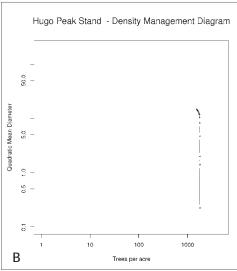
Figure 3— Density management diagram and mean annual increment (MAI) over periodic annual increment (PAI) curve for the modeled stand. Volumes are in cubic feet and quadratic mean diameters in inches. Images from Larsen (1991) are Douglas-fir (Pseudotsuga menziesii (Mirbel) Franco) from western Washington USA.
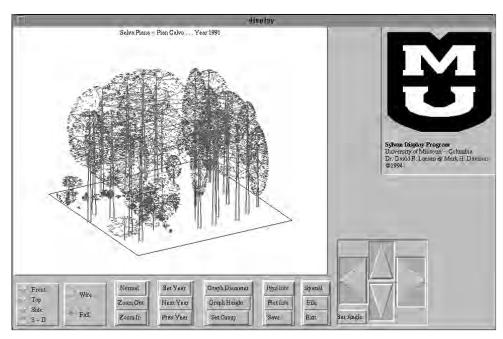
Figure 4 — An example of the Sylvan Display program (Davison 1995). The stand illustrated is European beech (Fagus sylvatica L.) in Central Italy.
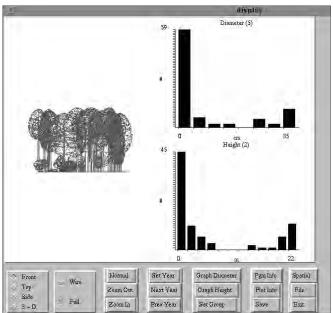
Figure 5— An example of the Sylvan Display program (Davison 1995). This view displays the diameter distribution and the height distribution. The stand illustrated is European beech (Fagus sylvatica L.) in Central Italy.

Figure 6— An example of the Sylvan Display program (Davison 1995). Trees selected for cutting are highlighted in black in both the stand map and the histograms of the size distributions, whereas residual trees are in light gray. The stand illustrated is European beech (Fagus sylvatica L.) in Central Italy.

STAND VISUALIZATION SYSTEM (SVS)

The Stand Visualization System (SVS) (McGaughey 1997) is a good stand-level visualization tool for the Windows operating system. In the initial phase of the recent Sylvan Stand Structure model development, SVS was considered our primary visualization tool. The Sylvan Stand Struc-ture model has modules that produce SVS-ready files for visualization.

However, after using the program for some time, we recognized several areas for improvement in the SVS interface. While the 3-dimensional interface (see Figure 7) looks nice, we found it difficult to determine specific information about individual trees. A model output visualization tool should
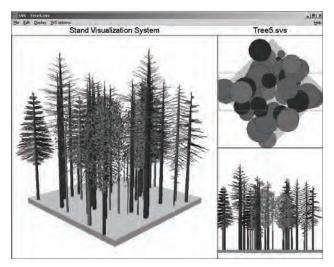
*Figure 7— An example of the Stand Visualization System (SVS) program (McGaughey 1997). The stand illustrated is Douglas-fir (*Pseudotsuga menziesii *(Mirbel) Franco) from western Washington USA*

*Figure 8— An example of the Stand Visualization System (SVS) program (McGaughey 1997). This image illustrates the multiple menus used to change the screen layout. The stand illustrated is Douglas-fir (*Pseudotsuga menziesii *(Mirbel) Franco) from western Washington USA.*

*Figure 9—An example of the Stand Visualization System (SVS) program (McGaughey 1997). This screen allows the user to change the 3-dimensional perspective for the 3-dimensional view seen under the pop-up window. The stand illustrated is Douglas-fir (*Pseudotsuga menziesii *(Mirbel) Franco) from western Washington USA*

be designed to convey information about the changes in tree dimensions and the interactions of neighboring trees.

Many components, while present in SVS, were not always in the most logical location for the user to access. For example, to change the display interface one must select "SVS Options", then "Screen Layout", then the desired screen configuration. This requires accessing a third-level menu item to accomplish a very common task (see Figure 8). Changing the perspective of the 3-dimensional view also required a pop-up window to set the viewing parameters requiring a multi-step process to change this view. Individual tree data is available in the interface, but requires entering the tree-marking interface and then selecting individual trees. All of these items are workable but not very convenient for the user to master.

We realized that there is a lot of information available in the Sylvan tree list that is not utilized by the SVS program. Additionally, the Sylvan Stand Structure model's main development platform is Linux and some team members were also using MacOS. We decided to create a new visualization tool, Sylview. The design criteria for this program are detailed in the following section.

SYLVIEW

The Sylview program was designed to be a stand-level visualization tool used to examine the output of the Sylvan Stand Structure model and allow the user to grasp the stand dynamics principles that are built into the Model. It was designed so that the viewer could fully utilize avail-

able information within the tree list, information which illustrates tree interactions likely to occur during stand development. The following design criteria for the Sylview software were established:

Practical Considerations
- It should present a plot of trees in map and profile views
- It should be very easy to see tree growth through time, both individually and collectively

- The user should be able to inspect the internal wood character of each tree

Technical Considerations

- It should work on multiple platforms (Linux, Windows, MacOS)
- It should relay 2-dimensional vector graphics for easy-to-understand views with smooth screen and print display

In Practice

- It is written in C++ language with the Qt cross-platform application framework
- It uses the Sylvan C++ libraries to allow common file format and access to the Sylvan functions

We Also Followed the Following Principles:

- Principle of least surprise—the user should not be surprised by the results of his or her actions. For example, if a user points to a tree object, then the user should get more information about that object.
- Intuitively obvious—the function of an object should be what the user expects.

Because we were calculating the internal character of the wood we used profile or taper equations to predict the diameter of the stem at any given height. These taper equations must be sensitive to crown dimensions to appropriately illustrate change in the internal structure of the stem as it

is influenced by stand density and crown competition. All depictions of a tree's vertical profile in Sylview are drawn with correctly scaled taper equations. The equations in the current version are based on the method of Walters and Hann (1986). The predicted wood-quality zones are based on the relationship of the wood to the crown at the time of wood formation.

In the Sylvan Stand Structure model we want users to be able to learn about the relationship of tree competition (in both species and density) and crown size to the resultant wood formed in the tree. Additionally, we would like this model to be easily adapted to different tree species in different places in the world. To accomplish this, the model can be parameterized using data collected in the plot to be simulated.

Currently, there is a set of R functions that are used to accomplish this task. They are cumbersome and require a large number of steps to confirm that the parameters are appropriate and reasonable. We are in the early stages of developing an additional module that will process users' plot data and produce a valid parameter file with statistical feedback on the nature of the selected parameters.

We feel that the Sylview program allows a user to examine model output at a level of interactivity that was difficult until now. The design of Sylview was also focused on visualizing data in a manner that provides users with clear information about the stand they are studying. We opted for graphical forms that convey information versus images that present

Figure 10— An example of the Sylview Program (Scott 2006). The stand illustrated is cherrybark oak (Quercus pagoda Raf.)-sweetgum (Liquidambar styraciflua L.) from Mississippi, USA. This is a one-acre plot plantation with alternating species in both directions. The profile view displays the trees in the grey horizontal box in the map view. The highlighted tree in black at left is also displayed at right showing internal wood structure, individual tree crown over time, and the stem cross-section. Also note that the tree-list data are displayed in the status bar at the bottom of the screen. This screen was captured under the Windows XP operating system.

Figure 11— An example of the Sylview Program (Scott 2006). The stand illustrated is cherrybark oak (Quercus pagoda Raf.)-sycamore (Platanus occidentalis L.) from Arkansas, USA. This is a one-acre plot natural stand. The profile view displays the trees in the grey horizontal box in the map view. The highlighted tree in black at left is also displayed at right showing internal wood structure, individual tree crown over time, and the stem cross-section. The screen was running on the MacOS.
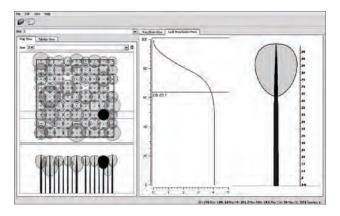
Figure 12— An example of the Sylview Program (Scott 2006). The stand illustrated is cherrybark oak (Quercus pagoda *Raf.)-sweetgum* (Liquidambar styraciflua *L.) from Mississippi, USA. This is a one-acre plot plantation with alternating species in both directions. The profile view displays the trees in the grey horizontal box in the map view. The highlighted tree in black at left is also displayed at right showing vertical cumulative leaf area index from the top of the stand to the neighbor trees of the selected tree. This information is used in the crown base change function.*

confusing visuals. We tried to make the software intuitive and easy to use, with a lot information available and few hidden menus to navigate. The submenus are typically software-preference dialogs and are seldom changed.

In our attempts to covey information we have provided model results using both traditional and innovative methods. Some of our traditional outputs include stand tables (stand statistics by diameter class), stock tables (stand statistics by species), and changes in the spatial statistics/density management diagrams (both Reineke and Gingrich). Figures 8 and 9 illustrate this type of output. Please note that the stand and stock tables also report the volume in clear wood, mixed knot wood, and green wood. These zones are specified by the relationship of the ring of wood to the tree's crown at the time of wood formation.

CONCLUSIONS

The Sylview program is one program in the set of programs called the Sylvan Stand Structure model. It is a vital component allowing users to fully appreciate the complex stand-development simulation data generated by the other programs. It allows users to comprehend the relationship of crown size and stand density to wood quality and stem shape. We have several new components planned for Sylview including the addition of branch size and number predictions based of the work of Oswalt (2007). We also plan to develop a log-sort table that will break the trees in the stand into logs of various wood characteristics. The current
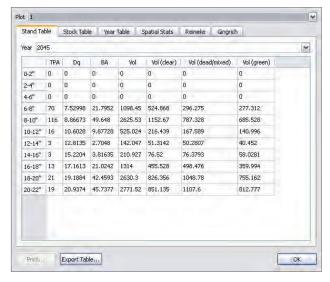
Figure 13— An example of the Sylview Program (Scott 2006). The stand illustrated is cherrybark oak (Quercus pagoda *Raf.)-sweetgum* (Liquidambar styraciflua *L.) from Mississippi, USA. This window is a standard stand table (average statistics by diameter class). Units are Dq in inches, BA in square feet per acre, and volume in cubic feet per acre. This table also provides the volume of clear wood, mixed knot wood, and green knot wood.*
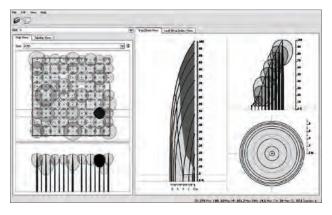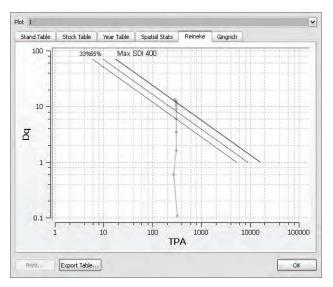

Figure 14— An example of the Sylview Program (Scott 2006). The stand illustrated is cherrybark oak (Quercus pagoda *Raf.)-sweetgum* (Liquidambar styraciflua *L.) from Mississippi, USA. This is a standard density-management diagram of the model's data from this plot.*

version of Sylview also includes a method to conduct stand treatments in the user interface. However, this component was not implemented at the time of the meeting.
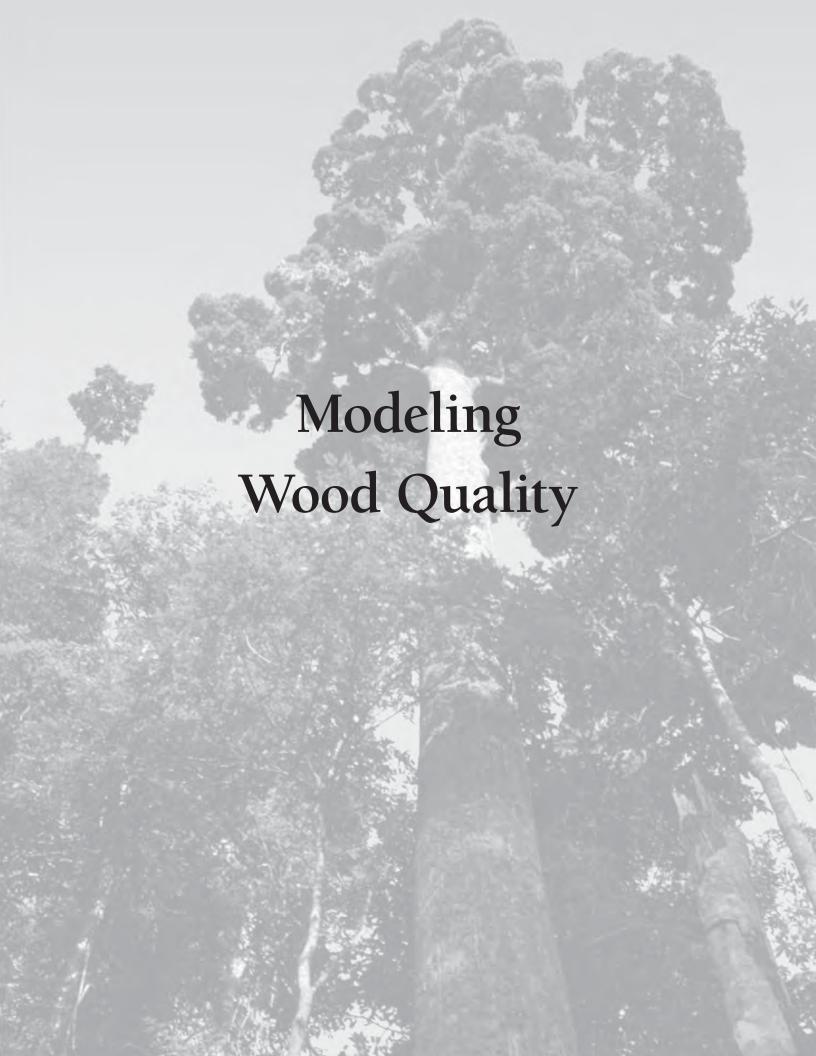
ACKNOWLEDGEMENTS

The Sylvan Stand Structure model is being calibrated to Southern Bottomland Hardwood through collaboration

with the USDA Forest Service, Southern Research Station, Southern Hardwoods Laboratory, Stoneville, MS and the US Forest Service, Forest Inventory and Analysis, Southern Research Station, Knoxville, TN.

LITERATURE CITED

Assmann, E. 1970. Principle of Forest Yield. Study. In: The Constitution and Development of Stands. Pergamon Press: 88.

Davison, M. 1995. The Sylvan display program. Master's thesis. University of Missouri-Columbia.

Gingrich, S. F. 1967. Measuring and evaluating stocking and stand density in Upland Hardwood forests in the Central States. Forest Science 13:38-53.

Larsen, D. 1991a. Projecting forest stand structures using stand dynamics principles: an adaptive approach. PhD thesis. University of Washington.

Larsen, D. 1991b. Silvicultural planning using a Bayesian framework. In: Buford, M., ed. 1991. Symposium on Systems Analysis in Forest Resources. United States Department of Agriculture: 262–267.

Larsen, D. 1994. Adaptable stand dynamics model integrating site-specific growth for innovative silvicultural prescriptions. Forest Ecology and Management 69: 245–257.

McGaughey, R. J. 1997. Visualizing forest stand dynamics using the stand visualization system. In: Proceedings of the 1997 Meeting of the American Society of Photogrammetry and Remote Sensing, vol. 4: 248–257.

Oswalt, C. M. 2007. Development of a Simulation System for Testing Hardwood Plantation Silviculture. Unpublished Dissertation. University of Tennessee. Wayne Clatterbuck, Advisor.

Reineke, L. H. 1933. Perfecting a stand density index for even-aged forests. Journal of Agricultural Research 46:627-638.

Scott, I. 2006. Sylview: A Visualization System for Forest Management. Unpublished Masters Thesis. University of Missouri-Columbia. Kannappan Palaniappan, Advisor.

Walters, D. K.; and Hann, D. W. 1986. Taper equations for six conifer species in southwest Oregon. Forest Research Laboratory, Oregon State University, Corvallis. Research Bulletin 56. 41p.

Modeling
Wood Quality

Modeling Wood Quality
Keynote Presentation

Modeling Wood Quality In the Context of Forest Management

S.Y. (Tony) Zhang

ABSTRACT
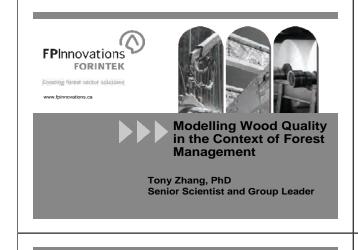
AS THE FOREST INDUSTRY IN CANADA IS shifting toward intensive forest management and value-added wood manufacturing, it is becoming increasingly important to take an integrated approach along the forest-wood value chain in order to produce quality wood and wood products and maximize the value of the forest resource. As a result, Forintek has undertaken a series of studies in recent years to examine the impact of intensive forest management on wood and lumber properties and on product recovery in major commercial species in eastern Canada. Through these studies, tree-level models have been developed to describe key stem, wood, and lumber properties as well as product recovery in relation to tree and stand variables. Based on these studies, this paper reviews wood-quality modeling in the context of forest management. Following a review of important wood-quality attributes and their evaluation methods, this paper highlights wood-quality variation and manipulation through forest management and compares different approaches to wood-quality modeling.

Editors' note: *The author elected not to provide a full paper for these proceedings because it was being submitted to a refereed journal. As with all of the keynote addresses, this presentation was designed to provide context for the related presentations that follow. In lieu of the keynote paper, the author's slides from the presentation are reproduced on the following pages to introduce the topic for this section of the proceedings.*

S.Y. (Tony) Zhang (tony.zhang@van.forintek.ca) is a senior scientist at FPInnovations—Forintek Division, 2665 East Mall, Vancouver, BC V6T 1W5, Canada.

Slide 1

FPInnovations
FORINTEK

Creating forest sector solutions

www.fpinnovations.ca

Modelling Wood Quality in the Context of Forest Management

Tony Zhang, PhD
Senior Scientist and Group Leader

Slide 2 — Contents

- What are important wood quality attributes
- Wood quality evaluation
- Wood quality variation and manipulation
- Wood quality modelling

Slide 3 — What is wood quality?

- **Foresters: mainly refer to external stem characteristics**
- **Manufacturers: attributes affecting wood processing (e.g. sawing, drying, machining)**
- **End users:**
  - **1) structural products (e.g. mechanical)**
  - **2) appearance-based products (e.g. surface)**

Slide 4 — What are important wood quality attributes?

Any characteristics which affect the wood value chain are considered as wood quality attributes

Slide 5

Silviculture	Site	GENETICS

SDM/Rotation Age

Height Growth

Crown Structure / Development

- Tree diameter/ volume
- Wood structure
- Juvenile wood
- Chemical composition
- Wood density
- Fibre morphology
- Branch growth
- Knottiness
- Visual aspect

- Tree taper

Lumber volume/ dimension recovery

Strength/stiffness stability
Lumber quality

- Appearance
- Stability
- Machinability
- Durability

Lumber value

Pulp/paper value

Secondary products value

Slide 6 — What are important wood quality attributes?

- **Wood quality attributes include a number of stem and wood characteristics (both external and internal stem characteristics)**
- **Wood quality attributes vary with end uses**

Important wood quality attributes for structural lumber

- Large diameter: low conversion cost, high recovery
- Straight stem: high recovery, large dimension,high quality
- Small taper: high recovery
- Clear log/small knots: high quality
- No decay: low conversion cost, high quality and high recovery
- High wood density: high strength/stiffness
- Low juvenile wood%: stability, strength/stiffness
- No grain deviationt/reaction wood: stability

Important wood quality attributes for pulp/paper

- Long & thin-walled fibres: form dense sheets with smooth surface, high tensile strength
- Transverse dimension of fibres: paper properties
- Uniformity in fibre morphology: paper properties
- **Low lignin % & high cellulose %:** high yield, low cost
- **High wood density**: high yield
- **Low extractives % & light colour**: low cost
- **Minimum defect**: high yield, low cost

Important wood quality attributes for panels

- **Large and straight logs**: high recovery
- **Minimum taper**: high recovery
- **Attractive wood appearance**: high quality
- **No drastic difference between earlywood & latewood**: peeling, surface quality
- **Moderate wood density:**: easy peeling, processing
- **Clear logs/minimum knots**: high quality, low cost, high recovery
- **Minimum decay/other defects**: low cost, high recovery

Important wood quality attributes for secondary products

- Attractive appearance *(colour, figure, surface roughness):* quality
- Excellent dimensional stability: quality
- Defect-free: quality
- Good machinability: easy processing
- Durability: quality
- Uniformity: quality

Key quality attributes for major end uses

- For structural lumber, piece size and wood strength should be a priority
- For secondary products, piece size, appearance & stability should be the focus
- For fibre-based products, fibre quality and wood density are important

Important quality attributes for major end uses

Aim at end-product quality attributes rather than intermediate wood attributes *(e.g., wood density for lumber)*

Contents

• What are important wood quality attributes

• Wood quality evaluation

Ideal tools for wood quality evaluation

– Nondestructive
– Reliable
– Affordable
– Not time-consuming
– Ideally portable

Advanced methods for evaluating wood quality

– Ray-based methods
– Stress wave methods
– Ultrasonic methods
– Vibration methods
– Advanced microscopes
– Others (e.g., mechanical)

Methods for evaluating wood anatomical/chemical attributes

• **Microscopes/image systems**: microscopic, ultrastructural features
• **Fibre quality analyzer/Kajaani**: fibre length & coarseness
• **Fiber strucutre analyzer**: fibre shape/cross sectional analysis
• **CT Scanner/Micro CT**: NDT systems for macro- and microscopic features
• **Silviscan**: MFA, cell size

Methods for evaluating wood anatomical/chemical attributes

• Windendro/WinCell: ring/cell characteristics

• NIR spectrometry: chemical composition, MFA, fibre & wood mechanical properties

• X-ray diffractometry: MFA, ultrastructure

• Others

Methods for evaluating physical/mechanical attributes

• X-ray densitometry: wood density/ring characteristics

• Stress wave: wood stiffness

• Ultrasonic: physico-mechanical properties

• Vibration: physico-mechanical properties

Methods for evaluating physical/mechanical attributes

- NIR: wood density, strength/stiffness

- Silviscan: wood density, stiffness

- Computer tomography *(CT scanner):* macro characteristics of wood/internal log

Techniques for the NDT of standing trees

- Pilodyne: wood density of the rings nearby bark
- SilvaTest: MOE
- Resistograph: wood density
- Fibergene: MOE
- Etc.

Real challenge is to develop more reliable, portable and cost-effective tools for the nondestructive evaluation of standing trees!

Contents

- What are important wood quality attributes

- Wood quality evaluation

- Wood quality variation and manipulation

Sources of variation in wood quality

- Silviculture
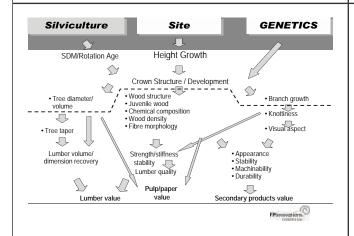
- Genetics

- Environment/site

- Processing

Sources of variation: silviculture

Clear log length
Knottiness
Stem taper
Sapwood%
Juvenile wood%
Bending properties
Ring characteristics and wood uniformity
Wood density

Sources of variation: Genetics

Chemical composition (e.g. lignin%)
Fibre length and MFA
Decay resistance
Wood density
Juvenile wood transition
Branchiness
Stem straightness

Sources of variation: Site

Occurrence of defects (decay, wetwood)
Wood color
Ring characteristics and wood uniformity
Sapwood%
Juvenile wood transition
Wood density

Sources of variation: processing

Wane
Grain deviation
Wood texture and figure
Surface roughness
Dimensional stability

Major management tools for wood quality manipulation

– Tree breeding
  – Forest genomics
    – Species selection
      – Site selection
        – Initial spacing
          – Thinning
            – Pruning
              – Fertilization
                – Rotation age

Wood quality manipulation by genetics

- Focus on <u>major heritable, internal quality traits</u>: fibre morphology, chemical composition, microfibril angle, decay resistance, wood density, juvenile wood%, etc.

- Pay attention to <u>external quality traits</u>: straightness and branch characteristics

Wood quality improvement by silviculture
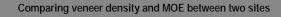
Focus on <u>external quality attributes</u>: Piece size, clear log length, branchiness/knottiness
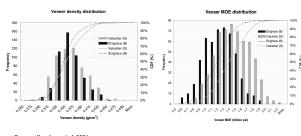
Pay attention to <u>selected internal quality attributes</u>: sapwood%, juvenile wood%, ring characteristics, bending properties, wood density,

Wood quality improvement

It is important that wood quality improvement target at <u>end-product quality attributes</u> rather than intermediate wood attributes *(e.g., wood density for lumber)*

Comparing veneer density and MOE between two sites

Source: Knudson et al. 2006
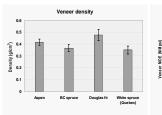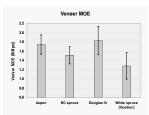
Comparing genetically improved white spruce veneer to those of other Species

Source: Knudson et al. 2006

Contents

• What are important wood quality attributes

• Wood quality evaluation

• Wood quality variation and manipulation

• Wood quality modelling

Modelling Approaches to wood quality attributes

• Empirical modelling

• Physics-based approach

• Process-based approach

---
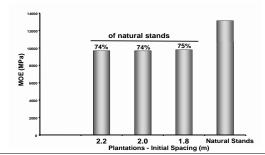
1. Empirical Modelling Approach

• Used to model most wood quality attributes such as
  1) Wood density & other physical properties
  2) Mechanical properties
  3) Fibre properties
  4) others
• But, most wood quaity attributes are <u>stand type-dependent</u>, <u>age-dependent, site-dependent.</u>

black spruce lumber stiffness between plantations and natural stands

Source: Zhang et al. 2002

---

1. Empirical Modelling Approach

- Models for lumber properties of natural stands (Liu et al. 2007)

  MOE = f (DBH, crown length, stem taper)
  MOR = f (DBH)

- Models for plantation-grown lumber properties (Lei & Zhang 2005)

  MOE = f (DBH, Crown length, stem taper)
  MOR = f (DBH, crown length, crown width)

---

1. Empirical Modelling Approach

- Most wood quaity attributes are **age-dependent**. While age can be taken into consideration for some attributes (e.g., wood density), it is difficult to incorporate age into the prediction models for some attributes (e.g. dimensional stability, bending properties)

- WD = f (cambial age, ring width, tree height)

---

1. Empirical Modelling Approach

- Some wood quaity attributes are also **site-dependent**. And we can not measure wood samples from various sites

---

1. Empirical Modelling Approach

- Relatively easy to develop and has some practical applications

- Difficult to integrate the empirical models into growth models

- Difficult to serve for forest management purposes

Variation of selected wood characteristics due to site, diameter class and age in balsam poplar

Characteristics	Source of variation	Degree of freedom	Mean squares	Variance components	V. C. (%)
Wood density (kg/m³)	Site	2	4776	173	25.6
	Diameter	4	489	0	0.0
	Age	4	1158	97	14.4
	Error	59	406	406	60.0
Initial moisture Content (%)	Site	2	6120	262.5	48.9
	Diameter	4	240	0.0	0.0
	Age	4	378	15.2	2.8
	Error	59	260	260.4	48.3
Sapwood thickness (cm)	Site	2	22.84	0.933	42.6
	Diameter	4	4.56	0.253	11.5
	Age	4	2.72	0.255	11.6
	Error	59	0.75	0.751	34.3
MOE (MPa)	Site	2	11779761	171458	13.5
	Diameter	4	1527873	0	0.0
	Age	4	5717434	400954	31.6
	Error	59	695738	695738	54.9
Decay (%)	Site	2	370	11.5	14.3
	Diameter	4	75	0.0	0.0
	Age	4	135	9.8	12.1
	Error	59	59	59.5	73.6

Source: Zhang and Chauret 1999

2. Physics-based approach

- Used to model selected wood quaity attributes such as

  1) Wood shrinkage and dimensional stability
  2) Mechanical properties

FPInnovations

2. Physics-based approach

- **Physics-based modelling approaches essentially link the properties of the individual elements (e.g. cells, microfibrils) to the properties of a lumber piece using finite element analysis and other analytical methods**

FPInnovations

2. Physics-based approach

- **Development of such physics-based models for physical and mechanical properties is technically complex and require micro/anatomical information**

- **Once developed and validated, they could be generalized with relative ease over a broad range of stands**

FPInnovations
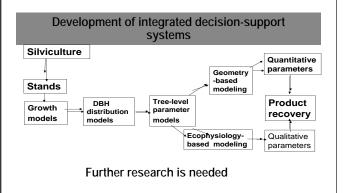
3. Process-based Approach

- Used to model those wood quaity attributes related to crown structure and development such as:

  1) sapwood content
  2) knottiness
  3) juvenile wood

FPInnovations

3. Process-based Approach

- Applied to stands of different sites and ages

- Require more input variables which are more difficult to measure

FPInnovations

Development of integrated decision-support systems

Silviculture → Stands → Growth models → DBH distribution models → Tree-level parameter models → Geometry-based modeling → Quantitative parameters → Product recovery

Ecophysiology-based modeling → Qualitative parameters → Product recovery

Further research is needed

FPInnovations

Resource Inventory for Conversion Modeling

Graeme Palmer and Jerry Vanclay

ABSTRACT

FORESTERS ROUTINELY ESTIMATE THE economic potential of a standing forest resource as lumber. It is usual to consider the straightness and size of a tree to estimate gross recovery and the range of lumber products that might be produced. However, such estimates are usually subjective and depend on the knowledge and experience of the assessor. Several conversion modeling packages are available to assist with such appraisals, but these require an established library of log data, or require detailed and expensive log measurements. Fortunately, many tree attributes that influence lumber out-turn can be easily and objectively appraised, and these easy-to-measure attributes can be used to infer a larger suite of log characteristics.

This paper briefly describes a computer-based conversion modelling system that emulates components of a wood-processing system and enables users to create a custom wood-processing facility producing lumber, veneer, or other products. It examines the attributes of trees that need to be quantified for such simulation to proceed, describes how routine timber cruising can record these details, and discusses how a user may modify these attributes to reflect different silvicultural regimes. It also describes the accounting module which enables detailed financial analysis of conversion strategies, and of the whole value chain. The system challenges forest managers to examine silvicultural options in a broader context, focusing not on a "better log", but on creating more value in the lumber marketplace.

INTRODUCTION

Wood production in Australasia has undergone considerable change over the last 30 years as the wood-using industries convert from native forest to plantation-grown wood. Change continues with pace now as hardwood plantation production emerges and native forests are conserved free of harvesting.

Sawmills are the primary wood users and are becoming more exposed to global markets; they are, consequently, reducing margins. The importance of management has never been so critical, nor the impact of wood quality more important to achieving commercial goals.

It is the goal of both producer and processors to optimize the profitability of the industry. Therefore, management is mainly about manipulating the character of wood, the design of processes, and as far as possible the price of products.

The problem that faces most managers is: How can resource quality be evaluated inexpensively so that different management scenarios can be compared?

The parameters contributing to this analysis are:
- Available processing options
- Market for products
- Average properties of clear wood and variation
- The presence and impact of defects

The important message from this discussion is that value, and therefore quality, is a "local" variable. That is, the resource produced in say Southeast Queensland needs to be different from wood grown in the Northwest of the United States.

Graeme Palmer (woody@biltechnologies.net.au) is a doctoral student and **Jerry Vanclay** is professor and head, School of Environmental Science and Management, Southern Cross University, PO Box 157, Lismore, NSW 2480, Australia.

For sawn-wood processing, the primary process-efficiency parameters are the scope and *variation* of wood properties and defect distribution. The *average* values contribute most substantially to product price. Simulation is ideal for this kind of problem because the variety in the character of a wood resource can be accommodated sensibly.

Industrial optimization, in the context discussed here, requires a resource simulator and a process simulator. That is, a component that can create virtual stems and a component to convert these stems into virtual products.

The resource description component is the most difficult because of the level of detail required by product grading systems, and the apparently wide variation in the relevant quality parameters. Both these features need to be accommodated if simulation is to incorporate both finished-product value estimates as well as process-cost estimates.

Models and simulators of various types span the range of application from standing stems to finished product. For example:

- Yield models are used extensively to program wood flows
- MARVL (NZFRI 1987) is an example of a system that provides yield by log quality classes
- CAPSIS and WinEPFN (Meredieu et al. 1999) are examples of simulators that combine yield or growth models with conversion simulators to provide estimates of processed product yield by value
- AUTOSAW (Todoroki 1990) is an example of a complex conversion simulator enabling optimization of saw pattern and grade recoveries using virtual logs that include knot defect information. This system has also been combined with production models to provide stand management optimization like WinEPFN
- GRASP (Occena and Schmoldt 1996) is a sawing simulator developed in the USA that uses sophisticated 3D solid-log representations with shape and defect derived from CT (computer tomography)
- SATECH (Saatech Systems Pty Ltd.) is a very simple saw pattern simulator that uses log sizes and minor variations in shape to optimize recovery
- WOODEYS SIM (Innovative Vision) is a docking simulator that can provide product yields by quality class from board character inputs collected by a scanner/docker system

In the view of the author, if these systems are considered in the context described above, potential problems exist that include:

- The localized nature of detailed resource character and process design inputs
- Limited breadth of resource characters that are supported by simple systems
- The high cost of detailed data such as provided by computer-aided tomography

Additionally, for many potential users, data and or models that describe stem features may not be available, e.g., growth and taper functions, knot models, density models, etc. For these users, inventory and general and known statements of correlation between stem characters are the only sources of input data.

In Queensland, the public wood producer has attempted to solve these problems by adapting WinEPFN to local parameters. This required a significant rebuild of the system to incorporate local models and grade rules which are "hard coded".

What is needed is a broadly applicable software system that can be used to define or describe detailed stem characteristics for a virtual resource using whatever input data that can be assembled easily and/or cheaply. In particular, the use of standing resource inventory data offers the best opportunity to capture local resource character.

A software system such as this could be applied to a variety of problems; for example, resource valuation, strategic planning of merchandising processes, and process design optimization to name a few. The application of such a system may also be widened if data can be manipulated by "skilled" users to reflect novel stands that may be the objective of breeding or silviculture.

INVENTORY DATA

For the purpose of developing and now demonstrating the operation of the system, the following inventory data were gathered to describe stems.

- Diameter at breast height and total tree height
- Taper formed from height and diameter
- Stem form assessed by measuring the height of each bend in the measured stems, the direction of the bend measured by compass, and the deviation of the bend from straight estimated as a proportion of stem diameter at the bend node
- Crown assessed by locating points in the stem that correspond to the bottom of the growing crown (identified by the lowest dead branch) and the bottom

of the live crown (identified as the branch node above the lowest dead branch)

o At each point on the stem, a collection of local branch nodes assessed—the number of branches, along with the size and the direction of each branch was recorded (branch size estimated by eye as a proportion or percent of stem diameter at the point of branch location)

While this format was implemented here, the system was designed to accommodate any format adopted by the user.

The important point to be made is that the nature of the inventory is not limited and, in practice, more detailed and expensive data collection can be accommodated with the obvious advantages of accuracy and detail that can be achieved through a more complex inventory.

A Resource Maker

The system described here attempts to meet the goal of generic application.

The system includes:

- An abstract data structure that describes a stem including all the characteristics that a user or application demands
- Tools to read data of various types
- Tools to display and manipulate data
- Tools to make new simulated data
- A tool to display the stems

An important concession is made in the design of the system in order to maintain reasonable cost and accessibility. A virtual stem of sufficient complexity to represent the characteristics that define product value is assumed to be resolved by a collection of 3D forms located in Cartesian space. These forms, in turn, are described by simple mathematical expressions.

The principle reason for making this concession is that any stem may be stored more efficiently within a computer as a collection of expressions rather than as a 3D-matrix or raster of point data values. The latter requiring large amounts of computer memory, e.g., 1m3 resolved to 1mm3 units equals 10^9 bytes potentially.

Finally, a sawmill simulator is also under development that will convert virtual stems

to product grade by recovery data. It is the resource maker that is the focus of this document.

The Data Type "Stem"

At the center of the system is the abstract stem data type. This data type must be designed to accommodate all of the usual features of a stem that might impact either conversion cost or product grade and recovery. The design also needs to accommodate expansion so that other features may be accommodated as a given simulation context requires.

The user can define any additional variables to add to the data structure, and this feature is used to accommodate any wood-quality variable the user wishes to add. For example, microfibril angle or heart/sap wood.

The data structure includes the following types:

- values—single value data
- functions—a mathematical expression that solves to produce value of y for all x
- sequences—a sequence is a series of values or sequence members that describe characteristics that may be correlated between members; for example, the distances between branch nodes will be correlated to

Table 1—The stem data structure.

Attribute or Sub-attribute	Type of Entry
Age	single value
BHt	single value
DBH	single value
THt	single value
Growth = Function of age	
GHt [f (GAge)]	expression
GDia [f (GAge))	expression
GAge	single value
Form = Sequence of Bends	
Bend = BndHt	single value
BndDir	single value
BndDev	single value
BndFrm	expression
HForm = Function of Direction	
Radius	expression
Taper = Function of height	
TprDia [f (TprHt)]	expression
TprHt	single value
Bark = Function of height and direction	
BrkHt	single value
BrkThk [f (BrkHt)]	expression
Crown = Probable sequence of Branch Nodes	
Branch Node = Node Ht, Array of Branches	
Branch = BrDia	single value
BrDir	single value
BrAng	single value
BrGnl	single value
BrDdl	single value
BrFrm	expression
Wood Properties = Array of Wood Property	
Wood Property = f (Age)	expression

the distance between previous branch nodes

- probable sequences—similar to a sequence except that the input data relating to a sequence is a census for any single tree while data for a probable sequence are in samples; these types vary the manner in which the system treats them during resource design

During run time, two data structures are formed and utilized by the system. One structure is formed for input, and a second is formed as the simulated stems. In practice, the user enters data via the input structure, and then uses tools to create the simulated structure.

Data Input Tools

Data that can be utilized by the system include both numeric values and expressions. To accommodate the input of numeric data, the system includes an input file format designer, and a reader. The capacity to design input files enables the reading of any data file for any feature of the stem.

Input is assumed to be hierarchical. For example, for the following data structure,

VarA, ArrayA

ArrayA = VarB, ArrayB

ArrayB = VarC, VarD

the input file will be arranged as a series of values as follows:

VarA1.

VarB11

VarC111, VarD111

VarC112, VarD112

VarC113, VarD113;

VarB12

VarC121, VarD121

VarC122, VarD122

VarC123, VarD123;;

VarA2.

VarB21

VarC211, VarD211

VarC212, VarD212

VarC213, VarD213;

VarB12

VarC221, VarD221

VarC222, VarD222

VarC223, VarD223;;;

The system interface is shown in the following figures. The upper dialog window in Figure 1 shows the data form through which the user defines DBH and total height, then opens a new form (lower dialog window) to enter data for the bend height, bend size, and bend direction of each bend within the stem.

The Function Design Tool

To accommodate input of functions, an interpreter is included within the system that can read and interpret functions (input as typed text) that may then be attached to data items. An analogy may be drawn with "macros" used in numerical analysis software such as spreadsheets. Figure 2 shows the function panel and an example expression defining growth in diameter at breast height as a function of age. This function has been formed by fitting a curve provided by the system of input data, by least squares. This approach or an external user-defined function may be used.

The Chart Tool

A data-charting module provides the user with data display capacity to view the manner in which variables are related. The chart tool also provides the interface for the "make" tools mentioned below.
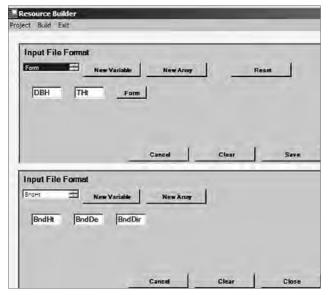
Figure 1: The input format definition panel. At level 1 (upper dialog window), diameter at breast height (DBH) and total height (THt) are defined. Then, the user accesses level 2 by clicking the "Form" button. This opens the lower dialog window through which the stem form is defined by entering, for each bend in the stem, the bend height (BndHt), bend deviation (BndDe), and bend direction (BndDir).
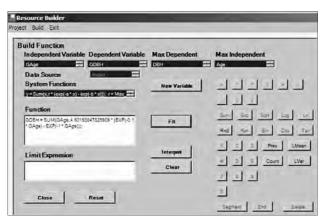
Figure 2. The function input panel.
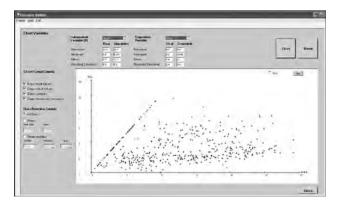
Figure 3: The data-charting panel showing input and simulated data values for inter-bend distance versus height in the stem.

"Make" Tools

At the core of the system is a set of tools that are designed to "make" data values or functions for simulated stems from input data or functions generated from real stems. The make tools include:

- Making single values
- Making functions
- Making sequences and
- Making probable sequences

Each uses the same general approach which is:

- Input data values are used to determine variability around an average value.
- This variation is used to select a simulated value either at random or biased to reflect a normal distribution in the input data. A further bias is applied to cause the make process to tend toward producing the same variability in the simulated data as is displayed by input data, i.e., the next value made will be selected to maintain the variance described by the input.
- Sequences are made from individual member data sets in sequence.

- Probable sequences use the average and variance of samples taken from the range of an independent variable to make simulated values.

Figures 4 and 5 illustrate the use of the "make" tools. Figure 4 shows the process through which one of the tools is used to define growth curves that display the development of simulated tree stems over time. Figure 5 illustrates the result of the "make" process for a specific example. The input values are shown by curves connecting light-colored points and the simulated growth curves are those connecting the black points.

The Display

Finally, a display tool is provided within the resource maker to visualise virtual stems. In Figure 6, profiles are displayed of a simulated stem showing the stem surface (upper image) and a cross section of wood density (lower image). Note that
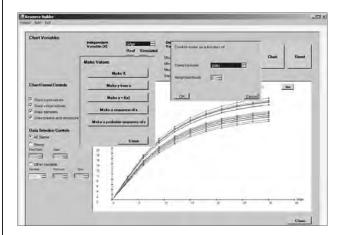
Figure 4. Using the "make" tools to form growth curves for simulated stems.
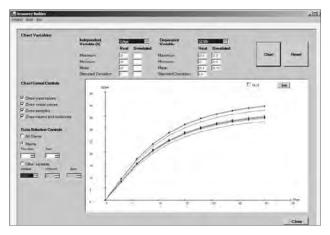
Figure 5: A display of input (curves connecting the light-colored points) and simulated (curves connecting the black points) growth curves for the first five stems of the input and simulated data sets.
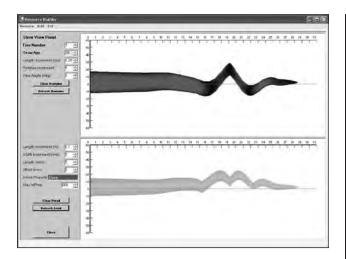
Figure 6: The display tool showing stem surface over bark (upper image) and cross-sectional variation in wood density (lower image).

in the stem-surface image, darker shading denotes bending into the image, giving information in the third dimension. For the wood-density image a simple relationship with diameter is displayed in only two dimensions.

Concluding Remarks

This discussion and demonstration have shown how the system may be applied to almost any application context that might arise. The system offers capacity for any user to exploit any form of input to create virtual 3D representations of tree stems that can be manipulated in Cartesian space by a conversion simulator.

While the system is fundamentally complete, minor developments continue to build a more robust system. In the next stages, the distribution of knots will be added to the system and display.

The system remains untested in any practical sense, however, and this is the subject of work that will go on over the next 3 years, using eucalypt hardwood plantations as the test environment.

The sawing simulator that is required to partner with the resource maker is also under development. The design of this system is similar to the resource maker in that it attempts to provide a design platform which would enable the user to design both saw patterns and the sequence of process stations that comprise process design. In this way, the system will attempt both to define product-grade volumes that form output and to estimate material flow rates and machine productivity.

LITERATURE CITED

Occena, L.; Schmoldt, D. 1996. Grasp: A prototype interactive graphic sawing program. Forest Products Journal 46(11/12):40-42.

Meredieu C.; Dreyfus P.; Saint-André L. ; Leban J.M. 1999. A chain of models from tree growth to properties of boards for *Pinus nigra* ssp. laricio Arn.: Simulation using CAPSIS and WinEpifn. In : Nepveu, G., ed. Workshop on Connection between Silviculture and Wood Quality through Modelling Approaches and Simulation Software, Proceedings of the IUFRO 5.01.04 workshop held at La Londe-Les Maures, France, 5-12 Sep 1999. Nancy, France: INRA: 505-513.

NZ Forest Research Institute. 1987. Stand assessment by log grades using MARVL. FRI Bulletin 132. Rotorua, New Zealand.

Todoroki, C.L. 1990. Autosaw system for sawing simulation. New Zealand Journal of Forestry Science 20(3):332-348.

Maximizing Benefits from Oval Logs Using Geometric Modeling with Finite Precision

Christine L. Todoroki, Robert A. Monserud, Dean L. Parry

ABSTRACT

OVER THE YEARS SAWMILLERS HAVE BY by trial and error determined the most advantageous way to improve recovery from their logs. For elliptical shapes, primary sawing along the longer axis has generally been accepted as the "correct" method. To verify this, we applied a series of sawing simulations to five replicate groups of oval logs, modeled from measurements of 52 western hemlock logs. Ovality of each group was controlled through transformations that progressively altered cross-sectional shape while maintaining constant log volume. The log models were sawn in a series of simulations with AUTOSAW that altered log orientation, elliptical representations, and error bounds. Log orientation was altered by 5-degree increments. At the 0-degree orientation (and at 180 degrees) logs were sawn with the primary saw parallel to the shorter axis, and at 90 degrees (and 270 degrees) were sawn "correctly" along the longer axis. Angular orientations yielding the maximum percentage of lumber volume to log volume were recorded. Maxima, rather than averages were of primary interest due to the closer alignment with sawmillers' requirements. Contrary to common belief, oval logs tended to produce more lumber than round logs—when rotated to their optimal orientation. Moreover, maximum responses tended to increase with increasing ovality. Maxima occurred more frequently at 90 degrees and 270 degrees. Because of the finite precision implementation, round-off errors were prevalent within proven geometric algorithms. Increasing the number of co-ordinates in the elliptical representations and increasing the error bound on numerical comparisons did not eliminate, but shifted the problem. Our ability to isolate round-off errors through visualization of the various stages, track back to individual boards, and add seemingly insignificant amounts of wane (0.004 inch) enabled us to overcome limitations due to finite precision arithmetic.

KEYWORDS: Log eccentricity, sawing simulation, conversion, yield, geometric algorithms, computational precision

INTRODUCTION

In spite of the myth that logs are round, oval logs are more common than truly circular shapes (Matérn 1956). Ovality tends to be greater for larger logs and for those logs from the lower parts of the stem (Asikainen and Panhelainen 1970, Williamson 1975, Singleton et al. 2003). If ovality is described by an ellipticity ratio, defined as the inverse ratio of the largest diameter to that perpendicular to it (Figure 1), then truly circular logs would have the maximum possible ellipticity ratio of 1.0 and oval logs would have an ellipticity ratio of less than 1.0.

The ellipticity ratio of log cross-sections typically lies between 0.80 and 1.00. Williamson's (1975) mean and standard deviation for Douglas-fir out-of-roundness corresponds to our ratios of 0.83 and 0.97, and Monserud's (1979) to 0.945 with a standard deviation of 0.04. Kellogg

Christine L. Todoroki (Christine.Todoroki@scionresearch.com) is a senior scientist, New Zealand Forest Research Institute Limited, Private Bag 3020, Rotorua, New Zealand; **Robert A. Monserud** (retired) was a research forester and team leader and **Dean L. Parry** (retired) was a research forester, USDA Forest Service, Pacific Northwest Research Station, PO Box 3890, Portland, OR 97208, USA.
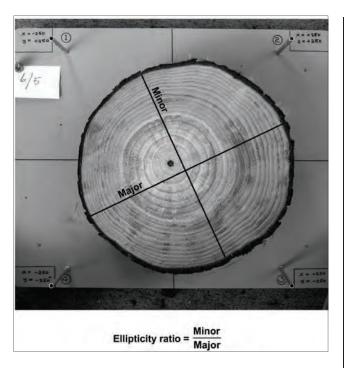
Figure 1— Definition of the ellipticity ratio as the inverse ratio of the largest diameter to that perpendicular to it.

and Barber (1981) found that the mean ratio (albeit not perpendicular) for western hemlock was 0.92, ranging from 0.85 to 0.96. Biging and Wensel (1988) reported an overall mean of 0.94, from which a sub-sample of 45 disks had a mean of 0.91 and range of 0.77 to 0.98. Ellipticity ratios between 0.82 and 0.94 were found for lodgepole pine (Koch et al.1990), and for Norway spruce Saint-André and Leban (2000) recorded a mean of 0.94 with the most extreme ellipticity ratio being 0.72.

Ovality is often perceived as being detrimental to sawn lumber recovery. Skatter and Høibø (1998) state that "any deviation in shape from circularity will normally reduce the yield" while Saint-André and Leban (2000) state concern "about the loss in yield due to the non-circular external log's shape" in citing Skatter and Høibø (1998). Skatter and Høibø's findings are, however, based on "mean simulated main yield" where "main yield" refers to yield from a central block within the log and ignores the contribution of side boards. In considering yield from both side boards and cant boards Asikainen and Panhelainen (1970) found that yield from oval logs depended on how the log was oriented relative to the saws. They found that when the log was sawn in its "correct" position, with the smaller radius perpendicular to the primary saws (equivalent to the longer axis being parallel to the primary saws), and with its volume determined

on the basis of the minimum diameter, that "the sawing yield of an oval log is better than that of a round log of the same size". Furthermore "when sawing is carried out in the wrong position, the opposite applies".

The effect on value recovery, due to ovality, has been investigated by Maness and Donald (1994). They found that although ovality caused significant reductions in value, significant benefits were gained with the optimal rotation of logs. They also found the benefits were more highly related to cross-sectional eccentricity than to log sweep.

We test the assumption that ovality is detrimental to lumber yield, and test the hypothesis that the best sawing position is as described by Asikainen and Panhelainen (1970). Our primary interest is with maximum responses with respect to log rotation because they correspond to logs rotated for optimal lumber yield. Our secondary interest is with finite precision arithmetic, data representation and error bounds, and the contribution of these factors to solution accuracy.

METHOD

The assumption and hypothesis are tested using sawing simulation with AUTOSAW (Todoroki 1990, 1997). The sawing simulator is based on geometric algorithms and, due to computer implementation, finite precision arithmetic (Higham 2002). Given that *"a finite precision implementation of a proven geometric algorithm is not necessarily correct; because of round-off error"* (Milenkovic 1988) we test three methods for improving accuracy by 1) increasing the number of discrete data representing cross-sectional shape, 2) increasing the error bound in numerical comparisons, and 3) increasing the error bound on isolated numerical comparisons with known round-off errors.

Log Models
Five groups of 52 digitized logs ranging from circular cross-sections (control) to those with ovality of 0.80 (in decrements in the ellipticity ratio of 0.05) were modeled from a sample of 52 measured western hemlock logs. The 52 logs comprised a range of small-end diameters, tapers, and volumes. Logs within the control group were modeled with circular cross-sections; the other four groups had progressively more elliptical cross-sections. Each oval log replicate had a cross-sectional area and volume identical to the corresponding circular log. The format of the log models was compatible with AUTOSAW log model input format,

thus cross-sections were represented using ordinates (x_c, y_c, z_c) to represent the geometric center, and polar notation (r_1, r_2, θ) to represent the semi-major and semi-minor axes, r_1 and r_2, and the angle of the ellipse to the horizontal, θ.

Sawing Simulation

The log models were processed in the AUTOSAW sawing simulator using a cant sawing pattern, cutting lumber that was primarily of 2-inch nominal thickness, between 4 and 12 inches wide, and tallied in 1-ft increments. The primary saw had a 0.14 inch kerf while that at the edger was 0.18 inch. A secondary thickness of 1 inch was also allowed. Lumber was edged and trimmed to remove wane. Thus the full extent of the effect of ovality on yield, defined as the percentage of lumber to log volume and known alternatively as "conversion", could be examined.

The sawpattern described above was repeatedly applied in a series of simulations that altered log orientation, elliptical representations, and error bounds. At the initial orientation of 0 degrees, the primary saw was parallel to the minor axis of the elliptical cross-sections and the cant processed in a perpendicular direction (Figure 2) while at 90 degrees (and 270 degrees) logs were sawn "correctly" along the longer axis. Logs were rotated and sawn in 5-degree increments allowing conversions to be tracked across rotations. Thus rotations at which maximum conversion occurred could be identified.

Elliptical representations of cross-sectional shape, used within geometric algorithms in AUTOSAW, were modeled by a number of discrete (x, y) co-ordinates. In the first series of simulations the number of co-ordinates was set to 30, and in a second series the number was increased to 72. In both of these simulation series an error bound, ε, equal to the available computational precision, 10^{-12}, was used in numerical calculations. The following simple numerical procedure that repeatedly divides a variable, u, by 2, starting from 1 until no difference is encountered, was used to calculate the error bound on computational precision, ε:

$$u = 1$$
$$\text{while } 1 + u > 1$$
$$\varepsilon = u; \quad u = u/2$$
$$\text{end};$$

In a third series of simulations the error bound was increased to 10^{-3} (while maintaining the number of co-ordinate pairs per ellipse at 72), effectively allowing an additional 0.001mm on measurement calculations. Within

0 degrees
lumber/log volume = 52%

45 degrees
lumber/log volume = 49%
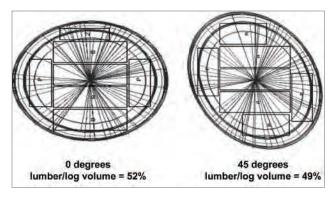
Figure 2— Initial (0-degree) and 45-degree orientations, with conversions, of a log with an ellipticity ratio of 0.80.

each series a total of 18,720 automated simulations were performed: 72 rotations x 52 logs x 5 ovality groups.

In a final set of sawing simulations AUTOSAW was invoked interactively, rather than in an automated fashion as in the previous simulations. Only those boards with known floating point errors, detected through analyzing the results for disparities, were re-sawn. For the circular logs, in the absence of floating point errors, log to lumber conversions were expected to be identical for all rotations. For elliptical logs, conversions across the range of orientations were expected to display symmetry, due to the symmetry of the log shape and consistency of all sawing factors. Logs with conversions that deviated from these expectations were identified and the rotational setting of the disparity recorded. The disparity was then tracked back to the individual board by re-invoked AUTOSAW with the sawing simulation history (binary) file. The board was then un-cut (a feature of AUTOSAW that enables cuts to be un-sawn), the wane tolerance changed from 0.0 to 0.1mm (0.004 inch), and then re-cut, invoking the same cutting algorithms as called for in the automated simulations.

Analysis

Simulated board dimensions were summarized by log, orientation, and ovality and combined into datasets that also incorporated log volume and diameter information. Microsoft Excel® was used to calculate conversions. Normalized responses were calculated by dividing through by the corresponding circular log's response at the initial orientation. In this way any effects due to differing log sizes, shapes, and branching configurations were eliminated. SAS® (1999) was used to analyze the data, calculate confidence intervals (CI), and test for significant differences between means using 95 percent confidence levels. Floating point errors were detected through comparison of conver-

sions. For circular logs, conversions at adjacent angles were compared, while for elliptical logs conversions that had been generated with equivalent planes of symmetry were compared, e.g., all conversions at 5 degrees from horizontal (5 degrees, 175 degrees, 185 degrees, and 355 degrees).

Table 1—Mean, standard deviation, and 95% confidence intervals for the normalized maximum conversions by ellipticity ratio. Comparisons are between the oval (ratio < 1.00) and circular (ratio = 1.00) log sets.

Ellipticity ratio	Sample mean	Standard deviation	Confidence interval
0.80	1.032	0.078	.011 – .053
0.85	1.031	0.063	.014 – .048
0.90	1.034	0.057	.018 – .049
0.95	1.021	0.028	.014 – .029
1.00	1.000	0.000	

RESULTS

Floating point errors were detected amongst some of the simulated boards. In the initial scenario with $\varepsilon = 10^{-12}$ and 30 co-ordinates per cross-section, about 60 of the 22,000 simulated boards per ovality group were sawn incorrectly due to floating point error. Neither increasing the number of points on the elliptical cross-sections nor increasing the error bound from 10^{-12} to 10^{-3} eliminated the problem. There was, however, a reduction in the number of affected boards (to about 50 per 22,000 per ovality group), and a shift to different boards. It was only through manual intervention, through changing the wane tolerance, that the remaining floating point errors were corrected. After correcting the floating point errors the following results were obtained.

Orientation for Maximum Log to Lumber Conversion

Overall, the 90-degree and 270-degree rotations provided the best orientations for placing oval logs (Figure 3) with about 60 percent of logs recording maximum conversions at those angles. At 0 degrees and at 180 degrees, nearly 40 percent of those logs with ellipticity ratio 0.80 also recorded a maximum. For circular logs, conversion remained constant over all angles.

Effect of Increasing Ovality on Conversion

Normalized maximum conversions due to oval logs were greater than those due to circular logs (Table 1). For the least oval set with an ellipticity ratio of 0.95, maximum conversion was greater than the circular set by an average of 2.1 percent (95-percent CI: 1.4–2.9 percent). For the most oval set with an ellipticity ratio of 0.80, conversion exceeded that of their circular counterparts by an average of 3.2 percent (95-percent CI: 1.1–5.3 percent).

Increased conversions at the optimal orientation with greater ovality can be seen through the logarithmic regression trends with log small-end diameter (Figure 4).

SUMMARY

Floating point errors were detected through observing small deviations from the expected flat response across rotations for circular logs, and through observing small deviations from the expected symmetry for oval logs. The occasional small differences of the order of 10^{-5} were caused through finite precision arithmetic and discrete, rather than continuous, data representations. These seemingly insignificant differences, arising from proven algorithms for determining the intersection between the plane of the

Figure 3— Frequency distributions by ellipticity ratio showing percentage of logs attaining maximum conversion at each orientation.
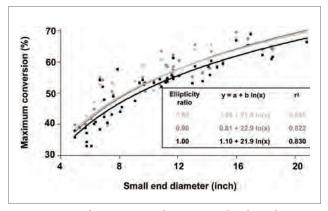
Figure 4— Logarithmic regressions demonstrating the relationship between maximum conversion and log small-end diameter by ellipticity ratio.

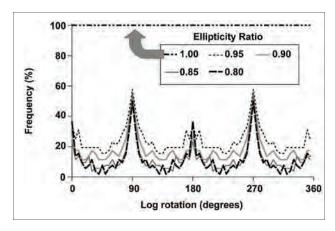saw and the log cross-section, resulted in a differing board width being fitted to the piece. In an attempt to eliminate the differences, simulations were rerun with error bounds increased from the bound for computational precision, 10^{-12} to 10^{-3}, and the number of points generated per ellipse increased from 30 to 72. This did not completely eliminate the problem although there was a small reduction in the number of affected pieces and a shift in affected pieces. Thus those affected pieces (about 50 amongst the 22,000 simulated for each log ovality group) were manually corrected by re-edging with a small allowance for wane (0.1 mm or equivalently 0.004 inch).

Floating point errors are likely to be inherent in any application that performs calculations and numerical comparisons. Because these seemingly insignificant errors can affect results, thorough validation procedures are needed to detect, isolate, and correct any anomalies.

Ovality was found to be beneficial to lumber yield, when the log was rotated to its optimal position. The increase was of the order of 2–3 percent. As a rule of thumb, the best rotation is as described by Asikainen and Panhelainen (1970), with the primary saw parallel to the major axis of the elliptical cross-section and the cant processed in a perpendicular direction.

LITERATURE CITED

Asikainen, K.; Panhelainen, A. 1970. Tukin soikeuden vaikutus sahaustulokseen. (The effect of the ovalness of the log on the sawing yield). (in Finnish with English summary). Papper och Trä 6: 395-402.

Biging, G.S.; Wensel, L.C. 1988. The effect of eccentricity on the estimation of basal area and basal area increment of coniferous trees. Forest Science 34: 621-633.

Higham, N.J. 2002. Accuracy and stability of numerical algorithms. Second edition. Society for Industrial and Applied Mathematics, Philadelphia. 710 p.

Kellogg, R.M.; Barber, F.J. 1981. Stem eccentricity in coastal western hemlock. Canadian Journal of Forest Research 11: 714-718.

Koch, P.; Côté W.A. Jr.; Schlieter, J.; Day, A.C. 1990. Incidence of compression wood and stem eccentricity in Lodgepole Pine of North America. Res. Pap. INT-420. Ogden, UT: U.S. Department of Agriculture Forest Service, Intermountain Research Station. 42 p.

Maness, T.C.; Donald, W.S. 1994. The effect of log rotation on value recovery in chip and saw sawmills. Wood and Fiber Science 26(4): 546-555.

Matérn, B. 1956. On the geometry of the cross-section of a stem. Meddelanden Från Statens Skogforsk 46(11), 28p.

Milenkovic, V.J. 1988. Verifiable implementations of geometric algorithms using finite precision arithmetic. Artifiical Intelligence 37: 377-401.

Monserud, R.A. 1979. Relations between inside and outside bark diameter at breast height for Douglas-fir in northern Idaho and northwestern Montana. Res. Note. INT-266. Ogden, UT: U.S. Department of Agriculture Forest Service, Intermountain Research Station. 8 p.

SAS Institute Inc. 1999. SAS Institute Inc. 1999. SAS OnlineDoc®, Version 8, Cary, NC: SAS Institute Inc., USA.

Saint-André, L. ; Leban, J.-M. 2000. An elliptical model for tree ring shape in transverse section. Methodology and case study on Norway spruce. Holz als Roh- und Werkstoff 58: 368-374.

Singleton, R.; Debell, D.S.; Marshall, D.D.; Gartner, B.L. 2003. Eccentricity and fluting in young-growth Western Hemlock in Oregon. Western Journal of Applied Forestry 18(4):221-228.

Skatter, S.; Høibø, O.A. 1998. Cross-sectional shape models of Scots pine (*Pinus silvestris*) and Norway Spruce (*Picea abies*). Holz als Roh- und Werkstoff 56: 187-191.

Todoroki, C.L. 1990. AUTOSAW system for sawing simulation. New Zealand Journal of Forestry Science 20(3):332-348.

Todoroki, C.L. 1997. Developments of the sawing simulation software, AUTOSAW: Linking wood properties, sawing, and lumber end-use. In: Proceedings of the Second Workshop "Connection between Silviculture and Wood Quality through Modelling Approaches and Simulation Softwares". Ed. G Nepveu, INRA-Nancy, France IUFRO S5.01-04, South Africa, August 26-31, 1996: 241-247.

Williamson, R.L. 1975. Out-of-roundness in Douglas-fir stems. Forest Science 21(4): 365-370.

Predicting Lumber Grade and By-Product Yields for Standing Scots Pine Trees

Henna T. Lyhykäinen, Harri Mäkinen, Annikki Mäkelä, Arto Usenius

ABSTRACT

THE PURPOSE OF THIS STUDY WAS TO develop models for estimating yields and grades of lumber, as well as by-products, of individual Scots pine (*Pinus sylvestris L.*) stems using stem and crown dimensions as explanatory variables. The process-based growth model, PipeQual, which provides information about stem form and branch properties, was used to generate the material for analysis. The model was used to predict the 3D structure of Scots pine stems in thinning regimes of varying intensity and rotation periods. The generated stems were sawn using the WoodCim sawing simulator and the yields and grades of the individual sawn pieces, as well as by-products, were recorded. The sawn timber was classified on A, B, C and D-grades for side and center boards separately (in accordance with Finnish export rules). By-products were pulpwood, sawmill chips, sawdust, and bark.

The response variables were formulated as cumulative proportions of the total volume of each stem. Logistic regression models were fitted to the data, and the best combination of the explanatory variables was found to be living crown height and the natural logarithm of diameter at breast height. The models were tested against simulated sawing of actual measured Scots pine stems and predictions for larger stems were found to be more biased than those used in model building.

The developed approach integrates wood production and the conversion chain. The models can be used in stand management optimization for comparing different management options, e.g., on a value-added basis from the sawmill's point of view.

KEYWORDS: *Pinus sylvestris,* timber products, product recovery, process-based growth model, sawing simulations

INTRODUCTION

Scots pine (*Pinus sylvestris L.*) timber is essential raw material for the Finnish mechanical wood industry; two-thirds of the forested area of Finland is pine-dominated, and pine sawn-goods alone represent one percent of the value of the total export in goods (Finnish Statistical 2006). During the last few decades the share of pine stands has increased, and there has been much public debate regarding whether or not wood quality has deteriorated in the end-users' point of view.

The number, type and size of branches are important determinants of grading of Scots pine logs (Heiskanen 1965, Uusvaara 1985, Uusitalo 1997). Both statistical (Colin and Houllier 1992, Roeh and Maguire 1997, Mäkinen et al. 2003) and mechanistic models (Mäkelä 2002) have been developed to predict branch dimensions along the stem. The branch models, with the growth model, have enabled predictions of the 3D structure of trees and logs. Since the structure can be described in detail, stems can be viewed and processed virtually. However, detailed 3D information on tree and log properties is often unnecessarily detailed for economical analysis based on timber utilization. Prediction of wood-quality distribution of raw material, without detailed 3D description and conversion simulations, would provide an adequate tool for understanding the connec-

Henna T. Lyhykäinen (henna.lyhykainen@helsinki.fi) is a doctoral student in the Department of Forest Economics, P.O. Box 27, FI-00014 University of Helsinki, Finland; **Harri Mäkinen** is a researcher at the Vantaa Research Centre, Finnish Forest Research Institute, P.O. Box 18, FI-01301 Vantaa, Finland; **Annikki Mäkelä** is a professor of silviculture (forest production) in the Department of Forest Ecology, P.O. Box 27, FI-00014 University of Helsinki, Finland; **Arto Usenius** is a research professor at the VTT Technical Research Center of Finland, P.O. Box 1806, FIN-02044 VTT, Finland.

tion between wood quality and tree growth in different management regimes. Therefore, more robust models can be used for assessing the potential product recovery from different stands and selecting the appropriate raw material for each end use.

The earlier models for predicting lumber grade yields of standing trees were based on regression analysis with continuous dependent variables (Stayton et al. 1971, Yaussy 1986, 1989). Howard and Gasson (1989) used a truncated normal distribution with a lower bound set to zero. Later, Prestemon (1998), Lynch and Clutter (1999), Gobakken (2000), and Prestemon and Buongiorno (2000) used discrete multinomial logit or tobit models for predicting the probability of a stem, or log, to belong to a certain quality class. These models assume that the whole stem or log belongs to the same class. Thus, the models predict how stems are, on average, distributed to sawn wood grades. The models can be used for comparing different silvicultural strategies or valuing stands, but not for predicting quality grade distributions of individual stems.

In Finland, Uusitalo (1997) developed multinomial logistic models for predicting average lumber-grade distribution of Scots pine logs from final fellings. Separate models of battens, outer, and inner boards were estimated for butt, second, and third log, and dependent variables were defined as polytomous responses so that a certain number of battens, inner boards, and outer boards represent certain grades. The results showed that timber grade distribution of logs was mainly related to dbh, height of the lowest dead branch, and the height of the tree.

The aim of this study was to develop models for predicting the lumber grade and by-product yield of individual Scots pine stems using simple stand and stem properties as explanatory variables. We used a process-based growth model, PipeQual (Mäkelä 1997, Mäkelä and Mäkinen 2003), for assessing the development of wood properties along tree growth and the effects of different silvicultural treatments on wood properties. In the PipeQual model, tree growth is derived from carbon acquisition and allocation, with a detailed description of branch structure. This allows the model to be applied to predictions of wood quality in individual stems. The model dynamically predicts the growth of individual trees at different dominance positions, from which the stand level is composed. The stems created by the PipeQual model were used as an input to the integrated wood conversion simulation system, WoodCim (Usenius 2002). The WoodCim was developed by the Technical

Research Centre of Finland for sawmilling companies. It enables the virtual sawing of individual logs, as well as predictions of grade distribution of sawn timber and by-product yields at tree level.

MATERIAL AND METHODS

Material

Stand developments according to several silvicultural strategies of varying intensity were simulated by the PipeQual simulator (Mäkelä 1997, 2002, Mäkelä and Mäkinen 2003). The model combines stem properties with carbon metabolism by means of a modular structure that consists of stand, whole tree, whorl, and branch modules interconnected through parametric inputs and outputs at a time resolution of one year. The stand level consists of ten size classes of trees, each size class is described by a mean tree. At the tree level, annual growth is calculated from tree-level photosynthesis (affected by shading from neighboring trees) and maintenance respiration. The annual growth is allocated to foliage, fine roots, and woody structures (stem, branches, and coarse roots). The tree module is connected to a whorl module, which contains models for the vertical structure of stem and branches. The branch module calculates the annual dynamics of individual branches and their properties in each whorl (Mäkinen and Mäkelä 2003).

The PipeQual requires initial values for stem height, dbh, crown length, and age for ten size classes of trees, as well as the initial number of trees per hectare in each size class. The initial size classes were defined in terms of initial seedling height with even class intervals, and assumed an exponential frequency or normal distribution of seedling height depending on the management strategy. In the simulations, site fertility of the stands was matched with *Myrtillus* site type (H_{100} = 28 m) (Cajander 1949) corresponding to sites of medium fertility in Southern Finland.

Different silvicultural schedules were formed in order to produce as much variation in stand development and growth rate of trees as possible. The different silvicultural strategies were divided into four main groups based on management intensity, named as open-grown, high, normal and low intensity (Table 1). Four planting densities (2000, 3000, 5000, and 10000 stems ha^{-1}) were simulated in all the strategies, except in the low intensity strategy where the sparsest planting density was excluded. In sapling stands at a dominant height of 6.6–6.8 m, tending treatment was carried out, i.e., the number of remaining stems was reduced

to 400, 1200, 1900, or 3000 in the strategies of open-grown, high, normal, and low intensity, respectively. In the normal and low intensity strategies, the first commercial thinning was carried out at dominant height of 14 m. In the open-grown and high intensity strategies, the stand density co-incided with or was lower than the density recommended for forestry practice (Tapio 2006) and, therefore, no actual first thinning was carried out. The later thinnings were carried out according to the recommendations for forestry practice, expressed as the minimum stand basal area to be retained after thinning (Tapio 2006). The final felling was carried out when the mean dbh of the stand exceeded 30 cm or the stand age was 85 years. If there was longer than a four-year difference between these two criteria of final felling, both alternatives were simulated. Altogether, different combinations of the planting densities, tending and thinning intensities, and final felling ages resulted in 48 different treatment schedules.

These mean trees of each diameter-class formed the data set of this study. The initial analysis of the data showed, that stem dimensions and wood quality of the stands in the open growth strategy with 85 year rotation differed

completely from the other data set. The attempts to force the equations through these diverging stems resulted in large biases in the other observations. For that reason, 20 stems from these strategies (Table 1, in parenthesis) were omitted. In addition, because some of the size classes were completely removed in treatments during the stand rota-
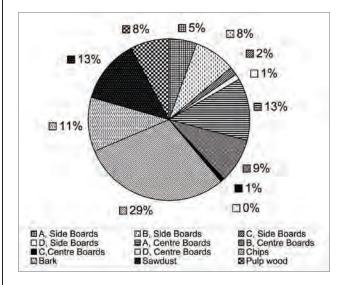
Figure 1. The average product distribution of the stems in the data set.

Table 1— Treatment strategies of the PipeQual simulations.

Strategy	Planting density	Tending of sapling stand	First commercial thinning	Number of later thinnings	Final felling age
	Stems ha^{-1}	Stems ha^{-1}	Stems ha^{-1}		Years
Open-grown	2000	400	-	-	48 or (85)
	3000	400	-	-	49 or (85)
	5000	400	-	-	51 or (85)
	10000	400	-	-	52 or (85)
High	2000	1200	-	1 or 2	80 or 85
	3000	1200	-	1 or 2	84
	5000	1200	-	1 or 2	85
	10000	1200	-	1 or 2	85
Normal	2000	1900	1200/ 600/ 400	0, 1 or 2	69, 79 or 85
	3000	1900	1200/ 600/ 400	0, 1 or 2	68, 81, 85, 89 or 98
	5000	1900	1200/ 600/ 400	0, 1 or 2	69, 83, 85, 98
	10000	1900	1200/ 600/ 400	0, 1 or 2	73 or 85
Low					
	3000	3000	1200/ 600/ 400	0 or 1	72 or 85
	5000	3000	1200/ 600/ 400	0 or 1	74 or 85
	10000	3000	1200/ 600/ 400	0 or 1	76 or 85

Table 2—Properties of the simulated stem data

	Minimum	Maximum	Mean	Std. Deviation
Height, m	11.70	26.70	21.28	3.88
dbh, cm	14.80	36.80	27.36	5.28
H_{db}, m	0.00	7.30	1.16	1.50
H_{lc},m	6.40	16.30	11.89	2.50
Age, years	33.00	98.00	70.90	18.23

Abbreviations: $H_{db} =$ Dead branch height, distance from ground to first dead branch greater than 15 mm.

$H_{lc} =$ Living crown height, m.

tion or provided no sawn-timber, the final data set consisted of 395 trees. Properties of the data are shown in Table 2.

The generated stems were used as an input for the Wood-Cim sawing simulations. In the simulations, two typical sets of sawn-timber dimensions and sawing set-ups were used (Appendix 1). The arithmetic means of the results from these two sawing set-ups were used for each stem in the modeling. The sawing method was the traditional Scandinavian pith-centred cant sawing, in which the first machine cuts side boards and a block, and the second machine cuts the block into center boards and side boards. The center and side boards were classified as A, B, C and D-grades according to Nordic Timber grading rules (Poh-joismainen sahatavara, 1994). Center boards were defined as sawn pieces from the center of the stem (32–75 mm thick, Appendix 1). By-products were pulpwood, sawmill chips, sawdust, and bark. The minimum lengths applied for logs and pulpwood boles were 3.1 m and 2.0 m and the minimum top diameters without bark were 6.5 m and 16.0 cm, respectively. The average product distribution of the data set is shown in Figure 1. On average, the proportion of sawn timber from the total stem volume with bark was 43.2 percent.

Methods

The volume of each quality class of side and center boards and by-products was related to the total volume of the stem with bark. Then, cumulative relative volumes of the quality classes and by-products for each stem were calculated as shown in Table 3. The share of pulp wood bole from the top can be calculated by subtracting Y_{11} (the total proportion of all lumber grades plus chips, sawdust and bark) from 1.

The models describing the cumulative relative volumes of the quality classes of center and side boards and by-products were developed using the logistic regression approach:

$$Y_i = \frac{1}{1+e^{(\alpha-\beta_{i1}X_{i1}-\beta_{i2}X_{i2}..\beta_{iy}X_{iy})}} + \varepsilon_i \tag{1}$$

The logistic multivariate models were fitted using SPSS, Inc. software. Parameters of the models were estimated by iterative linearization method in which linearization is done around the set of initial values of coefficients. Iteration is repeated until a convergence of parameters values is obtained. Standard statistical tests used to the evaluation of fit of the final linearized equations were also calculated (Pinduct and Rubinfeld 1998, pp. 266–268).

Different combinations of independent variables describing dimensions of the stems, crowns, and the growth rate (width of the annual rings around the pith), as well as their transformations, were tested until the models were finally accepted. The independent variables were restricted to conventional stand and tree measurements routinely collected in forest inventories or for forest management planning purposes. The average width of the annual rings around the pith was also tested as an independent variable because ring width near the pith and quality of Scots pine logs have been closely related (e.g. Heiskanen 1965, Kärkkäinen 2003). In addition, highly correlated independent variables were avoided. A correlation matrix was used for the preliminary analysis on the relationship between the dependent and independent variables.

In order to examine the performance of the models, the product distributions were predicted in two independent data sets of the Stem Data Bank collected by the Technical Research Centre of Finland (VTT). In the Stem Data Bank, the 3D structure of real stems, including the description of external shape, internal knot structure, other possible defects, and heartwood core, is mathematically reconstructed into virtual stems, based on image analysis of flitch surfaces (Usenius 2002, Pinto et al. 2003). The first data set consisted of 38 stems thinned

Table 3. Explanations of the symbols

Variable	Definition
H_{lc}	Height to the living crown base from the stem base (m)
Ln(Dbh)	Natural logarithm of stem diameter at breast height (cm)
Y_1	The proportion of A-grade side boards of the total volume of stem
Y_2	Y_1+ the proportion of B-grade side boards of the total volume of stem
Y_3	Y_2+ the proportion of C-grade side boards of the total volume of stem
Y_4	Y_3+ the proportion of D-grade side boards of the total volume of stem
Y_5	Y_4+ the proportion of A-grade center boards of the total volume of stem
Y_6	Y_5+ the proportion of B-grade center boards of the total volume of stem
Y_7	Y_6+ the proportion of C-grade center boards of the total volume of stem
Y_8	Y_7+ the proportion of D-grade center boards of the total volume of stem
Y_9	Y_8+ the proportion of chips of the total volume of stem
Y_{10}	Y_9+ the proportion of bark of the total volume of stem
Y_{11}	Y_{10}+ the proportion of sawdust of the total volume of stem
S_2	Residual variance

from 24 stands in Southern Finland. It is noteworthy that the stands were not a random sample from Finnish forests. Instead, they represented regularly managed stands of better-than-average wood quality. The data is described in detail in Wall et al. (2005). The second data set consisted of 191 stems from eight final fellings. The data set is described in detail in Mäkinen and Song 2002. Properties of the Stem Bank Data are shown in Table 4. The sawing of the stems in both data sets was simulated using the WoodCim simulator with the same parameters as the stems generated by the PipeQual model.

Table 4—Properties of the Stem Bank Data.

	Minimum	Maximum	Mean	Std. Deviation
Height, m	12.90	32.60	22.22	4.72
dbh, cm	16.20	49.50	30.18	6.87
H_{db}, m	0.00	17.00	6.21	3.30
H_{lc}, m	3.65	23.50	12.41	3.91
Age, years	30.00	194.00	127.64	31.72

Abbreviations: H_{db} = Dead branch height, distance from ground to first dead branch greater than 15 mm.
H_{lc} = Living crown height.

Table 5—Variables and parameters of models Y_1–Y_{11}.

Dependent variable	Independent variable	Coefficient	S.E	95 % Confidence Interval	
				Lower	Upper
Y_1 Adjusted R^2 = 0.67, s^2 < 0.001	Constant	11,5729	0.5502	10.4913	12.6547
	H_{lc}	2.1936	0.1625	1.8742	2.5131
	Ln(DBH)	0.1115	0.0114	0.0891	0.1339
Y_2 Adjusted R^2 = 0.87, s^2 < 0.001	Constant	10.6867	0.2657	10.1643	11.2091
	H_{lc}	2.3895	0.0804	2.2314	2.5475
	Ln(DBH)	0.0687	0.0053	0.0584	0.0791
Y_3 Adjusted R^2 = 0.92, s^2 < 0.001	Constant	11.0040	0.2035	10.6039	11.4042
	H_{lc}	2.5820	0.0616	2.4608	2.7032
	Ln(DBH)	0.0524	0.0039	0.0447	0.0601
Y_4 Adjusted R^2 = 0.93, s^2 < 0.001	Constant	10.0831	0.1778	9.7336	10.4325
	H_{lc}	2.3185	0.0544	2.2116	2.4254
	Ln(DBH)	0.0531	0.0036	0.0460	0.0601
Y_5 Adjusted R^2 = 0.82, s^2 = 0.003	Constant	9.4063	0.3142	8.7886	10.0241
	H_{lc}	2.2175	0.0980	2.0248	2.4102
	Ln(DBH)	0.0926	0.0069	0.0790	0.1061
Y_6 Adjusted R^2 = 0.96, s^2 = 0.001	Constant	11.4282	0.1685	11.0969	11.7595
	H_{lc}	3.0140	0.0525	2.9108	3.1172
	Ln(DBH)	0.0782	0.0035	0.0714	0.0851
Y_7 Adjusted R^2 = 0.98, s^2 = 0.001	Constant	12.1566	0.1331	11.8950	12.4182
	H_{lc}	3.2550	0.0413	3.1739	3.3362
	Ln(DBH)	0.0757	0.0027	0.0704	0.0809
Y_8 Adjusted R^2 = 0.98, s^2 = 0.001	Constant	12.1670	0.1319	11.9077	12.4263
	H_{lc}	3.2581	0.0409	3.1777	3.3385
	Ln(DBH)	0.0757	0.0027	0.0705	0.0809
Y_9 Adjusted R^2 = 0.98, s^2 < 0.001	Constant	7.8896	0.0754	7.7414	8.0378
	H_{lc}	2.4820	0.0269	2.4291	2.5349
	Ln(DBH)	0.0439	0.0023	0.0395	0.0484
Y_{10} Adjusted R^2 = 0.97, s^2 = 0.001	Constant	8.9923	0.1055	8.7850	9.1997
	H_{lc}	2.9965	0.0395	2.9187	3.0742
	Ln(DBH)	0.0491	0.0035	0.0423	0.0560
Y_{11} Adjusted R^2 = 0.98, s^2 < 0.001	Constant	16.0608	0.1929	15.6815	16.4401
	H_{lc}	5.6700	0.0738	5.5248	5.8151
	Ln(DBH)	0.0382	0.0057	0.0270	0.0493

Explanations of the symbols are given in Table 3. All the parameter values are significant (p<0.001).
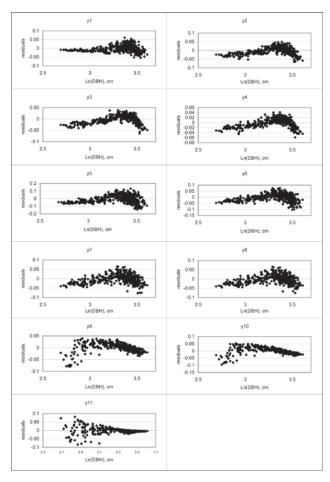
Figure 2. Residuals of the model Y_1–Y_{11} plotted against the logarithm of dbh.

Figure 3. Errors of the predictions of the models Y_1–Y_{11} plotted against the logarithm of dbh of stems (cm) in the Data Base Stems.

RESULTS

The logistic function (Equation 1) was used to model the cumulative relative proportions of the quality classes and by-products. All the models had the same independent variables and a constant. Using living crown height and natural logarithm of stem diameter at breast height as explanatory variables, the best model fit was achieved. The models and independent variables were significant at a risk lever smaller than 0.001, also 95-percent confidence intervals are shown in Table 5. The parameters of the models and their standard errors, as well as the R^2 values and variances of the residuals, are shown in Table 5. Explanations of the symbols are shown in Table 3.

The smallest adjusted R^2 value was 0.67 (Y_5) and the highest 0.98 (Y_7–Y_9, Y_{11}). For models in which the proportion of A-grade was added, Y_1 and Y_5, had the lowest R^2 values. Thus, for the proportion of the highest quality grades, both center and outer boards had the highest random variation. It is noteworthy that the adjusted R^2-value

of the model Y_8, which includes all sawn wood grades, was very high, 0.98.

The residuals of the models versus natural logarithm of dbh are shown in Figure 2. The variation of the residuals is relatively small, but notably related to logarithm of dbh. However, the models were not biased in relation to the height of the living crown. Variances of the errors of Y_1 increase when diameter increases with respect to increasing values of Y_1, which illustrates the proportion of A-grade outer boards. Correspondingly, errors of Y_{11} decrease when diameter increases because the relative amount of pulp wood (defined as [1 - Y_{11}]) becomes smaller when diameter increases.

Testing the Models

The real test of the prediction system is whether it accurately predicts yield for trees other than those used to develop the equations. In this study we used measured stems and results from the simulated sawing process for the testing purpose.

As can be seen in Figure 3, extrapolation of models does not work in testing data for larger stems than those used in model building (dbh greater than 37 cm) and the models were clearly biased. In larger diameters than those in the data, overestimations of the models increase when diameter increases. In diameters smaller than 37 cm, models behaved relatively well based on the preliminary examination. Models Y_5–Y_8, in which the proportion of center boards is added to the cumulative variable, give underestimations in the smallest stems which are all from thinnings. Additionally, in small stems symmetrical and wide variation can be seen in models Y_9 and Y_{10}. Finally, overestimations occur in model Y_{11}, which includes all products.

In model Y_{11}, bias decreases when diameter increases, because the share of pulp wood becomes smaller when stem volume increases. The average tree age in the Stem Data Bank was 143 years, i.e., the stems were, on average, much older and their diameters much larger than in the stems used for model building. Stems with large diameters and high quality (high living branch height) had systematic error in predictions, and because the proportions are calculated as the differences between two cumulative variables error causes dislocation to the quality classes. The dbh affects the quality distribution in two ways. First, the larger the sawn piece is the thicker the permitted knots are, and secondly, large amounts of best-quality boards can be sawn just from large butt logs (Uusitalo 1997). Based on the testing data, however, the effect is overestimated.

DISCUSSION

Earlier studies on modeling the quality of Scots pine have shown that the height of the lowest dead branch is an important quality indicator, because thick branches self-prune slowly (e.g. Kärkkäinen 1980, Uusitalo 1997). In this study, we found that the height of the living crown was a better quality indicator. Data of earlier studies have consisted of only stems from final fellings. In this study, the stems were from different stages of the rotation. In young stems, the height of the lowest dead branch is usually very low and, therefore, it doesn't account for the differences in sawn timber grades. The size of the sound knot may, however, determine the quality class of the board. In the smallest typical size class of boards (19*100 mm), on the flat side of the board a sound knot with diameter of 20mm or smaller is allowed in the pine A-grade, 35 mm or smaller in B-grade, and 50 mm or smaller in C-grade (Pohjoismainen sahatavara

1994). When using models for predicting the product distribution of stands, living crown height can be considered an accurate quantifier, both if stems are genuine and stem characteristics are measured, or if stems are generated by empirical or process-based stand simulators.

The PipeQual model probably overestimates the overall quality of stems because other defects than branches are not considered. The simulated stems are straight without warp, twist, forks and out-of-roundness in cross-section and defects like decay or splits do not appear. In Scots pine, knots are, however, the most important individual factor affecting quality grading. Therefore, the simulated stems were supposed to indicate stem quality well enough. The data set used for independent testing, however, consisted of only stems of good quality and systematic overestimations of the models need to be more closely dissected.

Stand development was simulated using a submesic site type (MT-type in Cajander's classification 1949) located in Southern Finland. These assumptions could restrict the applicability of the models for other site types or geographical locations, but more testing with suitable data is required.

Future Perspectives and Applications of the Models

The multiproduct predicting system presented in this paper has many application possibilities for optimization of forest management at the stand level with different objective functions. By combining models for a simulation-optimization system we are able to study the value of end products and simultaneously take other aims into account, for example carbon sequestration of different end and by-products. Carbon sequestration can be taken into account via life cycle analysis of different construction wood products, furniture products, and short cycle products, i.e., packaging and paper goods.

In earlier case studies, which have examined the value growth and optimal rotation age of pine stands, when the quality of timber was taken into account via different quality-pricing methods, improvements in quality (that is, in value of logs) didn't extend optimal rotation length (Pastila 2003, Makkonen 2006). These case studies examined value growth until age 100 years and, in this study, final felling criteria was either a diameter of 30 cm or an age of 85 years. Because the treatment history of the Stem Data Bank stem is well recorded, it is possible to study value growth of these stands by connecting the product recovery predictions of models (from earlier stages of experimental stands) and

recorded information of simulation sawings (final fellings) with the average costs of treatments, producers' prices of lumber and by-products, and appropriate interest rates. By examining net present values and value growths of stands we could study whether longer rotation would improve grade distribution remarkably enough that the investment in standing stock would be profitable.

The purpose of this study was to build a simple prediction system for standing pine stems for evaluation of the effects of different stand management regimes on the product distribution of stems. Outside of the stem diameter range of the data set used for model building, the models were clearly biased. We will continue to improve the preliminary models in the future. The next step is to develop multilevel multivariate models, because stems in same stands are not independent of each other and equation systems in which parameters have been estimated simultaneously may produce more consistent and efficient estimates than models constructed separately. Also, the structure of dependent variables, in which responses are volumes instead of properties, and sum of volumes is restricted to total volume of stem, will be applied to diminish bias of the models.

CONCLUSIONS

This paper has presented the current state of development of the model system. It was possible to develop models for predicting the quality distribution and yield of by-products of individual Scots pine stems using the simple stand and stem properties as explanatory variables. The models presented are, however, preliminary and not yet applicable for general use. In the near future, model development will be continued, more thorough tests of the models will be reported, and based on the test results, the models will be modified.

LITERATURE CITED

Cajander, A.K. 1949. Forest types and their significance. Acta forestalia fennica 56(5). 71 p.

Colin, F.; Houllier, F. 1992. Branchiness of Norway spruce in northeastern France: predicting the main crown characteristics from usual tree measurements. Annales des sciences forestières 49: 511-538.

Gobakken, T. 2000. Models for assessing timber grade distribution and economic value of standing birch trees. Scandinavian Journal of Forest Research 15: 570-578.

Heiskanen, V. 1965. On the relations between the development of the early age and thickness of trees and their branchiness in pine stands, Acta Forestalia FennicaActa For. Fenn. 80 (1965) (2): 1–62.

Howard, A.F.; Gasson, R. 1989. Recursive multiple-regression model for predicting yields of grade lumber from lodgepole pine sawlogs. Forest Product Journal 39 (4): 51-56.

Kärkkäinen, M. 1980. Mäntytukkirunkojen laatuluokitus [In Finnish, grading pine sawlogs stems.] Communicationes Instituti Forestalis Fenniae 96 (5): 152.

Kärkkäinen, M. 2003. Puutieteen perusteet. Metsälehti Kustannus. Karisto Oy. Hämeenlinna. 452 p. [In Finnish]

Kärkkäinen, M.; Uusvaara, O. 1982. Nuorten mäntyjen laatuun vaikuttavia tekijöitä. Folia Forestalia 515:1-28

Lynch, T.B.; Clutter, M.L. 1999. Predicting Loblolly pine plywood bolt grade with a multinomial logit model. Forest Product Journal 49 (5): 56-61.

Mäkelä, A. 1997. Carbon balance model of growth and self-bruning in trees based on structural relationship. Forest Science 43 (1): 7-24.

Mäkelä, A. 2002. Derivation of stem taper from the pipe theory in a carbon balance framework. Tree Physiology 22: 891-905.

Mäkelä, A.; Mäkinen, H. 2003. Generating 3D sawlogs with a process-based growth model. Forest ecology and management (184)1/3: 337–354

Mäkinen, H.; Mäkelä, A. 2003. Predicting basal area of Scots pine branches. Forest Ecology and Management 179: 351-362.

Mäkinen, H.; Saranpää, P.; Niemistö, P. 2003. Predicting branch characteristic of planted silver birch (*Betula pendula* Rouh.) On the basis of routine stand and tree measurements. Forest Science 49: 301-317.

Mäkinen, H.; Song, T. 2002. Evaluation of models for branch characteristics of Scots pine in Finland. *Forest Ecology and Management* (158) 1/3: 25-39

Mäkinen, H.; Uusvaara, O. 1992. Lannoituksen vaikutus männyn oksikkuuteen ja puuaineen laatuun. [Finnish with English summary: Effect on fertilization on the branchiness and the wood quality of Scots pine. Folia Forestalia 801: 1-23.

Makkonen, K. 2006. The effect of quality based pricing of raw wood on rotation age and net revenues to forest managers. Master thesis, Business Economics of Forestry, Department of forest economics, University of Helsinki. 105 p. [In Finnish with English summary.]

Pastila, S. 2003. Profitability of Timber Production and Value of Timber—Thinnings and their Impact on Harvested Timber Volume and Stem Value in Scots Pine Stands. Master thesis, Business Economics of Forestry, Department of forest economics, University of Helsinki. 121 p. [In Finnish with English summary.]

Peltola, A., ed. 2006. Finnish Statistical Yearbook of Forestry 2006. Finnish Forest Research Institute. 432 p.

Pinduct, R.S.; Rubinfield, D.L. 1998. Econometric models and economic forecasts. 4th edition. Irvin/McGraw-Hill Book Co. 634 p.

Pinto, I.; Pereira, H.; Usenius, A. 2003. Analysis of log shape and internal knots in twenty maritime pine (*Pinus pinaster* Ait) stems based on visual scanning and computer aided reconstruction. Annales des sciences forestières 60:137–144

Pohjoismainen sahatavara. 1994. Mänty—ja kuusisahatavaran lajitteluohjeet. Suomen Sahateollisuusmiesten Yhdistys. Helsinki. 64 p. [In Finnish]

Prestemon, J.P. 1998. Estimating tree grades for Southern Appalachian natural forest stands. Forest Science 44:73-86

Prestemon, J.P.; Buongiorno, J. 2000. Determinants of tree quality and lumber value in natural uneven-aged Southern pine stands. Canadian Journal of Forest Research 30:211-219.

Roeh, R.L.; Maguire, D.A. 1997. Grown profile models based on branch attributes in coastal Douglas-fir. Forest Ecology and Management 96: 77-100

Stayton, C.L.; Marden, R.M.; Gammon, G.L. 1971. Predicting lumber grade yields for standing hardwood trees. Research Paper NC-50. St. Paul, MN: U.S. Dept. of Agriculture, Forest Service, North Central Forest Experiment Station.

Tapio. 2006. Hyvän metsänhoidon suositukset. Metsätalouden kehittämiskeskus Tapio. Metsäkustannus Oy, Helsinki. (In Finnish)

Usenius, A. 2002. Experiences from industrial implementations of forest—wood chain models. Fourth Workshop IUFRO s5.01.04, Harrison Hot Springs, British Columbia, Canada-September 8-15, 2002.

Uusitalo, J. 1997. Pre-harvest measurements of Pine Stands for Sawing Production Planning. Acta Forestalia Fennica 259. 59 p.

Uusvaara, O. 1985. The quality and value of sawn goods from plantation-grown Scots pine. Communicationes Instituti Forestalis Fenniae 130. 53 p.

Wall, T.; Fröblom, J.; Kilpeläinen, H. [et al.]. 2005. Harvennusmännyn hankinnan ja sahauksen kehittäminen. WOOD WISDOM—tutkimusohjelman hankekonsortion loppuraportti. Metsäntutkimuslaitoksen tiedonantoja 943. 129 p. [In Finnish]

Yaussy, D.A. 1986. Green lumber grade yields from factory grade logs of 3 oak species. Forest Products Journal. 36(5):53-56

Yaussy, D.A. 1989. Green lumber grade yields from black cherry and red maple factory grade logs sawed at band and circular mills. Canadian Journal of Forest Research 19(11):1436-1444

Appendix 1

Setting series 1	Diameter Class		Centre Boards		Side Board Models		
	Dmin, mm	Dmax, mm	thickness, mm	width, mm	1. machine, mm	2. machine innermost board	2. machine outermost board
1	120	157	38	100		19	
2	158	162	38	115		25	
3	163	174	50	100	19	19	
4	175	182	50	125		25	
5	183	197	36	115	25	25	
6	198	207	50	150		25	
7	208	217	32	125	25	19	
8	218	222	63	150	25	25	
9	223	231	38	125	25	19	
10	232	237	75	150	25	25	
11	238	242	63	175	19	19	19
12	243	250	38	150	25	25	
13	251	256	50	175	25	25	
14	257	262	63	200	19	25	19
15	263	271	32	200	19	25	19
16	272	282	75	200	25	25	19
17	283	291	38	200	25	19	19
18	292	301	75	225	19	25	25
19	302	314	50	225	25	25	25
20	315	325	50	200	25	25	
21	326	334	50	200	25	25	
22	335	351	50	225	25	25	19
23	352	555	50	225	25	25	25
Setting series 2							
24	120	144	38	100		19	
25	145	150	32	100		19	
26	151	156	44	100	19	19	
27	157	168	32	125		25	
28	169	175	50	115	19	25	
29	176	182	50	125		25	
30	183	193	63	100	25		
31	194	202	50	150		25	
32	203	212	75	100	25	19	
33	213	215	50	150	19	19	19
34	216	221	44	175		25	19
35	222	225	75	125	25	25	
36	226	239	75	150	25	25	
37	240	252	50	200		25	25
38	253	261	38	150	25	25	
39	262	268	63	200	19	25	25
40	269	282	75	200	25	25	19
41	283	290	63	225	19	25	25
42	291	299	50	225	25	25	25
43	300	319	50	225	25	25	25
44	320	555	50	200	25	25	

Integrating a Wood-Quality Module with a Growth Simulator to Quantify Silvicultural Scenarios in Jack Pine Plantations (Are We Making the Right Choices?)

Robert Schneider, Frank Berninger, S.Y. (Tony) Zhang, Chhun-Huor Ung

ABSTRACT

Initial planting density has a critical effect on establishment costs, growth and yield, product quality, and value recovery. Initial planting density for major softwoods in Quebec was lowered in the early 1990's in order to increase the success of future thinnings and to reduce plantation establishment costs. While these reasons might seem sound, we still do not fully understand the impact of this decision on growth, yield, and wood quality of these plantations. Furthermore, not enough is known about the interaction between thinnings, initial stand density, and site fertility or the effects of these interactions on the growth, yield, and wood quality. To address some of these questions before experimental plots become mature enough to provide empirical evidence, a process-based growth simulator is being developed for jack pine plantations based on the CroBas model. The simulator has a wood-quality module that yields estimates of branch diameter and insertion angle as well as wood density and bending properties. Emphasis is placed on this module to quantify the impact of silvicultural regimes on wood quality and compare the simulated results with field data from several plantations sampled across Eastern Canada. Preliminary results indicate that total branch basal area of the stem decreases exponentially with increasing initial stand density, and this trend holds true over time. In addition, initial validation shows very little bias in height growth predictions in young plantations.

Robert Schneider (robert.schneider.1@ulaval.ca) and **Frank Berninger** are in the Département des sciences biologiques, Université du Québec à Montréal, c.p. 8888 succ. C.V., Montréal, Québéc H3C 3P8, Canada; **S.Y. (Tony) Zhang** is a senior scientist at FPInnovations—Forintek Division, 2665 East Mall, Vancouver, BC V6T 1W5, Canada; **Chhun-Huor Ung** is at the Laurentian Forestry Centre, Canadian Forest Service, P.O. Box 10380, Stn. Sainte-Foy, Québec, Quebec, G1V 4C7 Canada.

Optimizing Wood Quality and Stand Diversity in Uneven-Aged Forest Management[1]

Jingjing Liang, Joseph Buongiorno, Robert A. Monserud

ABSTRACT

WE DEFINED UNEVEN-AGED MANAGEMENT alternatives for Douglas-fir (*Pseudotsuga menziesii*)/western hemlock (*Tsuga heterophylla*) stands by the cutting cycle, C, the residual stand basal area, B, and the q ratio. Bootstrap simulation was used to predict the effects of B, q, and C on percentage of peeler logs, tree species diversity, and tree size diversity. Response surface analysis showed that adjusting B, q, and C could control for most of the variability in the percentage of peeler logs, tree species diversity, and tree size diversity. Other things being equal, a higher q ratio increased the percentage of peeler logs, tree species diversity and tree size diversity. The same combination of B, q, and C, maximized the percentage of peeler logs, stand species diversity, and tree size diversity. Thus, there was no apparent conflict between wood quality and stand diversity.

KEYWORDS: stand growth, bootstrap, response surface, stochastic, Douglas-fir, western hemlock

INTRODUCTION

One interesting issue concerning all-aged management is its effect on wood quality. Research on the relation between wood quality and product values has lagged behind research on growth and yield, stocking control, and fertilization (Briggs and Fight 1992). We still lack information linking tree growth to wood quality and product value. In most economic analyses, log values are functions only of tree size.

However, trees of a given size may vary highly in grades, due in part to stand characteristics such as density.

Biological diversity is a necessary condition of ecosystem resilience. Stands with greater tree size and species diversity provide better habitat for wildlife. They also tend to be more aesthetically pleasing (Guldin 1996).

Forest managers encounter risk in many diverse forms. Although research has begun to combine biological and economic risk in optimization, it remains difficult to optimize systems with risk in many variables. The method used in this study was bootstrap simulation, coupled with response surface analysis (Myers and Montgomery 2002). The aim was to obtain optimal management regimes, defined by a specific target distribution and cutting cycle, while recognizing stochastic forest growth, prices, and interest rates. In the process, we show the sensitivity to selected management regimes of financial returns, stand diversity, stand density, and wood quality in Douglas-fir/western hemlock stands.

STAND GROWTH MODEL

The stochastic stand growth model we used was an extension of the deterministic growth model for Douglas-fir/western hemlock stands developed by Liang et al. (2005). This model predicts the number and volume of trees for four species groups (Douglas-fir, other shade-intolerant species, western hemlock, and other shade-tolerant species) in nineteen 5.1-cm-wide diameter classes. The elements of the

Jingjing Liang (j.liang@uaf.edu) is an assistant professor, Department of Forest Sciences, University of Alaska, P.O. Box 757200, Fairbanks, AK 99775, USA; **Joseph Buongiorno** is a professor, Department of Forest Ecology and Management, University of Wisconsin-Madison, 1630 Linden Drive, Madison, WI 53706, USA; **Robert A. Monserud** (retired) was a research forester and team leader, USDA Forest Service, Pacific Northwest Research Station, PO Box 3890, Portland, OR 97208, USA.

[1.] This is an abbreviated and fully rewritten paper based on an analysis published in *Forest Science* 52(5):579–594.

matrix model were obtained with equations of individual tree growth, mortality, and stand recruitment, functions of tree and stand characteristics. These include species diversity, size diversity, stand basal area, and tree size. Diversity was measured with Shannon's index (Magurran 1988). The equations were estimated with individual tree and stand data from 2,706 permanent plots in western Washington and Oregon.

The deterministic model was made stochastic by adding a vector of random shocks. The vector was based on observations on the 2,706 sample plots used to calibrate the stand growth model. For each plot, the vector of stochastic shocks was the difference between the state predicted by the deterministic model, and the observed state.

In the simulations, the stochastic shock was obtained by bootstrapping (Diebold et al. 1998). At each time step a shock vector was drawn randomly, with replacement, from the sample of 2,706 vectors of errors. The advantage of bootstrapping is that it leaves the data as is, without imposing a particular distribution on the shocks, as when truncated multivariate normal distributions are used instead.

This stochastic stand growth model gave predictions of expected basal areas that were similar to those of the deterministic model (Liang et al. 2005) for Douglas-fir and other shade-intolerant species. The stochastic predictions were higher for western hemlock and other shade-tolerant species, suggesting that random shocks help the regeneration of shade-tolerant species.

WOOD QUALITY MODEL

The model-predicted log grade as a proxy for wood quality was based on the USFS Product Recovery Database (Stevens and Barbour 2000), which had data on 3,378 logs. The logs are classified into five grade categories, according to their diameter, branch size, growth rate, and minimum length. The grade codes are: I for peeler, II for #1 Sawmill, III for #2 Sawmill, IV for #3 Sawmill, and V for all other grades. For this study, the logs were divided into the four species groups used in the growth model.

The log grade was predicted by species group with a logistic regression and a nominal response variable. The parameters, estimated by iterative-reweighed least squares (McCullagh and Nelder 1992) are in Table 1. For both species, log grade was higher for larger trees on the lower sites. The positive correlation between tree size and log grade is consistent with the definition of log grade by the

Northwest Log Rules Advisory Group (1998). A possible explanation of the negative correlation between log grade and site is that lower site reduces growth rate (Liang et al. 2005), and consequently increases wood quality with smaller annual rings (Barnett and Jeronimidis 2003). The other variables (basal area, elevation, aspect, and slope) did not have a significant effect on log grade, at the $\alpha=5$ percent level, and were removed from the model.

For other shade-tolerant and shade-intolerant species, the observed percentage of total volume by log grade for each diameter class was assumed to be constant.

MANAGEMENT SIMULATIONS

A management regime was defined by the cutting cycle, and the target residual stand state. The harvest took the trees that exceeded the target residual stand. The simulations were for 50 years. The target residual stand was defined by basal area, diameter of largest tree, and q ratio, where q is the ratio of the number of trees in adjacent diameter classes. This BDq method is commonly used to define the target diameter distribution in uneven-aged stands. Along with the basal area and the diameter of the largest tree, q defines the distribution of the residual stand (Buongiorno and Gilless 2003, p. 291–293).

By assigning different values to basal area, maximum diameter, and the q ratio, the BDq rule defines a wide range of

Table 1. Estimation results of the equations of log grade

Dependent variable	Independent variable	Coefficient	Significance
Douglas-fir			
π_1/π_4	Constant	2.91	*
	D	0.04	**
	S	-0.10	**
π_3/π_4	Constant	1.66	
	D	0.04	**
	S	-0.10	*
Western Hemlock			
π_1/π_4	Constant	-8.94	*
	D	0.41	**
	S	-0.40	*
π_2/π_4	Constant	-8.37	*
	D	0.35	**
	S	-0.30	*
π_3/π_4	Constant	-5.90	**
	D	0.26	**
	S	-0.13	**

π_i = probability of log grade i (no Douglas-fir log was of grade 2).
D = tree diameter.
S = site index.
P = level at which the effect of the independent variable would be just significant: * = P less than 0.05; ** = P less than 0.01 for test of significance.

residuals stands. For a given basal area, increasing the value of q would progressively increase the number of trees in the small diameter classes relative to the number of trees in the large diameter classes. For a given q ratio, increasing the target basal area would increase the stand density without changing the distribution of trees by diameter class.

In the following simulations, the maximum diameter was set at 102 cm, the largest diameter recognized by the growth model. The cutting cycles were 10, 15, 20, 25, or 30 years. The target basal areas were 14, 23, 32, 41, or 51 m^2ha^{-1}; and the alternative q ratios used were 1.2, 1.4, 1.6, or 1.8. The target basal area by species group was kept at the average level observed on all the plots. All combination of these values gave 100 possible management regimes.

As the initial state for each management regime, 500 plots were randomly selected by bootstrapping, with replacement, from the 2,706 permanent plots used to calibrate the growth model. 500 replications were sufficient to obtain stable simulation results.

The following criteria were established to measure the performance of different management regimes:
• Percentage of peeler logs in total volume
• Tree species diversity
• Tree size diversity

Tree species diversity and tree size diversity were measured with Shannon's index, based on the basal area by size and species class.

RESPONSE SURFACE ANALYSIS

For each combination, $k=1,\ldots,100$, of control variables (cutting cycle, C_k, target basal area, B_k, and q ratio, q_k) the simulations gave 500 observations for each management criterion. The response surface analysis determined the effect of each control variable on the expected value of a management criterion, with other control variables held constant at their mean. This was done by regression analysis of the simulated mean responses obtained with a combination of control variables. For example, in the case of the percentage of peeler logs, the following quadratic response surface was fitted by ordinary least squares (OLS):

$$P_k = \omega_0 + \omega_c C_k + \omega_B B_k + \omega_q q_k + \omega_{cc} C_k^2 + \omega_{BB} B_k^2 + \omega_{qq} q_k^2$$
$$+ \omega_{CB} C_k B_k + \omega_{Bq} B_k q_k + \omega_{cq} C q_k + v_k$$

(1)

where P_k was the mean percentage of peeler logs over the 500 replications for the kth combination of control variables,

the ω's were parameters, and v_k was the residual error.

We then assessed the sensitivity of the expected response to a particular control variable by testing the joint significance of all terms containing a particular variable, and by calculating the effect of a variable on the response while other variables were held constant at their mean.

The results of estimation of the response surfaces for the different management criteria are in Table 2. The control variables explained 97–99 percent of the variation in the percentage of peeler logs and stand diversity.

As shown in Figure 1, the cutting cycle had a biologically significant effect only on the species diversity, which decreased slightly with longer cutting cycles.

Increasing the target basal area from 14 to 50 m^2ha^{-1}, other things being equal, decreased species diversity by 5 percent. Meanwhile, the percentage of peeler logs decreased only slightly, and the tree size diversity was unchanged.

The q ratio had a significant effect on all three criteria. Increasing the q ratio from 1.2 to 1.8, other things being equal, decreased percentage of peeler logs, species diversity, and size diversity.

When the results of all the management alternatives were pooled together, we found that the percentage of peeler logs was positively correlated to tree species diversity and to tree size diversity (Figure 2). The positive relationship between percentage of peeler logs and species diversity was statistically the most significant.

OPTIMIZATION

The last part of the analysis sought the combined values of the control variables that optimized a particular management criterion. For example, the maximum percentage of peeler logs was found by finding the values of C, B, and q such that:

$$\max_{\{C,B,q\}} P = \hat{\omega}_0 + \hat{\omega}_c C + \hat{\omega}_B B + \hat{\omega}_q q + \hat{\omega}_{cc} C^2 + \hat{\omega}_{BB} B^2 +$$
$$\hat{\omega}_{qq} q^2 + \hat{\omega}_{CB} CB + \hat{\omega}_{Bq} Bq + \hat{\omega}_{cq} Cq$$

subject to :
$$10 \leq C \leq 30$$
$$14 \leq B \leq 51$$
$$1.2 \leq q \leq 1.8$$

(2)

where the $\hat{\omega}$'s were the estimated values of the parameters
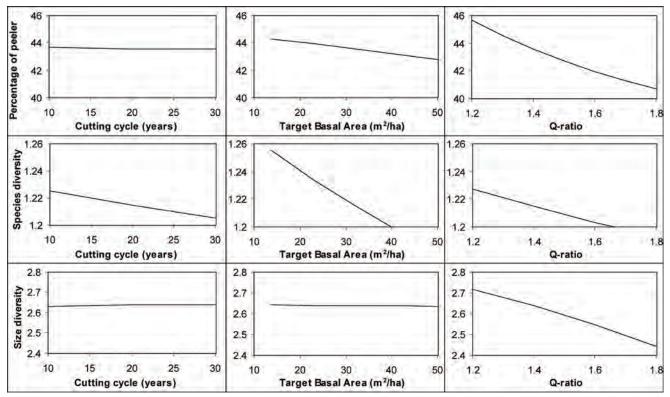
Figure 1— Effects of control variables on the expected value of management criteria, with other control variables being held constant at their mean
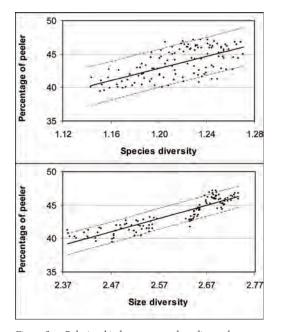
Figure 2— Relationship between wood quality and tree diversity

Table 2. Values of management criteria as functions of the control variables.

Equation	R^2
$P=71.20^{**} -1.61^{**}C +0.21B -26.63^{**}q +0.029C^2 -2.10B^2 +5.62^{**}q^2 -0.32CB -2.08Bq +1.09^{**}Cq$	0.97
$Hs=1.35^{**} +0.012C -0.15^{**}B -0.05q +0.0005C^2 +0.11^{**}B^2 +0.02q^2 -0.005CB -0.09^{**}Bq -0.02^{**}Cq$	0.98
$Hd=3.24^{**} -0.12^{**}C -0.09B -0.23^{**}q -0.005C^2 -0.03B^2 -0.16^{**}q^2 -0.01CB +0.07Bq +0.11^{**}Cq$	0.99

P = percentage of peeler logs.
Hs= species diversity.
Hd= size diversity.
BA= basal area.
C= length of cutting cycle (10y).
B= target basal area (10^2m^{2}ha^{-1}).
q= q ratio of target tree distribution.
*, P less than 0.05; **, P less than 0.01 for test of significance.

of the response surface for percentage of peeler logs, *P*. The constraints defined the range of the control variables, *C*, *B*, and *q*, in the simulations.

The optimization results showed that a 10-year cutting cycle, a target basal area of 14 m^2 ha^{-1}, and a *q* ratio of 1.2 led to the highest percentage of peeler logs, the highest tree species diversity, and the highest tree size diversity.

SUMMARY AND CONCLUSION

The *q* ratio had more influence on the management criteria than the residual basal area or the cutting cycle. Having a higher *q* ratio, which means more trees in the smaller size classes, reduced tree-species diversity, tree-size diversity, and the percentage of peeler logs.

Over all the simulated management regimes, there was a positive correlation between the percentage of peeler logs and species diversity, and between the percentage of peeler logs and tree-size diversity.

The combination of cutting cycle (10 years), target basal area (14 m^2 ha^{-1}), and *q* ratio (1.2), that maximized percentage of peeler logs also maximized tree-size diversity, and tree-species diversity.

Thus, there was no apparent conflict between the goal of stand diversity and the goal of wood quality. Stands with a higher diversity of structure (tree size) and a higher diversity of species also contained a higher percentage of high-grade logs.

LITERATURE CITED

Barnett, J.R.; Jeronimidis, G. 2003. Wood Quality and its biological basis. Blackwell Publishing, Oxford, UK. 226 p.

Briggs, D.G.; Fight, R.D. 1992. Assessing the effects of silvicultural practices on product quality and value of coast Douglas-fir trees. Forest Products Journal 42(1): 40-46.

Buongiorno, J.; Gilless, J.K. 2003. Decision methods for forest resource management. Academic Press, San Diego. 439 p.

Diebold, F.X.; Ohanian, L.E.; Bekowitz, J. 1998. Dynamic equilibrium economies: a framework for comparison models and data. Review of Economic Studies 65: 433–451.

Guldin, J.M., **1996.** The role of uneven-aged silviculture in the context of ecosystem management. Western Journal of Applied Forestry 11(1): 4–12.

Liang, J.; Buongiorno, J.; Monserud, R.A. 2005. Growth and yield of all-aged Douglas-fir/western hemlock forest stands: a matrix model with stand diversity effects. Canadian Journal of Forest Resources 35: 2369-2382.

Magurran, A.E. 1988. Ecological diversity and its measurement. Princeton University Press, Princeton. 179 p.

McCullagh, P.; Nelder, J.A. 1992. Generalized Linear Models. Chapman & Hall, London. 532 p.

Myers, R.H.; Montgomery, D.C. 2002. Response surface methodology, 2nd ed. John Wiley & Sons, New York. 798p.

Northwest Log Rules Advisory Group. **1998.** Official log scaling and grading rules. 8th ed. Eugene, Oregon. 48 p.

Stevens, J.A.; Barbour, R.J. 2000. Managing the stands of the future based on the lessons of the past: estimating western timber species product recovery by using historical data. USDA, Forest Service, Res. Note PNW-RN-528. 9 p.

Simulation in Sustainable Forest Management

Simulation in Sustainable Forest Management
Keynote Presentation

Tools for Sustainable Forest Management

Hubert Hasenauer and Stephan A. Pietsch

ABSTRACT

WITHIN THE PAST TWO DECADES, AND particularly since the "Brundtland Report", sustainability has become a key term in emphasizing the relationship between economic progress and nature conservation issues. One option for assessing and understanding these changes are forest ecosystem models, which are designed to reproduce, quantify, and describe forest ecosystem processes. Three major modeling concepts have been evolved and successfully applied within forest ecosystem modeling: (1) Management models, (2) Succession models, and (3) Biogeochemical-mechanistic models (BGC-Models). In this paper the different concepts including the main components, their advantages and disadvantages in assessing specific end-user needs are discussed. Three application examples are presented as well.

KEYWORDS: Ecosystem research, modeling, system analyses, sustainability

INTRODUCTION

Forest management within the context of economic progress is an essential issue when considering sustainability. Forests have been severely modified by humans. The results are a reduction in forest-covered land area (in Europe from a potential coverage of 80 percent to 40 percent), a change in tree-species distribution, and intensive management to enhance timber production. One tool used to assess and understand these changes is forest ecosystem modeling. Conflicting interests such as simplicity, observability and biological realism must be addressed to ensure a well balanced modeling approach. Because field observations are usually only available for short time periods or for a limited number of locations, models are an important tool used to extrapolate in space and time (Pacala et al. 1996).

An important constraint in our modeling efforts is that, in some research fields, the scientific knowledge has room for improvement. In such situations, models help to detect research needs and to inform the design of field studies. Simple input/output approaches can be used until a comprehensive understanding of missing research information is available.

Within science, the term model is defined as a simplified reproduction of a much more complex reality (Shugart 1998). Consequently, models will always include a certain level of abstraction by creating a system, which is less complex than reality, but still describes the pattern and behavior of a real-world scenario. Models are available in a wide variety of forms ranging from conceptual models to graphical models to computer simulation tools (Kimmins 1987).

Building models requires a system analytical approach (see Figure 1). First a problem must be formulated. Objectives need to be defined according to the criteria of simplicity, observability, and biological realism. While defining objectives, the framework of the model's function in terms of its application and expected model output is defined.

Hubert Hasenauer (hubert.hasenauer@boku.ac.at) is a professor and head of institute and **Stephan A. Pietsch** is an assistant in the Institute of Silviculture, BOKU University of Natural Resources and Applied Life Sciences, Peter Jordan Str. 82, A-1190 Vienna, Austria.

Next, resource planning is important because data collection is expensive and time consuming. Thus, a lot of our modeling efforts are limited by data constraints. This limits the scaling in space and time. If models are to be applied on a larger scale or to a longer time period the data structure used for calibration and model initialization has a major impact on the reliability of the expected output.

All modeling work must include validation and/or evaluation of the model. This is a continuous process because each model is based on the latest available knowledge to ensure reliability. Data not used for calibration are used for assessing the expected error range of key output variables. One important objective in modeling is to mimic nature as well as possible, to achieve biological realism in the model output. This may require procedures or experiences which are not always rigorously tested in typical statistical validation.

When using ecosystem models it is important to understand how a model responds to undisturbed "regular" conditions as well as to different scenarios (assumed disturbances). Such scenario simulations are important for sensitivity analysis. Thus, they are a major step in evaluating and testing the reliability of expected model output even if no adequate test data sets are available.

Ecosystem processes act at different levels, which may require different procedures for data collection and integration. Some processes may be on a leaf- or tree-level (such as photosynthesis) other processes may act at a regional or even global scale (such as expected change in climate). The same holds true for time; some processes operate within seconds or less (such as gas exchange within the stomata), while others take years or centuries to have an impact on a forest ecosystem (such as soil processes). If we wish to combine different processes, accommodating these differences in scale is critical. At this point, issues of formal conceptual implementation center around the three major modeling criteria: simplicity, observability, and biological realism. These criteria are essential for ensuring a "well balanced" model approach.
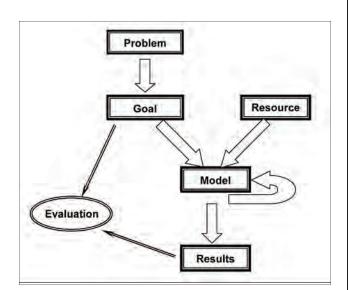
The term "well balanced" refers to the fact that it makes no sense to give one model driver a very careful and detailed description while others are less rigorously implemented or even inconsistant. An imbalanced approach such as this may lead to misleading and ill-defined modeling results since biological realism is not correctly addressed. From a statistical point of view, random variation may be removed. Such models pretend to produce accuracies in their predictions, which do not exist. Each model needs a "unit". While this is easy to achieve for typical production models (such as volume increment) achieving this may become complex within biogeochemical-mechanistic modeling, since these models integrate different ecosystem processes at various spatial and temporal scales.

Models are developed to combine existing knowledge, describe interactions between key ecophysiological processes, formulate hypotheses, identify gaps in our knowledge, and to perform scenario analysis to support decisions. With the development of the computer industry and the improvement in our ecological understanding, a wide variety of models have been developed. Nevertheless, from a

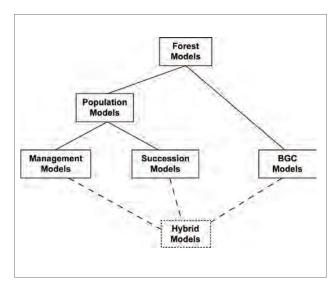Figure 1. System analytical approach in the design of ecosystem models (Hasenauer et al. 2000).

Figure 2: The three most common forest ecosystem modeling concepts according to implementation principles (see Hasenauer et al. 2000).

conceptual point of view, we may distinguish between the three following forest ecosystem model concepts (see also Hasenauer et al. 2000).

MODELING CONCEPTS

Management Models

Forest conditions are assessed by periodical forest inventories. However, for forest planning, models are needed to predict forest growth. Forest inventories combined with model-driven forest growth predictions provide the basic information from which to derive sustainable cutting plans at the company, regional, or national level. Traditionally, forest management has relied on yield tables (Weisee 1880). The main assumptions concerning yield tables are that the forest stands are pure, even-aged and undergo only one stand treatment, if any. Based on a given site quality (such as site index) the mean stand development over time—one rotation period—is described. This model type has existed for more than 100 years. It is important to note that the main interest in growth and yield models was always the prediction of future stand development in order to avoid over-cutting and exploitation of forest resources. These are the key features for developing sustainable management plans.

With the movement of forest management towards uneven-aged forests, existing yield tables have been improved and/or partly replaced by tree growth models. The idea is driven by the fact that uneven-aged mixed species stands may increase or at least maintain soil fertility, increase biodiversity, and improve stand resilience. As a result, tree growth models have been developed which operate at the individual tree level. Examples of these models in North America include Stage 1973, Wykoff et al. 1982, and Monserud 1975; and in Europe: Pretzsch 1992, Hasenauer 1994, Sterba et al. 1995, and Nagel 1999. The main advantage of tree models is that they are independent from any specific mixture, age, and stand treatment, because the growth and mortality of each tree within a stand is described.

From a conceptual point of view, we may distinguish between tree models which predict the periodical 5-year growth rates (diameter and height increment) based on a given potential (Hasenauer 1997) which is then reduced to the actual growth of a tree (see also the concept of gap models) versus those which predict periodical tree growth directly. Tree mortality is determined by a survival probability within a given period. Such models have been developed mainly to provide an alternative tool (replacing yield tables) within uneven-aged mixed-species stands and to ensure sustainable forest management. For further details related to this topic see Hasenauer (2005) and the ITM homepage: http://www.boku.ac.at/itm.

Succession Models

Succession, Gap, or Patch models describe the reproduction growth and mortality of trees (Botkin 1993). Old trees die, resulting in forest gaps or patches into which new trees will grow (Shugart 1998). The first and most famous succession model was JABOWA I (Botkin et al. 1972) developed for describing the stand dynamics of the Hubbard Brook experimental forest in the Northeastern United States. Since then, numerous applications have been developed (Shugart 1998, Pacala et al. 1996, Lexer and Höninger 2001).

In a succession model, predefined species-specific growth potential (considered as the maximum growth) is calculated in a way similar to the site-specific "growth potential" calculation of management models. Next, reduction factors for assessing the competition for light, temperature, water, and nutrients (nitrogen) are derived as so-called response functions. These response functions can be thought of as multipliers between 0 and 1, which reduce the species-specific growth potential to actual values according to site variation and the competitive status of the trees. Thus, succession models explicitly assess the impact of temperature, water, and nutrients on tree growth by applying multipliers while management models use individual tree competition measures to predict the 5-year growth rates of trees.

Although tree growth is simulated, the main goal of succession models is to describe vegetation patterns over time. The original aim of gap models was to understand and reproduce existing vegetation patterns that have developed since the last glacier periods. The stand dynamic as it has evolved during centuries was and still is one of the main features. The regeneration, growth, and death of individual trees and the interaction between different tree species are key features. Management impacts are usually not assessed, because a constant height-to-diameter ratio and a fixed mortality percentage are implemented. Interactions between the main driving forces of growth (energy, temperature, water, nutrients) are the main research areas used to enhance the functioning of this model type. Today, such models are used for assessing the potential vegetation pattern and potential changes in vegetation distribution under expected climate change.

Biogeochemical-mechanistic Models

Mechanistic models describe the circulation, transformation, and accumulation of energy within and through a forest ecosystem. The main goal is to assess the interaction between plants and their surrounding environment. BGC-Models are considered diagnostic tools to understand ecosystem behavior. Thus, they are often called process or biogeochemical models (BC-Models). In contrast to tree population models, such as management or succession models, BGC models incorporate a mechanistic description of the interaction between plants and the surrounding environmental conditions (Waring and Running 1998). Consequently, they are designed to be responsive to changes in environmental conditions.

BGC models operate on a monthly to daily time resolution to simulate the cycles of carbon, water, and nitrogen for generalized biome types (Thornton 1998) or species (Pietsch et al. 2005). Leaf area index (LAI, m^2 leaf area per m^2 ground area) controls canopy radiation absorption, water interception, photosynthesis, and litter inputs to detritus pools. BGC models operate on a stand level and simulate net primary production (NPP) calculated from a photosynthesis routine (Farquhar et al. 1980) minus autotrophic respiration. Autotrophic respiration comprises maintenance respiration, calculated as a function of tissue nitrogen concentration and growth respiration and a function of the amount of carbon allocated to the different plant components (leaf, root, and stem).

NPP is partitioned into the leaves, roots, and stems as a function of dynamic allocation patterns, with consideration for limitations due to availability of and competition for nitrogen. BGC models require meteorological input data, such as daily minimum and maximum temperature, incident solar radiation, vapor pressure deficit, and precipitation, which may be derived for any location within the area of interest using interpolation algorithms (see Hasenauer et al. 2003).

BGC models have been applied for large as well as small-scale applications. The specific strength of these models is the description of the carbon cycle as it can be used for assessing growth responses to environmental impacts (see Hasenauer et al. 1999). The daily time resolution adequately addresses the annual patterns of weather events. Other applications are the description of the water cycle (Running and Coughlan 1988, Pietsch et al. 2003) and the nutrient cycle as it may depend on the tree population. Major goals for improving mechanistic modeling techniques are enhancement of the species representation (Pietsch and Hasenauer 2001, Pietsch et al. 2005) and inclusion of management scenarios (Merganicova et al. 2005).

APPLICATION EXAMPLES

In this chapter a typical example for forest management and two mechanistic modeling examples are presented. In the first example, the distance tree growth model MOSES modeling stand response (Hasenauer 1994) is applied for uneven-aged mixed-species stands in Switzerland. The second and third examples demonstrate the application of our species-specific version of BIOME-BGC (Thornton 1998, Pietsch et al. 2005) to assess historic land use impacts and the carbon flux within old growth forests in Austria.

Modeling Uneven-aged Forests in Switzerland

The purpose of this study was to apply the tree growth model

Table 1: Differences in diameter increment (predicted-observed) for spruce, fir, and beech and three 5-year growth periods; n is the number of observations, id_{obs} is the mean of the observed increment, D_i is the mean of the differences between predicted and observed values, S_D the standard deviation of the differences and PI and TI are the prediction and tolerance intervals of the error (Reynolds 1984).

| Species	Period	n	$\overline{id_{obs}}$[cm]	$\overline{D_i}$[cm]	S_D[cm]	PI [cm]	TI [cm]
Spruce	1	3927	0.20	-0.08	0.26	-0.59 to 0.43	-0.59 to 0.42
	2	3421	0.21	-0.06	0.24	-0.53 to 0.41	-0.54 to 0.42
	3	3191	0.18	-0.21	0.87	-1.50 to 1.92	-1.93 to 1.50
Fir	1	2017	0.42	-0.22	0.22	-0.65 to 0.21	-0.65 to 0.20
	2	1849	0.35	-0.20	0.45	-1.08 to 0.68	-1.09 to 0.69
	3	1595	0.33	-0.38	1.07	-2.48 to 1.72	-2.49 to 1.74
Beech	1	18114	0.22	-0.08	0.19	-0.45 to 0.29	-0.45 to 0.29
	2	12762	0.21	-0.08	0.21	-0.49 to 0.33	-0.49 to 0.33
	3	10385	0.20	-0.11	0.45	-0.99 to 0.77	-0.99 to 0.77
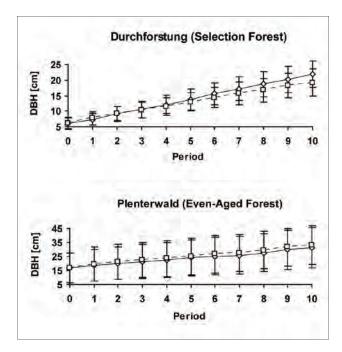
Figure 3. Development of mean diameter at breast height (DBH) for two plots between 1950 and 2004 (mean ± standard deviation). For both the selection forest and the uneven-aged forest, differences between observed values (represented by solid lines connecting diamond points) and predicted values (represented by dashed lines connecting square points) were not significant.

MOSES (Hasenauer 1994) to uneven-aged mixed-species forests (Schultz 1997). This model predicts the growth of each individual tree within a given forest. MOSES follows a potential growth concept where the actual increment results from different reduction factors. These reduction factors, according to Eke and Monserud (1974), are derived from two main competition factors: crown ratio and individual tree competition.

Data not used for calibration were obtained for this study. They consisted of 16.398 growth periods for Norway spruce (*Picea abies* L. Karst), 2.495 for silver fir (*Abies alba* Mill.), and 19.292 for Common beech (*Fagus sylvatica* L.). MOSES uses a distance dependent competition measure (Ek and Monserud 1974). Thus, it includes an algorithm for generating tree distributions (STAND-GEN) allowing the analysis of structural and textural effects (Kittenberger 2003). With these data, a comparison was done between predictions and observation. The results suggest no trends (see Table 1) and consistent prediction results for uneven-aged conditions. The range in the error limits are calculated according to Reynolds (1984) and can be interpreted as follows: The prediction interval (PI) gives—within 95 percent probability—the range where 95 percent of errors will be for any other plots not included in the validation data set.
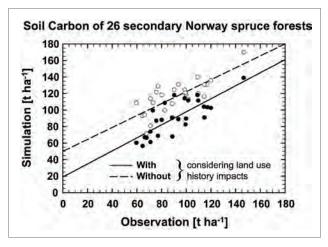
Figure 4. Predicted vs. observed tree volume including regression lines developed by using independent validation data

The tolerance interval (TI) shows—within 95 percent probability—the range of errors to be expected upon repeated model applications.

For spruce we can be confident that, with a probability of 95 percent, no bias for the prediction of the increment exists. For single future model applications (95 percent probability) the bias will be between -0.59 and 0.43 cm in period 1. When applying model simulations repeatedly there is a 95 percent probability that 95 percent of the errors will be between -0.59 and 0.42 cm in the first period.

In Figure 3, a long-term simulation of the diameter at breast height between 1950 and 2004 for two different plots is given. The upper plot is a 150-year-old selection forest composed of spruce, fir, and beech located 861 m above sea level. The lower plot is a 116-year-old even-aged forest that has been regularly thinned, located 570 m above sea level. In both plots, every treatment was simulated over 50 years. No trend or bias is evident.

Modeling Forest Ecosystem Restoration

For centuries, European forests have been influenced by humans resulting in a reduction of forest-covered land area, changes in forest species-distribution, and changes in soil conditions. Fast-growing tree species such as Norway spruce (*Picea abies* L. Karst) and Scots pine (*Pinus sylvestris* L.) were promoted in large areas typically covered with broadleaf or mixed-species stands in order to increase commercial timber growth.

One method to assess the effects of species composition is the use of mechanistic models because they integrate the main biogeochemical and physiological processes based on the current understanding of key ecophysiological
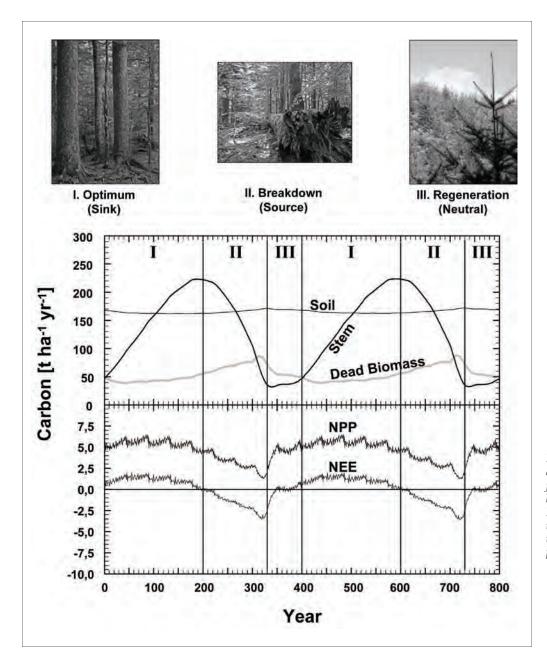
Figure 5. Two full carbon cycles within the old-growth forest, Rothwald, in Austria based on data. NPP is Net Primary Production and NEE is Net Ecosystem Exchange, indicating the source and sink potential of unmanaged forests.

mechanisms (Waring and Running 1998). The purpose of this study was to investigate potential degradation effects in the soil carbon content according to species change. The hypothesis was that historic land use change may affect the soil and that it might be possible to mimic theses changes with a biogeochemical model.

Data available for this study were from comparable sites with different management strategies: a typical broadleaf-dominated forest versus a secondary coniferous forest next to the broadleaf forest. With these data the water-, carbon- and nitrogen- cycle where assessed. For this study, the species-specific calibration described by Pietsch et al. (2005) was used. For model validation and testing, the 26 spruce and 18 beech plots established within the Forest Ecosystem Restoration research program (Sterba and Hasenauer 2000) were used. These plots varied in site index, stand density, and stand age and represented an excellent data source for studying land-use impacts on the flux dynamics of forest ecosystems. On each plot, soil nitrogen, soil carbon, and tree volume per hectare were available.

The main results (see Figure 4) clearly indicate that land-use impacts are essential to the flux dynamics and that soil is the key compontent. Ignoring such effects will lead to an overestimation in the soil carbon content and thus to biased assessments (Pietsch and Hasenauer 2001).

The Sink and Source Potential of Forests

An excellent test case for modeling the sink and source behavior of undisturbed forests is the flux dynamics of old growth or virgin forests. A very good example and application case is provided by the Central European virgin forest reserve Rothwald in Austria. Rothwald is located in the northern limestone Alps at 15°05'E and 47°46'N at an elevation between 950 and 1300 m above sea level. The parent rock is composed of limestone and dolomite. Soil types range from lithic and rendzic leptosols to chronic cambisols. Mean annual temperature is about 7°C and mean annual precipitation 1300mm. Living biomass is comprised of 68 percent Common beech (*Fagus sylvatica* L.), and admixture of Norway spruce (*Picea abies* L./Karst.) and silver fir (*Abies alba* Mill.). The documented history of the forest reserve starts in 1330, when Albrecht II Habsburg founded the charterhouse, Gaming, and endowed the area of Rothwald to the contemplative fraternity of the Carthusians. In 1782, Joseph II Habsburg eliminated the charterhouse. After this, the forest changed owners until it became part of the Rothschild estate in 1875. Today, Rothwald is a preserve area and was declared a wilderness area (IUCN category I) in 2001 (Splechtna and Gratzer 2005).

For our study we obtained 18 plots covering different successional stages within the Rothwald wilderness area. On each of the 18 plots, six sub-plots were randomly chosen from which we obtained soil and humus samples as well as the above-ground tree population conditions. The variables available for model testing are volume, dead wood volume, nitrogen and carbon within the humus and for three different soil layers. These data were used to validate the biogeochemical model for old growth forest conditions and to assess the carbon dynamics of such forests (see Figure 5).

The results show the sink and source potential of forest. During the optimum phase the ecosystem exhibits a net carbon sink (optimum phase), stationary phases with no net carbon exchange (old growth, juvenescence), and time periods where it constitutes a carbon source (breakdown, regeneration). Such source-sink transitions are part of natural ecosystem dynamics (Pietsch and Hasenauer 2006).

DISCUSSION AND CONCLUSION

Forest ecosystem models assess forest ecosystem processes. They are designed to detect, quantify, and reproduce the dynamics within our forests. These models are important tools used to extrapolate forest ecosystem processes at dif-ferent spatial and temporal scales such as from the point to the landscape level (bottom-up approach), or from the landscape to the plot level (top-down approach). Accommodation of these scales is important to ensure a successful application. According to the background of the model developer, the main subjects of interest and the three basic principles for building models are simplicity, observability, and biological realism. Three main modeling concepts may be distinguished (see Figure 2).

Management models are considered the classical approach developed within growth and yield sciences. They are designed to provide information for forest management purposes. Their main goal is to forecast timber to ensure sustainable harvesting and income. Succession models assess vegetation patterns. They are developed and used to understand the tree population dynamic as it has evolved over centuries. One main area of application for succession models is the assessment of potential forest-vegetation patterns. Mechanistic models are explicitly designed to understand the complex interaction between energy, water, and nutrient cycles within forest ecosystems. They are used for assessing the interactions and flows within forest ecosystems and the surrounding environment and may be thought of as classical carbon-cycle models.

In this study, two different modeling concepts were applied. The management-oriented tree growth model MOSES (Hasenauer 1994) was used to analyze the growth within an uneven-aged mixed-species forest in Switzerland. The main results of this modeling exercise suggest no bias and that tree growth modeling is an appropriate tool to use in meeting the increased silvicultural demand to manage structurally diverse forests.

Our second applied model—the species-specific version of the biogeochemical model BIOME-BGC (see Pietsch et al. 2005)—demonstrated that the flux dynamics of managed and unmanaged forest ecosystems can be addressed. This proves that BGC-Models are an appropriate tool for assessing land use changes as well as the sink and source potential of forests. The correct formal implementation of key ecosystem processes is essential to studying climate-change impacts and degradation effects, which are used in sustainable impact-assessment studies.

It is shown that both mechanistic as well as management-oriented modeling can be applied successfully for scenario calculations. Note that the level of detail and, thus, the complexity of the different approaches, though different, each adequately addressed the objectives and expected

needs. Choosing the correct level of model complexity is an important step within the modeling process because it ensures an efficient use of available resources, and the reliability of the model output.

ACKNOWLEDGMENTS

LITERATURE CITED

Botkin, D.B. 1993. Forest dynamics: an ecological model. Oxford University Press, Oxford. 309 p.

Botkin, D.B.; Janak, J.F.; Wallis, J.R. 1972. Some ecological consequences of a computer model of forest growth. Journal of Ecology. 60: 849-872.

Ek, A.R.; Monserud, R.A. 1974. FOREST: A computer model for simulating the growth and reproduction of mixed species stands. University of Wisconsin, College of Agriculture and Life Science. Res. Rep. R2635. 90 p.

Farquhar, G.D.; Caemmerer, von S.; Berry, J.A. 1980. A biochemical model of photosynthetic CO_2 assimilation in leaves of C_3 plants. Planta 149: 78-90.

Hasenauer, H. 1994. Ein Einzelbaumwachstumssimulator für ungleichaltrige Fichten-Kiefern- und Buchen-Fichtenmischbestände. Forstl. Schriftenreihe, Univ. f. Bodenkultur, Wien. Österr. Ges. f. Waldökosystemforschung und experim. Baumforschung an der Univ. f. Bodenkultur Band 8: 152 p. (In German)

Hasenauer, H. 1997. Dimensional relationships of open-grown trees in Austria. Forest Ecology and Management 96: 197-206.

Hasenauer, H. 2005. Sustainable Forest Management: Growth models for Europe. Springer, Berlin. 398 p.

Hasenauer, H.; Burgmann, M.; Lexer, M.J. 2000. Konzepte der Waldökosystemmodellierung. Centralbl. f. d. ges. Forstw 117: 137-164. (In German)

Hasenauer, H.; Kindermann, G. 2002. Methods for assessing regeneration establishment and height growth in uneven-aged mixed species stands. Forestry 75(4): 385-394.

Hasenauer, H.; Merganicova, K.; Petritsch, R. [et al.]. 2003. Validating daily climate interpolations over complex terrain in Austria. Agricultural and Forest Meteorology 119: 87-107.

Hasenauer, H.; Nemani, R.R.; Schadauer, K.; Running, S.W. 1999. Forest growth response to changing climate between 1961 and 1990 in Austria. Forest Ecology and Management 122: 209-219.

Kimmins, J.P. 1987. Forest ecology: models and the role in ecology and resource management. Macmillan Publishing Company, New York. pp. 460-474.

Kittenberger, A. 2003. Generieren von Baumverteilungsmuster. Diplomarbeit am Institut für Waldwachstumsforschung der Universität für Bodenkultur, Wien. 79 p.

Lexer, M.J.; Hönninger, K. 2001. A modified 3D-patch model for spatially explicit simulation of vegetation composition in heterogenous landscapes. Forest Ecology and Management 144: 43-65.

Merganicova, K.; Pietsch, S.A.; Hasenauer, H. 2005. Testing mechanistic modeling to assess forest management impacts. Forest Ecology and Management 207: 37-57.

Monserud, R.A. 1975. Methodology for simulating Wisconsin northern hardwood stand dynamics. Ph.D. Thesis. University of Wisconsin, Madison. 156 p.

Nagel, J. 1999. Konzeptionelle Überlegungen zum schrittweisen Aufbau eines waldwachstumskundlichen Simulationssysttems für NW Deutschland. J. D. Sauerländer´s Verlag, Frankfurt/Main. 122 p.

Pacala, S.W.; Canham, C.D.; Saponara, J. [et al.]. 1996. Forest Models Defined by Field Measuremensts: Estimation, Error Analysis and Dynamics. Ecological Monographs 66 (1): 1-43.

Pietsch, S. A.; Hasenauer, H. 2001. Using mechanistic modeling within forest ecosystem restoration. Forest Ecology and Management (159): 111-131.

Pietsch, S.A.; Hasenauer H. 2006. Evaluating the self-initialization procedure for large scale ecosystem models. Global Change Biology 12: 1-12.

Pietsch, S.A.; Hasenauer, H.; Kucera, J.; Cermak, J. 2003. Modeling the effects of hydrological changes on the carbon and nitrogen balance of oak in floodplains. Tree Physiology 23: 735-746.

Pietsch, S.A.; Hasenauer, H.; Thornton, P.E. 2005. BGC-Model parameters for tree species growing in central European forests. Forest Ecology and Management 211: 264-295.

Pretzsch, H. 1992. Konzeption und Konstruktion von Wuchsmodellen für Rein- und Mischbestände. Institut für Ertragskunde der Forstl. Forschungsanstalt München 115: 332 p.

Reynolds, M.R. 1984. Estimating the error in model predictions. Forest Science 30: 454-469.

Running, S.W.; Coughlan, J.C. 1988. A general model of forest ecosystem processes for regional applications. I. Hydrologic balance, canopy gas exchange and primary production processes. Ecological Modelling 42: 125-154.

Schütz, J.P. 1997. Sylviculture 2: La gestion des forêts irrégulières et mélangées. Collection gérer l'environnement, Presses Polytechniques et Universitaires Romandes, Lausanne. 178 p.

Shugart, H.H. 1998. Terrestrial ecosystems in changing environments. Cambridge University Press, Cambridge. 537 p.

Splechtna, B.E.; Gratzer, G. 2005. Natural disturbances in central European forests: approaches and preliminary results from Rothwald, Austria. Forest Snow and Landscape Research 79: 57-67.

Stage, A.R. 1973. Prognosis model for stand development. USDA Forest Service Res. Pap., INT-137: 32 p.

Sterba, H.; Hasenauer, H. 2000. The special research program "Forest Ecosystem Restoration". In: Hasenauer, H. (ed.). Proc. Int. Conference on Ecosystem restoration FER 2000. Vienna, Austria. pp. 257-263.

Sterba, H.; Moser, M.; Hasenauer, H.; Monserud, R.A. 1995. PROGNAUS ein abstandsunabhängiger Wachstumssimulator für ungleichaltrige Mischbestände. Deutscher Verband Forstl. Forschungsanstalten-Sektion Ertragskunde. Eberswalde/Berlin. pp. 173-183.

Thornton, P.E. 1998. Description of a numerical simulation model for predicting the dynamics of energy, water, carbon and nitrogen in a terrestrial ecosystem. University of Montana, Missoula, Montana. 280 p.

Waring, R.H.; Running, S.W. 1998. Forest ecosystems: analysis at multiple scales. 2nd Edition. Academic Press, San Diego, California. 370 p.

Weise, W. 1880. Ertragstafeln für die Kiefer. Verlag Springer, Berlin. 156 p.

Wykoff, W.R.; Crookston, N.L.; Stage, A.R. 1982. User's Guide to the Stand Prognosis Model. USDA Forest Service GTR INT-133. 112 p.

Reconstruction of Stand Structure and Growth Following Partial Cutting of Southeast Alaska Forests: Sustainable Forest Management or Highgrading?

Robert L. Deal

ABSTRACT

THE EFFECTS OF PARTIAL CUTTING ON STAND structure, growth, mortality, and species composition were evaluated on 73 plots in eighteen stands that were harvested 12–96 years ago in southeast Alaska. Stands were reconstructed using historical records and tree increment cores from 986 western hemlock, Sitka spruce, western red-cedar, and yellow-cedar trees. Site-specific regression equations were developed to predict diameter at breast height (DBH) at time of cutting for all trees, relating former DBH with current DBH, basal area, species, and plot cutting intensity. These equations explained 77–99 percent of the variation in DBH at the time of cutting. Stand mortality was estimated using snag class and snag age. Results were used to test assumptions that partial cutting of older forests results in reduced stand growth and vigor, increased wounding and mortality, and changes in tree species composition. The current stand basal area, tree species composition, and stand growth for all cutting intensities was strongly related to trees left after harvest. Residual trees, including larger remnant trees and small advance regeneration, grew rapidly after partial cutting and became a significant and dominant component of the current stand. The net basal-area growth was greater in the partially cut plots than in the uncut plots, and stand basal-area growth generally increased with increasing cutting intensity. Mortality, however, was not significantly different between cut and uncut plots. Concerns about greatly reduced stand growth and vigor, lack of spruce regeneration, and increased stand mortality were largely unsubstantiated. Sustainable forest management using silvicultural systems based on partial cutting could provide a sustainable timber resource while maintaining complex stand structures similar to old-growth stands.

KEYWORDS: Partial cutting, stand reconstruction, Sitka spruce, southeast Alaska, stand structure, western hemlock

INTRODUCTION

Southeast Alaska is a coastal temperate rainforest region with large areas of old-growth forests that are renowned for their scenic quality, fish and wildlife habitat and timber resources. Forest managers in the region have been working to develop management strategies that will provide wood resources to the local economy without compromising scenic quality, or aquatic and wildlife habitat. Managers are interested in developing silvicultural solutions to enhance options for multiple-resource management.

The coastal rain forests of southeast Alaska have simple tree composition but complex forest age and tree-size structure. The two predominant tree species, Sitka spruce (*Picea sitchensis* (Bong.) Carr.) and western hemlock (*Tsuga heterophylla* (Raf.) Sarg.), contain more than 90 percent of the total forest volume (Hutchison 1967). The forests are generally multi-aged, and stands developed following high frequency, small-scale natural disturbances such as

Robert L. Deal (rdeal@fs.fed.us) is a research forester, U.S. Department of Agriculture, Forest Service, Pacific Northwest Research Station, 620 SW Main Street, Suite 400, Portland, OR 97205.

windthrow, landslides, and endemic tree disease (Deal et al. 1991, Kramer et al. 2001, Hennon and McClellan 2003). These multi-aged stands contain complex forest structures with many forest canopy layers, abundant understory vegetation, large trees and snags, heartrot cavities in live trees, large woody debris, and other important ecological characteristics of old-growth forests (Franklin et al. 1981, Alaback and Juday 1989, Franklin and Spies 1991).

Since the 1950s, clearcutting has been the dominant timber management practice in southeast Alaska forests (Harris and Farr 1974). Forest development following stand-replacing disturbances such as clearcutting is different than typical forest development following natural small-scale disturbances. Post-harvest conifer regeneration is frequently abundant (greater than 10,000 trees ha^{-1}) with the development of a dense new cohort of western hemlock and Sitka spruce trees. The forest canopy closes in 20–30 years followed by a dense, long-lasting stage of stem exclusion (Alaback 1982, Deal et al. 1991). Canopy closure eliminates most herbs and shrubs (Alaback 1982) and attempts to re-establish understory plants by thinning dense young-growth stands has led mostly to conifer regeneration (Deal and Farr 1994) with little success in herbaceous plant colonization (Tappeiner and Alaback 1989). These dense young-growth stands have relatively uniform tree height and diameter distributions, and notably lack the multi-layered, diverse forest structures and shrub/herb layers
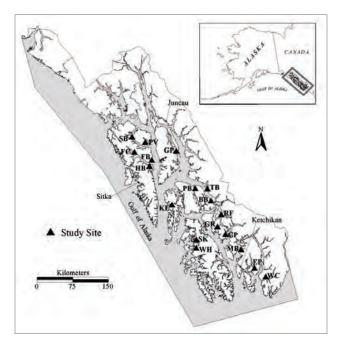
found in old-growth or multi-aged stands (Alaback 1984, Deal 2001, Hennon and McClellan 2003).

Stand development in partially cut stands happens differently than in young-growth stands, which develop after clearcutting. In a study that assessed several stands that were partially cut between 1900–1950, results indicated that stand structural diversity, plant diversity, and plant abundance were much greater in these partially cut stands than in young-growth stands developing after clearcutting (Deal 2001, Deal and Tappeiner 2002). Recent forest-management plans have prescribed forest practices using a variety of silvicultural systems including even-aged, two-aged, and uneven-aged management (TLMP 1997), even though there is little information available on their silvicultural or ecological effects. A large scale alternatives-to-clearcutting (ATC) study has been established in the region (McClellan et al. 2000) to assess the long-term effects of experimentally manipulated forests but it will be many years before results are available.

There is increasing interest in developing forest-management practices that maintain or enhance biodiversity and assure long-term sustainability of forest products, wildlife, and aquatic resources. Some major silvicultural concerns with the use of partial cutting (and highgrading of forests) have been previously reported in southeast Alaska (Harris and Farr 1974). However, most of these concerns are speculative or based on research done in other regions. In this paper I assess the effects of partial cutting in 18 stands throughout southeast Alaska and evaluate the following concerns with partial cutting:

- partial cutting will cause changes in tree species composition and loss of Sitka spruce
- trees left after partial cutting will be of low vigor with poor growth
- partial cutting will lead to significant increases in tree mortality

METHODS

Study Areas and Site Selection

Eighteen partially-harvested sites were selected to sample a range of time-since-cutting and intensity of cutting throughout southeast Alaska (Figure 1) using the following criteria: a) range of time-since-cutting from 10–100 years ago; b) only one partial cutting; c) a wide range of cutting intensities at each site, including an uncut area; and d) uniform topography, soils, and forest type. At each site

Figure 1. The 18 study sites in southeast Alaska. See Table 1 for definitions of the site codes.

I located an uncut control and generally three partially cut areas (light, medium, and heavy) and installed 0.2 ha plots in each cutting intensity area with a total of 73 0.2-ha overstory plots installed in 18 stands (Table 1).

Stand Structure and Growth

In each plot, tree species, DBH, height, and crown class was recorded for all live trees with a DBH greater than 2.5 cm (1.3 m). Species, DBH, and decay class were recorded for each snag to characterize current stand structure. On each plot, I reconstructed basal area of cut trees from stump diameter and took increment cores from 10–20 trees of each tree species and crown class to determine tree age, basal area growth, and cutting date for each stand. I reconstructed stand structure, basal area, species composition, and cutting intensity for each plot from this information (see section below on stand reconstruction methodology and Table 1). Differences in tree species composition, tree-age cohorts, and stand growth were assessed among cut and uncut plots (Deal and Tappeiner 2002). Tree radial growth increments were used to investigate the effects of partial cutting on the growth of hemlock and spruce trees, and the size and growth of new and residual trees (new trees include new regeneration and trees shorter than 1.3 m at time-of-cutting, and residual trees were at least 1.3 m tall at date of cutting).

Tree Wounding and Tree Mortality

For each dead tree with a DBH greater than 25 cm, DBH, species, decay class and status (uprooted, standing dead, or broken bole) were recorded. Snag and log decay classes and estimated time since death for hemlock and spruce are reported elsewhere (Hennon et al. 2002). Only trees that were determined to have died after partial cutting were used in reconstructing tree mortality. Analysis of variance with site as a blocking independent variable was used to test for differences in the incidence of tree wounding and mortality between uncut and cut plots. Regression analysis tested for correlation between these variables and the intensity of cutting, (i.e., percent basal area removed). Tests were conducted for both understory and overstory trees.

Stand Reconstruction Methodology

Tree increment cores and stem sections were measured in the laboratory. Cores were mounted on grooved boards with rings vertically aligned to provide the best resolution of tree-ring boundaries. Cores and stem sections were sanded, and tree rings were measured under a dissection

Table 1—Descriptions of research sites listed from the oldest to the most recently cut site. Cutting intensity data show the range for the partially cut plots at each site. The current stand data include the range of both uncut and cut plots at each site. The forest type is the major overstory tree species at each site.

Research Site	Cutting Intensity				Current Stand[a] Composition					
	Cutting Date (year)	Cut (%)	Basal Area		Basal Area (m^2 ha^{-1})	All Trees (trees ha^{-1})	Picea (%)	Tsuga (%)	Other[b] (%)	Forest Type
			Cut (m^2 ha^{-1})	Left (m^2 ha^{-1})						
WC - Weasel Cove	1900	17-51	9-23	22-45	53-75	450-1220	0-24	67-100	0-17	*Picea sitchensis*
GP - Glass Peninsula	1911	23-69	15-41	17-47	60-84	147-397	11-34	28-83	0-49	*Picea sitchensis*
FB - Florence Bay	1914	50-57	33-38	26-38	56-83	120-360	18-75	25-82	0	*Picea sitchensis*
PB - Portage Bay	1918	26-65	7-28	14-25	47-56	459-1202	5-33	67-95	0	*Tsuga heterophylla*
KL - Kutlaku Lake	1920	31-63	17-31	18-37	58-139	305-525	5-49	35-95	0-16	*Picea sitchensis*
HB - Hanus Bay	1922	49-96	24-85	3-25	56-83	413-1180	6-62	38-94	0	*Picea sitchensis*
SK - Sarkar	1925	27-59	14-28	19-37	57-76	467-1163	0-11	89-100	0	*Tsuga heterophylla*
EP – Elf Point	1927	17-73	12-36	13-57	42-116	453-1443	2-4	72-96	0-24	*Tsuga heterophylla*
CP - Canoe Passage	1927	16-75	9-57	19-46	44-66	815-2452	2-13	74-92	6-19	*Tsuga heterophylla*
SB - Salt Lake Bay	1928	48-55	28-35	29-31	63-87	158-642	17-73	27-83	0	*Picea sitchensis*
WH - Winter Harbor	1932	24-38	19-39	56-70	73-95	785-1311	2-33	67-98	0	*Picea sitchensis*
FC - Finger Creek	1941	18-41	11-33	44-51	58-75	331-522	5-60	40-95	0	*Tsuga heterophylla*
RF - Rainbow Falls	1942	34-61	15-25	16-29	44-66	348-1108	0-28	63-100	0-10	*Picea sitchensis*
MB - Margarita Bay	1958	23-83	9-48	10-30	41-63	694-2695	4-24	76-96	0	*Tsuga heterophylla*
BB - Big Bear Creek	1958	17-36	9-27	47-63	53-79	270-754	15-47	53-85	0	*Picea sitchensis*
PV - Pavlof River	1977	36-58	21-43	31-47	37-69	288-823	4-29	42-96	0-46	*Picea sitchensis*
GR -Granite	1983	18-86	9-51	9-50	13-70	368-1440	0-7	93-100	0	*Tsuga heterophylla*
TB - Thomas Bay	1984	20-29	18-19	42-77	49-70	237-766	1-17	83-99	0	*Tsuga heterophylla*

[a] Stand data for trees and basal area includes all trees that are at least 2.5 cm DBH

[b] The other minor species include western red-cedar (*Thuja plicata* Donn ex D. Don), yellow-cedar (*Chamaecyparis nootkatensis* (D. Don) Spach), red alder (*Alnus rubra* Bong.), and mountain hemlock (*Tsuga mertensiana* (Bong.) Carr.).

microscope using the methods of Swetnam et al. (1985). Each tree's radial growth since time-of-cutting was calculated. Tree DBH at time-of-cutting was determined by using radial-width adjustment equations for off-center cores and species-specific bark thickness equations (Deal 1999).

The date-of-cutting was determined by using tree-radial growth analyses (Lutz 1928, Henry and Swan 1974, Oliver 1982, Lorimer 1985, Bailey and Tappeiner 1998) and verified by historical data if available. Patterns of tree release indicating an abrupt and sustained increase in growth for at least 10 consecutive years averaging at least 50–100 percent greater than the previous 10 years (Lorimer et al. 1988) were used to determine the cutting date. Nine of the twelve stands with historical records matched cutting dates within ± 1 year of the cutting date determined from increase in tree radial growth.

I developed stem-taper equations to predict tree DBH from the stump diameter, by using forward stepwise regression analysis (Snedecor and Cochran 1980). The tree DBH and basal area of each stump was used to determine the amount of basal area cut for each plot. The diameter at time-of-cutting of current live trees was determined by using increment cores and stem sections from 986 western hemlock, Sitka spruce, western red-cedar (*Thuja plicata* Donn ex D. Don), and yellow-cedar trees (*Chamaecyparis nootkatensis* (D. Don) Spach). I developed site-specific regression equations to predict DBH at time of cutting for all trees, relating DBH at time of cutting to current tree DBH, basal area, species, and plot cutting intensity (Deal and Tappeiner 2002). These equations ($p < 0.001$) explained 77–99 percent of the variation in tree DBH at time-of-cutting (Table 2). The basal area of all trees at time-of-cutting was multiplied by the appropriate plot-expansion factor to determine stand basal area per hectare for each plot at time-of-cutting.

I used snag class and snag age data to determine the snag DBH at cutting date, and then estimated stand mortality since cutting. Each snag was assigned a decay class, and an average age for each decay class was determined (Hennon et al. 1990, 2002, Table 3). The DBH for snags at the date-of-cutting were predicted using the live tree regression equations and growth calculated for the period of time snags were alive. Periodic basal-area mortality per hectare was estimated for each plot.

I determined the proportion of stand basal-area cut (P%CUT) for each plot from:

P%CUT = [CUTBA/(RESBA + CUTBA + MORTBA)]*100

$$(1)$$

where CUTBA is the stand basal area cut, RESBA is the live-tree stand basal area at cutting date, and MORTBA is the periodic stand basal-area mortality since the cutting date. I then used the proportion of stand basal area cut as a continuous variable in regression analyses to analyze changes in tree species composition, tree-age cohorts, growth of tree-diameter, and stand basal-area growth since cutting.

Table 2—Regression models with regression R^2, MSE, and P for tree DBH at the cutting date for stands at 18 research sites.

Dependent variable	n	B_0	B_1	X_1	B_2	X_2	B_3	X_3	B_4	X_4	R^2	MSE
Tree DBH (mm) at cutting date												
Thomas Bay	39	9.1389	0.8955	DBH	-15.9034	TRMT	0.000066	DBH^2			0.9964	26.5359
Granite	31	-25.9198	0.9950	DBH	-14.3791	TRMT					0.9904	33.3668
Pavlof River	65	-49.5589	0.9829	DBH							0.9932	30.9784
Big Bear Creek	55	-1.1164	0.8715	DBH	-18.5378	TRMT	0.00005	DBH^2			0.9859	46.2153
Margarita Bay	60	87.9575	0.3145	DBH	-55.4578	TRMT	0.00051	DBH^2			0.8442	78.2703
Rainbow Falls	42	168.731	0.00044	DBH^2	-63.4244	TRMT	-96.1845	SPEC	0.3127	DBH	0.9031	100.775
Finger Creek	62	64.5816	0.00034	DBH^2	0.4176	DBH	-73.4940	SPEC			0.9062	92.4447
Winter Harbor	53	-62.9720	0.8104	DBH	0.000074	DBH^2					0.9667	80.1479
Salt Lake Bay	62	109.198	0.00034	DBH^2	-34.7033	TRMT	-72.5692	SPEC	0.3798	DBH	0.9111	103.593
Canoe Passage	64	14.2886	0.00094	DBH^2	-23.6187	TRMT					0.8958	98.6757
Elf Point	61	-276.472	0.00047	DBH^2	-60.2159	TRMT	82.3128	ln(DBH)			0.8517	125.299
Sarkar	45	167.7315	0.8323	DBH	-114.774	TRMT	-114.499	SPEC			0.8757	133.490
Hanus Bay	49	191.108	0.00056	DBH^2	-61.2362	TRMT	-94.5875	SPEC			0.8345	145.447
Kutlaku Lake	54	1968.728	1.4432	DBH	-69.3543	SPEC	-74.1878	TRMT	-383.626	ln(DBH)	0.8616	181.251
Portage Bay	64	-93.3010	0.7059	DBH	0.00015	DBH^2					0.9091	96.0436
Florence Bay	60	353.259	0.00055	DBH^2	-90.3223	TRMT	-136.677	SPEC			0.8173	148.229
Glass Peninsula	54	-85.8333	0.8576	DBH	-61.5255	TRMT	-43.6595	SPEC			0.8124	187.423
Weasel Cove	63	111.536	0.00070	DBH^2	-47.8378	TRMT					0.7733	132.780

Note: n is the number of observations; B_0 is the intercept and B_1-B_4 are slope coefficients of the regression line; R^2 is adjusted coefficient of determination; MSE is mean square error; P is the probability value; DBH is current tree diameter breast height (1.3 m); SPEC is tree species; and TRMT is intensity of cutting.

RESULTS AND DISCUSSION

Tree Species Composition

Partial cutting had little effect on current tree species composition. We found no significant difference between cut and uncut plots in the proportion of either western hemlock trees or Sitka spruce trees. The proportion of Sitka spruce trees averaged 17.5 percent in the cut plots and 15.2 percent in the uncut plots. The proportion of spruce trees and basal area increased slightly with increasing cutting intensity, but cutting intensity explained only 3–5 percent of the variation in tree-species proportion. We found no significant relation between cutting intensity and the proportion of either spruce or hemlock trees or the proportion of spruce and hemlock basal area.

The results of this study show that the establishment of new regeneration and the growth of large, uncut trees of both hemlock and spruce can maintain species composition similar to that of study plots before cutting. New regeneration was generally plentiful on cut plots, most new trees were hemlock, and cutting more than 50 percent of the stand basal area always led to the establishment of new regeneration (Deal and Tappeiner 2002). New cohort spruce trees were found on 44 percent of the cut plots and on only 11 percent of the uncut plots. These results indicate that partial cutting can generally help establish tree regeneration, and, in contrast to other opinions (Andersen 1955), spruce will regenerate after partial cutting. Our results indicate that silvicultural systems using partial cutting can be successfully applied to maintain spruce in mixed western hemlock-Sitka spruce forests in southeast Alaska.

Stand Structure and Growth

Most trees cut were large-diameter spruce trees, and more residual hemlock than residual spruce trees were left in almost all plots. However, after cutting, there were usually some large trees left in the stand. The number of trees left after cutting in diameter class L-(>100 cm), M-(71-100 cm), and S-(41-70 cm) averaged 7, 14 and 43 trees ha^{-1}, respectively (Figure 2). Before cutting, an average of 18, 32 and 64 trees ha^{-1} were in these diameter classes, and we found significant differences ($p < 0.005$) between stands before and after cutting in the number of L-,M-, and S-class trees. After 60 years, however, the number of trees in these size classes was similar to the stands before cutting, with an average of 16, 29 and 81 trees ha^{-1} in the L-, M-, and S-classes, respectively (Figure 2). The current stands had slightly more trees in class S (+17 trees ha^{-1}) and slightly fewer trees in M (-3 trees ha^{-1})

Table 3—Snag decay classes for Sitka spruce (*Picea sitchensis* **(Bong.) Carr.), western hemlock (***Tsuga heterophylla* **(Raf.) Sarg.), western red-cedar (***Thuja plicata* **Donn ex D. Don), and yellow-cedar (***Chamaecyparis nootkatensis* **(D. Don) Spach).**

	Picea sitchensis[1] and *Tsuga heterophylla*[1]	*Thuja plicata*[2] and *Chamaecyparis nootkatensis*[2]
Class 1	Some twigs retained; most bark intact; logs with little outer decay	Some twigs retained; most bark intact; logs with little outer decay
Age	10 years (range 0-12)	14 years (range NA)
Class 2	Twigs gone, long primary branches and some secondary branches retained; bark beginning to slough; top usually broken; sapwood decaying	Twigs gone, long primary branches and some secondary branches retained; bark beginning to slough; top usually intact; sapwood decaying
Age	20 years (range 12-33)	26 years (range NA)
Class 3	Secondary branches gone, but short primaries or stubs present; height decreasing; most bark gone; logs decaying but can support themselves	Primary branches retained; top usually Intact; bark mainly gone; sapwood decaying, heartwood sound but beginning to check
Age	50 years (range 33-63)	51 years (range 27-96)
Class 4	Branch stubs mainly gone; height decreasing; most bark gone; considerable decay of heartwood at base; logs slumping and colonized by moss or other vegetation	Primary branches mainly gone; bole usually intact coming to point; surface deeply checked, bark and sapwood mainly gone
Age	80 years (range 63-117)	81 years (range 49-128)
Class 5	Broken stumplike appearance; top portion with branch stubs gone; bark almost completely gone; wood decaying and sloughing away; colonized by vegetation; log cannot support itself, becoming oval as slumps into forest	Bole broken often with jagged top; downed portion covered by vegetation or unrecognizable
Age	100+ years	100+ years

[1] From Hennon et al. (2002).
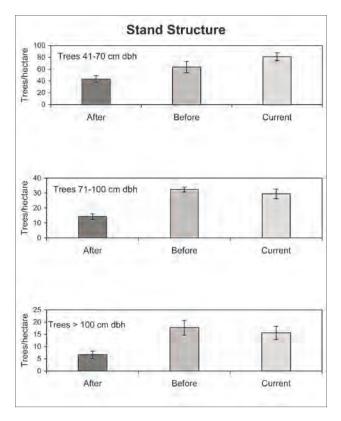[2] From Hennon et al. (1990).

Figure 2. The number of trees per hectare by size class in the partially cut plots immediately after and before cutting, and in the current stand 60 years after cutting. Vertical bars indicate standard errors.

and L (-3 trees ha^{-1}) classes than the stands before cutting, but no significant differences were found in the frequency of trees for any diameter class.

Sitka spruce diameter growth was slightly greater than western hemlock growth for all tree-diameter classes, but growth differences between species were not statistically significant (p > 0.05) for any diameter class. Residual trees of both species in all size classes increased diameter growth after cutting. The current stand basal area, tree species composition, and stand growth for all cutting intensities was strongly related to trees left after harvest. These results are contrary to conventional thinking about partial cutting in southeast Alaska where residual trees are assumed to be of poor quality and low vigor. In this study, we found that these small advance regeneration and larger residual trees responded with rapid and sustained growth after overstory removal and became a major part of the current stand.

Tree Wounding and Mortality

Overstory trees had significantly greater incidence of wounding (p = 0.04) in cut than uncut plots and wounding increased with intensity of cutting (p = 0.03). Many

wounds could not be attributed to logging, however, as falling trees and porcupine damage were other causal factors on some sites.

For trees of all sizes, mortality was not significantly different between cut or uncut plots. However, estimating mortality over time is the most difficult piece of stand reconstruction and the wide ranges in average age of snags highlights the difficulty of accurately estimating stand mortality (Table 3). The reported average age of snag classes includes a considerable amount of variation and these snag classes provide only a rough estimate of stand mortality. Another concern in partially harvested stands is windthrow and the fate of large residual trees is of particular interest. In this study, the percentage of dead, large residual trees in cut plots (27 percent) was not significantly different than in uncut plots (22 percent). Of large residual trees that died, an average of 37 percent and 28 percent, respectively, died through uprooting in partially cut and uncut plots; the remainder died standing or by bole breakage. Windthrow did not significantly increase after partial cutting; indeed, mortality of residual trees was only marginally higher in partially cut than in uncut stands. For residual trees that died, the higher rate of uprooting associated with cutting does suggest that wind has an increased role in tree death. Thus, our results may underestimate the severity of wind-damage risk in some landscape settings. Managers concerned about windthrow should consider wind exposure (Kramer et al. 2001) when designing partial cutting treatments.

CONCLUSION

The stands reported here were cut to provide specific wood products and cutting occurred without a planned silvicultural system. Little effort was taken to ensure spruce regeneration, encourage stand growth, control or reduce tree damage agents, or maintain the complex stand structures found in old-growth forests. Nevertheless, Sitka spruce was maintained in these stands and greatly reduced stand growth did not occur. There were not large changes in tree species composition, greatly reduced diameter growth and vigor, or higher incidence of tree wounding, decay, and windthrow-mortality with partial cuts. Stand structural diversity and plant diversity and abundance were much greater in partially- cut stands than in young-growth stands developing after clearcutting. These results indicate that new silvicultural systems that use partial cutting could alleviate some of the problems associated with conventional

clearcutting in southeast Alaska while also providing a sustainable timber resource.

LITERATURE CITED

Alaback, P.B., 1982. Dynamics of understory biomass in Sitka spruce-western hemlock forests of southeast Alaska. Ecology 63: 1932-1948.

Alaback, P.B., 1984. A comparison of old-growth forest structure in the western hemlock-Sitka spruce forests of southeast Alaska. In: Fish and Wildlife Relationships in Old-Growth Forests. Meehan, W.R., Merrell, T.R.J., Hanley, T.A. (Eds.), American Institute of Fishery Research Biologists, Morehead City, NC. pp. 219-226.

Alaback, P.B.; Juday, G.P. 1989. Structure and composition of low elevation old-growth forests in research natural areas of southeast Alaska. Natural Areas Journal 9: 27-39.

Andersen, H.E. 1955. Clearcutting as a silvicultural system in converting old forests to new in southeast Alaska. Society of American Foresters Proceedings 1955: 59-61.

Bailey, J.D.; Tappeiner, J.C. 1998. Effects of thinning on structural development in 40- to 100-year-old Douglas-fir stands in western Oregon. Forest Ecology Management 108: 99-113.

Deal, R.L. 1999. The Effects of Partial Cutting on Stand Structure and Growth, and Forest Plant Communities of Western Hemlock-Sitka Spruce Stands in Southeast Alaska. Ph.D. Thesis. Oregon State University, Corvallis, OR. 191 p.

Deal, R.L. 2001. The effects of partial cutting on forest plant communities of western hemlock-Sitka spruce stands of southeast Alaska. Canadian Journal of Forest Resources 31: 2067-2079.

Deal, R.L.; Farr, W.A. 1994. Composition and development of conifer regeneration in thinned and unthinned natural stands of western hemlock and Sitka spruce in southeast Alaska. Canadian Journal of Forest Resources 24 (5): 976–984.

Deal, R.L.; Oliver, C.D.; Bormann, B.T. 1991. Reconstruction of mixed hemlock-spruce stands in coastal southeast Alaska. Canadian Journal of Forest Resources 21: 643-654.

Deal, R.L.; Tappeiner, J.C. 2002. The effects of partial cutting on stand structure and growth of western hemlock-Sitka spruce stands in southeast Alaska. Forest Ecology Management 159 (3): 173-186.

Franklin, J.F.; Cromack, K.J.; Denison, W. [et al.]. 1981. Ecological characteristics of old-growth Douglas-fir forests. Gen. Tech. Rep. PNW-GTR-118. USDA Forest Service, Pacific Northwest Research Station, Portland, Oregon. 48 p.

Franklin, J.F.; Spies, T.A. 1991. Composition, function, and structure of old-growth Douglas-fir forests. In: Ruggiero, L.F., Aubry, K.B., Carey A.B., Huff, M.H., eds. Wildlife and vegetation of unmanaged Douglas-fir forests. Gen. Tech. Rep. PNW-GTR-421. USDA Forest Service, Pacific Northwest Research Station, Portland, Oregon. 25p.

Harris, A.S.; Farr, W.A. 1974. The Forest Ecosystem of Southeast Alaska, 7: Forest Ecology and Timber Management. Gen. Tech. Rep. PNW-GTR-25. USDA Forest Service, Pacific Northwest Research Station, Portland, Oregon. 109 pp

Hennon, P.E.; Hansen, E.M.; Shaw, C.G. III. 1990. Causes of basal scars on *Chamaecyparis nootkatensis* in southeast Alaska. Northwest Science 64: 45-54.

Hennon, P.E.; McClellan, M.H. 2003. Tree mortality and forest structure in temperate rain forests of southeast Alaska. Canadian Journal of Forest Resources 33: 1621-1634.

Hennon, P.E.; McClellan, M.H.; Palkovic, P. 2002. Comparing deterioration and ecosystem function of decay-resistant and decay-susceptible species of dead trees. Gen. Tech. Rep. PSW-GTR-25. USDA Forest Service, Pacific Southwest Research Station, Albany, CA. pp. 435-443.

Henry, J.D.; Swan, J.M.A. 1974. Reconstructing forest history from live and dead plant material—an approach to the study of forest succession in southwest New Hampshire. Ecology 55: 772-783.

Hutchison, O.K. 1967. Alaska's forest resource. Res. Bull. PNW-19. USDA Forest Service, Pacific Northwest Research Station, Portland, Oregon. 74pp.

Kramer, M.G.; Hansen, A.J.; Taper, M.L.; Kissinger, E.J. 2001. Abiotic controls on long-term windthrow disturbance and temperate rain forest dynamics in southeast Alaska. Ecology 82: 2749-2768.

Lorimer, C.G. 1985. Methodological considerations in the analysis of forest disturbance history. Canadian Journal of Forest Resources 15: 200-213.

Lorimer, C.G.; Frelich, L.E.; Nordheim, E.V. 1988. Estimating gap origin probabilities for canopy trees. Ecology 69: 778-785.

Lutz, H.J. 1928. Trends and Silvicultural Significance of Upland Forest Successions in Southern New England. Environmental Studies Bulletin 22. Yale University School of Forestry, New Haven, CT. 68 p.

McClellan, M.H.; Swanston, D.N.; Hennon, P.E. [et al.]. 2000. Alternatives to clearcutting in the old-growth forests of southeast Alaska: study plan and establishment report. Gen. Tech. Rep. PNW-GTR-494. USDA Forest Service, Pacific Northwest Research Station, Portland, Oregon. 40p.

Oliver, C.D. 1982. Stand Development—Its Uses and Methods of Study. In: Means, J.E., ed., Forest Succession and Stand Development Research in the Northwest: Proceedings of the Symposium. Oregon State University, Forestry Research Laboratory, Corvallis, OR. pp. 100-112.

Snedecor, G.W.; Cochran, W.G. 1980. Statistical Methods, 7th ed. The Iowa State University Press, Ames, IA. 507 p.

Swetnam, T.W.; Thompson, M.A.; Sutherland, E.K. 1985. Spruce budworms Handbook: Using Dendrochronology to Measure Radial Growth of Defoliated Trees. Agricultural Handbook 639. USDA Forest Service, Cooperative State Research Service, Washington, DC. 39 p.

Tappeiner, J.C.; Alaback, P.B. 1989. Early establishment and vegetative growth of understory species in the western hemlock-Sitka spruce forests in southeast Alaska. Canadian Journal of Botany 67: 318-326.

Tongass Land Management Plan (TLMP) Record of Decision. 1997. Record of Decision for Tongass National Forest Land and Resource Management Plan Revision, Alaska. Alaska Region, R10-MB-338a. USDA Forest Service, Region 10, Juneau, AK. 44 pp.

Combining Tree- and Stand-Level Models: A New Prediction System to Improve Growth Prediction in Norway Spruce (*Picea abies*)

C. Yue, U. Kohnle, S. Hein

ABSTRACT

A NEW PREDICTION SYSTEM IS PRESENTED to improve the estimation of single tree diameter and stand basal area growth. The prediction system consists of three steps: prediction, combination, and modification. The prediction of stand basal area is based on a tree-level diameter growth model and a stand-level basal area growth model. A cumulative diameter-rate model is developed for the tree-level diameter growth model. The two models working at different levels are combined based on variance and covariance method. The combined estimator is further used to modify the two models (the tree-level as well as the stand-level model). In contrast to a straightforward linking approach (such as for disaggregation) the new prediction system works in a feedback process.

For the estimation of the annual growth model parameters from periodical measurements, a general loss function is introduced to counterbalance possible effects of irregular measurement intervals. Based on an independent validation data set, projections of stand basal area with the combined estimator gain in efficiency from 14–43 percent compared to projections with the tree-level model alone, and from 4–16 percent compared to projections with the stand-level model, depending on the temporal horizon of the projection (5–30 years).

C. Yue, U. Kohnle (presenter; ulrich.kohnle@forst.bwl.de) and **S. Hein** are researchers at the Forest Research Institute of Baden-Wuerttemberg, Freiburg, Germany.

The Use of Airborne LiDAR Data to Estimate the Relationship Between Crown Surface Area and Stem Surface Area of *Chamaecyparis obtusa* Stands

Tohru Nakajima, Yasumasa Hirata, Naoyuki Furuya, Katsutoshi Takezoe,
Makoto Suzuki, Satoshi Tatsuhara, Norihiko Shiraishi

ABSTRACT

IN THIS STUDY, WE CALCULATED the relationship between the average crown surface area and the stem surface area of dominant trees. The study site was the University of Tokyo Forest in Chiba. First, we estimated the crown surface area based on a digital surface model (DSM) and a digital elevation model (DEM) obtained from airborne light detection and ranging (LiDAR) data acquired on August 14, 2005. The region of interest (ROI) from which the data were extracted was 200 m wide and 1,700 m long. The airborne LiDAR data had a footprint diameter of 50 cm, a distance between neighboring footprints of 25 cm, and a laser pulse rate of 70,000 Hz. Next, we estimated the stem surface area based on ground survey data. We established seven circular plots in *Chamaecyparis obtusa* plantations and measured the diameter at breast height (DBH), and tree height in each plot. We applied a relative-crown curve and a relative-taper curve to these data, and estimated the average crown surface area and stem surface area of dominant trees. A linear regression between the crown surface area and stem surface area was carried out, resulting in a coefficient of determination of 0.97. This result showed a strong relationship between the average crown surface area and the stem surface area estimated from airborne LiDAR data and ground survey data.

KEYWORDS: Airborne LiDAR, *Chamaecyparis obtusa*, crown surface area, stem surface area

INTRODUCTION

A forest grows due to the photosynthesis of its trees. As previous studies have shown, the greater the respiration volume of trees, the less forest growth (Bosc et al. 2003, Arain and Restrepo-Coupe 2005). This suggests that one can predict forest growth based on the balance between the photosynthesis and respiration of trees.

The main parts of a tree involved in photosynthesis and respiration are the canopy and wood including the stems, branches, and roots, respectively. To estimate forest resources, one can collect direct, ground-based data on woodiness, such as the diameter at breast height (DBH) and the stem number. Various growth models have been developed based on stem information, including the tree height and DBH (Castedo-Dorado et al. 2007, Qin et al. 2007, Shiraishi 1986). However, it is difficult to measure a crown structure that is high and complex. It is even more difficult to measure crown information over a wide area. Chiba (2005) introduced crown-length information into a growth model for estimating the DBH and stem form.

Tohru Nakajima and **Katsutoshi Takezoe** are graduate students, **Satoshi Tatsuhara** is an associate professor and **Norihiko Shiraishi** is a professor in the Graduate School of Agricultural and Life Sciences, the University of Tokyo, 1-1-1 Yayoi, Bunkyo-ku, Tokyo 113-8657, Japan; **Yasumasa Hirata** is a group leader, Shikoku Research Center, Forestry and Forest Products Research Institute, 2-915 Asakuranishimachi, Kochi 780-8077, Japan; **Naoyuki Furuya** is a researcher, Forestry and Forest Products Research Institute, 1 Matsunosato, Tsukuba, Ibaraki 305-8687, Japan; **Makoto Suzuki** is a lecturer, University Forest in Chiba, Graduate School of Agricultural and Life Sciences, the University of Tokyo, 770 Amatsu, Kamogawa, Chiba 299-5503, Japan.

However, no growth models that include crown information have been developed for Japanese mountainous areas at the regional scale.

Previous studies have suggested the usefulness of remotely sensed data for measuring forest resources such as stand age (Farid et al. 2006), tree height (Hirata 2005, Takahashi et al. 2005, Næsset and Bjerknes 2001), and forest biomass (Labrecque et al. 2006). In addition, airborne light detection and ranging (LiDAR) data enable us to obtain a wide range of canopy information, including the leaf area (Roberts et al. 2005), canopy fuel (Andersen et al. 2005), and canopy structure (Coops et al. 2007) information. For a mountainous forest in Japan, where the terrain was very complex and steep, Nakajima et al. (2006) reported that the average crown length of dominant trees could be estimated using airborne LiDAR data.

As mentioned above, it is important to analyze the relationship between woody information and canopy information for developing a growth model that considers the balance of respiration and photosynthesis. However, few previous studies have analyzed the relationship of crown information estimated from LiDAR and woody information measured by a ground survey in Japan. The objective of our study was to estimate the relationship between the average crown surface area and the woody surface area of dominant trees using airborne LiDAR data. For calculating the crown surface area and stem surface area, we used the relative-crown curve reported by Kajihara (2000) and the relative-taper curve reported by Nagumo and Tanaka (1981), respectively. We then conducted a linear regression between the crown surface area and the stem surface area. Considering the balance of tree photosynthesis and respiration for development of the growth model, we discuss the relationship between the crown surface area and the stem surface area.

METHODS

Study Site

The study focused on *Chamaecyparis obtusa* plantation forests in the University of Tokyo Forest in Chiba, Japan. The University Forest in Chiba is located in the southeastern Boso Peninsula. The plantation forests are 824 ha in area, occupying 37 percent of the total forest area of 2,226 ha. Natural forests cover the rest of the forest area. The total stem volume of the University Forest is approximately 500,000 m^3. Of this stem volume, 300,000 m^3 is stocked
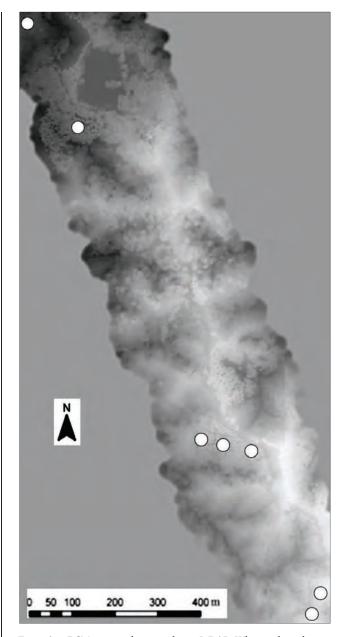
Figure 1— DSM measured using airborne LiDAR. White circles indicate the locations of sample plots used for ground surveys of Chamaecyparis obtusa stands.

in plantation forest and 200,000 m^3 is stocked in natural forest. The total annual growth volume is approximately 8,069 m^3, which converts to approximately 3.6 m^3 per ha. The average yearly temperature in this area is 13.8 degrees Celsius. The hottest month is August, with the average temperature of 24.2 degrees Celsius. The coldest months are January and February, in which the average temperature is 4.4 degrees Celsius. The altitude above sea level ranges from approximately 50 m to 370 m, and the terrain of the area is complex and precipitous for its altitude range.

Table 1. Sample plots used for ground surveys of *Chamaecyparis obtusa* **stands.**

Plot No.	Compartment	Subcompartment	Stand age	Stand density (stems ha⁻¹)
1	11	C1	68	450
10	20	C1	27	3925
11	20	C1	27	2350
14	4	C1	44	2025
21	11	D2	55	700
22	11	D2	55	700
23	11	D2	55	1475
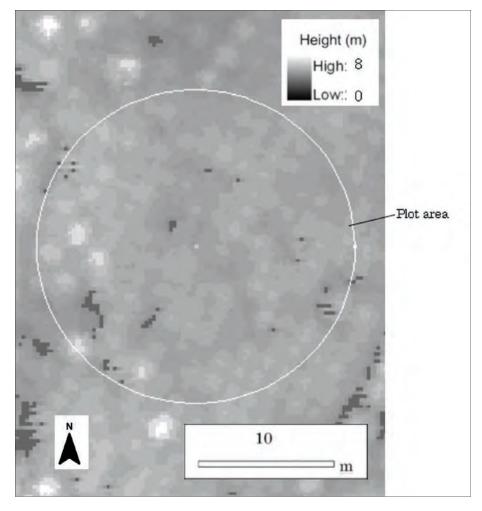
Figure 2— Enlarged view of airborne LiDAR data of Plot 10.

Data Collection

Airborne LiDAR data were acquired on August 14, 2005. The region of interest (ROI) from which the data were extracted was 200 m wide and 1,700 m long. The LiDAR data specifications were as follows; flying height, 500 m; speed, 70 km h⁻¹; footprint diameter, 50 cm; distance between neighboring footprints, 25 cm; and laser pulse rate, 70,000 Hz. We used a digital surface model (DSM) (Figure 1) and a digital elevation model (DEM) derived from the LiDAR data to extract information on the crowns of standing trees.

In the region covered by the LiDAR data, we established seven circular sample plots for ground surveys. These sample plots were approximately 22.6 m in diameter (0.04 ha) and were located in *Chamaecyparis obtusa* plantations of various stand densities. At least 450 stems ha⁻¹ were measured in each plot (Table 1). The central coordinates of each plot were found using a differential global positioning system (DGPS) receiver (ProMark2, Ashtech and Pathfinder ProXR, Trimble Navigation). The four highest trees in each plot were selected as the dominant trees, equivalent to 100 stems ha⁻¹ selected as dominant trees. The DBH of each standing tree in each plot was measured. The heights of more than 40 percent of all trees were measured using a Vertex III system (Haglöf), and were estimated for other trees using a Näslund height-diameter curve.

Data Analysis

Estimating the crown cross-sectional surface from LiDAR data—

The crown cross-sectional surface of the dominant trees was estimated from LiDAR data with TNTmips ver. 6.6 (MicroImages 2001). Using the DEM and DSM data, we estimated the crown cross-sectional surface of dominant trees in each plot. First, we selected four trees (100 stems ha⁻¹) as dominant trees. In this case, the dominant trees were the highest in each plot. Because the DSM includes the height above sea level, it is difficult to calculate the exact tree height from DSM data. Accurate tree height can be obtained from the digital crown model (DCM) calculated by

subtracting the DEM, i.e., the height above sea level, from the DSM. The tree height was defined as the height of the top of the tree derived from the DCM. Figure 2 shows that airborne LiDAR can identify the canopy of each individual tree. The four highest trees in each plot were selected as the dominant trees from the DCM and overlapped on the vector data from the DGPS for the circular plots.

Second, we estimated the crown cross-sectional surface.
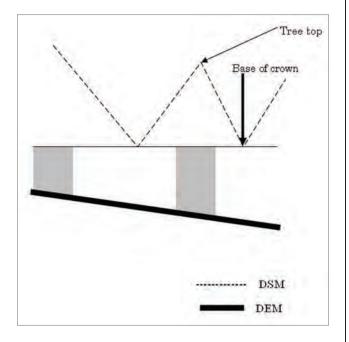
Figure 3— Position at which tree height was measured to determine the base of the crown. The base of the crown is indicated by a bold arrow.

The crown length of each tree was estimated by subtracting the height to the base of the crown from the total tree height. We measured the height to the base of the crown on the rebound point obtained from the DSM cross-sectional surface, because we considered the far side canopy from the rebound point to be the crown of the neighboring tree (Figure 3). The direction of the DSM cross-sectional surface was estimated from the average slope aspect derived from the DEM in each plot, because there is normally more space for branch and leaf expansion on the slope side of trees. Figure 4 shows an example of a cross-sectional surface of a dominant tree. We calculated the crown length, crown width, and width at approximately the middle point of the crown length for this figure. Nakajima et al. (2006) reported that the average crown length of dominant trees could be estimated accurately by airborne LiDAR data. Thus, we assumed that the crown widths of dominant trees could be estimated by LiDAR data without large differences from ground-truth measurements. These crown information data were used for estimating the crown surface area as follows.

Relationship Between the Crown and Stem Surface Areas

Finally, we obtained the relationship between the surface areas of the crown and stem using data derived from airborne LiDAR and the ground survey. In this study, we assumed that the stem surface and crown surface would be the main sites of respiration and photosynthesis, respec-
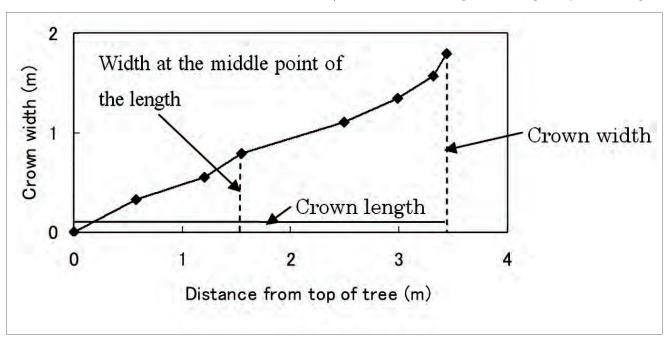
Figure 4—Example of the cross-sectional surface of a dominant tree.

tively. This assumption is based on suggestions by previous studies that photosynthesis activity is very high on the crown surface (Kajihara 2000). Bosc et al. (2003) reported that the surface area of wood has a stronger relationship with respiration than with woody volume. With this assumption, we calculated the crown surface area and stem surface area and estimated the relationship of the size of the average photosynthetic organ and woody organ of the dominant trees.

Calculation of the crown surface area—

In this procedure, we applied formula (1), the relative crown curve reported by Kajihara (2000), to the crown profile:

$$y = \frac{x}{a + bx}$$

(1)

where x: relative distance from the top of the tree (0 - 1.0)

  y: relative crown width (0 - 0.5)

  a, b: parameters

By definition, this curve passes the point (1, 0.5). Therefore, the relationship between parameter a and b is shown as formula (2):

$$a + b = 2$$

(2)

Formula (1) could be transformed into formula (3) through formula (2):

$$y = \frac{x}{a + (2 - a)x}$$

(3)

Formula (4) is the actual crown curve based on the relative crown curve, formula (3):

$$Y = \frac{DX}{aL + (2 - a)X}$$

(4)

where X: distance from the top of the tree (m)

  Y: width at distance X (m)

  D: crown width (m)

  L: crown length (m)

We estimated parameter a with formula (3), to which we assigned the coordinate value exchanged from the crown width and the distance from the top of the tree at the middle point of the crown derived from LiDAR data on the relative crown curve. By assigning parameter a to formula (4), we can derive the actual crown curve. The crown surface area is estimated with formula (5) showing the surface of the solid revolution of formula (4):

$$S_c = 2\pi \int_0^L Y \left\{ 1 + \left(\frac{dY}{dX} \right)^2 \right\}^{\frac{1}{2}} dX$$

(5)

where S_c: crown surface area (m^2)

We calculated the crown surface area by integrating formula (5) with Romberg quadrature. We applied these calculations to the four dominant trees in each plot and estimated the average crown surface area of the dominant trees.

Calculation of the stem surface area—

We calculated the stem surface area based on the tree height, DBH, observed during the ground survey, and the relative taper curve. We applied the relative taper curve estimated in the University Forest in Chiba (formula (6) as reported by Nagumo and Tanaka (1981)):

$$y_s = \alpha x + \beta x^2 + \gamma x^3$$

(6)

Where y_s: relative stem radius (0 - 0.5)

  a, β, γ: parameters

Formula (7) is the actual taper curve based on the relative taper-curve, formula (6):

$$Y_s = \frac{D_s \left(\dfrac{\alpha X}{H} + \dfrac{\beta X^2}{H^2} + \dfrac{\gamma X^3}{H^3} \right)}{\alpha \left(1 - \dfrac{1.3}{H} \right) + \beta \left(1 - \dfrac{1.3}{H} \right)^2 + \gamma \left(1 - \dfrac{1.3}{H} \right)^3}$$

(7)

where Y_s: stem radius (m)

  D_s: radius at breast height (1.3m)

  H: tree height (m)

The stem surface area is estimated with formula (8) showing the surface of the solid revolution of formula (7):

$$S_s = 2\pi \int_0^H Y_s \left\{ 1 + \left(\frac{dY_s}{dX} \right)^2 \right\}^{\frac{1}{2}} dX$$

(8)

where S_s: stem surface area (m^2)

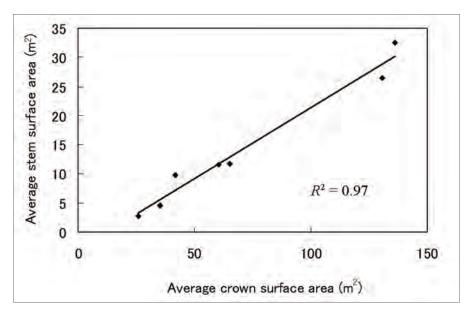 We calculated the stem surface area by integrating

Figure 5—The crown surface area obtained from airborne LiDAR data versus the stem surface area estimated by ground survey data.

formula (8) with Romberg quadrature. The average stem surface area is the average value of the stem surface areas of the four dominant trees. The stem surface areas based on ground survey data were regressed against the crown surface areas based on airborne LiDAR data. We then calculated the coefficient of determination. This result and the relationship between the average crown surface area and average stem surface area are discussed below.

RESULTS AND DISCUSSION

The relationship between the average stem surface area and the crown surface area of the dominant trees can be seen in Figure 5. The constant term and slope of the regression line were 0.2442 and -3.0999, respectively. As shown in this figure, the average stem surface area per tree was smaller than the crown surface area per tree. The coefficient of determination was 0.97. This result suggests a very strong correlation between the average stem surface area and the crown surface area of dominant trees. This finding is also consistent with those of previous studies, which found that in general, the greater the respiration volume, the more photosynthesis is required (Arain and Restrepo-Coupe 2005). In this study, we established sample plots in plantations with various stand densities. Figure 5 shows the strong relationship between the crown and stem surface area for various stand densities. These plots established in *Chamaecyparis obtusa* stands have been regularly managed

by staff of the University Forest in Chiba in an integrated fashion based on standard density control measures (Shiraishi 1986). Thus, the relationship between the crown surface area and the stem surface area had been controlled throughout various stand densities at the management unit level. This could be one of the reasons for the very high coefficient of determination even though the plots included stands of various densities. However, the dominant trees were not suppressed by other trees because the tops of these trees were relatively high. This situation could also account for the very strong relationship between the average crown surface area and the stem surface area of the dominant trees throughout low- and high-density stands. This observation will be verified in a further case study in another experimental forest belonging to the University of Tokyo managed under the standard density control.

In our study, we estimated the crown length by the DSM obtained from the first pulse. The first pulse reflected against the sunlit canopy does not include information on the shaded portion of the canopy, where sunlight is blocked by other tree branches. In other words, Figure 5 suggests a strong relationship between the sunlit crown surface area and the stem surface area. This result is also consistent with previous reports that the shaded canopy does not contribute to tree growth (Kajihara 1985).

Note that we considered only the stem surface area as the main contributor to respiration. However, a tree respires not only on the surface of its stem but also on the surface of its branches and roots. Thus, to obtain an accurate estimation of the relationship between photosynthesis and respiration, we should compare the crown surface area with the sum of the surface area of stems, branches, and roots. If the surface area of the stems, branches, and roots were summed up, the graph of the figure would move upward, and the regression line would pass closer to the coordinate origin. If this were the case, the rate of the crown surface area to the total surface area of stems, branches, and roots could be more constant.

Another general relationship is that the larger the crown,

the larger the branches and roots (Fukuda et al. 2003). If the branch and root surface areas are added to the stem surface area, the increase in the upper-right side value in Figure 5 is larger than that of the lower-left side value. Thus, if we plot the total stem, branch, and root surface area and the crown surface area on the figure, the slope of the regression line would become steeper.

CONCLUSIONS

In this study, we estimated the relationship between the average crown surface area and the stem surface area of dominant trees in *Chamaecyparis obtusa* stands. First, we estimated the crown surface area based on a DSM and DEM obtained from airborne LiDAR data. In this procedure, the relative crown curve was applied to these LiDAR-derived data. Second, we estimated the stem surface area based on ground survey data such as the DBH and tree height. The relative taper curve was applied to these ground-survey data in this procedure. Finally, a linear regression between the crown surface area and the stem surface area was carried out, resulting in a coefficient of determination of 0.97. The results of our study suggest a strong relationship between the average sunlit crown and stem surface area.

The next challenge is estimating the branch and root surface area in more plots and developing a growth model to consider the relationship between the crown surface area and the surface areas of stems, branches, and roots.

ACKNOWLEDGMENTS

LITERATURE CITED

Andersen, H.E.; McGaughey, R.J.; Reutebuch, S.E. 2005. Estimating forest canopy fuel parameters using LIDAR data. Remote Sensing of Environment 94: 441-449.

Arain, M.A.; Restrepo-Coupe, N. 2005. Net ecosystem production in a temperate pine plantation in southeastern Canada. Agricultural and Forest Meteorology 128: 223-241.

Bosc, A.; De Grandcourt, A.; Loustau, D. 2003. Variability of stem and branch maintenance respiration in a *Pinus pinaster* tree. Tree Physiology 23: 227-236.

Castedo-Dorado, F.; Dieguez-Aranda, U.; Alvarez-Gonzalez, J.G.; 2007. A growth model for *Pinus radiata* D. Don stands in north-western Spain. Annuals of Forest Science 64: 453-465.

Chiba, Y. 2005. Changing crown and stem form as related to thinning regime. Kanto Japanese Forest Research 56: 151-154. (in Japanese)

Coops, N.C.; Hilker, T.; Wulder, M.A. [et al.]. 2007. Estimating canopy structure of Douglas-fir forest stands from discrete-return LiDAR. Trees—Structure and Function 21: 295-310.

Farid, A.; Goodrich, D.C.; Sorooshian, S. 2006. Using airborne lidar to discern age classes of cottonwood trees in a riparian area. Western Journal of Applied Forestry 21: 149-158.

Fukuda, M.; Iehara, T.; Matsumoto, M. 2003. Carbon stock estimates for sugi and hinoki forests in Japan. Forest Ecology and Managemen*t* 184: 1-16.

Hirata, Y. 2005. Relationship between tree height and topography in a *Chamaecyparis obtusa* stand derived from airborne laser scanner data. Journal of Japanese Forestry Society 87: 497-503. (in Japanese with English summary)

Kajihara, M. 1985. Estimation of stem-volume increment by using sunny crown-surface area and stem-surface area. Journal of Japanese Forestry Society 67: 501-505. (in Japanese with English summary)

Kajihara, M. 2000. The stem growth and form viewed in canopy information. Tokyo: Japanese Society of Forest Planning Press. 139 p. (in Japanese)

Labrecque, S.; Fournier, R.A.; Luther, J.E.; Piercey, D. 2006. A comparison of four methods to map biomass from Landsat—TM and inventory data in western Newfoundland. Forest Ecology and Management 226: 129-144.

MicroImages, Inc. 2001. TNTmips ver.6.6. Lincoln, NE, USA.

Næsset, E.; Bjerknes, K.-O. 2001. Estimating tree heights and number of stems in young forest stands using airborne laser scanner data. Remote Sensing of Environment 78: 328-340.

Nagumo, H.; Tanaka, M. 1981. Construction of a volume table with a relative stem-curve. Journal of Japanese Forestry Society 63: 278-286. (in Japanese with English summary)

Nakajima, T.; Hirata, Y.; Furuya, N. 2006. Developing methodology for estimating canopy information by LiDAR. Proceedings of the International Conference Silvilaser 2006: 249.

Qin, J.; Cao, Q.V.; Blouin, D.C. 2007. Projection of a diameter distribution through time. Canadian Journal of Forest Research 37:188-194.

Roberts, S.D.; Dean, T.J.; Evans, D.L. [et al.]. 2005. Estimating individual tree leaf area in loblolly pine plantations using LiDAR-derived measurements of height and crown dimensions. Forest Ecology and Management 213:54-70.

Shiraishi, N. 1986. Study on the growth prediction of even-aged stands. Bulletin of the Tokyo University Forests 75:199-256.

Takahashi, T.; Yamamoto, K.; Senda, Y.; Tsuzuki, M. 2005. Estimating individual tree heights of sugi (*Cryptomeria japonica* D. Don) plantations in mountainous areas using small-footprint airborne LiDAR. Journal of Forest Research 10:135-142.

Evaluation of an Ecosystem-Based Approach to Mixedwood Modeling

B. Seely, C. Hawkins, J.A. Blanco, C. Welham, J.P. Kimmins

EXTENDED ABSTRACT

KEYWORDS: FORECAST, mixedwood management, model testing, process-based model, resource competition

INTRODUCTION

MIXED CONIFER-BROADLEAF FORESTS (mixedwoods), covering more than a third of the productive forest landbase in British Columbia, are highly valuable both as sources of fiber and as areas rich in biodiversity. Historically, these forest types have been managed as single-species stands with herbicide and manual brushing treatments employed to promote conifer plantations (Comeau et al. 2000, Harper and Kabzems 2003). More recently, the benefits of retaining and managing for intimate mixtures of conifers and hardwoods have been recognized (Grover and Greenway 1999) and management paradigms have transitioned from a focus on promoting conifer plantations in mixedwood areas to the management of intimate mixtures. Research with respect to the production ecology of mixedwood ecosystems has illustrated that mixtures of conifers and broadleaf species can be more productive than pure stands (Man and Lieffers 1999) and that reasonably good conifer growth can be maintained in intimate mixtures if steps are taken to reduce broadleaf competition (Simard and Hannam 2000, Simard et al. 2004, Comeau et al. 2000). Explanations for these findings have focused on the differential utilization of resources by broadleaves and conifers (light, nutrients, and water) (Man and Lieffers 1999), the positive impacts of broadleaf species on nutrient cycling rates (Comeau 1996, Cote et al. 2000) and shared mycorrhizal networks (Simard et al. 1997).

The dynamic nature of mixedwood forests presents a number of management challenges, not the least of which is how best to project their growth and development under different management systems. One model that utilizes a mechanistic approach for projecting forest growth and ecosystem dynamics is FORECAST (Kimmins et al. 1999). FORECAST was designed to accommodate a wide variety of harvesting and silvicultural systems in order to compare and contrast their effect upon forest productivity, stand dynamics, and various biophysical and social indicators of non-timber values. The model has been applied to a variety of mixedwood stand types (Welham et al. 2002, Seely et al. 2002, Seely et al. 2004, Sachs 1996), but establishing its utility as a decision-support tool for mixedwood management still requires evaluations of its performance against long-term, mixedwood forest growth data from well-documented field trials. Here we evaluate the ability of a mechanistic forest growth model (FORECAST) to project patterns of stand growth and dynamics in a spruce-aspen mixedwood forest type subjected to different silvicultural treatments. Model output is compared against field measurements from long-term silviculture trials in the Sub Boreal Spruce (SBS) biogeoclimatic zone in British Columbia, Canada.

METHODS

Model Description

FORECAST is a management-oriented, stand-level forest growth and ecosystem dynamics simulator. A detailed de-

B. Seely (brad.seely@ubc.ca), J.A. Blanco, C. Welham, and J.P. Kimmins are in the Department of Forest Sciences, University of British Columbia, 2424 Main Mall, Vancouver, BC, V6T 1Z4, Canada; C. Hawkins is in the Faculty of Natural Resources and Environmental Studies, University of Northern British Columbia, 3333 University Way, Prince George, BC V2N 4Z9, Canada.

scription of the FORECAST model is provided in Kimmins et al. (1999) and Seely et al. (In press), only a summary is provided here. The model was designed to accommodate a wide variety of harvesting and silvicultural systems in order to compare and contrast their effect on forest productivity, stand dynamics, and a series of biophysical indicators of non-timber values. Projection of stand growth and ecosystem dynamics is based upon a representation of the rates of key ecological processes regulating the availability of, and competition for, light and nutrient resources (a representation of moisture competition is being completed but was not included in this study). The rates of these processes are calculated from a combination of historical bioassay data (biomass accumulation in component pools, stand density, etc.) and measures of certain ecosystem variables, (e.g., decomposition rates, photosynthetic saturation curves) by relating 'biologically active' biomass components (foliage and small roots) with calculations of nutrient uptake, the capture of light energy, and net primary production. Using this 'internal calibration' or hybrid approach, the model generates a suite of growth properties for each tree and plant species to be represented. These growth properties are subsequently used to model growth as a function of resource availability and competition. FORECAST performs many of its calculations at the stand level but it includes a submodel that disaggregates stand-level productivity into the growth of individual stems with user-inputted information on stem size distributions at different stand ages. Top height and diameter at breast height (DBH) are calculated for each stem and used in a taper function to calculate total and individual stem gross and merchantable volumes.

Test Site

Site description—
The study site was located approximately 50 km east of Prince George in the SBSwk1 variant (MacKinnon et al. 1990). The site was established in 1985 in an area that was clearcut in 1969, broadcast burned in 1970, and planted in 1971 with 2+1 bare-root white spruce (*Picea glauca*) seedlings. Following the burn, the plantations had a vigorous regeneration of aspen (*Populus tremuloides*) such that when plots were established in 1985, the aspen canopy was well above that of the spruce. A validation data set was derived from long-term monitoring plots established as part of a study of spruce weevil (*Pissodes strobi*) attacks on young spruce plantations treated to have varying degrees of aspen cover (see Taylor and Cozens 1994, for a complete

description). The study area contained three separate sites intended as replicates, but because of differences in species and density among the sites, only one site (Site 2) was selected for model evaluation.

Treatments and plot establishment—
Long-term plots were installed to examine the impact of two levels of aspen removal on both weevil attack rates and spruce growth. The first treatment was the mechanical removal all of the aspen (referred to as 'brushed') and the second treatment was a partial removal of the aspen using strip cuts (partial brushed). A control plot was also established in which no aspen were removed. All plots were rectangular in shape with dimensions of 50 m x 115 m. In the partial brushed plot, 5-meter wide strips with no aspen removed were left adjacent to 7-meter wide strips in which all the aspen had been removed mechanically. Strips were made perpendicular to the long axis of the rectangular plot. This treatment resulted in the removal of approximately 60 percent of the overstory aspen.

All spruce trees were measured (top height and DBH) in each plot in 1986, 1988, 1991 and 2003 (18 years after treatment). Tree mortality was also recorded. Aspen trees were measured (top height and DBH) in 2003 only. Estimates of total volume and stem biomass were made for both species in years where both height and DBH data were available using standard species specific volume (BCFS 1976) and biomass equations (Standish et al. 1985).

Simulation of Treatments
Prior to the simulation of the specific management treatments an initial site condition was established in the model using a procedure described by Seely et al. (In press). Simulations were conducted to represent each of the 2 treatments (brush & partial brush) and the control. In each simulation, spruce was planted in year 1 (1971) at 1500 stems per hectare and aspen regeneration occurred in year 1 at 2000 stems per hectare. A small population (5 percent cover) of a general (medium height) *Vaccinium* sp. shrub was also initiated in year 2. In the case of the brushed treatment, 100 percent of the aspen was harvested in year 15 (1985) and regenerated at 5000 stems per hectare the following year (to represent suckering). In the case of the partial brushed treatment, 60 percent of the aspen stems were removed with stems distributed evenly across all size classes. Since FORECAST has an aspatial representation of tree distribution, the simulation was based on the assumption that the removal strips were

narrow enough (7 m) that the spruce would behave as if the residual aspen were distributed evenly throughout the treated area, particularly as the residual aspen matured and crown expansion occurred. It was assumed that there was some regeneration of aspen by suckering (2500 stems per hectare) following the thinning treatment. The control scenario had no management interventions following the initial planting of spruce.

Evaluation of Model Performance

Model performance was evaluated using graphical comparison to examine treatment response with respect to standard growth and yield variables. In addition, overall model fit was assessed for each species and variable using the modelling efficiency (ME) statistic described in Vanclay and Skovsgaard (1997):

$$ME = 1 - \frac{\sum D_i^2}{\sum (Observed_i - \overline{predicted})^2}$$

This statistic provides a simple index of performance on a relative scale, where ME = 1 indicates a perfect fit, ME = 0 indicates that the model is no better than a simple average, while negative values indicate poor model performance.

RESULTS
Evaluation of Model Performance

ME values were greater than 0.9 for all variables tested with the exception of total stand spruce stemwood biomass (ME=0.88), average DBH for spruce (ME = 0.76) and average DBH for aspen (ME =0.77) (Table 1). The model did a better job of predicting the diameters of the top 200 spruce trees relative to that for all spruce trees in a given simulation (Table 1). It also performed well in projecting the treatment effects on patterns of total stand wood production for both spruce and aspen in both treatments and the control.

Table 1—Goodness of fit of model relative to field data as measured by modeling efficiency (ME) for the spruce-aspen simulations (n: number of data).

Variable	Spruce		Aspen	
	ME	n	ME	n
Average top height	0.97	12	0.93	3
Average stem biomass	na	na	na	na
Top 200 top height	0.98	12	na	3
Average DBH	0.76	6	0.77	3
Top 200 DBH	0.93	6	na	3
Stand volume	0.97	6	0.98	3
Stand stem biomass	0.88	6	0.96	3
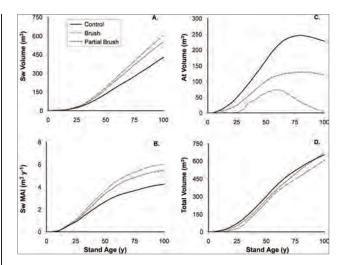
Figure 1. Simulation results for a 100-year time period for the spruce-aspen mixedwood showing A) total Sw Volume, B) Sw mean annual increment (MAI), C) total At volume, and D) total volume for all species for the two treatments and the control site. The treatment occurred in year 15.

The simulated long-term impacts of the brushing treatments on spruce volume, mean annual increment of spruce volume, aspen volume, and total stand volume are shown in Figure 1. The impact of the treatments on spruce growth rates was subtle for more than a decade following the treatment but was substantial over a longer time period (Fig. 1A, B). Impacts on aspen volume happened quickly and were more dramatic (Fig. 1C). The influence of the treatments on total stand volume was relatively small (Fig. 1D) with the control stand producing slightly more (15 percent) volume than the fully brushed stand at rotation age (approximately 75 years). However, the aspen content of the total stand volume changed significantly with the different treatments.

Simulated Competitive Interactions

Light competition—

Foliage shading index, an integrated measure of simulated competition for available light between species, is shown for the spruce-aspen mixedwood stand type in Figure 2. Specifically, the foliage shading index represents the relative decline in foliar N productivity caused by shading (including self-shading and shading by other species). The index is calculated based on the quantity of light captured by the foliage of each tree species summed throughout the canopy profile (see Kimmins et al. 1999 for more detail). The relative productivity of the foliage (per unit foliar N) is determined as a function of the species-specific light response curves shown in Figure 2C.
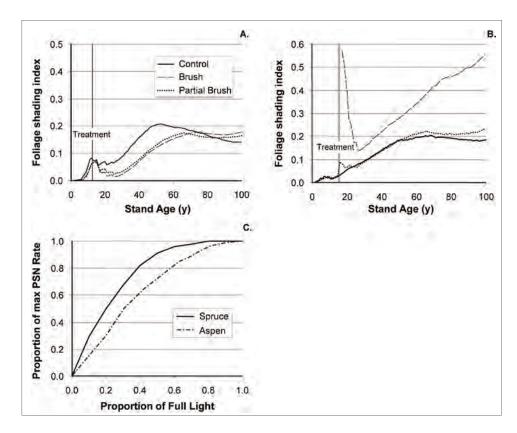
Figure 2. Simulated foliage-shading index as a measure of light competition for A) spruce and B) aspen for the two aspen brushing treatments and the control in the spruce-aspen mixedwood stand type. Panel C shows the relative photosynthetic rates (per unit foliar N) for spruce and aspen as a function of light levels calculated throughout the canopy profile.

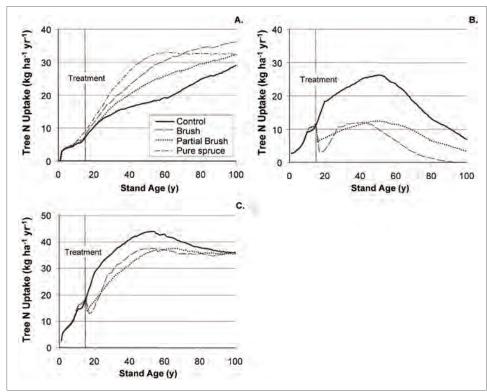*Figure 3. Simulated annual nitrogen (N) uptake for A) spruce and B) aspen and C) total tree for the two aspen brushing treatments and the control in the spruce-aspen mixedwood stand type.*

The foliage shading index of spruce was reduced for several decades following both brushing treatments relative to the control but gradually returned to levels similar to that in the control stand by year 70 (Fig. 2A). In the case of aspen, the foliage shading index increased dramatically immediately following the full brushing treatment and resprouting and remained high relative to the control (Fig. 2B). In contrast, the foliage shading index for aspen in the partial brushing treatment (for both residual and resprouting trees combined) increased only slightly following the treatment after which it remained at a level similar to that for aspen in the control stand.

Nitrogen competition—

The simulated impact of the aspen brushing treatments on N competition, as measured by total tree N uptake, is shown for the spruce-aspen mixedwood stand type in Figure 3. Total annual N uptake by spruce increased gradually but substantially over the long-term with increasing aspen removal relative to the control stand (Fig 3A). Total N uptake for the simulated pure spruce reference plantation (Fig. 3A) provides an indication of total potential N uptake in the absence of aspen competition. The simulated N uptake pattern for aspen was opposite to that observed for spruce (Fig. 3B). Following the brushing treatments, total tree N uptake rates were highest in the control stand for the duration of the 100-year simulation period (Fig. 3C).

DISCUSSION

The overall fit of the model to observed values (as measured by ME) was good for all the simulated treatments examined. Model predictions of DBH, particularly for smaller trees, were among the least accurate of all variables examined. While comparisons of average measures of individual stems are informative and useful, comparisons of stand-level summaries of total volume and stem biomass are perhaps the best measures of overall model performance as they represent an integrated accounting of total production for all of the trees (whether measured or simulated) in the stand. FORECAST performed well in predicting the effects of the different brushing treatments on these stand-level measures of production for spruce and aspen. The model was able to simulate these effects by representing the impact of the silviculture interventions on interspecific competition for light and nutrient resources.

Simulation results indicate that competition for both light and nutrients is important in the dynamics of these mixedwood forest types although it is difficult to isolate specific effects as there are interactions between them. The analysis also highlighted the fact that long-term response data and modeling are required to adequately assess the rotation-length effects of treatments on stand development. The projected 15 percent higher total stand volume in the control treatment relative to the full brushing treatment is consistent with field-based estimates made by Man and Leiffers (1999). The main effect of the treatments was an increase in the relative spruce content of the total stand volume. The brushed and alternative brushed treatments had 45 percent and 31 percent more spruce volume at rotation relative to the control, respectively. Managers evaluating these options based on model output may make different decisions depending upon which species is favored for specific resource values.

As management practices shift increasingly towards the management of complex stand types it is critical that we develop a range of models with the capability to project the short and long-term impacts of alternative stand management systems on both timber and non-timber values. Given our general lack of field experience with many of the silvicultural systems employed under ecosystem-based management and the uncertainty associated with natural disturbance agents and changing climate, models which incorporate some level of causality and/or understanding through the representation of key ecological processes are generally better suited for this purpose than models driven predominantly by empirical relationships (Korzuhkin et al. 1996, Johnsen et al. 2001). The analysis described herein provides a level of confidence for the use of the model as a decision-support tool in these ecosystem types, but more validation work should be conducted across a range of different mixedwood forest types and management interventions as long-term datasets become available.

LITERATURE CITED

BC Forest Service. 1976. Whole stem cubic metre volume equations and tables: centimetre diameter class merchantable volume factors. Forest Inventory Division, British Columbia Forest Service, Dept. of Forests, Victoria, BC. 103 p.

Comeau, P.G. 1996. Why mixedwoods? In: Comeau, P.G., Thomas, K.D., eds. Silviculture of temperate and boreal broadleaf-conifer mixtures. British Columbia Ministry of Forests, Victoria, British Columbia. Land Managers Handbook 36:1–7.

Comeau, P.G.; Biring, B.S; Harper, G.J. 2000. Conifer

response to brushing treatments, a summary of B.C. data. British Columbia Ministry of Forests, Victoria, British Columbia. Ext. Note 41. 12 p.

Côté, L.; Brown, S.; Paré, D. [et al.] 2000. Dynamics of carbon and nitrogen mineralization in relation to stand type, stand age and soil texture in the boreal mixedwood. Soil Biology and Biogeochemistry 32: 1079-1090.

Grover, B.E.; Greenway, K.J. 1999. The ecological and economic basis for mixedwood management. In: Veeman T.S, Smith D.W., Purdy B.G., Salkle F.J., Larkin G.A., eds. Proc. 1999 sustainable forest management network conference: Science and practice: sustaining the boreal forest. February 14–17, 1999. University of Alberta, Edmonton, Alberta, Canada. Pp. 419–428.

Harper, G.; R. Kabzems. 2003. Growing-space Management in boreal-mixedwood Forests—The establishment of EP 1192.02, Fort Nelson River Site. British Columbia Ministry of Forests, Victoria, British Columbia. Ext. Note 64.

Huang, S.; Titus, S.J. 1994. An age-independent individual tree height prediction model for boreal spruce-aspen stands in Alberta. Canadian Journal of Forest Research 24: 1295-1301.

Johnsen, K.; Samuelson, L.; Teskey, R. [et al.] 2001. Process models as tools in forestry research and management. Forest Science 47: 2-8.

Kimmins, J.P.; Mailly, D.; Seely, B. 1999. Modelling forest ecosystem net primary production: the hybrid simulation approach used in FORECAST. Ecological Modelling 122: 195-224.

Korzukhin, M.D.; Ter-Mikaelian, M.T.; Wagner, R. 1996. Process versus empirical models: which approach for forest management? Canadian Journal of Forest Research 26: 879-887.

Mackinnon, A.; DeLong, C.; Meidinger, D. 1990. A Field Guide for Identification and Interpretation of Ecosystems of the Northwest Portion of the Prince George Forest Region. LMH 21. British Columbia Ministry of Forests.

Man, R.; Lieffers, V.J. 1999. Are mixtures of aspen and white spruce more productive than single species stands? Forestry Chronicle 75: 505-513.

Sachs, D. 1996. Simulation of the growth of mixed stands of Douglas-fir and paper birch using the FORECAST model. In: Comeau, P.G, Thomas, K.D., eds. Silviculture of temperate and boreal broadleaf-conifer mixtures. British Columbia Land Management Handbook No. 36: 152-158.

Seely, B.; Hawkins, C.; Blanco, J.A. [et al.] In Press. Evaluation of a mechanistic approach to mixedwood modelling. The Forestry Chronicle.

Seely, B.; Nelson, J.; Wells, R. [et al.] 2004. The application of a hierarchical, decision-support system to evaluate multi-objective forest management strategies: A case study in north-eastern British Columbia, Canada. Forest Ecology and Management 199: 283-305.

Seely, B.; Welham, C.; Kimmins, J.P. 2002. Carbon Sequestration in a Boreal Forest Ecosystem: Results from the Ecosystem Simulation Model, FORECAST. Forest Ecology and Management 169: 123-135.

Simard, S.W.; Hannam, K.D. 2000. Effects of thinning overstory paper birch on survival and growth of interior spruce in British Columbia: implications for reforestation policy and biodiversity. Forest Ecology and Management 129: 237-251

Simard, S.W.; Perry, D.A.; Jones, M.D. [et al.] 1997. Net transfer of carbon between tree species with shared ectomycorrhizal fungi. Nature 388: 579-582.

Simard, S.W.; Sachs, D.L.; Vyse, A.; L. Blevins. 2004. Paper birch competitive effects vary with conifer tree species and stand age in interior British Columbia forests: implications for reforestation policy and practice. Forest Ecology and Management 198: 55-74.

Standish, J.T.; Manning, G.H.; Demaershalk, J.P. 1985. Development of biomass equations for British Columbia tree species. Rep. No. BC-X-264. Canadian Forestry Service, Pacific Forest Research Centre, Victoria, British Columbia. 47 p.

Taylor, S.P.; Cozens, R.D. 1994. Limiting white pine weevil attacks by side and overstory shade in the Prince George Forest Region. Journal of the Entomological Society of British Columbia 91: 37-42.

Vanclay, J.K.; Skovsgaard, J.P. 1997. Evaluating forest growth models. Ecological Modelling 98: 1-12.

Welham, C.; Seely, B.; Kimmins, J.P. 2002. The utility of the two-pass harvesting system: an analysis using the FORECAST ecosystem simulation model. Canadian Journal of Forest Research 32: 1071-1079.

Assessing Forest Productivity: Satellite versus Terrestrial Data-Driven Estimates in Austria

Richard Petritsch, Céline Boisvenue, Steve Running, Hubert Hasenauer

ABSTRACT

FOREST PRODUCTIVITY HAS ALWAYS BEEN A major issue within sustainable forest management. While in the past, terrestrial forest inventory data have been the major source for assessing forest productivity, recent developments of modeling techniques and satellite-derived information have become of increasing interest for productivity estimates. Using a mechanistic model enables us to analyze the pools and fluxes within a forest ecosystem. On the other hand, satellite data as they can be derived from, say, the Moderate Resolution Imaging Spectroradiometer (MODIS) Sensor may be used for monitoring global and/or regional Net Primary Production (NPP). In this study we first present the incorporation of management within a mechanistic ecosystem model and then use this approach for comparing satellite vs. terrestrial driven NPP based on different estimation procedures: (1) NPP estimates derived from MODIS satellite, (2) estimates from the species specific adaptation of Biome-BGC, and (3) NPP estimates derived from inventory data using biomass expansion functions (BEF). First results suggest that the scaling issue is of major concern since the area covered by the satellite images is much larger than the area which is commonly assumed to be represented by inventory plots. Thus, satellite-based approaches may overlook details which are covered by inventory data. After aggregating the available inventory information to ecological growth regions, the correlation between satellite vs. terrestrial data-driven NPP estimates improved substantially.

KEYWORDS: Forest production, NPP, ecosystem modeling, MODIS

INTRODUCTION

Forests play a large role in the global carbon cycle, and they are already responding to global climate and atmospheric changes (Boisvenue and Running 2006). Forest NPP, however, cannot be directly measured (Clark et al. 2001). It must be inferred even for on-site estimates. Reliable and globally available estimates of NPP at a site level would support the monitoring of carbon sequestration. NPP estimates enter into the global carbon budget (Nemani et al. 2003) and large-scale patterns of food and fiber production (Running et al. 2004). They are essential in understanding physiological processes in forests and the effects of climate change on individual forests as well as on whole biomes (Richardson et al. 2007).

Terrestrial forest inventory data has always been a major source for assessing the productivity of forest ecosystems. Due to the demanding efforts for large area inventories they are usually limited to measuring routine data like diameter at breast height of a sample of a forest stand. Biomass of the whole stand is then projected using allometric equations (Wirth et al. 2004). As an alternative to the purely statistical approach, different types of models have been developed. Biogeochemical mechanistic (BGC) models assist in obtaining knowledge on key ecosystem processes as they focus on the interaction between soil, plants, and

Richard Petritsch (richard.petritsch@boku.ac.at) and **Hubert Hasenauer** are in the Department of Forest- and Soil Sciences, University of Natural Resources and Applied Life Sciences, Peter-Jordan-Strasse 82, A-1190 Vienna, Austria; **Céline Boisvenue** and **Steve Running** are in the Numerical Terradynamic Simulation Group, University of Montana, Missoula, Montana, USA.
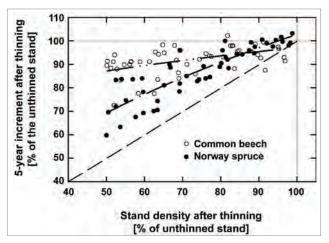
Figure 1. Five-year total stem volume increment rates in percent of the unthinned conditions using Monte-Carlo simulations.
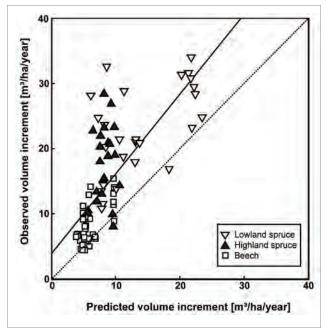

Figure 2. Predicted vs. observed volume increments following thinning using the current model setup.

the atmosphere by assessing the fluxes of energy, water, nitrogen, and carbon within a given ecosystem (Waring and Running 1998).

An important limitation of BGC models is that they operate on fully stocked even-aged stands since they are not explicitly designed to be sensitive to varying stand density. It is important to distinguish between historic management (Pietsch and Hasenauer 2002) and current management, which mainly addresses density changes. As forest management has been, and still is, the main driving impact for changes in forest growth in Europe (Kauppi et al. 1992) the conceptual integration of thinning is essential.

Recent developments in satellite-derived information

become of increasing interest, as they are able to provide globally available estimates of NPP at a site level. Sensors, such as the Moderate Resolution Imaging Spectroradiometer (MODIS) on NASA's Terra satellite, are being used for monitoring global NPP (Running et al. 2004). Comparisons of MODIS production estimates, which are globally available, to ground-based estimates have taken place (Turner et al. 2006). In these studies, site-level estimates were scaled up. In the present study, we compare the unaltered smallest common spatial denominator of NPP estimates from MODIS, Biome-BGC, and routine inventory data with Biomass Expansion Factors (BEFs).

Thus the objectives of this study can be summarized as:

1. Application of the mechanistic ecosystem model Biome-BGC to managed forest stands in Central Europe.

2. Comparison of satellite vs. terrestrial data-driven NPP estimates using a set of sample plots across Austria.

INCORPORATING FOREST MANAGEMENT

We use the mechanistic ecosystem model Biome-BGC Version 4.1.1 (Thornton et al. 2002) with improvements regarding hydrology (Pietsch et al. 2003), species representation (Pietsch et al. 2005) and self-initialization (Pietsch and Hasenauer 2006). Land-use history for considering potential soil degradation from past human impacts is addressed (Pietsch and Hasenauer 2002). Applications for managed forest stands assumed that thinnings only produced changes in the stem, leaf, coarse and fine root pools. Six parameters are available to characterize intervention in terms of stem removal, stem to coarse woody debris (cwd), leaf removal, leaves to litter, coarse roots to cwd, and fine roots to litter. These values are given in percent (Merganicová et al. 2005). The original model assumes a fully stocked stand but forest
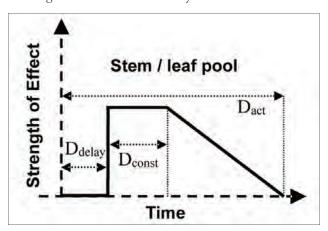

Figure 3. Allocation change after thinning.

management options usually change stand density. Thus, we are interested in how the model performs immediately after biomass removal.

Model Analysis

For studying management impacts we use the species parameters for Common beech (*Fagus sylvatica*) and Norway spruce (*Picea abies*) (Pietsch et al. 2005). Within 50 Monte-Carlo simulations we applied thinnings where we randomly chose time and intensity of the intervention. The reaction of the model was evaluated by calculating the volume increment immediately after thinning relative to the volume increment of the unthinned forest stand. Since there is no explicit stand density within the model, it is determined as the remaining stem biomass in percent of the stem biomass before thinning (Assmann 1970). This assumption is only valid immediately after the intervention.

Although the original model is set up for fully stocked stands it was sensitive to management (Figure 1). This response is species specific and the more shade-tolerant species, beech, is less responsive than spruce. Although this is consistent with findings from growth and yield studies the response seems to be too optimistic and requires some further adjustments. The volume increment after thinning increased compared to the unthinned stand with the same biomass fraction (1:1 line). This can be attributed to the fact that there is more access to resources (water, nitrogen, and light) after thinning. With increased thinning intensity the simulated growth acceleration of beech was higher than that of spruce. Although the situation is consistent with findings in growth and yield studies (e.g. Assmann 1970), the application of the model to managed forest stands produced significant under-estimations in volume increment (Figure 2).

Allocation Change

Trees change their physiology as a result of reduction in competition. This affects the distribution pattern between above- and below-ground biomass and between wood and leaf biomass as they may change in response to specific environmental conditions (Mooney and Winner 1991). A management submodel was developed, with changed allocation pattern after thinning (Petritsch et al. 2007), using 66 sample plots from 12 different regions in Central Europe. Model behavior after thinning was investigated using 8 sample plots per species. The allocation pattern was changed after the intervention to stimulate stem
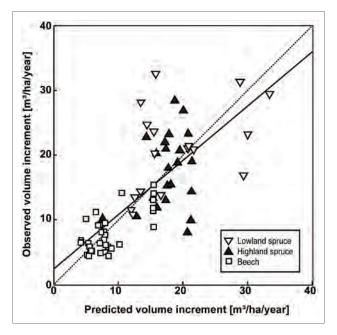
Figure 4. Predicted vs. observed volume increments after thinning for the improved (with allocation change) model.

growth (Figure 3). The values of the parameters Ddelay, Dconst, and the maximum of change in the proportions were optimized using the evaluation plots. The duration of the effect (Dact) is estimated from the thinning intensity while the change decreased linearly until it vanished after a maximum duration of 20 years (Figure 3).

Results

Using the remaining sample plots as a validation dataset the application of the improved model gave unbiased volume increment (Figure 4) as well as stand volume predictions by species. Although the parameters for spruce were established using only sample plots with lowland spruce they are also valid for the application to highland spruce. A detailed description of the management submodel with all results of the model validation can be found in Petritsch et al. (2007).

COMPARING NPP ESTIMATES

Satellite NPP

NASA's Earth Observation System (EOS) satellite carries the Moderate Resolution Imaging Spectroradiometer (MODIS). Several products are derived from these raw data on a daily basis. We use NPP (Heinsch et al. 2003) as it is calculated by the Numerical Terradynamic Simulation Group (NTSG) at the University of Montana. NPP estimates (MOD17)

are available as annual values on 1km spatial resolution. MOD17 requires meteorological data, and up-stream MODIS products such as GPP (MOD17A2), Leaf Area Index (LAI), Fraction of Photosynthetically Active Radiation (FPAR; MOD15), and MODIS Land Classification (MOD12). The meteorological data used for the web-available NPP estimates are retrieved from NASA's Global Modeling and Assimilation Office (GMAO).

Due to georeferencing constraints, and to ensure pixel-to-site coherence, satellite estimates were obtained for a 3 x 3 km area around the site latitude and longitude. Each of these nine pixels has an attached land classification from an up-stream MODIS product, MOD12. The MODIS productivity estimates are highly dependent on the land classification of each pixel, because the land classification defines which biome and therefore which ecophysiological parameter value will be used in the algorithm (see Heinsch et al. 2003 for details).

Terrestrial NPP

The first approach uses the mechanistic ecosystem model Biome-BGC (Thornton 1998) Version 4.1.1 with extensions (Pietsch et al. 2003, Pietsch et al. 2005, Pietsch and Hasenauer 2006) and daily climate data from the Austrian version of DAYMET (Hasenauer et al. 2003). In addition to daily climate data only generally available site data are used as input parameters for the model.

The second procedure is based on allometric equations. Total biomass is estimated using Lehtonen et al. (2004) for conifers and VandeWalle (2005) for broadleaves, aggregated for the whole stand and converted to carbon for each site. NPP is assumed to be the annual biomass increment of the forest stand. This is a completely statistical approach depending on constant biomass expansion factors (BEFs).

Comparison Dataset

We obtained MODIS data for 624 sites across Austria where terrestrial measurements were also available. Some of the locations (144 of the 624) were previously used in a validating effort to produce species-specific parameter estimates of the ecosystem model (Pietsch et al. 2005). The remaining 480 sites are from the Austrian National Forest Soil Survey (Englisch et al. 1992) and include soils, humus, as well as forest growth information.

To assess NPP as the increment in stand biomass it is essential to have re-measurements of stand data. Thus only 166 (Figure 5) plots which have more than one measurement could be used in the analysis. These are all forested sites.
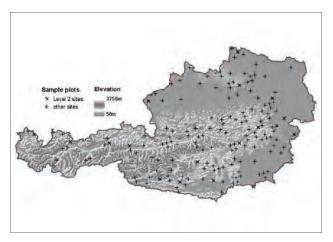
Figure 5. Location of the 166 sample plots for the comparison of NPP estimates.
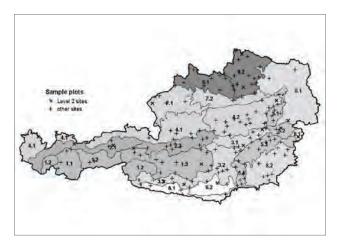
Figure 6. Growth districts and ecoregions in Austria (Killian, 1994).

Table 1. Correlations of the NPP estimates on different aggregation levels.

	N	BGC vs. MODIS	BEF vs. MODIS	BGC vs. BEF
plots	166	0.08	0.02	0.35
growth districts	22	0.58	0.28	0.60
eco-regions	9	0.54	0.51	0.82

Results

We found that NPP estimates using Biomass Expansion Factors (BEF) show the largest variation. On the plot level only BGC vs. BEF are significantly correlated (r=0.35; t=4.82; α=0.05; N=166). The correlation between satellite and terrestrial data-driven estimates were low (r<0.1; t<1.0; α=0.05; N=166). As NPP is estimated on different scales, we expected low correlation on plot level. Thus, we spatially aggregated

the estimates to growth districts and ecoregions (Figure 6) as given in Killian (1994). These aggregated estimates improved the correlations and resulted in higher r values (r>0.5; t>1.5; α=0.05; N=9) for all combinations (Table 1). Correlation between BGC and BEF further improved to 0.82 (t=3.79; α=0.05; N=9).

Discussion and Conclusion

Since forest NPP cannot be directly measured it must be inferred even for on-site estimates. In the present study we compared three different methods for estimating forest NPP. The mechanistic ecosystem model Biome-BGC provides NPP on a daily basis as GPP minus respiration. Since this model operates on fully stocked even-aged stands we had to adapt it for managed forests in Central Europe. Application of the original model gave unbiased results in terms of an under-estimation of volume increment after thinning. By implementing a management submodel, which changes the allocation pattern after thinning, we achieved unbiased results for the volume and volume-increment prediction (Petritsch, et al. 2007).

Terrestrial forest inventory data from the Austrian National Forest Soil Survey (Englisch et al. 1992) combined with allometric equations (BEF, Lehtonen et al. 2004, VandeWalle 2005) were used to calculate total biomass increment. This number was used as the second estimate. The inventory data consist of repeated 5-year measurements. Due to the purely statistical properties and the long measurement cycle no climate impact or inter-annual variation was expected. Thus the estimates are mainly driven by site characteristics.

Satellite NPP estimates come from MODIS and are available online as annual averages. For the calculation, meteorological data and upstream MODIS products such as GPP, LAI, FPAR, and land classification are required. MODIS productivity estimates strongly depend on the ecophysiological parameters. They are chosen according to the land classification (Heinsch et al. 2003).

On plot level BGC and BEF were significantly correlated (r=0.35; t=4.82; α=0.05; N=166) but satellite versus terrestrial approaches showed no significant correlation (r<0.1; t<1.0; α=0.05; N=166). According to the different scales of satellite and terrestrial data this result was expected. Holman and Peterson (2006) analyzed growth pattern at multiple scales (plot, forest type, watershed, and subregion) and found that at larger scales (watershed and subregion), forest-type growth patterns show coherence. Our BGC estimates

probably capture more of the variation due to larger scale factors such as climate, as compared to the BEF estimate. The satellite estimates probably capture even more than the BGC estimates. Satellite estimates do not capture variability due to inter-tree competition but do capture variability due to processes of larger-scale influence.

Correlations strongly improved after grouping the results to growth districts and ecoregions (Killian 1994). For terrestrial vs. satellite estimates we calculated r>0.5 (t>1.5; α=0.05; N=9) and BGC vs. BEF r=0.82 (t=3.79; α=0.05; N=9).
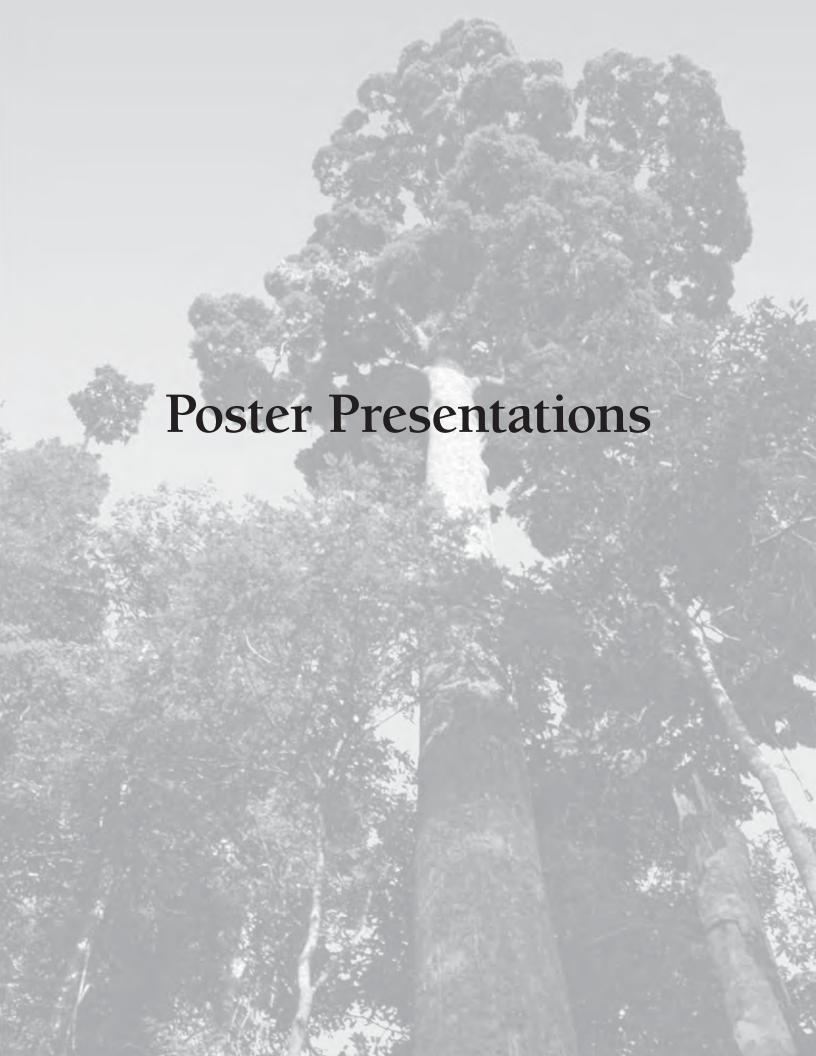
Scaling is obviously very important when comparing satellite vs. terrestrial data. Since MODIS-driven productivity estimates are assessed on a 3 x 3 km area the grouping of inventory-driven estimates strongly affected the correlation between the different methods. Although scaling biases are quantifiable, the data required for doing so are beyond the scope of this study.

LITERATURE CITED

Assmann, E. 1970. The principles of forest yield study. Pergamon Press, New York. 506p.

Boisvenue, C.; Running, S.W. 2006. Impacts of climate change on natural forest productivity—evidence since the middle of the 20th century. Global Change Biology 12: 862–882.

Clark, D.A.; Brown, S.; Kicklighter, D.W. [et al.]. 2001. Measuring Net Primary Production in Forests: Concepts and Field Methods. Ecological Applications 11: 356–370.

Englisch, M.; Karrer, G.; Mutsch, F. 1992. Österreichische Waldboden-Zustandsinventur. Teil 1: Methodische Grundlagen.. Mitt. Forstl. Bundesversuchsanst. Wien 168:5-22. (in German)

Hasenauer, H.; Merganicová, K.; Petritsch, R. [et al.]. 2003. Validating daily climate interpolations over complex terrain in Austria. Agriculture and Forest Meteorology 119: 87-107.

Heinsch, F.A.; Reeves, M.; Votava, P. [et al.]. 2003. User's Guide GPP and NPP (MOD17A2/A3) NASA MODIS Land Algorithm. University of Montana, Missoula, Montana. 57p.

Holman, M.; Peterson, D.L. 2006. Spatial and temporal variability in forest growth in the Olympic Mountains,

Washington: sensitivity to climatic variability. Canadian Journal of Forest Research 36:92-104.

Kauppi, P.E.; Mielikäinen, K.; Kuusela, K. 1992. Biomass and carbon budget of European forests, 1971–1990. Science 256: 70–74.

Kilian, W.; Müller, F.; Starlinger, F. 1994. Die forstlichen Wuchsgebiete Österreichs. Berichte der Forstlichen Bundesversuchsanstalt No. 82, Vienna. 60p. (in German)

Lehtonen, A.; Mäkipää, R.; Heikkinen, J. [et al.]. 2004. Biomass expansion factors (BEFs) for Scots pine, Norway spruce and birch according to stand age for boreal forests. Forest Ecology and Management 188: 211-224.

Merganicová, K.; Pietsch, S.A.; Hasenauer, H. 2005. Testing mechanistic modeling to assess impacts of biomass removal. Forest Ecology and Management 207: 37–57.

Mooney, H.A.; Winner, W.E. 1991. Partitioning Response of Plants to Stress. In: Mooney, H.A., Winner, W.E., Pell, E.J., eds. Response of Plants to Multiple Stresses. Academic Press, San Diego. pp.129-141.

Nemani, R.R.; Keeling, C.D.; Hashimoto, H. [et al.]. 2003. Climate-driven increases in global terrestrial net primary production from 1982 to 1999. Science 300: 1560-1563.

Petritsch, R.; Hasenauer, H.; Pietsch, S.A. 2007. Incorporating forest growth response to thinning within Biome-BGC. Forest Ecology and Management 242: 324-336.

Pietsch, S.A.; Hasenauer, H. 2002. Using mechanistic modelling within forest ecosystem restoration. Forest Ecology and Management 159: 111-131.

Pietsch, S.A.; Hasenauer, H. 2006. Evaluating the self-initialization procedure of large scale ecosystem models. Global Change Biology 12: 1658-1669.

Pietsch, S.A.; Hasenauer, H.; Kucera, J.; Cermák, J. 2003. Modeling effects of hydrological changes on the carbon and nitrogen balance of oak in floodplains. Tree Physiology 23: 735-746.

Pietsch, S.A.; Hasenauer, H.; Thornton, P.E. 2005. BGC-model parameters for tree species growing in central European forests. Forest Ecology and Management 211: 264-295.

Richardson, A.D.; Hollinger, D.Y.; Aber, J.D. [et al.]. 2007. Environmental variation is directly responsible for short- but not long-term variation in forest-atmosphere carbon exchange. Global Change Biology 13: 788-803.

Running, S.W.; Nemani, R.R.; Heinsch, F.A. [et al.]. 2004. A Continuous Satellite-Derived Measure of Global Terrestrial Primary Production. BioScience 54: 547-560.

Thornton, P.E. 1998. Description of a numerical simulation model for predicting the dynamics of energy, water, carbon and nitrogen in a terrestrial ecosystem. Ph.D. Thesis. University of Montana, Missoula, Montana. 280p.

Thornton, P.E.; Law, B.E.; Gholz, H.L. [et al.]. 2002. Modeling and measuring the effects of disturbance history and climate on carbon and water budgets in evergreen needleleaf forests. Agricultural and Forest Meteorology 113:185-222.

Turner, D.P.; Ritts, W.D.; Cohen, W.B. [et al.]. 2006. Evaluation of MODIS NPP and GPP products across multiple biomes. Remote Sensing of Environment 102: 282-292.

Vande Walle, I.; Van Camp, N.; Perrin, D. [et al.]. 2005. Growing stock-based assessment of the carbon stock in the Belgian forest biomass. Annales of Forest Sciences 62: 853-864.

Waring, R.H.; Running, S.W. 1998. Forest ecosystems: analysis at multiple scales, 2nd Edition. Academic Press, San Diego, California. 370p.

Wirth, C.; Schumacher, J.; Schulze, E.D. 2004. Generic biomass functions for Norway spruce in Central Europe—a meta-analysis approach toward prediction and uncertainty estimation. Tree Physiology 24: 121-139.

Poster Presentations

The Simulation of Allelopathy in Ecosystem-Level Forest Models: A Study Case in the Pacific Northwest

Juan A. Blanco and J.P. (Hamish) Kimmins

ABSTRACT

ALLELOPATHY IS ONE OF THE FACTORS THAT determine interactions among plants. Allelochemicals have been found in many forest ecosystems, but the importance of allelopathic interactions depends on forest type and environmental conditions. Despite the wide presence of this phenomenon, its modelization has been little developed, but its inclusion should be carefully considered in forest models dealing with environmental stress, exotic plant invasions (or introduction) and ecological succession. In these situations, multiple factors influence allelochemical production or toxicity such as nutrient availability, soil moisture and texture, solar radiation, and temperature, among others. Ecosystem-level effects of allelopathy are changes in germination rates, inhibition of seedling growth, mycorrhizal function, insect and bacterial growth, inhibition of nitrification or litterfall decomposition and dieback of mature trees. In this work, a comprehensive conceptual model on the interactions between different factors suitable to be incorporated in ecosystem-level models is presented. In addition, to illustrate the utility of simulating allelopathy, a virtual experiment was carried out with the forest ecosystem-level model FORECAST applied in a forest of western red-cedar (*Thuja plicata*) interacting with the ericaceous understory shrub salal (*Gaultheria shallon*) in coastal British Columbia, Canada. Our results showed different effects of allelopathy on several ecological variables depending on the type of allelopathic influence simulated, with important reductions in predicted merchantable volume when reduction in germination and litterfall decomposition by allelopathy was simulated. Furthermore, a great increase in understory biomass was also predicted as consequence of allelopathy. This experiment showed the suitability of ecosystem-level models to simulate, if not directly allelopathic interactions, at least the ecological effects of allelopathy at the ecosystem level. Overall, this work pointed out that forest managers and researches should think carefully about the inclusion of allelopathy as a way of improving the accuracy of forest models.

KEYWORDS: allelopathy, allelochemicals, phytotoxicity, ecosystem-level models, silviculture practices, conceptual model, virtual experiment, FORECAST

ALLELOPATHY AND FORESTRY

Historically, the study of allelopathic interactions has been focused mainly on relationships between crops and weeds (Pellissier and Souto 1999). Studies about allelopathic relationships in forest soils are scarce and dispersed. Nevertheless, several studies have identified the importance of allelopathy in forest ecosystems. For example, Rietveld et al. (1983) have reported premature birch (*Betula papyrifera* Marsh) death in mixed plantations with walnut (*Juglans nigra* L.). Problems of conifer regeneration caused by ericaceous understory species have also been described (Mallik 2003). These examples show the importance of chemical interactions among plants in forest development and, therefore, show the necessity of including these relationships in forest models dealing with similar situations. The objective of this work is to provide suggestions concerning the most

Juan A. Blanco (juan.blanco@ubc.ca) is a postdoctoral research fellow in forest ecology and **J.P. (Hamish) Kimmins** is a professor of forest ecology in the Department of Forest Sciences, Faculty of Forestry, University of British Columbia. 2424 Main Mall, Vancouver, BC, V6T 1Z4, Canada.

important issues that should be taken into account when modeling allelochemical relationships in forests, presenting an example of ecosystem-level simulation using FORECAST to illustrate the use of allelopathy in modeling forests at an ecosystem-level. The paper presented here is an extended abstract of the work by Blanco (2007).

The presence of allelochemicals able to influence forest growth and development seems to be widespread in all ecosystem types (McKey et al. 1978, Williamson et al. 1992, Mallik 2003). The inclusion of allelopathy in forest models would be a good way to analyze the potential role of this phenomenon in ecosystem dynamics, and could be a useful contribution to the controversial debates over the ecological role of allelopathy. Three special cases have been mentioned as situations in which allelopathy should be analyzed; stress, invasion, and succession (Chuo 1986, Calloway 2001). Plants may use a passive interference in the development of their competitors by releasing allelochemicals (Reigosa et al. 2002) under nutrient or water stress (Koeppe et al. 1976, Kohl 1993), or other stress conditions such as UV radiation and physical damage by herbivores (Baldwin 1989, Reigosa et al. 1999). Given that natural communities have been evolving together for centuries, the most important effects of allelochemicals might appear in resource competition between species which did not share a common environment in the past (Rabotnov 1974). Recent studies have pointed out that allelochemical production and tolerance could be a key factor in determining success in exotic species invasion and in defining the new community resulting from the invasion process (Bais et al. 2003, Hierro and Callaway 2003). Understanding the role of allelopathy in succession following disturbances could be important in forest regeneration success (Rizvi et al. 1992).

Different factors affect allelopathy at various points within a tree. Additionally, scale is important in the modeling of allelopathy, and additional factors stand out at the stand-level. Plants growing in nutrient-rich environments tend to have lower allelochemical production than plants growing on nutrient-poor sites (McKey et al. 1978, Tang et al. 1995). Water stress can increase allelochemical production (Melkiana 1992, Reigosa et al. 2002). Water soil potential determines the rate of microorganism activity, allelochemical movement, and leaching (An et al. 2002). Differences in allelochemical production as a function of altitude and latitude have been reported by Anaya et al. (1992). Radiation affects donor plants, depending on wavelength, intensity and photoperiod (Reigosa et al. 1999). Temperature is an-

other parameter affecting allelopathy (Melkania 1992). In addition, other local factors such as edaphic microclimate, intensity and duration of rainfall, pH or oxygen concentration may also be important (Weidenhamer et al. 1989, Fisher et al. 1994). Plant-related factors such as age or type of allelochemical produced are also important. Ecological factors include fire or the presence of other organisms able to degrade allelochemicals to less toxic forms or to stimulate allelochemical production in plants (Williamson and Black 1981, Melkiana 1992, Reigosa et al. 1999). Nitrification in later seral stages may be strongly inhibited for this reason (Pellissier et al. 2002) and succession may be directed towards the selection of plants that inhibit nitrification of other organisms to reduce interspecific competition (Rice and Pancholy 1973, Chou 1986).

Allelopathy effects at the ecosystem level are directly related to forestry issues. Phenomena such as the delay and reduction of germination by allelochemicals, restricted root development, altered water balance, or decrease in mycorrhizal formation due to allelopathy have been widely reported (Einhellig 1986, Mallik and Pellisier 2000). One of the most important effects may be change in site fertility due to alteration of humus decomposition (Damman 1971) or changes in the influence of the understory on tree regeneration (Mallik 2003). Allelochemical activity can be reduced by mechanical elimination of donor plants or by using steam to reduce allelochemical activity. Fertilization has also been used, with contradictory results (Prescott et al. 1993, Mallik 1996). In addition, if the number and intensity of wildfires are reduced, it is possible that allelochemicals can reach levels that cause dieback in established tree species (Ellis et al. 1980) or may make tree regeneration after harvesting or windthrow almost impossible (Mallik 2003).

AN EXAMPLE OF SIMULATION OF ECOSYSTEM-LEVEL ALLELOPATHIC EFFECTS WITH FORECAST

To our knowledge, FORECAST is the only forest ecosystem-level model specifically designed to allow the simulation of allelopathic effects. FORECAST is a stand-level, non spatially-explicit, ecosystem model. A complete, detailed description of the model can be found in Kimmins et al. (1999). The model was calibrated for western red-cedar (*Thuja plicata* Don.) stands in the Coastal Western Hemlock biogeoclimatic zone of the Duncan Forest District (Vancouver Forest Region, British Columbia, Canada). Four

different simulations were carried out, all of them with the same starting conditions: site index 24 m at 50 years, 3000 stems ha⁻¹ as initial density, and initial aboveground biomass of salal (*Gaultheria shallon* Pursh) of 35 kg ha⁻¹. The rotation length was fixed at 100 years for all simulations. The first run did not simulate any allelopathic effect, and was considered a reference situation. For subsequent runs, we selected the two effects most frequently described and analyzed in the literature: a germination decrease of 15 percent for trees (Mallik and Pellissier 2000), and a reduction of decomposition rates by 10 percent (Damman 1971), but no effects micorrhizal effects were simulated in any run. Finally, the fourth run simulated both effects simultaneously. In addition, fertilization was simulated (addition of 225 kg N ha⁻¹ at years 22 and 40).

The least sensitive variable to allelopathy was dominant top height (Figure 1), with changes lower than 3 percent. On the other hand, merchantable volume showed a high sensitivity to allelopathy. At the end of the rotation, in the unfertilized scenario, both decomposition and germination decreased and caused a reduction of 7 percent in merchantable volume. When both effects are simulated simultaneously the reduction is close to 11 percent. A similar pattern can be observed in the total aboveground biomass of red-cedar, although in this case the reduction in biomass started more than 10 years sooner than for merchantable; volume. Finally, the most sensitive variable was salal aboveground biomass. When allelopathy was simulated as a reduction in decomposition rates, changes in salal biomass were small, but when red-cedar germination was reduced a significant relative increase in salal biomass was observed around year 80 (Figure 1). It also must be pointed out there was very little fertilization influence on stand response to allelopathy, with results almost identical in the fertilized and non-fertilized scenarios. The only important difference between these two scenarios was for salal aboveground biomass. Changes in germination and decomposition rates had opposite effects on stand development. Lower germination reduced nutrient competition between survivor trees, emulating an early self-thinning. By contrast, reduction in decomposition rates caused a general reduction in stand growth. This reduction was due to lower availability of soil nutrients, which were sequestered for more time in litterfall than in the simulation without allelopathy. In addition, maximum differences caused by decomposition alteration were generally reached at the end of the rotation. However, changes in germination reduction reached the maximum differences earlier in the
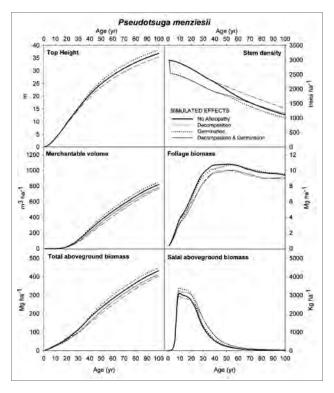
Figure 1—Simulated development of Douglas-fir and other plants in a red-cedar stand under some effects of allelopathy (decomposition and germination rates reduction) in two different scenarios: Non-fertilized (left column) and fertilized with 225 kg⁻¹ N ha at years 22 and 40 (right column). Arrows indicate fertilization schedule.

rotation (Figure 1). This situation clearly points out that reduction of decomposition had a longer lasting effect on stand growth, and probably is one of the most important allelopathy effects (Damman 1971). This effect was caused because decomposition rates were reduced by the presence of salal during the whole rotation length, while germination reduction was important only at the establishment of the new stand. For this reason, economic and ecological analysis of stand development in situations with potential allelopathic inhibition of important species growth should consider this natural phenomenon. Finally, it must be emphasized that fertilization had little influence in the severity of allelopathic inhibition of growth.

Our results showed different effects of allelopathy on several ecological variables depending on the type of allelopathic influence simulated. In addition, this experiment showed the suitability of ecosystem-level models to simulate, if not directly allelopathic interactions, at least the ecological effects of allelopathy at the ecosystem level. Overall, our work points out that forest managers and researches should think carefully about the inclusion of allelopathy as a way of improving the accuracy of forest models.

ACKNOWLEDGMENTS

LITERATURE CITED

An, M.; Johnson, I.R.; Lovett, J.V. 2002. Mathematical modelling of residue allelopathy: the effects of intrinsic and extrinsic factors. Plant and Soil 242: 11-22.

Anaya, A.L.; Ortega, R.C.; Nava Rodríguez, V. 1992. Impact of allelopathy in the traditional management of agroecosystems in Mexico. In: Rizvi, S.J.H.; Rizvi, V. eds. Allelopathy. Basic and applied aspects. London, UK: Chapman & Hall Editors. pp. 272-301.

Bais, H.P.; Vepachedu, R.; Gilroy, S., [et al.]. 2003. Allelopathy and exotic plant invasion: from molecules and genes to species interactions. Science 301: 1377-1380.

Baldwin, I.T. 1989. Mechanism of damage-induced alkaloid production in wild tobacco. Journal of Chemical Ecology 15:1 661–1680.

Blanco, J.A. 2007. The representation of allelopathy in ecosystem-level forest models. Ecological Modelling 209: 65–77.

Callaway, R.M. 2002. The detection of neighbors by plants. Trends in Ecology and Evolution 17: 104–105.

Chou, C.-H. 1986. The role of allelopathy in subtropical agroecosystems in Taiwan. In: Putnam, A.R.; Tang, C.S., eds. The science of allelopathy. New York, U.S.A.: Johan Wiley & Sons Editors. pp. 57-73.

Damman, A.W.H. 1971. Effect of vegetation changes on the fertility of a Newfoundland forest site. Ecological. Monographs 41: 253-270.

Einhellig, F.A. 1986. Mechanisms and modes of action of allelochemicals. In: Putnam, A.R.; Tang, C.S., eds. The science of allelopathy. New York, USA: Johan Wiley & Sons Editors. pp. 171-188.

Ellis, R.C.; Mount, A.B.; Mattay, J.P. 1980. Recovery of *Eucalyptus delegatensis* from high altitude dieback after felling and burning the understorey. *Australian Forestry Journal* 43: 29-35.

Fisher, N.H.; Williamson, G.B.; Weidenhamer, J.D.; Richardson, D.R. 1994. In search of allelopathy in the Florida scrub: the role of terpenoids. Journal of Chemical Ecology 20: 1355-1380.

Hierro, J.H.; Callaway, R.M.,2003. Allelopathy and exotic plant invasion. Plant and Soil 256: 29-39.

Kimmins, J.P.; Mailly, D.; Seely, B.,1999. Modelling forest ecosystem net primary production: the hybrid simulation approach used in FORECAST. Ecological Modeling 122: 195-224.

Koeppe, D.E.; Southwick, L.M.; Bittell, J.E. 1976. The relationship of tissue chlorogenic acid concentration and leaching of phenolics from sunflowers grown under varying phosphate nutrient conditions. Canadian Journal of Botany 54: 593-599.

Kohl, K. 1993. Allelopathy and water stress of purple nutsedge (*Luperus rotundus* L.). Master thesis. Honolulu, Hawaii, USA: University of Hawaii.

Mallik, A.U. 1996. Effect of NPK fertilizations on *Kalmia angustifolia*: implications for forest disturbance and conifer regeneration. Forest Ecology and Management 81: 135-141.

Mallik, A.U. 2003. Conifer regeneration problems in boreal and temperate forest with ericaceous understory: role of disturbance, seedbed limitation, and keystone change. Critical Reviews in Plant Science, 22: 341-366.

Mallik, A.U.; Pellissier, F. 2000. Effects of *Vaccinium myrtillus* on spruce regeneration: testing the notion of coevolutionary significance of allelopathy. Journal of Chemical Ecology 26: 2197-2207

McKey, D.; Waterman, P.G.; Mbi, C.N., [et al.]. 1978. Phenolic content of vegetation in two African rain forests: ecological implications. Science 202: 61-63.

Melkiana, N.P. 1992. Allelopathy in forest in forest and agroecosystems in the Himalayan region. In: Rizvi, S.J.H.; Rizvi, V. eds. Allelopathy. Basic and applied aspects. London, UK: Chapman & Hall Editors. pp. 371-388.

Pellissier, F.; Souto, X.C. 1999. Allelopathy in northern

temperate and boreal semi-natural woodland. Critical Reviews in Plant Sciences 18:637–652.

Pellissier, F.; Gallet, C.; Souto, X.C. 2002. Allelopathic interaction in forest ecosystems. In: Reigosa, M.J.; Pedrol, N. eds. Allelopathy: from molecules to ecosystems. Plymouth, UK: Science Publishers Inc. pp. 257–269.

Prescott, C.E.; Coward, L.P.; Weetman, G.F.; Gessel, S.P. 1993. Effects of repeated nitrogen fertilization on the ericaceous shrub, salal (*Gaultheria shallon*), in two coastal Douglas-fir. Forest Ecology and Management 61: 45-60.

Rabotnov, T.A. 1974. On the allelopathy in the phytocenoses. Izo Akad Nauk SSSR Ser. Biol 6. Moscow, Russia. pp. 811-820.

Reigosa, M.J.; Pedrol, N.; Sánchez-Moreiras, A.M.; González, L. 2002. Stress and allelopathy. In: Reigosa, M.J.; Pedrol, N. eds. Allelopathy: from molecules to ecosystems. Plymouth, Massachusetts, USA. Science Publishers Incorprated. pp. 231-256.

Reigosa, M.J.; Sánchez-Moreiras, A.M.; González, L. 1999. Ecophysiological approach in allelopathy. Critical Reviews in Plant Science 18: 577-608.

Rice, E.L.; Pancholy, S.K. 1973. Inhibition of nitrification by climax ecosystems II, Additional evidence and possible role of tannins. American Journal of Botany 60: 691-702.

Rietveld, W.J.; Schelinger, R.C.; Kessler, K.J. 1983. Allelopathic effects of black walnut on European black alder coplanted as a nurse species. Journal of Chemical Ecology 9: 1119-1133.

Rizvi, S.J.H.; Haque, H.; Sing, V.K.; Rizvi, V. 1992. A discipline called allelopathy. In: Rizvi, S.J.H.; Rizvi, V. eds. Allelopathy. Basic and applied aspects. London, UK: Chapman & Hall Editors. pp. 1-10.

Tang C.H.; Cai, W.F.; Kohl, K.; Nishimote, R.K. 1995. Plant stress and allelopathy. In: Inderjit; Dakshini, K.M.M.; Einhellig, F.A. eds. Allelopathy, organisms, processes and applications. Washington, DC, USA. American Chemical Society. pp. 142-157.

Weidenhamer, J.D.; Hartnett, D.C.; Romeo, J.T. 1989. Density-dependent phytotoxicity: distinguishing resource competition and allelopathic interference in plants. Journal of Applied Ecology 26: 613-624.

Williamson, G.B.; Black, E.M. 1981. High temperature forest fires under pines as a selective advantage over oaks. Nature 293: 634-644.

Williamson, G.B.; Richardson, D.R.; Fischer, N.H. 1992. Allelopathic mechanism in fire-prone communities. In: Rizvi, S.J.H.; Rizvi, V. eds. Allelopathy. Basic and applied aspects. London, UK: Chapman & Hall Editors. pp. 57-75.

Simulation of Density Effects on Tree Growth and Stem Form in Plantation Forests Using a Stand Growth Model

Yukihiro Chiba

ABSTRACT

I N THIS STUDY, A FOREST GROWTH MODEL WAS developed to describe the effect of stand density using mathematical models of tree architecture that quantify the relationships among tree organs. This stand-growth model was developed in conjunction with a mechanistic stability model of tree form representing branching structure (Chiba 1990, 1991), a stem-form model approximated by a hyperbolic function (Chiba 1990), and crown shape of forest trees reflecting density effects.

Tree growth is dependent on soil condition rather than stand density. Thus, the present model is driven by height growth of trees that is given by the Mitscherlich growth curve with a maximum height specific to forest site. Crown form of forest trees changes depending on growing space (determined by stand density) therefore, crown length also changes. In the model presented, crown length is a key parameter to represent crown (leaf and branch mass), and thus individual tree growth. Examining the stem-form model, it is clear that all the parameters in the stem-form model can be determined by tree size (i.e., tree height and crown length).

Applicability of the stand growth model was validated using the data on stand growths obtained for various thinning regimes. Employing this model, tree growth and biomass partitioning were well modeled along stand development with various initial tree densities and subsequent thinning regimes, showing serrated growth pattern. The growth patterns exhibiting a time trajectory between tree weight and stand density will be discussed in relation to density effects on tree growth in plantation forests.

REFERENCES

Chiba, Y. 1990. Plant form analysis based on the pipe model theory. I. A statistical model within the crown. Ecological Research 5: 207–220.

Chiba, Y. 1991. Plant form analysis based on the pipe model theory. II. Quantitative analysis of ramification in morphology. Ecological Research 6: 21–28.the ecosystem

Yukihiro Chiba (chiro@ffpri.affrc.go.jp) is a researcher at the Forestry and Forest Products Research Institute, Tsukuba, Ibaraki, 305-8687 Japan.

Analyzing High-Resolution Stem Growth Data and Re-Mapping Wood Property Data onto Time-Axes Using a Database Management System

David M. Drew, Derek Hohls, Geoffrey M. Downes

ABSTRACT

OVER THE LAST 50 YEARS, A LARGE NUMBER of researchers have made use of high-resolution electronic dendrometer systems to finely measure stem growth. More recently, use has been made of this kind of data to estimate the dates of formation of woody tissue, where the properties of this wood were analyzed at high resolution on pith-to-bark profiles. Stem growth and time-based wood property variation measured at this resolution is critical for developing and testing models that can explain short-term responses in the growing tree to changing environmental conditions. This kind of data is extremely voluminous, however, and its storage and management can be complex. We developed a 3-point integrated approach to dealing with all aspects of this kind of data, using the MySQL database management system (DBMS) in conjunction with custom-designed software and a web portal, so that all stakeholders in the research project/s could easily access data. This provides a generic means of dealing with this kind of data, which means that multiple researchers can apply the basic design to their research. The internet-based access provides powerful opportunities for collaborative work. In addition, we believe this data can be easily extracted and compared with predicted data from multiple modeling platforms with a small amount of customisation, since the data format is standardized.

David M. Drew (david.drew@sci.monash.edu.au) is at the School of Biological Sciences, Building 18, Monash University, Victoria 3800 and CSIRO Ensis, Private Bag 12, Hobart 7001, Tasmania, Australia; **Derek Hohls** is at CSIR Environmentek, PO Box 395, Pretoria , Gauteng 0001 South Africa; **Geoffrey M. Downes** are at CSIRO Ensis, Private Bag 12, Hobart 7001, Tasmania, Australia, Private Bag 12, Hobart 7001, Tasmania, Australia.

Crown Shape Dynamics in Managed Stands of Pedunculate Oak (*Quercus robur* L.) and Common Hornbeam (*Carpinus betulus* L.)

Tomislav Dubravac, Stjepan Dekanić, Valentin Roth

ABSTRACT

SPECIES-SPECIFIC CROWN SHAPE, EXPRESSED as a relation of crown diameter and crown length ($D\,l_k^{-1}$) changes during the tree lifetime in concordance with the ecological constitution of the species, productive capacities of the stand, and implemented management activities. In young stands (at the time of maximum current annual height increment) the crown is usually elongated, and becomes shorter as the stand reaches maturity. This is more evident in deciduous tree species.

We investigated average crown shapes (models) of pedunculate oak and common hornbeam trees, as well as their change over time and with respect to diameter at breast height (DBH). Results are based on the measurements of 2,235 trees from 47 permanent experimental plots with a total area of 33.45 ha. The plots are situated in two-layered, even-aged pedunculate oak and common hornbeam stands of different age classes.

Pedunculate oak trees develop crowns with maximum width roughly between one half and one third of the upper crown length. In more open canopies (as a result of management activities or degraded stand conditions) height of the maximum crown width decreases and the relative length of the sun-exposed crown increases. Common hornbeam trees constitute the lower layer of the canopy with the maximum crown width in the lower third of the crown length. Length of the sun-exposed crown in common hornbeam trees is always greater than half of the total crown length.

Knowledge about the development of crown shape in oak and hornbeam trees across stands of different age classes is indispensable for further calculations of crown volume. These calculations are widely used in diverse models of energy and material exchange within forest ecosystems and between forest ecosystems and the larger environment.

KEYWORDS: crown shape, pedunculate oak, common hornbeam, managed stands, tree age

Tomislav Dubravac and **Valentin Roth** are scientists and **Stjepan Dekanic** (presenter; stjepan.dekanic@zg.t-com.hr) is a research assistant in the Department of Ecology and Silviculture, Forest Research Institute Jastrebarsko, Trnjanska 35, HR-10000, Sagreb, Croatia.

Growth Performance of a Hill Dipterocarps Forest Five Years After Harvesting at Angsi Forest Reserve, Negeri Sembilan, Malaysia

Frisco Nobilly (presented by Kamziah Abd Kudus)

ABSTRACT

THE FUTURE LONG-TERM TIMBER SUPPLY FROM sustainably managed forests in Peninsular Malaysia is largely dependant on the availability of timber from the productive Permanent Forest Estate, particularly from the hill dipterocarps forests. Since little virgin forest of this kind remain, much of the future log-production will come from the second and successive cuts in regenerated logged-over forest. Therefore, specific information on behaviors of particular forest stands pertaining to growth performance, mortality, density, structure, and species-composition is urgently required to evaluate management systems and their suitability in different types of forests. The study was conducted in a logged-over hill dipterocarps forest in Angsi Forest Reserve, Negeri Sembilan, Malaysia. The data consists of five early measurement periods (2000–2005) collected from 4 permanent sample plots. The sample plots were 100m x 100m, and designed based on the International Tropical Timber Organization (ITTO) guidelines. The residual stand showed signs of growth five years after logging. Stocking of trees, both over 5 cm diameter at breast height (DBH) and over 30 cm DBH showed an increase in DBH over the measurement period. However, the overall increment rates of all trees over 30 cm dbh were relatively low, when compared to the rates assumed under the Selective Management System (SMS). Though the mean annual diameter increment of the dipterocarps was higher than that of the non-dipterocarps, the overall contribution to forest growth was small due to a lower stocking of dipterocarps in the residual stand. The overall mean annual mortality (3.51 percent) of all trees over 30 cm DBH for the 5-year period was higher than that assumed under the SMS (0.9 percent). Besides poorer-than-average site conditions, the low growth rates could be attributed to the lack of post-harvest silvicultural treatment. Based on these growth rates, anticipating a second cut in 25–30 years as stipulated under SMS, would be overly optimistic for this area.

Frisco Nobilly (frisco@putra.upm.edu.my) and **Kamziah Abd Kudus** (kamziah@putra.upm.edu.my) are at the Faculty of Forestry, Universiti Putra Malaysia, 43400 UPM Serdang, Selangor, Malaysia.

Effects of Management on Timber Production and Carbon Stocks in a Boreal Forest Ecosystem Under Changing Climate: A Model-Based Approach

Jordi Garcia-Gonzalo

ABSTRACT

A PROCESS-BASED MODEL WAS USED TO investigate how management, forest structure (in terms of age-class distribution), and climate change affect the growth, timber yield, and carbon (C) stocks in a boreal forest ecosystem, (i.e., forest management unit (FMU)). Moreover, an approach to calculate the cost of C sequestration was used. In addition, it was demonstrated that the combined use of a process-based growth model, a wood products model, and a multi-objective optimization heuristic in the analysis of optimized management plans considering timber production, C sequestration *in situ* as well as in wood products, and biodiversity (in terms of deadwood) for the FMU under changing climatic conditions. In this context, we also analyzed the potential benefits of considering climate change in forest management planning. For the optimization, three objective scenarios were analyzed to represent contrasting views on forest management objectives within multiple-purpose forestry.

Simulations covered 100 years using three climate scenarios (current climate, ECHAM4, and HadCM2) and six management regimes (also called stand treatment programs (STP)) including five thinning regimes and one unthinned regime. The management regimes were based on forest management recommendations applied until recently in Finland and differed from each other in the sense that the mean tree stocking varied in the stand over the rotation. Simulations were undertaken with ground-truthed stand inventory data of a forest management unit (1451 hectares) made up of a mosaic of Scots pine- (*Pinus sylvestris*), Nor-

way spruce- (*Picea abies*), and silver birch- (*Betula pendula*) dominated stands in central Finland.

A wood products model (WPM) was used to estimate carbon sequestration in products produced from simulated harvesting, with the results of the stand simulations being used as input. The output data from the WPM was used along with the results of forest stand simulations as input data for the multi-objective optimization. Thereafter, a combined random and direct search optimization heuristic was employed to find, for each stand, a STP that optimizes an additive utility function consisting of stand-level and unit-level components. A total of three management-objective scenarios were analyzed: timber production (maxTP), carbon sequestration (maxCS), and multi-objective management (MO: timber production, carbon sequestration, and biodiversity).

Regardless of the climate scenario and initial age-class distribution used, stand management had a clear effect on the mean C stock in the forest ecosystem. Any management regime allowing a higher tree stocking than usual over the rotation increased timber production and simultaneously maintained or increased the C stock in the forest ecosystem. On the other hand, the maximum C stock in the forest and the lowest net present value (NPV) were observed when no thinning was applied before the final cut. The gradual increase in temperature and precipitation with a concurrent elevation in CO_2 over the simulation period enhanced the timber production and C stocks. When using the same management for the entire management unit, the initial

Jordi Garcia-Gonzalo (jordi.garcia@joensuu.fi) is a doctoral student in forestry at the University of Joensuu, PO Box 111, Joensuu, FIN-80101 Finland.

age-class distribution had a large influence on the results of timber production (up to 20 percent difference) but not on C stock in the forest ecosystem (3 percent difference).

As a result of the optimization under changing climatic conditions, significant differences were found in the share of allocated STPs within the FMU between different management-objective scenarios as well as between climate scenarios within each objective scenario. The relative increase in the utility of optimized plans due to climate change differed somewhat between the objective scenarios. For maxTP, the maximum increase was 16.8 percent (ECHAM4), while for maxCS it was 9.9 percent (HadCM2), and for MO 11.3 percent (ECHAM4). Depending on the management objectives and climate scenario, optimization contributed between 30 percent and 50 percent of that gain, the rest comes from increased production due to climate change. In conclusion, the combined use of process models and multi-objective optimization appears to be a promising approach for multiple-use management planning under conditions of climate change.

A Standardized Measure of Goodness-of-Fit for Forest Projection Models Involving Repeated Measurements

Shongming Huang

ABSTRACT

Forest projection models are commonly used to provide quantitative forward and backward projections of complex stand dynamics over time. In order to judge the goodness-of-fit of these models, various statistical measures, and graphic techniques such as residual and studentized residual plots have traditionally been used, with the most common ones being R^2 (coefficient of determination), root mean square error, and chi-square related statistics. Unfortunately, many of these measures usually apply only to one-time measurement data. They could provide very misleading results when applied to repeatedly measured data (RMD). In this study, data structures and model types from RMD were discussed. The dangers of using these measures to gauge the goodness-of-fit of a model or to discriminate the goodness-of-fit of alternative models were illustrated. An alternative measure of goodness-of-fit, based on a vector of R^2 values each calculated in a way similar to the prediction sum of squares (PRESS) concept, was proposed. The usefulness and the robustness of this alternative measure for differentiating the goodness-of-fit of models that would otherwise be undistinguishable, was demonstrated based on repeatedly measured height-age, mortalitym and basal area increment data from permanent sample plots.

INTRODUCTION

REPEATEDLY MEASURED DATA (RMD) REFERS TO data sets with multiple measurements of a variable or variables on the same experimental unit over a period of
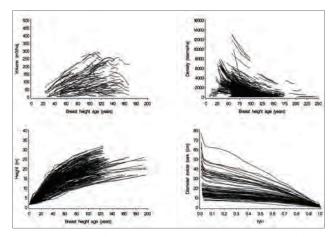
Figure 1. Examples of repeatedly measured data: volume-age (top-left) and density-age (top-right) trajectories from permanent sample plots, and height-age trajectories (bottom-left) and diameter-relative height curves (bottom-right) from stem analysis trees, where h is the height above ground corresponding to the point of diameter measurement, and H is total tree height.

time (Davidian and Giltinan 1995, Little et al. 2006). In forestry, the most common experimental unit (or "subject") is a permanent sample plot (PSP), or a stem analysis tree (Gregoire et al. 1995). In a PSP, all trees that meet a minimum threshold, (e.g., 0.3 m or 1.3 m in height) are measured repeatedly over time for their heights, diameters, conditions and mortality status, etc. When conducting stem analysis (tree sectioning) studies, the trajectories of height-age, diameter-age, and height-diameter can be re-constructed to determine how the heights and diameters of the trees change over time. Fig. 1 illustrates some of the most common RMD obtained from PSPs and stem analysis trees.

RMD can also refer to data sets with multiple measure-

Shongming Huang (shongming.huang@gov.ab.ca) is in the Forest Management Branch, Alberta Ministry of Sustainable Resource Development, 8th Floor, 9920-108 Street, Edmonton, Alberta T5K 2M4, Canada.
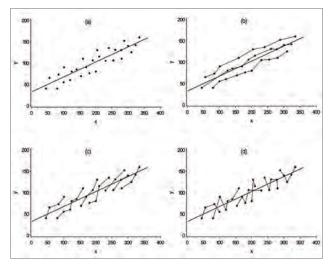
Figure 2. Twenty-right hypothetical data points unconnected (a), and connected in different ways (b, c and d). The data points and the connected trajectories in (b), (c) and (d) are listed in Table 1. The simple linear regression line (y = 31.9217 + 0.35189x) obtained from the ordinary least squares fit is overlaid on the data. Note that the same data points appear in all four graphs.

ments over distance or space. A typical example of such data is the diameter measurement taken along the stems of sectioned trees at intervals of equal or unequal lengths (as shown in Fig. 1, bottom-right graph), for developing tree volume or taper functions (Gregoire and Schabenberger 1996, Trincado and Burkhart 2006).

When RMD from different experimental units (plots or trees) are pooled together for model development, the pooled data are frequently referred to as longitudinal data, cross-sectional data, or panel data in different contexts (Judge et al. 1985, Diggle et al. 1994, Gregoire et al. 1995, Baltagi 2005). In practice, these different terms for data sets are

often used interchangeably, and are commonly referred to as RMD in a generic sense.

RMD is the foundation for developing forest growth and yield models. There are a number of distinct, yet very flexible features about the RMD analysis. Different data structures could be formulated from the observed data, different modeling approaches could be taken, and different goodness-of-fit measures could be reported. Because of its flexibility and the lack of a common, intuitive goodness-of-fit measure, it can be very difficult to judge the goodness-of-fit of models developed using RMD. Many of the reported goodness-of-fit measures appear to be uninformative, futile, misleading, or just plain wrong.

The main objective of this study was to propose and evaluate a goodness-of-fit measure for models developed using RMD. Data structures and modeling approaches associated with RMD were first reviewed, along with an assessment of the traditional goodness-of-fit measures. A goodness-of-fit index (GOFI) was then proposed and evaluated using data obtained from PSPs. The concept was first illustrated on a hypothetical data set based on simple linear regression.

DATA
Hypothetical Data
Table 1 lists 28 hypothetical data points used for this study, where *x* is the explanatory variable and *y* is the response variable. A scatter plot of the data is shown in Fig. 2(a). The same data were also connected in different ways in Fig. 2(b)-2(d) to create RMD, emulating data obtained from PSPs and stem analyses.

Table 1—Twenty-eight hypothetical data points.

		Subject					Subject		
x	*y*	Fig. 2(b)	Fig. 2(c)	Fig. 2(d)	*x*	*y*	Fig. 2(b)	Fig. 2(c)	Fig. 2(d)
45	40	3	1	1	200	80	2	4	4
56	65	1	1	1	204	130	1	3	4
80	40	2	2	2	210	115	3	4	4
84	73	1	1	1	230	105	2	5	3
100	55	2	2	1	240	135	1	4	5
101	90	1	1	2	254	106	2	6	5
120	60	2	2	2	260	131	3	5	5
125	80	3	2	2	278	130	3	6	5
140	85	3	2	2	280	110	2	7	5
154	69	2	3	3	288	152	1	5	6
160	110	1	2	2	300	140	3	6	6
170	90	3	3	3	310	125	2	7	6
180	76	2	4	3	323	142	3	7	6
190	106	3	3	3	335	160	1	7	6

Note: Fig. 2(a) shows a scatter plot of the data points. Subject refers to the trajectories shown in Fig. 2(b), 2(c) and 2(d). For example, the x-y values were assigned to 3 subjects (trajectories) in Fig. 2(b).
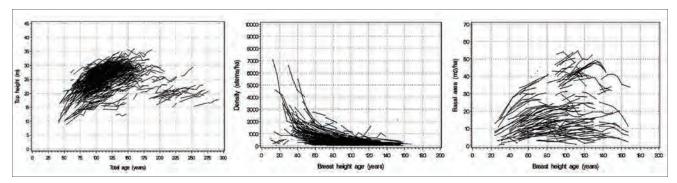
Figure 3. Repeatedly measured data from permanent sample plots: white spruce top height–age data (left), aspen density–age data (middle), and black spruce basal area–age data (right).

Table 2. Growth intervals and data structures based on a trajectory measured four times.

Structure I	Structure II	Structure III	Structure IV	Structure V	Structure VI
$y_1, x_1 - y_4, x_4$	$y_1, x_1 - y_4, x_4$	$y_1, x_1 - y_2, x_2$	$y_1, x_1 - y_2, x_2$	$y_1, x_1 - y_2, x_2$	$y_1, x_1 - y_2, x_2$
	$y_4, x_4 - y_1, x_1$	$y_2, x_2 - y_3, x_3$	$y_2, x_2 - y_3, x_3$	$y_1, x_1 - y_3, x_3$	$y_1, x_1 - y_3, x_3$
		$y_3, x_3 - y_4, x_4$	$y_3, x_3 - y_4, x_4$	$y_1, x_1 - y_4, x_4$	$y_1, x_1 - y_4, x_4$
			$y_2, x_2 - y_1, x_1$	$y_2, x_2 - y_3, x_3$	$y_2, x_2 - y_3, x_3$
			$y_3, x_3 - y_2, x_2$	$y_2, x_2 - y_4, x_4$	$y_2, x_2 - y_4, x_4$
			$y_4, x_4 - y_3, x_3$	$y_3, x_3 - y_4, x_4$	$y_3, x_3 - y_4, x_4$
					$y_2, x_2 - y_1, x_1$
					$y_3, x_3 - y_1, x_1$
					$y_4, x_4 - y_1, x_1$
					$y_3, x_3 - y_2, x_2$
					$y_4, x_4 - y_2, x_2$
					$y_4, x_4 - y_3, x_3$

RMD from Permanent Sample Plots

Repeatedly measured PSP data collected by the Forestry Division of Alberta Ministry of Sustainable Resource Development were used for this study. The PSPs were installed across the province. They covered typical ranges of stand and site conditions. Details of the data collection procedure can be found in the PSP manual (http://srd.alberta.ca/forests/managing/manuals.aspx).

Three data sets from the PSP database were selected for use in this study (see Fig. 3): white spruce (*Picea glauca* (Moench) Voss) top height–age data, aspen (*Populus tremuloides* Michx.) density–age data, and black spruce (*Picea mariana* (Mill.) B.S.P.) basal area–age data. Two main characteristics of these three data sets are 1) the response variable for each plot was measured repeatedly over time, and 2) each plot was measured at irregular time intervals. As a result, the measurements were unequally spaced and the total number of measurements per plot were different (e.g., some were measured three times, others five and six times following different, irregular schedules).

Data Structure from RMD

Different growth intervals can be obtained from RMD and arranged into one of the six data structures to estimate model parameters (Huang 1997): I (longest forward), II (longest), III (non-overlapping forward), IV (non-overlapping), V (all possible forward), and VI (all possible combinations). These growth intervals and the data structures derived from them are summarized in Table 2 and illustrated in Fig. 4, based on a trajectory measured four times. For a trajectory that is measured k times, the number of growth intervals are 1, 2, (k-1), 2(k-1), k(k-1)/2, and k(k -1) for data structures I, II, III, IV, V, and VI, respectively.

In the past, many models were estimated based on data structures arranged in a forward direction. This restriction appears unwarranted because there are many cases in which an earlier value or an initial condition must be predicted from a later value. For instance, tree/plot height at age 50 (site index) is predicted from the height-site index model, based on the observed height at 100 years. The data structures II, IV, and VI shown in Fig. 4 and Table 2 removed

233
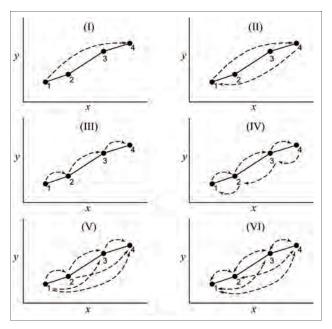
Figure 4. An illustration of the growth intervals and data structures: I (longest forward), II (longest), III (non-overlapping forward), IV (non-overlapping), V (all possible forward), and VI (all possible combinations).

this restriction. They incorporated the backward growth intervals into the estimation process to ensure that the data structures to be encountered in model applications were fully represented during model estimation. Otherwise, the reported goodness-of-fit measures and other fit statistics resulting from the model estimation might not be as relevant or compatible.

Common Measures of Goodness-of-fit

Numerous goodness-of-fit measures have been developed to judge how well a model fits the data. The most common ones are R^2 (coefficient of determination or fit index), adjusted R^2, and mean square error (MSE) or root mean square error (RMSE):

$$[1] \quad R^2 = 1 - \frac{\sum (y_i - \hat{y}_i)^2}{\sum (y_i - \bar{y})^2}$$

$$[2] \quad R^2_{adj} = 1 - \left(\frac{n-1}{n-p}\right)(1 - R^2)$$

$$[3] \quad RMSE = \sqrt{MSE} = \sqrt{\frac{SSE}{n-p}} = \sqrt{\frac{\sum (y_i - \hat{y}_i)^2}{n-p}}$$

where y_i and $\hat{y}_i$ are the ith observed and predicted y values, $\bar{y}$ is the arithmetic mean of y_i (i = 1, 2, 3, …n), SSE is sum of square errors, and p is the number of model pa-

rameters. Eqs. [1]–[3] (plus residual plots) have been used ubiquitously as the criteria for gauging the goodness-of-fit of a model, and for comparing and discriminating among alternative models.

Many other goodness-of-fit measures have also been developed, such as Amemiya's adjusted R^2, Mallow's C_p, random walk R^2, Akaike's information criterion, Schwarz Bayesian information criterion, and Amemiya's prediction criterion (Judge et al. 1985). They are all modified or scaled forms of R^2, MSE or SSE. For instance, the least squares based Akaike's information criterion (AIC_{LS}) and the Schwarz Bayesian information criterion (BIC_{LS}) take the following forms:

$$[4] \quad AIC_{LS} = n\ln(MSE) + 2p$$

$$[5] \quad BIC_{LS} = n\ln(MSE) + p\ln(n)$$

Various χ^2–based goodness-of-fit statistics can also be used (Huber-Carol et al. 2002, Yang et al. 2004). Most of them are derived from Pearson's χ^2 test statistic, $\chi^2 = \sum_{i=1}^{c}(O_i - E_i)^2 / E_i$ where O_i is the observed frequency and E_i is the expected frequency from a theoretical distribution, and i is the number of classes (i = 1, 2, …, c). For classical ordinary least squares regression where each response observation is assumed to come from a normal distribution centered vertically at the level implied by the fitted model, and where the variance of each normal distribution is assumed to be the same (σ^2, estimated by MSE), the χ^2 goodness-of-fit statistic can be written as:

$$[6] \quad \chi^2 = \sum_{i=1}^{n} \frac{(y_i - \hat{y}_i)^2}{\hat{y}_i}$$

The χ^2 statistic expressed in [6] is asymptotically $\chi^2_{(n-p-1),\alpha}$ distributed with ($n - p - 1$) degrees of freedom at a given α level (α = 0.05 throughout this study).

Since the size of the RMSE (or MSE), AIC_{LS}, BIC_{LS} and χ^2 are dependent on the scale and the type of data involved (e.g., an RMSE of 0.1 or an AIC_{LS} of 2000 may indicate a very good or a really bad model), the most common single overall goodness-of-fit measure is R^2 (or adjusted R^2 when comparing competing models). R^2 indicates the proportion of total variation explained or accounted for by a fitted model. In most practical applications, the R^2 value for an appropriately fitted model is generally between 0 and 1, with 0 indicating no relationship and 1 indicating a perfect relationship. Poorly fitted models, especially those without

an intercept term, can have negative R^2 values.

While R^2 has its own limitations (Kvalseth 1985, Anderson-Sprecher 1994), it does give modelers and model users an overall indication of the goodness-of-fit of a model, in addition to being suitable for comparing competing models. For instance, an R^2 value of 0.98 represents a good fit, as 98 percent of the total variations in the data were accounted for by the model. An R^2 value of 0.10 represents a poor fit, as the model only accounted for 10 percent of the total variation and the remaining 90 percent was unaccounted for.

Modeling Approaches Based on RMD

To appreciate different modeling approaches that can be used for RMD analysis, RMD was first treated as if it were one-time, temporary measured data (TMD).

RMD Treated as TMD

If repeatedly measured data are treated as one-time, temporary measured data, the trajectories shown in Fig. 2(b)–2(d) would be disconnected and all three graphs would become scatter plots of 28 data points, as shown in Fig. 2(a). The same simple linear regression line would be obtained for all four data sets, based on the ordinary least squares (LS) method:

[7] $y = b_0 + b_1 x$ ($b_0 = 31.9217$ and $b_1 = 0.35189$)

More detailed fit statistics are listed in Table 3. Residual plots from the LS fits treating the data as TMD looked the same, as shown in Fig. 5(a). For illustration, the residuals were connected in Fig. 5(b)–5(d) to form residual trajectories that correspond to the data trajectories shown in Fig. 2(b)–2(d).

Once the parameters were available, the χ^2 statistic could be calculated using eq. [6] ($\chi^2 = 66.3673$). The calculated χ^2 statistic is greater than $\chi^2_{(n-p-1),\alpha} = \chi^2_{25,0.050} = 37.6525$, which means that the agreement between observed y_i and predicted $\hat{y}_i$ values is poor and there is a lack of fit. This is bewildering considering that the regression line fitted the data in Fig. 2(a) reasonably well. Yang et al. (2004) observed a similar phenomenon in which the χ^2 test was found to

be overly sensitive. Narsky (2003) discussed the problems associated with the χ^2 test and presented a new method using distance to nearest neighbor. Schunn and Wallach (2005) discussed reasons why the use of χ^2 test could be disastrous for most applications.

When RMD was treated as TMD, the first key point to note is that many important fit statistics, such as the R^2 and RMSE values, lose their ability to represent and/or differentiate the goodness-of-fit of models. This is illustrated in Fig. 2, where a reasonable fit, as in Fig. 2(a), and a poor fit, as in Figs. 2(c)–2(d), have the same R^2 and RMSE values given in Table 3. It is often futile and sometimes very misleading to report the conventional fit statistics when RMD was treated as TMD.

The second key point to note is that any judgement on the goodness-of-fit of a model, or the determination of the 'best' model among alternative models, is better handled by ocular methods guided by a reasonable understanding of the relevant biological theory. For instance, visually inspecting the graphics, such as the plots of the fitted model overlaid on the original data (e.g., Fig. 2), or the plots of residual trajectories (rather than residual points) against the predicted y (e.g., Fig. 5), provides a much more powerful tool than many fit statistics for discerning the goodness-of-fit of a model.

The more fundamental question to be addressed is: if RMD are recognized as repeatedly measured data (i.e., not as one-time TMD), are the conventional fit statistics such as R^2 and RMSE appropriate for judging the goodness-of-fit of a model?

In order to answer this question, we first need to look at the type of models that can be developed based on the data structures associated with RMD.

Model Types Based on RMD

Three general approaches can be used to develop three types of models based on RMD.

1) Cumulative function—
All cumulative functions can be expressed in a general

Table 3. Summary statistics from the least squares fit of eq. [7] on data shown in Fig. 2.

Model	Type	Data structure	n	Estimate	Std. Err.	t-value	Pr > |t|	RMSE	R^2	$R^2_{adj.}$
[7]	Cumulative	Scatter	28	$b_0 = 31.9217$ $b_1 = 0.35189$	7.20586 0.03418	4.43 10.30	0.0002 <.0001	15.160	0.8031	0.7955

Note: Cumulative type refers to $y = b_0 + b_1 x$, which can be expressed as a cumulative function of the general form $y = f(x)$. RMSE, R^2 and $R^2_{adj.}$ are defined and calculated in [3], [1] and [2], respectively. Std. Err. is standard error of the estimate.
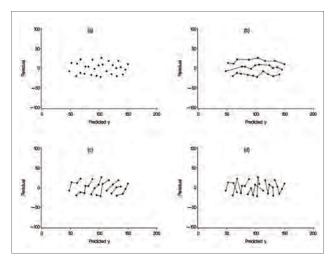
Figure 5. Residual plot (a) and residual trajectories (b, c, d) from the ordinary least squares fits of the simple linear regression $y = b_0 + b_1x$ on the data shown in Figure 2.

form as:

[8] $y = f(x)$

where the response variable y is expressed as a linear or nonlinear function of the explanatory variable x (x can be a single variable or a multiple variable matrix). Cumulative functions are typically developed by treating RMD as TMD, as illustrated in the preceding section.

Cumulative functions have been widely used in forest growth and yield studies. They are appropriate for many purposes, including obtaining averages for RMD. However, these functions have a number of serious limitations, the most important one being that they generally don't take into account the growth patterns embedded in the observed growth trajectories in RMD. Seemingly reasonable cumulative functions as judged by fit statistics could in

fact be very poor representations of RMD. This was clearly evident in Figs. 2(c). and 2(d). In most cases when RMD are treated as TMD, ocular methods are the only methods that can be used to correctly determine the goodness-of-fit of cumulative functions.

2) Difference equation—
Difference equations can be expressed in the following general form, where y_1 and y_2 are the y values at (typically) times x_1 and x_2, respectively:

[9] $y_2 = f(y_1, x_1, x_2)$

Difference equation techniques have been widely used in growth and yield modeling, particularly in the development of site index models (Clutter at al. 1983). They have also been used to develop mortality (density-age) and other types of models (Huang et al. 2001). Using the simple linear regression [7] as an example, difference equations can be obtained by expressing any two y-x pairs on the same growth trajectory as follows:

[10] $y_1 = b_0 + b_1x_1$ $y_2 = b_0 + b_1x_2$

Isolating b_0 in [10] and solving for y_2 produces:

[11] $y_2 = y_1 + b_1(x_2 - x_1)$

Alternatively, if b_1 is isolated in [10], we have:

[12] $y_2 = b_0 + (y_1 - b_0) x_2 / x_1$

For a function with p parameters, p difference equations can be formulated.

There are two different approaches for obtaining the parameter estimates for difference equations. The first ap-
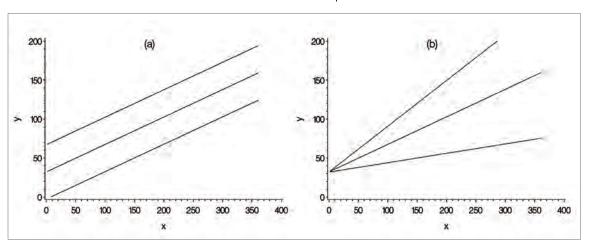
Figure 6. Difference equation growth curves generated from eqs. [11] (left) and [12] (right), based on the estimated coefficients ($b_0 = 31.9217$, $b_1 = 0.35189$) for the cumulative function $y = b_0 + b_1x$, and given y_1 values of 50, 85 and 120 at a fixed reference x_1 value of 150.

proach involves fitting a cumulative function first. After the parameters are estimated, the cumulative function with p parameters could be converted into p difference equations. For instance, *after* the two parameters in $y = b_0 + b_1 x$ are estimated, they could be constrained to formulate two difference equations [11] and [12]. Fig. 6 shows two sets of curves generated from eqs. [11] and [12], based on the estimated coefficients ($b_0 = 31.9217$, $b_1 = 0.35189$) for the cumulative function, and given y_1 values of 50, 85 and 120 at a fixed reference x_1 value of 150. Note that, from the same original cumulative function $y = b_0 + b_1 x$, two very different sets of difference equation growth curves are obtained.

The first approach applies to other more complex functions. For instance, once the cumulative Chapman-Richards function $y = a(1-e^{-bx})^c$ has been estimated, any one of the three parameters could be isolated to form three difference equations and to generate growth curves (Clutter et al. 1983). Depending on which parameter is chosen for isolation, the resulting curves would have very different shapes. There really is not a way of selecting the best parameter to isolate from among all the parameters that could be isolated, even though modelers provided all sorts of justifications to contend why a particular parameter related to the asymptote, rate or shape should be isolated (the likely truth is that the asymptote, rate and shape can all change). Additional analyses must be conducted to find out the 'best' parameter to isolate, and to determine which, if any, set of curves may be considered the most reasonable. Such analyses are best carried out by ocular methods, guided by the suggestions of relevant theory, by a modeler's knowledge of the data and the understanding of the innate relationship to be built, and (unfortunately sometimes) by a desire to produce a

pre-conceived or "wanted" answer for various purposes.

Since the first approach entails the fitting of cumulative functions, it does not require RMD. Even if RMD is available, cumulative functions are often developed by treating RMD as TMD, which could cause serious problems as previously discussed. The most critical problem is that the goodness-of-fit measures and the other fit statistics obtained in the model estimation process become irrelevant when a cumulative function is re-formulated into difference equations. The goodness-of-fit of the difference equations is unknown and shall not be misinterpreted.

The second approach involves directly estimating difference equations based on one of the data structures formulated from RMD. Rather than first fitting a cumulative function, parameters of a difference equation are directly estimated on one of the RMD structures. As an example, for the three trajectories shown in Fig. 2(b), six data structures as described in Table 2 and Fig. 4 can be formulated, and the parameters for the difference equations [11] and [12] directly estimated. The estimates obtained in this manner (Table 4) are different from those obtained from fitting the cumulative function (Table 3).

Compared to the first approach, the goodness-of-fit measures (RMSE, R^2, $R^2_{adj.}$) from the second approach (as shown in Table 4) differ depending on the model and the data structure used, particularly for model [12] where the RMSE and R^2 vary greatly. For [11], the estimated coefficients are identical for data structures I and II, III and IV, as well as V and VI. Growth curves (not shown here) based on the direct estimates shown in Table 4 were different from those shown in Fig. 6. The goodness-of-fit measures obtained from the second approach are relevant

Table 4. Fit statistics for equations [11] and [12] on the data shown in Fig. 2(b)

Model	Type	Data structure	n	Estimate	Std. Err.	t-value	Pr > |t|	RMSE	R^2	$R^2_{adj.}$
[11]	Difference equation	I	3	$b_1 = 0.35770$	0.00943	37.92	0.0007	4.302	0.9396	0.9396
		II	6	$b_1 = 0.35770$	0.00597	59.96	<.0001	3.848	0.9948	0.9948
		III	25	$b_1 = 0.36713$	0.03740	9.82	<.0001	6.535	0.9511	0.9511
		IV	50	$b_1 = 0.36713$	0.02620	14.03	<.0001	6.468	0.9557	0.9557
		V	118	$b_1 = 0.35620$	0.00538	66.19	<.0001	7.232	0.9214	0.9214
		VI	236	$b_1 = 0.35620$	0.00380	93.80	<.0001	7.217	0.9514	0.9514
[12]	Difference equation	I	3	$b_0 = 29.7931$	8.8174	3.38	0.0775	74.43	-17.08	-17.08
		II	6	$b_0 = 29.7366$	5.6029	5.31	0.0032	47.95	0.1952	0.1952
		III	25	$b_0 = 24.2689$	4.2158	5.76	<.0001	8.847	0.9104	0.9104
		IV	50	$b_0 = 25.6332$	3.3410	7.67	<.0001	7.843	0.9348	0.9348
		V	118	$b_0 = 28.7940$	1.2286	23.44	<.0001	22.305	0.2528	0.2528
		VI	236	$b_0 = 28.9035$	0.8913	32.43	<.0001	16.814	0.7360	0.7360

Note: RMSE, R^2 and $R^2_{adj.}$ are defined in [3], [1] and [2], respectively. Std. Err. is standard error of the estimate. Data structures are illustrated in Table 2 and Fig. 4.

only to the specific difference equation formulation and to the data structure used.

The second approach also applies to other more complex functions. For instance, parameters a, b and c of the Chapman-Richards function $y = a(1-e^{-bx})^c$ can be isolated first to produce the following difference equations, and then the remaining parameters in the difference equations can be directly estimated, or related to other variables through the parameter prediction method and estimated (Clutter et al. 1983, Huang 1997):

$$[13] \quad y_2 = y_1 \left(\frac{1 - \exp(bx_2)}{1 - \exp(bx_1)} \right)^c$$
$$(b = b_0 y_1^{b_1} b_2^{y_1/x_1} \quad c = b_3 y_1^{b_4} x_1^{b_5})$$

$$[14] \quad y_2 = a(1 - m^{x_2/x_1})^c, \quad m = 1 - (y_1/a)^{1/c}$$
$$(a = b_0 y_1^{b_1} \quad c = b_3 y_1^{b_4})$$

$$[15] \quad y_2 = a \left(\frac{y_1}{a} \right)^m, \quad m = \frac{\ln[1 - \exp(-bx_2)]}{\ln[1 - \exp(-bx_1)]}$$
$$(a = b_0 y_1^{b_1} \quad b = b_2 y_1^{b_3})$$

where the parameter prediction functions are expressed in parentheses. Once the parameters of a difference equation are related to other variables through the parameter prediction method, the difference equation may not possess the standard difference equation characteristics any more (Huang 1997). Typically, the parameters of difference equations are estimated based on one of the six data structures presented earlier *after* the difference equations are formulated.

3) Increment (or decrement) function—

An increment (or decrement) function is also referred to as a change function. It usually models the change in y as a function of initial conditions:

$$[16] \quad y_{inc} = \frac{y_2 - y_1}{x_2 - x_1} = f(x_1)$$

where y_{inc} is the change in y per unit of x (e.g., per year), and $f(x_1)$ indicates a linear or nonlinear function of the initial condition x_1. In the simple linear regression case, [16] can be expressed more explicitly as:

$$[17] \quad y_{inc} = f(x_1) = b_0 + b_1 x_1$$

Alternatively, the increment y_{inc} can also be expressed as periodic increment, where $y_{inc} = (y_2 - y_1)$. If this is the case, the interval length $(x_2 - x_1)$ must be appropriately accounted for on the right-hand side of the equation. There are also cases where the increment function [16] might be expanded to include other additional variables:

$$[18] \quad y_{inc} = \frac{y_2 - y_1}{x_2 - x_1} = f(y_1, x_1, x_2)$$

However, since such an expression allows a variable or its transformations (e.g., y_1 or x_1) to appear on both sides of an equation, some specialized techniques such as two- or three-stage least squares (Judge et al. 1985, LeMay 1990, Huang and Titus 1999) may need to be used to obtain the most appropriate estimates, and the interpretations must be made pertinently and carefully. Otherwise, both the fit statistics (usually with an overstated R^2 value) and the interpretations could be very misleading. In this study the more common type [17] was fitted on six data structures

Table 5. Fit statistics for increment function [17] on the data shown in Fig. 2(b).

Model	Type	Data structure	n	Estimate	Std. Err.	t-value	Pr > |t|	RMSE	R^2	$R^2_{adj.}$
[17]	Increment function	I	3	$b_0 = 0.343292$	0.05330	6.44	0.0981	0.0217	0.0840	-0.8320
				$b_1 = 0.000260$	0.00086	0.30	0.8128			
		II	6	$b_0 = 0.359345$	0.01160	31.06	<.0001	0.0161	0.0003	-0.2496
				$b_1 = -1.85E\text{-}6$	0.00005	-0.04	0.9721			
		III	25	$b_0 = 0.589959$	0.12680	4.65	0.0001	0.2460	0.1415	0.1042
				$b_1 = -0.00128$	0.00066	-1.95	0.0638			
		IV	50	$b_0 = 0.604899$	0.09330	6.49	<.0001	0.2410	0.1398	0.1219
				$b_1 = -0.00125$	0.00045	-2.79	0.0075			
		V	118	$b_0 = 0.462134$	0.02910	15.88	<.0001	0.1320	0.1214	0.1139
				$b_1 = -0.00075$	0.00019	-4.00	0.0001			
		VI	236	$b_0 = 0.446895$	0.02230	20.04	<.0001	0.1347	0.0771	0.0731
				$b_1 = -0.00047$	0.00011	-4.42	<.0001			

Note: RMSE, R^2 and $R^2_{adj.}$ are defined in [3], [1] and [2], respectively. Std. Err. is standard error of the estimate. Data structures are illustrated in Table 2 and Fig. 4.

formulated from the data shown in Fig. 2(b). Results are given in Table 5.

Compared to the difference equation results shown in Tables 4, the goodness-of-fit measures from the increment model shown in Table 5 also differ depending on the data structure used. However, the most striking aspect is that the R^2 values from the increment model are much lower than those from the difference equations (except for data structure I where only three observations were used). Given the R^2 values from the increment model (in the range of 0.0003 to 0.1415), one would without hesitation conclude that the model gave very poor fits to the data. Later it will be shown why such a conclusion could be erroneous.

A fitted cumulative function may sometimes be converted into an increment model indirectly by taking the derivative of y with respect to x. For the simple linear regression function [7], the increment function (i.e., the rate of change per unit of x) is a constant b_1:

[19] $\partial_y / \partial_x = b_1$

While the concept of taking the derivative of a cumulative function to obtain the increment function is fairly straightforward, in practice the execution may not be easy because the derivative could be very complex and computationally very expensive to obtain, especially for nonlinear models with multiple, interrelated variables. In addition, the derivative obtained from a cumulative function is supposed to represent growth rate. Many have suggested taking derivatives as one of the methods for developing increment models, and some have used derivatives to compute growth rates, as illustrated in eq. [19]. However, this approach would be valid only if the function and the data follow the same trend, as in Fig. 2(b). Otherwise, the growth rate does not reflect the true growth rate embedded in RMD at all, as in Fig. 2(c)–(d). Although this may be relatively easy to understand for a simple linear model, it could be very difficult to comprehend in a multivariate, multi-dimensional situation. The deficiencies associated with the fitting of a cumulative function by treating RMD as TMD could be found in a derivative-based increment model. Furthermore, the goodness-of-fit of an increment model obtained in such a manner is unknown, as the goodness-of-fit measures obtained for the cumulative function are no longer applicable to the derivative-based increment model.

A Goodness-of-Fit Index on RMD

The conventional R^2 value on model fitting data indicates the proportion of total variation explained by a fitted model. It is scale-independent. Given an R^2 of 0.8, we know that 80 percent of the total variation in the data is accounted for by the fitted model. This gives us a direct, intuitive indication about the overall goodness-of-fit of the model on the data.

In the analysis of RMD, the reported R^2 values vary considerably depending on the model type and the data structure used. When RMD was treated as TMD and a cumulative function estimated, the R^2 value (e.g., in Table 3) ignored repeated measures and pertained only to the scattered point data. When RMD was treated as RMD and a difference equation or an increment function estimated, the R^2 values (e.g., in Tables 4 and 5) fluctuated greatly (and are typically misleading, as will be shown later), which made the choice of a better approach almost impossible. This may explain why R^2 has typically not been reported in standard RMD analysis (Pinheiro and Bates 2000, Littell et al. 2006).

The reported statistics in RMD analysis are likelihood-based statistics such as: -2 log-likelihood, Akaike's information criterion (AIC) and Schwarz Bayesian information criterion (BIC):

[20] $AIC = -2\ln(L) + 2p$

[21] $BIC = -2\ln(L) + p\ln(n)$

where L is the likelihood function, p is the number of model parameters and n is the sample size (Judge et al. 1985, Littell et al. 2006). Note that the likelihood-based AIC and BIC are different from the LS-based AIC_{LS} and BIC_{LS} (eqs. [4] and [5]). Both AIC and BIC are used to compare competing models. BIC charges a heavier penalty for a large number of parameters (similar in concept to adjusted R^2). The model with the smaller information criteria is said to be a better fit. Both AIC and BIC can also be utilized for choosing amongst several covariance structures.

While AIC and BIC have been used extensively in comparing competing models, when all models are poor, the model with the smaller information criteria is considered relatively better, but it is still a poor model. An AIC (or BIC) value of 200 or 1800 does not connote to any direct, intuitive, and scale-independent R^2-type indication about the overall goodness-of-fit of the model, or about how much total variation was explained by the model. In other words, an AIC (or a BIC) value of 200 or 1800 could mean
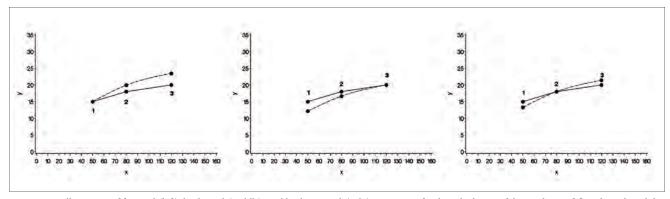
Figure 7. An illustration of forward (left), backward (middle), and bi-directional (right) projections for the calculation of the goodness-of-fit index. The solid lines represent observed trajectories. The dashed lines represent model projections. The first, third (last), and second (middle) observations are used as the starting point in forward, backward, and bi-directional (forward and backward) projections, respectively.

a superb model, or an abysmal fit.

Without a direct, intuitive, and scale-independent R^2-type indicator, we really do not have any idea about the overall goodness-of-fit of a model, and we do not know how much total variation was explained by the model. However, if the conventional R^2 values were reported (as in Tables 3, 4 and 5), they could be very misleading. Reporting the AIC and BIC values would help to differentiate competing models, but they do not indicate the goodness-of-fit of a model as is normally understood. This creates a dilemma for model developers and model users alike.

For linear models estimated based on likelihood methods, researchers (mostly economists) have developed pseudo-R^2s and other types of measures to help in assessing model fit (Hardin and Hilbe 2007, Pan and Lin 2005). They include McFadden's R^2 (1 − likelihood (intercept only model) / likelihood (full model)), Ben-Akiva and Lerman's R^2, maximum likelihood R^2, Craig and Uhler's R^2, and Makelvey and Zavoina's R^2. However, the pseudo-R^2s have some serious limitations. Even the software that adopted the pseudo-R^2s stated that "we do not intend that our pseudo R^2 should be reported in formal write-ups of results" (http://www.stata.com/).

The proposed goodness-of-fit index (GOFI) on RMD uses the same basic formula for the standard R^2, but it is modified as described below and illustrated in Fig. 7, to alleviate the problems and to provide a consistent measure of goodness-of-fit for RMD analysis.

First, assume that a forward projection from a fitted model is made for a trajectory measured three times at 50, 80, and 120 years (solid lines in Fig. 7). Forward projection uses the first data pair at the beginning of the trajectory (at time 1) as input into the model to project forward to get predicted y values at other times (e.g., times 2 and 3). Once the predicted values were obtained, the differences (errors or residuals) between the observed and predicted values are assessed and a forward coefficient of determination, denote as R^2_F or R^2_1 in this example, is calculated:

$$[22] \quad R^2_F = R^2_1 = 1 - \frac{\sum_{i=1}^{n-k}(y_i - \hat{y}_i)^2}{\sum_{i=1}^{n-k}(y_i - \overline{y})^2}$$

where all variables are as defined before, except the summation is over $i = 1, 2,…(n - k)$, and k is the number of trajectories. The first pair of each trajectory was excluded from the calculation because there was no error for the first pair (the model passes through the pair, see Fig. 7).

Similarly, a backward projection that uses the last pair (at time 3) as the starting point was made, and a backward coefficient of determination, denote as R^2_L (or R^2_3 in this example), was calculated using the same formula [22], but with the last data pair with zero error excluded. For the data pair 2 in the middle of the trajectory, bi-directional (forward and backward) projections were made, with this data pair as the starting point (see Fig. 7). An R^2_M (or R^2_2 in this example) was calculated in the same manner, but with the data pair 2 excluded. The goodness-of-fit index is simply the average of the three R^2 values:

$$[23] \quad GOFI_3 = (R^2_1 + R^2_2 + R^2_3) / 3$$

For a trajectory measured n times, a general expression for GOFI is:

$$[24] \quad GOFI_n = (R^2_1 + R^2_2 + R^2_3 + … + R^2_n) / n$$

The interpretation of GOFI is similar to that of the model fitting coefficient of determination. It provides an

overall performance measure for the developed model on model fitting data.

Since RMD is often unequally spaced and unbalanced, a recommended simplified GOFI can be computed using only the forward projection from the first data pair and the backward projection from the last data pair (see Fig. 8):

$$[25] \quad GOFI = \frac{R_F^2 + R_L^2}{2}$$

where R_F^2 is the forward coefficient of determination based on the first pair, and R_L^2 is the backward coefficient of determination based on the last pair. Because the computation of R_F^2 and R_L^2 involves the longest possible intervals, the prediction errors are typically the largest. The GOFI calculated in [25] generally represents the worst goodness-of-fit on a given data set—a feature that guards against an inflated goodness-of-fit that might otherwise be obtained. It is interval length dependent—a feature that echoes a general fact that short-term predictions are usually more accurate than long-term predictions. This second feature should be interpreted carefully, as a high GOFI obtained from short intervals may not be pertinent if the desired prediction intervals that a model should be assessed against need to be longer.

Many other related standard goodness-of-fit measures could also be calculated, for example:

$$[26] \quad RMSEP = \sqrt{\frac{\sum_{i=1}^{n-k}(y_i - \hat{y}_i)^2}{n-k}}$$

$$[27] \quad ME = \frac{\sum_{i=1}^{n-k}(y_i - \hat{y}_i)}{n-k} \qquad \text{or}$$

$$MAD = \frac{1}{n-k} \cdot \sum_{i=1}^{n-k}|y_i - \hat{y}_i|$$

$$[28] \quad MPE = \frac{100}{n-k} \cdot \sum_{i=1}^{n-k}\left(\frac{y_i - \hat{y}_i}{y_i}\right) \qquad \text{or}$$

$$MAPE = \frac{100}{n-k} \cdot \sum_{i=1}^{n-k}\left|\frac{y_i - \hat{y}_i}{y_i}\right|$$

where RMSEP is root mean square error of prediction, ME is mean error, MAD is mean absolute difference, MPE is mean percent error, and MAPE is mean absolute percent error. The summation is to $(n-k)$ because there are k trajectories and the starting points used in projections have zero errors and are removed from the calculations.

In the cases where a model can only make forward or backward projection, [25] reduces to:

$$[29] \quad GOFI = R_F^2 \qquad \text{or} \qquad GOFI = R_L^2$$

The GOFI statistic obtained in this manner would be similar to the standard R^2 statistic, except that it does not use the first or the last data pair in its calculation. If RMD is treated as TMD and a cumulative function fitted, GOFI would be equivalent to the standard R^2 statistic.

RESULTS AND DISCUSSION

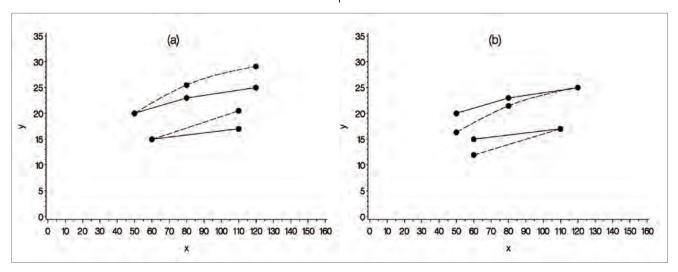The coefficients shown in Tables 4 and 5 were used to make

Figure 8. An illustration of forward (left) and backward (right) projections on unequally spaced, unbalanced repeatedly measured data, for the calculation of the goodness-of-fit index. The solid lines represent observed trajectories. The dashed lines represent model projections.

forward and backward projections on the data shown in Fig. 2(b). Prediction errors were obtained. Table 6 lists the summary statistics from the projections. Compared to the results presented in Tables 4 and 5, the results shown in Table 6 are striking on several aspects, as detailed below.

1) If the traditional R^2 fit statistics (as in Table 5) were used to judge the goodness-of-fit of the models, the increment function, with R^2 ranges from 0.0840 to 0.1415, would have been considered very poor. This could have led to some erroneous conclusions. The increment function in fact provided some of the best fits to the data, especially for data structures III, IV, and VI (see Table 6).

2) Judging from Table 4, the difference equation [12] had R^2 values exceeding 0.9 (for data structure III and IV). This could have meant that the model provided a fairly reasonable fit to the data. In truth, however, the estimates obtained from [12] would generate growth curves similar to those shown in Fig. 6(b), which were poor representations of the true trajectories shown in Fig. 2(b). Only the GOFI statistics shown in Table 6 adequately reflected the poor fits by [12], regardless of the data structure used. The GOFI statistics are also more consistent (ranging from 0.1469 to 0.2093, Table 6) than the R^2 values (ranging from -17.08 to 0.9348, Table 5).

3) The reported R^2 values for [11] range from 0.9214 up to 0.9948 (Table 4), the latter means an almost perfect fit. Four of the reported R^2 values for [11] exceed 0.95. The GOFI statistics are almost identical (range from 0.9270 to 0.9279, Table 6), and they are always lower than the R^2 values except for the data structure V. The reported R^2 values from the difference equation [11] were mostly inflated and unachievable in application, particularly those that exceeded 0.95.

4) The value in reporting R^2 from a difference equation formulation $y_2 = f(y_1, x_1, x_2)$ is questionable to say the least. The R^2 values vary considerably depending on the

Table 6. Forward and backward projection summary statistics on the data shown in Fig 2(b)

Model-data structure	Type	n − k	Prediction error				RMSEP	R^2_F or R^2_L	GOFI
			Mean	SD	Min.	Max.			
[11]-I & II	Forward	25	5.9885	5.672	-4.798	15.980	8.1698	0.9239	0.9279
	Backward	25	5.4086	6.221	-5.653	16.859	8.1486	0.9318	
[11]-III & IV	Forward	25	4.5857	5.802	-7.429	14.424	7.3042	0.9391	0.9270
	Backward	25	6.7639	6.217	-4.616	18.094	9.1023	0.9150	
[11]-V & VI	Forward	25	6.2117	5.660	-4.380	16.227	8.3268	0.9209	0.9275
	Backward	25	5.1931	6.229	-5.818	16.662	8.0136	0.9341	
[12]-I	Forward	25	13.4598	35.509	-80.406	55.655	37.3045	-0.5874	0.1469
	Backward	25	4.0084	10.192	-14.363	20.950	10.7604	0.8811	
[12]-II	Forward	25	13.3074	35.510	-80.687	55.493	37.2504	-0.5828	0.1491
	Backward	25	4.0336	10.191	-14.321	20.990	10.7692	0.8809	
[12]-III	Forward	25	-1.4378	36.773	-107.928	39.773	36.0589	-0.4832	0.1856
	Backward	25	6.4709	10.204	-10.264	24.809	11.9092	0.8544	
[12]-IV	Forward	25	2.2414	36.240	-101.131	43.695	35.5788	-0.4439	0.2093
	Backward	25	5.8627	10.185	-11.276	23.856	11.5741	0.8625	
[12]-V	Forward	25	10.7654	35.558	-85.383	52.783	36.4654	-0.5168	0.1804
	Backward	25	- 4.4537	10.181	-13.621	21.648	10.9248	0.8775	
[12]-VI	Forward	25	11.0607	35.549	-84.838	53.098	36.5449	-0.5234	0.1773
	Backward	25	4.4049	10.182	-13.703	21.572	10.9058	0.8779	
[17]-I	Forward	25	2.2470	7.199	-14.924	12.909	7.4032	0.9375	0.8711
	Backward	25	11.9747	6.986	-2.396	24.167	13.7931	0.8047	
[17]-II	Forward	25	5.7857	5.680	-5.157	15.747	8.0279	0.9265	0.9283
	Backward	25	5.5836	6.212	-5.524	17.009	8.2595	0.9300	
[17]-III	Forward	25	0.4096	4.453	-9.368	6.570	4.3825	0.9781	0.9694
	Backward	25	-3.7304	5.045	-16.079	2.621	6.1924	0.9606	
[17]-IV	Forward	25	-2.4919	4.255	-11.663	5.140	4.8569	0.9731	0.9729
	Backward	25	-0.5867	5.232	-13.592	7.635	5.1602	0.9727	
[17]-V	Forward	25	7.4287	5.336	-3.480	16.151	9.0838	0.9059	0.9253
	Backward	25	-4.4958	5.933	-15.244	4.317	7.3487	0.9446	
[17]-VI	Forward	25	3.3580	4.769	-5.760	11.111	5.7544	0.9622	0.9625
	Backward	25	2.6152	5.541	-9.051	11.919	6.0263	0.9627	

Note: RMSEP is root mean square error of prediction computed by [26], R^2_F and R^2_L are computed by [22], GOFI is the goodness-of-fit index computed by [25], and SD is standard deviation.

parameter(s) to be constrained and the data structure used (see Table 4). In many cases, a difference equation formulation tends to give unrealistically high R^2 values that look 'nice' but are not relevant in applications when predictions are made. This could be a result of the high correlation between y_2 and y_1, or an artefact of this particular type of formulation.

5) The GOFI statistic can be used more reliably than other statistics for determining the 'best' parameter(s) to constrain. This is evident in Table 6, where constraining parameter a (eq. [11]) is found to be consistently better than constraining parameter b (eq. [12]). Using the R^2 (and/or RMSE) values to determine the best parameter(s) to constrain could sometimes lead to erroneous conclusions (see Table 4). More importantly, the R^2 values (e.g., 0.9104 and 0.9348 for [12] on data structures III and IV, Table 4) are not appropriate for assessing the goodness-of-fit in applications where the attainable goodness-of-fits were much poorer (e.g., 0.1856 and 0.2093 for [12] on the same data structures III and IV, Table 6). Clearly the difference equation R^2 values were grossly overstated.

6) Data structures from RMD play an important role in parameter estimation and model development. Previous studies (e.g., Goelz and Burk 1992, Cao 1993, Huang 1997, Wang et al. 2004) showed that the 'best' data structure was model dependent, but in general, data structures III, IV, V, and VI were all reasonable. Those results were further confirmed in this study. It was found that data structure III was the most efficient and that data structure VI was the most consistent and stable. Since the longest growth interval data structures I and II ignore the observed information from intermediate measurement(s), their use should be limited. Additional studies may be needed to evaluate the bias and efficiency of various data structures from other repeatedly measured data sets. This is an area for further research.

To see if the results obtained from the hypothetical data still hold for real RMD from PSPs, three models corresponding to the data sets shown in Fig. 3 were fitted:
White spruce height-site index model:

[30] $$H_2 = H_1 \times \left(\frac{1 + \exp(b_1 + b_2\sqrt{\ln(1 + totage_1)} + b_3[\ln(H_1)]^2 + b_4\sqrt{totage_1})}{1 + \exp(b_1 + b_2\sqrt{\ln(1 + totage_2)} + b_3[\ln(H_1)]^2 + b_4\sqrt{totage_1})} \right)$$

where H_2 and H_1 are top height (i.e., average height of the 100 largest DBH trees per ha) at total age 1 and 2 ($totage_1$ and $totage_2$), respectively, and total age refers to the total age from the time of germination.

Aspen mortality (density-age) model:

[31] $$N_2 = N_1 \times \left(\frac{1 + \exp(a + b\ln(SI) + c[\log(1 + bhage_1)])}{1 + \exp(a + b\ln(SI) + c[\log(1 + bhage_2)])} \right)$$

$$a = -\left(\frac{1}{\sqrt{N_1/1000}} + \sqrt{1 + \sqrt{\frac{bhage_1}{N_1}} \ln(1 + bhage_1)} \right) \times \ln(1 + bhage_1)$$

$$b = b_1\left(\sqrt{N_1}\right)^{1/N_1} \qquad c = (1 + b_1)N_1^{\left[\frac{b_2 + \ln(N_1)}{N_1}\right]}$$

where N_2 and N_1 are stems/ha (for trees > 1.3 m) at breast height age 1 and 2 ($bhage_1$ and $bhage_2$), respectively, and SI is site index (m), i.e., top height at 50 years bhage.

Black spruce basal area increment model:

[32]
$$BAINC = \left(a_1 \exp(-a_2 bhage_1)bhage_1^{(1+a_3)} SC_1^{a_3} \times \right.$$
$$\left. [\ln(1 + N_0\sqrt{1 + bhage_1})]^2 \ln(1 + SI) \right) / \left((1 + BA_1)^{a_2} \right)$$

where BAINC = annual basal area increment (m²/ha/year), SC_1 = black spruce species composition ($BA_{black\,spruce}/BA_{all\,species}$) at time one, BA_1 = black spruce basal area (m²/ha) at time one, $bhage_1$ = breast height age (years) at time one, N_0 = initial density (stems/ha for trees > 1.3 m) at bhage zero, and SI = site index (m), i.e., top height at 50 years bhage.

All three models are parts of the GYPSY model (Growth and Yield Projection System) used in Alberta (Huang et al. 2001). Both [30] and [31] were developed from a combination of the difference equation and the parameter prediction formulation of the logistic-type model (Monserud 1984). Fit statistics for the models on data structure VI are listed in Table 7.

Table 7. Fit statistics for models [30], [31], and [32] on repeatedly measured data from PSPs

Model	Type	b_1	b_2	b_3	b_4	RMSE	R^2	$R^2_{adj.}$
[30]	Difference	13.079210	-6.03800	-0.25712	0.178732	1.1675	0.9904	0.9904
[31]	Difference	0.738940	6.53357			245.30	0.8584	0.8584
[32]	Increment	0.000112	0.05690	0.40459		0.2001	0.2668	0.2653

Note: RMSE, R^2, and $R_{adj.}^2$ are defined and calculated by [3], [1], and [2], respectively
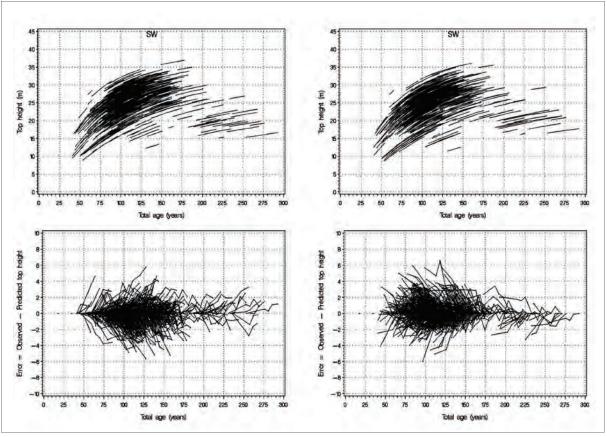
Figure 9. Forward (left graphs) and backward (right graphs) projections and associated error trajectories from model [30] on the white spruce top height-age data shown in Fig. 3.

The R^2 values shown in Table 7 would suggest that, the difference equation site index model [30] fitted the data extremely well (R^2 = 0.9904), with more than 99 percent of the total variation accounted for by the model. The basal area increment model [32] fitted the data poorly (R^2 = 0.2668), with less than 27 percent of the total variation accounted for by the model.

The estimated coefficients shown in Table 7 were used to make forward and backward projections for the relevant data sets shown in Fig. 3. As an example, Fig. 9 shows the forward and backward projections and associated error trajectories from the white spruce height-site index model [30]. Similar graphs from [31] and [32] were also produced (available upon request). They displayed similar patterns as shown in Fig. 9. Summary statistics from forward and backward projections for all three models are listed in Table 8.

The results shown in Table 8 confirmed most of the

Table 8. Summary statistics from forward and backward projections based on the PSP data.

Model	Type	n – k	Prediction error				RMSEP	R_F^2 or R_L^2	GOFI
			Mean	SD	Min.	Max.			
[30]	Forward	1496	-0.1811	1.478	-5.654	5.807	1.48819	0.8748	0.9065
	Backward	1496	0.1102	1.040	-4.531	6.587	1.04526	0.9382	
[31]	Forward	1054	20.7475	157.699	-1047.11	1019.49	158.984	0.9219	0.8611
	Backward	1054	4.0670	254.241	-2052.97	3192.27	254.153	0.8003	
[32]	Forward	459	0.8301	3.286	-14.144	14.096	3.3856	0.9361	0.9425
	Backward	406	0.2452	2.980	-14.166	14.122	2.9866	0.9488	

Note: RMSEP is root mean square error of prediction computed by [26], R_F^2 and R_L^2 are computed by [22], GOFI is the goodness-of-fit index computed by [25], and SD is standard deviation.

earlier observations. The reported R^2 (0.8584, Table 7) for the difference equation [31] was in line with the calculated GOFI (0.8611, Table 8). However, the reported R^2 (0.9904, Table 7) for the difference equation [30] was overstated and not achievable in application when predictions were made. The GOFI for [30] was 0.9065 (Table 8), an achieved number that was lower than the reported R^2.

For the basal area increment model [32], the reported R^2 (0.2668, Table 7) is much lower than the GOFI (0.9425, Table 8) achieved in application. If the R^2 statistic was used to assess the goodness-of-fit of the basal area increment model, the model would be deemed as a poor model. However, as shown in Table 8 (and figures showing the forward and backward projections and associated error trajectories, available upon request), the increment model provided very reasonable fits to the data. When predictions were made, the fitted model accounted for about 94 percent of the total variation.

While all previous analyses and results were demonstrated on model fitting data, it is worthwhile to note that the logic embedded in them is equally applicable to independent model validation data in which the GOFI could be more aptly called goodness-of-prediction index (GOPI). When the data were split into a model-fitting data set and a model-validation data set by two groups of distinct regions (i.e., not a random split), the results and subsequent inferences obtained from the validation data set (to be reported elsewhere) were very close to those obtained from the model-fitting data set, with the marginal differences likely caused by the so-called optimism principle of model validation (Picard and Cook 1984, Yang et al. 2004).

All previous analyses and results were based on the ordinary least squares method, which assumes that the error terms of a model are independently and identically distributed (i.i.d.) with mean zero and a constant variance. However, for RMD from PSPs (and stem analysis), serial correlation (i.e., correlation between the errors within the same plot), contemporaneous correlation (i.e., correlation between the errors of different plots), and various within- and between-plot heteroskedasticity (unequal error variance) might be present. In addition, the correlations could be both temporal and spatial. Furthermore, the RMD obtained from PSPs and stem analysis is typically unequally spaced (i.e., measurements were taken over intervals of varying times or distances) and unbalanced (i.e., different number of measurements were made on different experimental units).

Violation of the i.i.d. error assumption may have some important statistical consequences for LS regression. It invalidates standard regression hypothesis testing and interval estimations. The problem may be solved using the generalized least squares (GLS) method (Judge et al. 1985, LeMay 1990, Baltagi 2005) or the mixed model technique (Davidian and Giltinan 1995, Gregoire et al. 1995, Littell et al. 2006). The use of GLS and three nonlinear mixed model methods (i.e., approximate first-order, second-order, and marginal structures) was demonstrated in Huang (1997) on the stem analysis data for the development of site index models. To avoid the digression from the main purposes of this study, only the results obtained from the nonlinear mixed model fittings of [30] from the marginal structures method (Method 3) of the nonlinear mixed model estimations described in Littell et al. (2006), were presented here.

Since the PSP data used in this study are unequally spaced, unbalanced RMD, many of the time-series covariance structures such as AR(1), AR(2), MA(1), and ARMA(1,1), which all assume that the measurements are made at equally spaced time intervals, are inappropriate. Instead, spatial covariance structures used in spatial data analyses were used (Littell et al. 2006). With spatial covariance structures, the covariance is assumed to be a function of the distance (e.g., time interval) between two locations:

[33] $Cov(e_i, e_j) = \sigma^2[f(d_{ij})]$

where σ^2 is the overall error variance, d_{ij} is the distance between two measurements at times or distances i and j ($d_{ij} = |t_i - t_j|$), and $f(d_{ij})$ represents a function of d_{ij}. Seven functions listed in Littell et al. (2006) were examined to determine the most appropriate function for the data used in this study:

[34a] $f(d_{ij}) = [1 - 1.5(d_{ij}/\rho) + 0.5(d_{ij}/\rho)^3] \times 1\{d_{ij} < \rho\}$

(Spherical)

[34b] $f(d_{ij}) = \exp(-d_{ij}/\rho)$ (Exponential)

[34c] $f(d_{ij}) = \exp(-d_{ij}^2/\rho^2)$ (Gaussian)

[34d] $f(d_{ij}) = (1 - \rho d_{ij}) \times 1\{\rho d_{ij} < 1\}$ (Linear)

[34e] $f(d_{ij}) = [1 - \rho \log(d_{ij})] \times 1\{\rho \log(d_{ij}) < 1\}$ (Linear Log)

[34f] $f(d_{ij}) = \rho^{d_{ij}}$ (Power)

[34g] $f(d_{ij}) = (d_{ij} / 2v)^v \, 2K_v(d_{ij} / \rho) / \Gamma(v)$ (Matérn)

where ρ is the correlation parameter ($|\rho| < 1$). The term $1\{d_{ij} < \rho\}$ used in the spherical function is an indicator function that equals to 1 when $d_{ij} < \rho$ and equals 0 otherwise. Similar $1\{\cdot\}$ terms were used in the linear and linear log functions to indicate that they equal 1 when the condition within the parentheses holds and equal 0 otherwise. The additional parameter v in Matérn's function is a smoothness parameter, and the $K_v(\cdot)$ is the modified Bessel function. Littell et al. (2006) provided more details about these functions. The covariance structure associated with the power function [34f] for unequally spaced data, $Cov(e_i, e_j) = \sigma^2 \rho^{d_{ij}} = \sigma^2 \rho^{|t_i - t_j|}$, provides a direct generalization of the continuous autoregressive AR(x) structure for equally spaced data (Pinheiro and Bates 2000). It has been used in a number of recent studies (e.g., Nord-Larsen 2006, Trincado and Burkhart

2006, Fortin et al. 2007).

The potential problem of heteroskedasticity associated with the height-site index model [30] is relatively easier to tackle. First, White's test and the modified Breusch-Pagan test were conducted to examine the significance of the heteroskedasticity (results showed that it was significant at $\alpha = 0.05$ level). Then, following the procedures described in Huang (1997), several assumptions about the nature of the heteroskedasticity were proposed and evaluated. The variance of errors was assumed to be (1) a linear or nonlinear function of the predicted height, (2) a linear or nonlinear function of the independent variables, or (3) a factor of age or predicted height (with weight = age^k or weight = pred. ht^k, where k is a constant, e.g., k = -2, -3/2, -1, -1/2, 1/2, 1, 3/2, 2). Plots of studentized residuals against predicted height resulted from various fittings based on different weighting factors were examined. It was found that the weighting factor w = 1/pred.ht produced the most satisfactory studentized residual plot, an outcome that coincides

Table 9. Nonlinear mixed model estimation of equation [30] with generalized error structures.

Covariance	Estimate	Std. Err.	t-value	Pr > |t|	Lower	Upper	AIC	BIC
Spherical	b_1 = 12.6712	0.1487	85.22	<.0001	12.3795	12.9629	6180.8	6203.7
Exponential	b_2 = -5.9990	0.1124	-53.37	<.0001	-6.2195	-5.7785		
Matérn	b_3 = -0.1749	0.01811	-9.66	<.0001	-0.2105	-0.1394		
	b_4 = 0.1176	0.03002	3.92	<.0001	0.05872	0.1765		
Gaussian	b_1 = 12.6667	0.1494	84.79	<.0001	12.3736	12.9597	6182.8	6210.2
	b_2 = -5.9941	0.1138	-52.69	<.0001	-6.2173	-5.7709		
	b_3 = -0.1749	0.01815	-9.64	<.0001	-0.2105	-0.1393		
	b_4 = 0.1171	0.03015	3.88	0.0001	0.05793	0.1762		
Linear	b_1 = 12.6656	0.1495	84.71	<.0001	12.3723	12.9589	6182.7	6210.2
Linear Log	b_2 = -5.9929	0.1140	-52.57	<.0001	-6.2165	-5.7693		
	b_3 = -0.1749	0.01816	-9.63	<.0001	-0.2105	-0.1393		
	b_4 = 0.1169	0.03017	3.88	0.0001	0.05774	0.1761		
Power	b_1 = 12.6705	0.1488	85.14	<.0001	12.3785	12.9624	6182.8	6210.3
	b_2 = -5.9983	0.1127	-53.22	<.0001	-6.2194	-5.7772		
	b_3 = -0.1749	0.01811	-9.66	<.0001	-0.2104	-0.1394		
	b_4 = 0.1175	0.03004	3.91	<.0001	0.05859	0.1765		

Note: AIC and BIC are Akaike's information criterion and Schwarz Bayesian information criterion computed by [20] and [21], respectively. A weighting factor of one over predicted height (w_i = 1/pred.H_2) was used.

Table 10. Ordinary nonlinear least squares fit statistics for equation [30]

Parameter	Estimate	Std. Err.	t-value	Pr > |t|	RMSE	R^2	$R^2_{adj.}$
b_1	13.0021	0.2679	48.54	<.0001	1.3800	0.9851	0.9851
b_2	-6.48752	0.2176	-29.82	<.0001			
b_3	-0.16233	0.0225	-7.22	<.0001			
b_4	0.163142	0.0367	4.45	<.0001			

Note: RMSE, R^2 and $R^2_{adj.}$ are defined in [3], [1] and [2], respectively. Data structure III defined in Fig. 4 was used.

with the results of the site index model derived from stem analysis data (Huang 1997).

Final fittings of [30] under seven covariance structures with heteroskedastic errors were implemented using the nonlinear mixed model macro NLINMIX (Littell et al. 2006). Results based on the RMD data structure III (which is the most efficient, see Wang et al. 2004), are shown in Table 9. The covariance structures that produced identical estimates (e.g., spherical, exponential, and Matérn) were grouped together. For comparison, results (see Table 10) from an ordinary nonlinear least squares fit of [30] without accounting for the correlated and heteroskedastic errors were also obtained, based on the same RMD data structure III.

The estimated coefficients shown in Tables 9 and 10 were used to make forward and backward projections. Summary statistics about the prediction errors, along with the calculated GOFI values and other statistics, are presented in Table 11.

The results shown in Table 11 indicate that the GOFI values from different fits with and without accounting for the heteroskedastic and correlated errors are marginally different. The practical benefits of using more complex estimation techniques are subtle. The important fact to recognize is that they all are lower than the reported, inflated R^2 value shown in Table 10. One might argue that this R^2 value was specific and unique to the particular data and model used, and as such, it could still be interpreted meaningfully with regard to the particular data and model. Such an argument would have been valid for TMD analysis. However, for RMD analysis, the argument becomes less

relevant, as the R^2 value loses its quality of reflecting and representing the goodness-of-fit of a model.

When an R^2 value is reported, it is generally assumed that when the model is used in application, a similar accuracy as represented by the R^2 can be expected. Unfortunately, this was not the case when a fitted model such as [30] was used in a way consistent with how it should be used in application. The traditional R^2 for difference equations expressed by $y_2 = f(y_1, x_1, x_2)$ tends to always overstate the performance accuracy. Readers should not be deceived by the reported high R^2 for such equations, as it is very easy to obtain. On the other hand, the R^2 for increment functions expressed by $y_{inc} = f(x_1)$ routinely understates the performance accuracy. A low R^2 for an increment function can in fact mean a good fit to the data and very reasonable performance accuracy in application when predictions are made. This was clearly evident for the basal area increment function [32] (see Tables 7 and 8). In both cases the GOFI provided a consistent, reliable, and intuitive alternative to the traditional R^2. The GOFI can also be used to reliably determine the best parameter to constrain when deriving difference equations.

In the cases where the heteroskedastic and correlated errors were accounted for by the nonlinear mixed model methods (as in Table 9), a reported AIC value such as 6182.8 for the power function had little relationship to how good or bad the height-site index model [30] may be. The only conclusion one can arrive at from Table 9 is that, since a smaller AIC (or BIC) indicates a better fit, the spherical covariance structure is the most reasonable one for model

Table 11. Summary statistics from forward and backward projections on the top height-age data

| Covariance structure | Type | n | Prediction error | | | | RMSEP | R^2_F or R^2_L | GOFI |
			Mean	SD	Min.	Max.			
Spherical	Forward	1496	0.1684	1.500	-5.122	6.607	1.5092	0.8712	0.9066
	Backward	1496	-0.0115	1.013	-4.504	6.257	1.0126	0.9420	
Gaussian	Forward	1496	0.1662	1.500	-5.126	6.604	1.5091	0.8712	0.9066
	Backward	1496	-0.01064	1.013	-4.503	6.259	1.0126	0.9420	
Linear	Forward	1496	0.1668	1.500	-5.126	6.605	1.5091	0.8712	0.9066
	Backward	1496	-0.01079	1.013	-4.503	6.259	1.0126	0.9420	
Power	Forward	1496	0.1686	1.500	-5.122	6.607	1.5092	0.8712	0.9066
	Backward	1496	-0.01156	1.013	-4.504	6.257	1.0126	0.9420	
Ordinary NLS	Forward	1496	0.4990	1.489	-4.624	7.053	1.5699	0.8606	0.9007
	Backward	1496	-0.13190	1.015	-4.705	5.967	1.0235	0.9408	

Note: RMSEP is root mean square error of prediction computed by [26], R^2_F and R^2_L are computed by [22], GOFI is the goodness-of-fit index computed by [25], and SD is standard deviation. The original data are shown in Fig. 3

[30]. However, if the model itself was a poor one, a smaller AIC may mean little, and we still do not have any direct, intuitive idea about how much total variation may have been explained by the model and how good the model fits the data.

With GOFI, model developers and users attain a direct, intuitive, consistent and reliable measure for gauging the goodness-of-fit of a model in a more realistic manner (as compared to reporting the traditional R^2). In the case of model [30], for instance, one can infer that approximately 90 percent of the total variation in predictions was accounted for by the fitted model. Together with plots of residual or studentized residual trajectories, this provides model developers and model users with an immediate indication about the goodness-of-fit of the model. The GOFI can also provide a common basis for comparing competing models developed using different methodologies, and reported with different R^2 values each claimed to be "higher" than the others.

CONCLUSIONS

The conventional goodness-of-fit measure represented by R^2 was found to be inadequate in reflecting the goodness-of-fit of a model when repeatedly measured data were involved. The R^2 usually overstates the performance accuracy of difference equations and understates the accuracy of increment functions. It is often futile and misleading to report the R^2 for repeatedly measured data when difference equations or increment functions are used. The reported R^2 does not relate to the performance accuracy of a model in application. A modified goodness-of-fit measure, termed GOFI (goodness-of-fit index), was proposed. It was shown that the GOFI provided a direct, intuitive, consistent and reliable goodness-of-fit measure for models developed from different methodologies, data structures, and estimation techniques. It is recommended that the GOFI should be reported as a standard goodness-of-fit measure and used as a common basis for determining the goodness-of-fit of a model, and for comparing alternative models when repeatedly measured data are used in model development.

ACKNOWLEDGMENTS

LITERATURE CITED

Anderson-Sprecher, R. 1994. Model Comparisons and R^2. The American Statistician 48: 113-117.

Baltagi, B.H. 2005. Econometric analysis of panel data. 3rd ed. John Wiley & Sons, New York. 314 p.

Cao, Q.V. 1993. Estimating coefficients of base-age-invariant site index equations. Canadian Journal of Forest Research 23: 2343-2347.

Clutter, J.L.; Fortson, J.C.; Pienaar, L.V.; [et al.]. 1983. Timber management—a quantitative approach. John Wiley & Sons, New York. 333p.

Davidian, M.; Giltinan, D.M. 1995. Nonlinear models for repeated measurement data. Chapman and Hall, New York. 360 p.

Diggle, P.J.; Liang, K.Y.; Zeger, S.L. 1994. Analysis of longitudinal data. Oxford University Press, New York. 396 p.

Fortin, M.; Daigle, G.; Ung, C.H.; [et al.]. 2007. A variance-covariance structure to take into account repeated measurements and heteroscedasticity in growth modeling. European Journal of Forest Resources (in press).

Goelz, J.C.G.; Burk, T.E. 1992. Development of a well-behaved site index equation: jack pine in north central Ontario. Canadian Journal of Forest Research22: 776-784.

Gregoire, T.G.; Schabenberger, O. 1996. Nonlinear mixed-effects modeling of cumulative bole-volume with spatially correlated within-tree data. Journal of Agricultural, Biological, and Environmental Statistics 1(1): 107-119.

Gregoire, T.G.; Schabenberger, O.; Barrett, J. 1995. Linear modelling of irregularly spaced, unbalanced, longitudinal data from permanent-plot measurements. Canadian Journal of Forest Research 25: 137-156.

Hardin, J.W.; Hilbe, J.M. 2007. Generalized linear models and extensions, 2nd Edition. Stata Press, College Station, TX. 387 p.

Huang, S. 1997. Development of compatible height and site index models for young and mature stands within an ecosystem-based management framework. In:

Amaro, A., Tomé, M., (eds.) Empirical and process-based models for forest tree and stand growth. Lisbon, Portugal. pp. 61-98.

Huang, S.; Morgan, D.J.; Klappstein, K.; [et al.]. 2001. A growth and yield projection system for natural and regenerated stands. Alberta Sustainable Resource Development Tech. Rep. T/485, Edmonton, Alberta.

Huang, S.; Titus, S.J. 1999. Estimating a system of nonlinear simultaneous individual tree models for white spruce in boreal mixed-species stands. Canadian Journal of Forest Research 29: 1805–1811.

Huber-Carol, C.; Balakrishnan, N.; Nikulin, M.; and Mesbah, M. (eds.). 2002. Goodness-of-fit tests and model validity. Birkhäuser, Boston. 551 p.

Judge, G.G.; Griffiths, W.E.; Hill, R.C.; [et al.]. 1985. The theory and practice of econometrics. 2nd edition, John Wiley & Sons, New York. 1056 p.

Kvalseth, T.O. 1985. Cautionary note about R^2. The American Statistician 39: 279-285.

LeMay, V.M. 1990. MSLS: a technique for fitting a simultaneous system of equations with a generalized error structure. Canadian Journal of Forest Research 20:1830-1839.

Littell, R.C.; Milliken, G.A.; Stroup, W.W. [et al.]. 2006. SAS for mixed models. 2nd ed., SAS Institute Inc., Cary, NC, USA. 841 p.

Monserud, R.A. 1984. Height growth and site index curves for inland Douglas-fir based on stem analysis and forest habitat type. Forest Science 30: 943-965.

Narsky, I. 2003. Goodness of fit: what do we really want to know? In: Proceedings of the PHYSTAT 2003 Conference, Stanford, California. pp.70-74.

Nord-Larsen, T. 2006. Modeling individual-tree growth from data with highly irregular measurement intervals. Forest Science 52(2): 198-208.

Pan, Z.; Lin, D.Y. 2005. Goodness-of-fit methods for generalized linear mixed models. Biometrics 61: 1000-1009.

Picard, R.R.; Cook, R.D. 1984. Cross-validation of regression models. Journal of the American Statistical Association 79: 575-583.

Pinheiro, J.C.; Bates, D.M. 2000. Mixed-effects models in S and S-PLUS. Springer, Heidelberg. 528 p.

Schunn, C. D.; Wallach, D. 2005. Evaluating goodness-of-fit in comparison of models to data. In: Psychologie der Kognition: Reden und Vorträge anlässlich der Emeritierung von Werner Tack. Saarbrueken, Germany: University of Saarland Press. pp. 115-154.

Trincado, G.; Burkhart, H.E. 2006. A generalized approach for modeling and localizing stem profile curves. Forest Science 52(6): 670-682.

Wang, Y.; Huang, S.; Yang, R.C.; Tang, S. 2004. Error-in-variable method to estimate parameters for reciprocal base-age invariant site index models. Canadian Journal of Forest Research 34: 1929-1937.

Yang, Y.; Monserud, R.A.; Huang, S. 2004. An evaluation of diagnostic tests and their roles in validating forest biometric models. Canadian Journal of Forest Research 34: 619-629.

Simulation Model of a Hill Dipterocarp Forest Five Years After Harvesting at Angsi Forest Reserve, Negeri Sembilan, Malaysia

Kamziah Abd Kudus and Frisco Nobilly

ABSTRACT

DIPTEROCARP FORESTS ARE OF VITAL economic and ecological importance in Peninsular Malaysia. Despite their economic importance, dipterocarp forests have been greatly depleted. The *Selective Forest Management System* (SMS) was introduced in 1978 and is the current forest-management system practiced. The SMS is designed to optimize the management objectives of economical and efficient forest harvesting, forest sustainability, and minimum forest development costs.

This study was conducted at Compartment 19, Angsi Forest Reserve, Negeri Sembilan, Malaysia. Compartment 19 is comprised of 399 hectares of forest from the total concession, which covers 12,741 hectares. The Forestry Department of Peninsular Malaysia Four established four growth and yield study plots in 1999, before logging activities started. The area is classified as a hill dipterocarp forest. At the end of 1999, the forest was logged under SMS with cutting limits of at least 65 cm diameter at breast height (dbh) for *Neobalanocarpus* species (chengal), at least 55 cm dbh for dipterocarp species, and at least 45cm dbh for non-dipterocarp species. Since the study plot establishment, data were collected in 2000, followed by annual visits from 2002 to 2005. Stem identity class, wood-quality group, species name, status of tree, dbh, and commercial bole height were recorded during each visit. Stems per hectare, basal area per hectare, gross volume, and net volume were calculated. A forest simulation model based on an empirical approach was developed for growth and yield prediction of the regenerated forest. Ideal cutting cycle will be recommended from this study.

Kamziah Abd Kudus (kamziah@putra.upm.edu.my) and **Frisco Nobilly** are at the Faculty of Forestry, Universiti Putra Malaysia, 43400 UPM Serdang, Selangor, Malaysia.

Timber Properties of Norway Spruce Predicted by RetroSTEM

Anu Kantola, Sanna Härkönen, Harri Mäkinen, Annikki Mäkelä

ABSTRACT

IN THE SAWMILL INDUSTRY, STEM FORM, branchiness, and wood density are the most important factors of Norway spruce (*Picea abies* [L.] Karst.) defining the yield and quality of sawn products. This study tests the prediction power of the Retrospective Stand and Tree Evaluation Model (RetroSTEM) in terms of timber properties (stem taper, branchiness, wood density) of Norway spruce. RetroSTEM reconstructs a measured tree from its current age and size (*h*, *DBH*, crown length), using the pipe model and regular crown allometry as constraints, and generates 3-dimensional objects with growth rings and knots. The model employs empirical sub-models for branch population dynamics and wood properties, the latter embedded by the visual tool TreeViz.

Material and Methods

RetroSTEM was tested against the stems from an independent data set, collected in Southern Finland in 1988–90 as a sub-sample of the temporary plots of the 8th National Forest Inventory in Finland (NFI8). The data consists of 31 trees from 9 stands, with varying fertility. The age of the sample trees varied between 46 and 134, DBH was between 11 and 45 cm, and crown ratio was between 0.6 percent and 1 percent. In the felled trees, maximum branch diameters per measured even meter over stem, stem taper, and sample disks were measured. Wood properties and the accuracy of stem properties were measured in terms of estimation bias.

Results

The simulated taper curves, branch sizes, and wood densities were compared with those of the sample trees. The simulated taper curves showed some overestimation of stem diameter (cm) in the mid part of the stem, with -0.4 cm bias. The measured and predicted diameters of branches (cm) increased at the top third of the crown, then stabilized and finally decreased below the living crown, showing a bias of 0.3 cm. If the crown ratio of a measured tree was high (greater than 90 percent), the largest measured branches occurred at the bottom of the stem, and the model prediction at this area was underestimated. TreeViz estimation for wood basic density (kg m^{-3}) over stem was generally similar in simulated and measured trees as well as in measured stem disks.

Conclusions and Further Analysis

The RetroSTEM model provides a feasible tool for describing stem characteristics in Norway spruce. However, a further evaluation of the crown development in trees of large crown ratio and growing space is required. Our future work will focus on finding out reasons for the observed bias in the distribution of branch and stem diameter over the stem. Similarly, the model will be tested against stand-level quality distributions of timber.

KEYWORDS: Branchiness, Norway spruce, process-based models, stem taper, wood density

Anu Kantola (anu.kantola@metla.fi) and **Harri Mäkinen** are researchers at the Vantaa Research Centre, Finnish Forest Research Institute, PO Box 18, 01301 Vantaa, Finland; **Sanna Härkönen** is at the Faculty of Forestry, P.O. Box 111, FIN-80101 University of Joensuu, Finland; **Annikki Mäkelä** is professor of silviculture (forest production), Department of Forest Ecology, University of Helsinki, PO Box 27, 00014 Helsinki, Finland.

Modeling the Distribution of Foliar Biomass for Pinus contorta var. latifolia in Interior British Columbia

Roberta Parish, James W. Goudie, Lin Ju

ABSTRACT

LODGEPOLE PINE (*PINUS CONTORTA* var. *Latifolia*) is a widespread and valuable commercial species in interior British Columbia. The amount and vertical distribution of foliar biomass in the crown of lodgepole are important characteristics of stand structure, which influence many aspects of ecosystem function. We developed a mixed effects model based on 60 trees in 13 stands to predict foliar biomass from branch size and location within the crown. We then fitted a mixed-model β-function to the internodal foliar biomass data. Positions in the crown and growth increment were important predictors of internodal biomass accumulation.

Roberta Parish (roberta.parish@gov.bc.ca), **James W. Goudie**, and **Lin Ju** are research scientists in the Research Branch of the BC Ministry of Forests, PO Box 9536, Victoria, BC V8N 2S8, Canada.

Working Plan: A Tool for Forest and Wildlife with Special Attention to Impacts on Habitat and Timber Quality in the Teak Forests of Central India

Ajit K. Shrivastava

ABSTRACT

Since the mid-19th century in India, scientific management of forests has been practiced in accordance with the prescriptions of a Working Plan. The objective of forest management has always been sustained yield of timber with less emphasis on wildlife habitat. India prepares, and periodically revises, Working Plans for management of established forest divisions. About 72 percent of all India's forests are managed according to the prescription of Working Plans. Nearby 10 million hectares of production forests are managed under such plans. Several different silviculture systems are followed as models in India including a selection system, a shelterwood system, clear cutting, and artificial regeneration with valuable species. There are various tropical timber species in production and trade such as, *Shorea robusta*, *Eucalyptus, Acacia* spp., *Dalbergia sisoo,* and *Tectona grandis* (teak). Teak is a high quality, high-priced timber largely available in central India. Timber harvesting cannot be done without following the Working Plan prescription, which is prepared for a large area of forest.

Forest management under a Working Plan has great impact on wildlife habitat, a fact that has been overlooked for some time. In Madhya Pradesh, the central state in India, 11 percent of forested area is protected as wildlife habitat under such designations as National Parks and Wildlife Sanctuaries. The remaining 89 percent of forested area is managed according to Working Plan prescriptions.

Currently, what is needed most for the efficient, systematic, and scientific management of India's forests is the ability to estimate the quality of timber available from a teak tree of any given diameter and height class within permissible limits. This is not part of the Working Plans at present.

It is common to see a wide variation between estimated quality of timber in a stand and actual quality assessed after felling. Local volume tables are easily applicable to those areas of restricted range of locality, but only with the assumption that trees of the same diameter have the same height. These tables are based mainly on one parameter, i.e., diameter at breast height. The crown size and shape is not taken into account. Timber quality is not taken into consideration under current forest management plans, even though it can be a strong indicator for forest protection and, in turn, better conservation efforts for wildlife habitat.

This paper deals with the effect various silviculture systems and treatments have on timber quality and methods of estimating timber volume in teak trees. It assesses and evaluates the relationship between timber quality and wildlife habitat in the rich teak areas of Mandla, Seoni, and Chhindwada in Central India.

Out of the 23.38 percent of forested area in Central India, 4.75 percent is under a Protected Area Network and is not available for utilization. In such a scenario, there is a tremendous amount of pressure on the managed forests. If the Protected Areas and wildlife are to survive for long, the future of the production forests needs to be secured. It needs to be borne in mind that the majority of the wildlife in this country occupies the managed forests. Thus, the man-

Ajit K. Shrivastava (ajitshri@gmail.com) is Chief Conservator of Forest Research and Extension, Indian Forest Service, Jabalpur, Madhya Pradesh 480 661, India

aged forests need more attention so that they can perform a production function as well as ensure a better future for the Protected Areas by conserving biodiversity.

INTRODUCTION

A Working Plan for a forest area is a management plan, which coordinates all planning activities for development and growth of the forests. It is an instrument to effectively monitor and evaluate forestry operations. The primary objective of the plan is to maximize timber production from the forests. It aims at evolving a felling program so that forests are harvested within a definite period. Recently, in order to achieve sustained timber yields a regeneration strategy was included in the Working Plan. The timber projection was first done through thumb rules for partial enumeration of trees. Recently, detailed inventories of forest resources have come into practice. Forest management objectives are currently changing. Emphasis is shifting from a purely timber-oriented management approach while social and conservation issues are gaining more importance. The National Working Plan Code (Government of India 2004) emphasizes the necessity of writing Working Plans that are consistent across the nation with specific prescriptions for wildlife management along with forest management. The main objectives of the Working Plan Code are:
- increasing the productivity of forests to meet essential national needs
- preserving the national forests with an emphasis on biological diversity and natural resources
- meeting the natural resource requirements of rural and tribal populations with a need for fuel-wood, fodder, minor forest produce, and small timber.

OBJECTIVES

Forest management for timber production, as wildlife habitat, and for other resources is most efficiently accomplished by considering all objectives simultaneously and by:
- Evaluating the present systems of forest management, i.e., silviculture systems

- Improving co-ordination between managed forests and protected areas
- Delineating wildlife habitat and corridors in protected areas
- Retaining existing old growth forests
- Retaining snags and hollow trees
- Maintaining grassy openings
- Providing for weed control
- Balancing the removal of exotic shrubs (such as lantana) with the restoration of native shrubs

STUDY AREA

The Satpuda Maikal landscape is about 50,000 km^2 in area, covering 178 forest ranges and 3,150 beats with an abundance of tiger and ungulate. Tigers are present in 290 beats with 78 having a high, 57 having a medium, and 155 beats having a low abundance of tiger sign. Ungulates are prey to tiger in 1,678 beats (Mathur 2002). The study area is a heterogeneous mosaic of large contiguous forest that includes the protected areas Kanha and Pench National Park along with a few sanctuaries where resource use has been stopped or controlled for some time. These areas are managed for wildlife and wild plants. The remaining second-category forests are managed for goods and services. These are regulated through Working Plan prescriptions. The forests are among the most economically valuable of the dry deciduous types. *Tectona grandis* (teak), also known as "king of timbers" is the principal timber species. The area is home to one of the contiguous populations of critically endangered tiger—estimated as 48 individuals living in managed forests. Other endangered species found here include mammals, birds, reptiles, amphibians, fishes and insects. Tree species found in the area are: *Tectona grandis, Terminalia Tomentosa* (Saja), *Adina cordifolia* (Haldu), *Anogeissus latifalia* (Dhawda), *Diospyros melanoxylcm* (Tendu), *Ougeinia oogeirsis* (Tinsa), *Pterocarpus marsupium* (Bija). Details of the forest area in the three districts considered here are shown in Table 1.

Table 1. The total areas and forest cover in the three districts of the study area, in km^2.

District	Total Area	Area in Forest Cover Types				Percent of Forest Cover
		Very Dense	Moderately Dense	Open Forest	Total Forest	
Mandla	5,800	443	1,309	980	2,732	47.10
Seoni	8,758	239	1,412	1,387	3,038	34.69
Chhindwara	11,815	203	2,368	1,838	4,409	37.32
Total	26,373	885	5,089	4,205	10,179	

SYSTEM OF FOREST MANAGEMENT IN THE STUDY AREA

The seven Working Plans for the three forest divisions in the study area are for East Mandla, West Mandla, North Seoni, South Seoni, East Chhindwara, West Chhindwara, and South Chhindwara. The different silvicultural systems in use here are modified versions of European systems and are described below:

Selection System (SCI):

Involves the removal of mature and over-mature trees singularly over a large area of forested land, on a periodic basis, and without creating gaps. This system is mainly used for managing teak crop. Trees that are dead, dying, discarded, defective, of undesirable species, and of exploitable diameter are removed. This is the most flexible system used, and is practiced under all the plans. A total of 410,580 hectares are managed under the SCI system in the study area.

Improvement Working Circle (IFS):

This system is used for management of young and middle-aged crops, which are mainly pole crop. These areas do not produce good quality timber. A total of 54,586 hectares is managed under the IFS system in the study area.

Rehabilitation of Degraded Forest (RDF):

This management system is practiced in the degraded forest areas with very sparse density. These areas contain good rootstock and are supplemented by artificial planting. A total of 224,961 hectares is managed under the RDF system in the study area.

Modified Clearcut System (Plantation Establishment):

This management system is practiced in the areas managed by the forest corporation in Madhya Pradesh. Under this system areas of even-aged mature crop are felled. An average of 2,100 hectares in two divisions in Seoni and Mandla districts are partially clearcut each year for plantation. In each clearcut hectare, 70–80 young to middle-aged trees are left with a green belt of 10 m separating adjacent 20–hectare clearcuts.

The total area managed under each of these systems per year for the three districts and their subdivisions is shown in Table 2.

PRINCIPLES OF YIELD REGULATION IN THE CURRENT WORKING PLANS

Yield regulation is considered an important aspect of forest management; and influences forest management practices. Productivity of Indian forests is on the decline, due to immense biotic pressure. Hence, conservation of existing dense forest and restoration of degraded forest is of great significance. It is a fact that the primacy of timber production over other management objectives has come to an end and conservation of forest ecosystems, including wildlife, have taken precedence over other objectives. As a result, yield regulation is losing its previous importance and relevance. In dense forests, suitable methods of yield regulation need to be developed while maintaining the principles of sustainable forest management. Yield is regulated based on volume and/or increment of growing stock. The concept of a "normal forest" is a dream in the mind of forest managers. The time has come to give importance to

Table 2. Annual areas allotted to different forest management systems within the three districts and their subdivisions, in hectares.

Management System	Mandla		Seoni		Chhindwara			Total for 10 years	Area allotted each year
	East	West	North	South	East	West	South		
SCI	37,473	64,606	44,799	80,246	29,326	79,238	74,892	410,580	41,058
IFS	-	24,258	19,885	10,443	-	-	-	54,586	5,459
RDF	26,767	26,525	30,744	22,444	65,989	32,613	19,879	224,961	22,496
Plantation	-	-	8,630	2,178	-	8,676	12,248	31,732	3,173
Total	**64,240**	**115,389**	**104,058**	**115,311**	**95,315**	**120,527**	**107,019**	**721,859**	**72,186**

the quality instead of the quantity of timber.

Yield Tables:

- Yield tables are a standard of reference available for growth of teak in even-aged plantations
- A rotation of maximum continuous net income is considered the most economically rewarding rotation on which to grow teak plantations on government plantations
- Yield tables are based on number of trees per unit area and average diameter for each quality class (Sharma 1998)

Local Volume Tables:

These are compiled from the measurements of trees growing in a restricted geographical area or locality, based on one independent variable, i.e., diameter at breast height (dbh), in an area of or more or less uniform crop or site quality. (Tiwari 1996)

These are applicable to such restricted areas as coupe/compartment or to a felling series in a small area, with the assumption that trees of the same diameter will have the same height and will hold good.

CALCULATION OF YIELD (SHRIVASTAVA 2006)

1. Von Mantle's formula:

    $I = 2\ GS/R$, where

    I = increment, in m^3/year

    GS= growing stock volume, in m^3,

    R= rotation age, in years.

    It gives an unrealistic forecast of yield.

2. Brandis's method: Based on data generated from strip enumeration and stump analysis of teak forests. Yield is calculated based on average number of trees reaching exploitable size annually plus a fraction of surplus trees in a diameter class above the exploitable class or size.

3. Smethie's Safeguarding Formula: Yield calculation is done on the basis of volume.

    Because it is based on the principles of sustained yield, Smethie's method is the most widely used for calculation of yield in selection forests in India.

    $X = f/t\ (II - Z\%\ II)$

    X: No. of trees selected for felling.

    f : Felling cycle in years.

    t: Time taken by class II trees to pass into class I

Table 3. Estimated yield and actual teak yield in the South Seoni Forest Division for the year 2006.

Division	Range	Coupe	Trees harvested (no.)	Estimated Yield			Actual Yield		
				Timber (m^3)	Poles (no.)	Fuelwood Stacks (no.)	Timber (m^3)	Poles (no.)	Fuelwood Stacks (no.)
South Seoni	West Khawasa	III Bawanthari	40,855	377.790	685	7,693	209.943	13,761	2,331
		III Khawasa	8,502	124.020	264	42	85.903	355	278
		III Kohka	4,080	22.705	128	719	28.149	1,226	136
		III Kothar	23,835	24.685	280	1,334	31.653	1,339	470
		Total	77,272	549.200	1,357	9,788	355.648	16,681	3,215
	Rukhar	III Banjari	1,861	230.353	196	197	187.369	335	104
		III Karhaiya	1,268	380.970	322	10	528.374	364	487
		III Karmajhira	5,086	72.555	224	1,954	49.469	2,661	270
		III Khapa	616	57.306	52	62	60.356	336	42
		III Nayegaon	3,072	349.555	186	303	279.002	781	200
		III Richhi	8,138	405.210	324	3,693	299.393	4,240	459
		III Rukhar	1,642	175.000	173	579	138.920	1,090	162
		Total	21,683	1,670.949	1,477	6,798	1,542.883	9,807	1,724
	West Khawasa	IV Bawanthari	27,069	835.085	13,653	773	512.037	12,702	2,370
		IV Khawasa	992	45.800	3	316	16.053	24	474
		IV Kohka	6,128	160.950	904	112	129.328	1,021	450
		IV Kothar	3,957	91.030	1,282	112	74.904	1,667	257
		Total	38,146	1,132.865	15,842	1,313	732.322	15,414	3,551

category.

Z : Percentage of class II trees that do not pass into class I stage in years on account of mortality or removal in thinning etc.

The estimate for teak timber production is done with the help of form factors and yield tables. For teak, current form factors give an estimate higher than the actual yield due to variation in size and shape of trees and a long gap in the revision of the volume tables and form factors. Table 3 shows differences in estimated yield and actual production for several forest areas.

TEAK AREA IN MANDLA, CHHINDWARA AND SEONI

Teak, a species of the *Tectona* genus, is the most important tree of India producing timber of worldwide reputation. It is a large deciduous tree that is quite variable in size depending on climatic conditions and soils. In favorable conditions, it has a long, straight, clean bole carrying its girth well up the stem. With advanced age, the stem becomes more fluted and buttressed towards the base. The sapwood of teak is white to pale yellowish-brown, whereas the heartwood is dark golden, turning brown, dark brown, and finally darker brown with age. It is a coarse and uneven textured timber without taste. However, it possesses a characteristic smell similar to the smell of old leather. In the study area, teak trees grow up to 30-meters in height, are fluted near the base, have pale brown bark, and gray leaves which are opposite, broadly elliptical, rough, 20–50 cm long, and 15–20 cm wide. The history of the planting of teak dates back in central India to 1891. Regular teak plantation started in 1928. Teak is found mostly on hilly or undulating country up to 900 m elevation with good sub-soil drainage. In recent years, some areas have been converted to high-tech plantations as high input areas and artificial irrigation are provided.

Teak is one of the most widely distributed and one of the most economically important timber species in India. Owing to the much higher prices of teak timber, it has been planted more extensively than any other single species.

Species associated with teak in central India:
• *Terminalia tomentosa* (Saja)
• *Bombax ceiba* (Semal)
• *Cassia fistula* (Amaltas)
• *Madhuca indica* (Mahua)
• *Lagerstroemia parviflora* (Lendia)
• *Buchanania lanzan* (Achar)

Salient features of teak wood:
• Principal timber tree in peninsular (central) India
• Major timber source for buildings, bridges, furniture, cabinetwork, wheel spokes, and general carpentry
• Termite-, fungus-, and weather-resistant while also lightweight, strong, attractive, workable, and seasons without splitting, cracking, warping, or significantly altering shape
• Coarse textured, oily, and scented when fresh
• Suitable for carpentry, it can have a smooth finish and fair polish
• Light to moderately heavy, moderately hard, somewhat brittle, straight or wavy grained, coarse and uneven textured
• Growth rings are distinct

Table 4. Teak forest area compared to total forest area in the three study divisions.

Divisions		Total Forest Area (ha)	Teak Area (ha)	% of Teak
Mandla	East	118,240.880	19,715.150	
	West	141,990.000	61,149.180	
Total		**260,230.880**	**80,864.330**	**31.07%**
Seoni	North	122,319.820	31,868.570	
	South	119,535.799	53,991.390	
Total		**241,855.619**	**85,859.960**	**35.50%**
Chhindwara	East	128,713.532	41,444.451	
	West	168,111.770	47,493.370	
	South	99,128.719	77,432.961	
Total		**395,954.021**	**166,370.782**	**42.02%**
Grand Total		**898,040.520**	**333,095.072**	**37.09%**

Table 5. Annual teak production in the study divisions.

Divisions	Teak	
	Timber (m^3)	Fuelwood Stacks (count)
Mandla	9,472	3,482
Seoni	10,185	4,162
Chhindwara	12,608	6,216
Total	32,265	13,860

TIMBER QUALITY IN CENTRAL INDIA

To assess timber-quality of teak, logs were obtained from working circles and plantations from the Mandla, Seoni and Chhindwara districts. For each sample, a teak log with a diameter of 60 cm and length of 120-cm was cut and converted into a standard size for use in determining the compressive strength of the wood, both parallel and perpendicular to the grain.

A total of 38 samples were tested by the timber mechanics division of the Forest Research Institute (FRI), Dehradun. The test samples are obtained from logs according to the standard schedule given in IS:2455-1974. All the samples are surfaced to a smooth, finished standard cross-section of 5 x 5 cm. The mechanical property of compressive strength is measured using the procedure described in IS:1708-1969. We are awaiting test results from FRI, Dehradun.

The average value of standard teak from Malabar, Nilambur, and Coimbatore in south India are taken as standards and used for the purpose of comparing the strength of teak under testing.

The number of samples taken was not a sufficient representation of the vast area and locality factor. However, the samples clearly show that the compressive strength of teak grown here is greater than that found in other plantations under other silvicultural treatments. This gives a clear idea about variation in compressive strength. In other studies of teak wood at the Forest Research Institute, it was found that there is variation in wood properties from the pith to periphery of the log and that the central portion is often weaker, especially in fast-grown woods probably due to the presence of a greater proportion of juvenile wood. (Rajpoot et al 1983, 1990; Shakula et al 1998, 1991). There may be significant variation in wood properties among individual teak trees. This is often a reflection of the different silvicultural systems used to grow teak. Previous studies have shown that with increases in growth rate, there is an increase in wood quality following an initial decrease in wood quality.

This was a unique study with a small number of samples. The results need to be further investigated through more detailed studies in order to establish a strong relation between silvicultural systems, timber quality, and habitat health. The results do indicate a direct relationship with high timber quality and high standards of forest management that, in turn, benefit wildlife and the conservation of wildlife habitat.

THE EFFECT OF FOREST MANAGEMENT SYSTEMS UNDER THE WORKING PLAN ON WILDLIFE

Timber harvesting and road building affect wildlife habitat more than any other forest management activity. Every year in the Mandla, Seoni, and Chhindwara districts of Central

Table 6. Notable wildlife occurring within the study area.

Name	Species	Mandla		Seoni		Chhindwara			Total	Kanha NP (PA)	Pench NP (PA)	Total	Grand Total
		East	West	North	South	East	West	South					
Tiger	*Panthera tigris*	6	2	21	2	6	6	5	48	131	-	131	179
Panther	*Panthera pordus*	7	8	15	12	6	13	6	67	112	39	151	218
Deer (Cheetal)	*Cervus axis*	774	550	370	1,928	1,053	698	654	6,027	21,484	14,850	36,334	42,361
Sambhar	*Cervus unicolor*	43	101	480	173	125	205	312	1,439	3,472	2,835	6,307	7,746
Barking Deer	*Muntiacus muntjak*	405	872	1,003	1,410	332	1,140	776	5,938	1,197	199	1,396	7,334
Blue bull	*Boselaphus traqocamelus*	-	-	16	129	153	211	142	651	104	2,143	2,247	2,898
Sloth Bear	*Melursus ursinus*	-	5	16	70	95	60	53	299	158	26	184	483
Wild Boar	*Sus scrofa*	2,367	6,826	5,094	4,300	1,906	3,180	1,906	25,579	8,941	3,289	12,230	37,809
Indian Bison	*Bos gaurus*	33	-	-	-	-	-	-	33	1,639	735	2,374	2,407

The three study districts (Mandla, Seoni and Chhindwara) are managed forest dominated by teak. Kanha and Pench national parks are protected areas in the vicinity of the study area.

India, 72,186 hectares are utilized for timber production and management. It recent years, forest managers been responsible specifically for the enhancement of wildlife habitat in managed forests. It is necessary to develop an understanding of wildlife habitat in managed forests, to predict the impact of forest management practices on wildlife, and to take an interest in how the system can be applied for the benefit of wildlife. Current scenarios suggest that it is of utmost importance to protect wildlife habitats in managed forests.

Opinions regarding wildlife management:
- Good forestry leads to good wildlife management
- Forest managers must learn sound wildlife management principles
- It is necessary to have proper communication and co-operation when implementing a Working Plan
- There should be an interdisciplinary attitude towards the management of natural resources
- In current budgets, insufficient funds are allotted for the implementation of wildlife habitat management
- Few studies focused on wildlife management are available
- Loss of species-diversity and extinction of species should be of great concern to every forester under every system

There is an urgent need for the study of:
- Research on the ecological effects of logging operations
- Distributional ranges, lifecourse, habitat association, and diet of wildlife in the Satpuda Maital area of central India
- Temporary rises in wildlife population densities immediately after logging
- Reduction of wildlife food supply
- Overpopulation and degraded habitat
- Loss of key microhabitats and changes in microclimate and microhabitat
- Juvenile mortality due to increased predation and loss of forage
- Non-resident or invasive-species spreading and increasing competition for reduced resources such as food, shelter, and mating grounds
- Increased morbidity due to new diseases and declining population health
- Increased hunting pressure
- Mortality and injury to wildlife directly caused by tree felling, skidding, and other timber extraction activities

Logging and Wildlife:
- There is an urgent need for research regarding the biological and ecological requirements wildlife.
- Attributes of each species and species group need to be investigated from a natural history perspective to understand what makes them particularly vulnerable to the impacts associated with timber harvesting.
- Existing forest management guidelines need to be refined with the goal of enhancing wildlife habitat in teak forests.
- While there is much literature available on vertebrates in general, more studies need to be done specifically on amphibians and fishes, as well as on insects and other invertebrates. These species are more sensitive to the effects that logging operations play a role in healthy ecosystems.
- Although still in the initial phases, flagship species studies represent a good starting point for improving wildlife habitat in managed forests.
- Special attention should be paid to the birds most affected by logging such as trogons, woodpeckers, babblers, barbets and flycatchers (the paradise flycatcher is the state bird).

Importance of the Working Plan in wildlife management:
- Even-aged crops should be grown under current silvicultural systems with the goal of creating edges and edge effects.
- Annual cuts should be no more than 40 hectares in size.
- Permanent gaps in the forest are to be avoided.
- During harvesting, intense human disturbance should not be permitted in two neighboring drainage areas simultaneously.
- No felling is to be allowed in riparian zones.
- Felling in areas used by wildlife for mating, nesting, calving, and fawning during the season of intensive use is to be avoided. Felling of trees and other vegetation bearing nests or surrounding nets, caves, and shelters should be prohibited.
- Removal of evergreen trees and shrubs, which remain green during summers, should be prohibited.
- Wood should be extracted from the forest in the shortest amount of time possible.
- Monkeys inhabit large trees and in the process cause a large amount of leaf fall which is, in turn, utilized by deer. These large trees should not be felled.
- Trees and shrubs bearing edible fruits used by wildlife

should not be felled.

• Bamboo is a very important fodder species and should be conserved. Sowing and planting of fruit and fodder species like Peepal, Gular, Anjan, Bamboo, and Ber should be encouraged.

Some factors that are detrimental to wildlife conservation:

• Presence of roads—including type of roads, location, and degree of use

• Harvesting operations:
  - should be limited to smallest possible area.
  - should be done in shortest possible time.
  - should have a no-activity zone adjoining cuts.
  - should be limited to cutting in only one drainage area per watershed at a time

• Fire—necessary measures should be taken to prevent forest fires

RECOMMENDATIONS

1. Close co-operation is required between forest and wildlife managers in the area of study. Forest management is the process of manipulating the forest environment to produce a mix of products and desired states.

2. It is necessary to practice forest management in such a way as to maintain forest tree species as well as soil, air, and water resources while providing a habitat for wildlife and aquatic life.

3. Wildlife habitat is a by-product of timber management. Instead of managing for larger yield in timber management, the focus should shift to managing for high quality timber.

4. Care must be taken in selecting and using forest management systems that will promote forest sustainability and species-diversity.

5. In a selection system, generally 50 percent of the trees of an available selection diameter are removed. The forests managed under this system have a high degree of vertical diversity. They are irregular in height, with great variation in tree size. There is competition between unequal age-classes of trees, with the larger trees suppressing the smaller trees.

6. In a selection system, initially there is an observed increase in diversity of plants and animals due to a temporary increase in shade-intolerant plants and forage plants in small openings.

7. A strong process should be developed to consider the impact of timber management on wildlife.

8. More should be done to research and understand wildlife requirements in particular areas.

9. Important wildlife areas in managed forest need to be given consideration.

10. A system should be developed to predict the affect of timber management on wildlife habitat, with the recognition that timber management inevitably affects wildlife habitat.

11. Alternatives should be investigated before actual cutting operations begin.

12. Any change in forest structure or composition will favor some wildlife species while adversely affect others.

13. Such changes can affect the number and type of wildlife species and their use of habitat.

14. The selection system tends, over time, to reduce the diversity of plants and animals in the forest. In this system there is a gradual reduction of shade-intolerant trees and understory plants. This system tends to produce large blocks of continuous forest cover dominated by relatively mature trees. Such forests lack the array of distinct successional stages that ensure diversity and a myriad of habitat niches.

SUMMARY

The teak forests in Central India are under increasing pressure to prove their economic viability and to offer land use options. Optimizing the impact of logging is an essential task in the improvement of teak forest management—both for timber production and for wildlife conservation. The empirical formulas used in the past need to be improved to provide realistic estimates of timber production to aid in planning production activities. The current Working Plans should focus on the quality of timber products and modify management prescriptions to protect rich timber areas, which will result in an improved wildlife habitat. Better harvesting practices with better reinforcement of the prescriptions should be the norm when implementing Working Plans.

Long-term sustainability, conservation, restoration of biodiversity, and forest productivity will be achieved in concert only by ensuring that objectives are consistent between forest management and wildlife management. There is a need to co-ordinate data, and analyze the technical aspects of resource planning across forest management and wildlife management. It will be necessary to redefine or

modify procedures for thinning and other forest harvesting operations to meet broader biodiversity goals.

LITERATURE CITED

Bali, B.I.; Singh, K.R. 1983. A note on the physical and mechanical properties of *Tectona grandis* (Teak) from Gorakhpur division, Uttar Pradesh. Timber Mechanics Branch, Forest Research Institute and Colleges, Dehradun. pp. 25-33.

Dudley, N.; Jeanrenaud, J.P.; Sullivan, F. 1996. Bad Harvest?: The Timber Trade and the Degradation of the World's Forests. Earthscan Publications, Ltd., London, UK. 224 p.

Forest Survey of India in Collaboration with Food and Agriculture Organization (FAO). 2004. Pilot Study on Assessment of Status of Sustainability of Forest Resources in India. Forest Survey of India, Ministry of Environment and Forests, Government of India, Dehradun. pp 82-83.

Gopal, R.; Qureshi Q.; Jhala Y.V. 2005. Focus on Tiger Conservation. The Indian Forester 131 (10): 1393-1398.

Government of India. 2004. National Working Plan Code. Government of India, Ministry of Environment & Forests, New Delhi. 52 p.

Grieser Johns, A. 1997. Timber Production and Biodiversity Conservation in Tropical Rain Forests. Cambridge Studies in Applied Ecology and Resource Management. Cambridge University Press, Cambridge, U.K. 248 p.

Kadambi, K. 1993. Silviculture and Management of Teak. Natraj Publishers, Dehradun. 137p.

Kimmins, H. 1997. Balancing Act: Environmental Issues in Forestry. University of British Columbia Press, Vancouver, B.C., Canada. 305 p.

Laurie, M.; Ram, B. 1939. Yield and Stand Tables for Teak (*Tectona Grandis,* Linn. F.) Plantations in India and Burma. Indian Forest Record Silviculture 4-A (1). Forest Research Institute, Dehra Dun, India.

Mathur, P.K.; Lehmkuhl, J.F.; Sawarkar, V.B. 2002. Management of Forests in India for Biological Diversity and Forests Productivity, A New Perspective—Volume I: Concepts, Approaches and Project Overview. WII-USDA Forest Service Collaborative Project Report, Wildlife Institute of India, Dehra Dun. 70p.

Ministry of Environment and Forests. 2003. State of Forest Report. Forest Survey of India, Ministry of Environment and Forests, Dehradun. pp. 72-75.

Negi, Y.S.; Jain, J.D. 2001. Physical and mechanical properties of plantation grown timbers tested at forest research institute. Forest Products Division, Forest Research Institute, Dehradun. TDA 47 (3–4): 27–30.

Panayotou, T.; Ashton, P.S. 1992. Not By Timber Alone: Economics and Ecology for Sustaining Tropical Forests. Island Press, Washington, D.C. 302 p.

Principal Chief Conservator of Forests MP. 2004. Statistics of Forest wealth in Madhya Pradesh. Madhya Pradesh Forest Department. Pp. 25-33.

Rajput, S.S.; Shukla, N.K.; Lal, M. 1991. Some studies on the variation of strength properties of *Tectona grandis* from Mizoram. Forest Research Institute and Colleges, Dehra Dun. Journal of the Timber Development Association 37(2): 33-38.

Sanyal, S.N.; Bali, B.I.; Singh, K.T.; Sharma, B.D. 1987. A note on the physical and mechanical properties of plantation grown *Tectona grandis* (Teak) from Tanjavur district, Tamilnadu. Timber Mechanics Branch, Forest Research Institute and Colleges, Dehradun. Journal of the Timber Development Association 33(4) 15-22.

Sanyal, S.N.; Saxena, R.D. 1980. Physical and Mechanical Properties of Some Maharashtra Timbers. N.B.O. Journal 25(2): 1-5.

Sawarkar, V.B. 1995. A Manual for Planning Wildlife Management in Protected Areas and Managed Forests. Wildlife Institute of India, Dehradun. Director WII Dehradun India. pp.48-73.

Shrivastava, A.K. 2006. Working Plan of West Mandla Division. Conservator of Forest Working Plan Jabalpur MP. pp. 24-148.

Shukla, N.K.; Lal, M. 2004. Physical and mechanical properties of plantation grown *Tectona Grandis* (Teak)

from Mizoram. Forest Products Division, Forest Research Institute, Dehradun. Journal of the Timber Development Assocation XL (3): 38-48.

Thomas, J.W. (ed.). 1979. Wildlife Habitats in Managed Forests the Blue Mountains of Oregon and Washington. Agriculture Handbook No. 553. USDA, Forest Service. 512 p.

Tiwari, K.P.; Pandey, R.L. 1996. Local Volume Tables for Teak, Sal and Other Species for Central Circle, Jabalpur (M.P.). Mensuration Branch. State Forest Research Institute, Jabalpur.

Tiwari, K.P.; Sharma, M.C.; Pandey, R.L. 1998. Yield and Stand Tables of Teak in Madhya Pradesh. Mensuration Branch, State Forest Research Institute, Jabalpur. Director State Forest Research Institute Jabalpur MP India. pp. 3-11.

Impact of Land Use and Climatic Changes on Pulpwood and Carbon Sequestration Sustainability at the Landscape Level

Paula Soares, José Loff, Paulo Borges, Ana Rodrigues, Susete Marques,
Luís Fontes, José Guilherme Borges, Margarida Tomé

ABSTRACT

THE EXPANSION OF TASMANIAN BLUEGUM (*Eucalyptus globulus* Labill.) in Portugal occurred in the second half of the twentieth century as a consequence of the implementation and development of the pulpwood industry in the country. Nowadays, and according to provisory data presented by the national forest inventory in July 2006, eucalyptus plantations represent 22.9 percent of the national forest area, corresponding to 743, 000 hectares. These plantations produce mainly raw material for the pulp industry. The importance assumed by the pulp companies in the national economy justifies the development of specific applications to simulate the impact of land use and climatic changes on the sustainability of pulpwood production and carbon sequestration at the landscape level. To achieve this goal, it is essential to develop computer-based decision support systems (DSS) adapted to the actual reality. To model the pulpwood production and carbon sequestration it was necessary (1) to select and parameterize a process-based model, (2) to improve a growth and yield empirical model specifically developed for Portuguese eucalyptus plantations, (3) to develop methodologies to link both types of models resulting in a hybrid model, and (4) to implement the models at landscape level. In general, process-based models are based on the knowledge of the physiological processes in the interfaces of plant-soil and carbon-nutrients-water. In this work the 3PG model was selected. This is a stand-level model that uses monthly time steps. It requires as inputs initial stand data (stem number, stem, foliage, and roots biomasses) and soil and weather data. A detailed analysis pointed out some weak points: (1) the stand density module is not appropriate for the stand density x rotation ages presently used in Portugal, and (2) output is not detailed enough for most management decisions. The Globulus model is a stand-level growth and yield empirical model. In this work, Globulus version 3.0 was used. In order to obtain models that (1) can work using regular forest inventory data as input, (2) are able to give good predictions under climate change, (3) provide information on the effect of different silvicultural alternatives, not only on tree growth but also on other forest products and services, (4) provide reliable information on stand structure and wood quality, and (5) account for the possible occurrence of several damages, a methodology was developed to link growth and yield models with process-based models. The result is the GLOB-3PG model that uses stand variables as linking functions. All the referred models were implemented in a DSS that encompasses the simulation of stand-specific management alternatives and the evaluation of total wood production and the respective net present value for each combination of prescriptions. The developed software, GLOBfLOR, is used to show results obtained in a case-study area predominantly occupied by eucalyptus plantations in central Portugal.

Paula Soares (paulasoares@isa.utl.pt), **José Loff**, **Paulo Borges**, **Ana Rodrigues**, **Susete Marques**, **Luís Fontes**, **José Guilherme Borges** and **Margarida Tomé** are at the Universidade Técnica de Lisboa, Instituto Superior Agronomia, Centro de Estudos Florestais, Tapada Ajuda, 1349-017 Lisboa, Portugal.

Estimating Future Carbon Sequestration at the National/Regional Level Using National Forest Inventory Data: The Impact of Data Aggregation

Margarida Tomé, Susana Barreiro, Joana A. Paulo, Paula Soares, José Tomé

ABSTRACT

THE EVALUATION OF THE CONTRIBUTION OF forests to climate change mitigation through the carbon cycle is of utmost importance due to the Kyoto Protocol to the United Nations Framework Convention on Climate Change. The National Forest Inventory (NFI) provides information on the current status of the forest but there is a need to predict future carbon sequestration under alternative forest management and land-use-change scenarios. Problems such as data aggregation and choice of appropriate growth models, among others, are important points to be considered for the development of national/regional simulators of carbon sequestration. The objective of the present presentation is to compare the use of alternative simulators, based in different levels of data aggregation as input, for the case of the Portuguese forests: from intensive plantations (*Eucalyptus globulus*) to private poorly-managed pine plantations (*Pinus pinaster*) to slow-growing sparse oak stands (*Quercus suber* and *Quercus ilex* ssp. *rotundifolia*). There is a lot of variation concerning the available data and the existing growth models for each of the species and forest types. Therefore, different methodologies had to be adapted for each case, which makes this case study an interesting one. Finally, preliminary estimations for the period of 1995–2005, obtained with each of the proposed methodologies, will be presented.

Margarida Tomé (magatome@isa.utl.pt), **Susana Barreiro**, **Joana A. Paulo**, **Paula Soares**, and **José Tomé** are at the Universidade Técnica de Lisboa, Instituto Superior de Agronomia, Centro de Estudos Florestais, Tapada da Ajuda, 1349-017 Lisboa, Portugal.

Modeling Branch Growth and Mortality to Silvicultural Treatments in Coastal Douglas-fir Plantations: Implications for Predicting Tree Growth

Aaron Weiskittel, Doug Maguire, Robert A. Monserud

ABSTRACT

STATIC MODELS OF INDIVIDUAL TREE CROWN attributes such as height to crown base and maximum branch diameter profile have been developed for several commercially important species. Dynamic models of individual branch growth and mortality have received less attention, but have generally been developed retrospectively by dissecting felled trees; however, this approach is limited by the lack of historic stand data and the difficulty in determining the exact timing of branch death. This study monitored the development of individual branches on 103 stems located on a variety of silvicultural trials in the Pacific Northwest, USA. The results indicated that branch growth and mortality were significantly influenced by precommerical thinning, commercial thinning, fertilization, vegetation management, and a foliar disease known as Swiss needle cast [*Phaeocryptopus gaeumannii* (T. Rohde) Petr.]. Models developed across these datasets accounted for treatment effects through variables such as tree diameter growth and the size and location of the crown. Insertion of the branch growth and mortality equations into an individual-tree modeling framework, significantly improved short-term predictions of crown recession on an independent series of silvicultural trials, which increased mean accuracy of diameter growth prediction (reduction in mean bias). However, the static height to crown base equation resulted in a lower mean square error for the growth predictions. Individual branches were highly responsive to changes in stand and site conditions imposed by silvicultural treatments, and therefore represent an important mechanism explaining tree and stand growth responses.

Aaron R. Weiskittel (aaron.weiskittel@umit.maine.edu) is a forest modeling assistant professor, University of Maine, Orono, ME 04471, USA; **Douglas A. Maguire** is a professor of silviculture, Oregon State University, College of Forestry, Corvallis, OR 97331, USA; **Robert A. Monserud** (retired) was a research forester and team leader, USDA Forest Service PNW Research Station, Portland, OR 97208, USA.

Urban Tree Crown Condition: Training and Evaluation Tools

Matthew F. Winn, Neil A. Clark, Philip A. Araman, Sang-Mook Lee

ABSTRACT

The USDA Forest Service Southern Research Station in Blacksburg, Virginia is in the process of constructing a website that will provide web-based training to FIA crews, urban foresters, university scientists, urban and citizen foresters in the area of urban tree monitoring. Initially, the website will focus primarily on tree crown characteristics but will eventually contain information on site and bole characteristics as well. In addition to the training module, the website will also include a testing module and crown analysis software. The testing module will be used to examine the repeatability of observer estimates of crown measurements using controlled tree models. The crown analysis software will allow users to assess the health of urban trees using digital photographs.

Matthew F. Winn is a forestry technician, **Neil A. Clark** was a research forester, **Philip A. Araman** (presenter; paraman@fs.fed.us) is a research team leader, and **Sang-Mook Lee** is a postdoctoral fellow at the Southern Research Station, USDA Forest Service, 1650 Ramble Road, Blacksburg, VA 24060, USA.

Digital Picture Tree Crown Evaluation Software

Matthew F. Winn, Sang-Mook Lee, Philip A. Araman

ABSTRACT

The USDA Forest Service Southern Research Station in Blacksburg, Virginia is developing stand-alone software to analyze digital pictures of tree crowns, partial tree crowns, or groupings of tree crowns for foliage transparency. One program called URBANCROWNS can be used to evaluate density and transparency of complete or partial trees in an urban setting from digital pictures. We are also developing software to determine leaf area estimates. The second program called FORESTCROWNS can be used to evaluate digital pictures of crowns from below in forested settings. Single trees, multiple intersecting trees, or canopy areas pictures can be analyzed to determine transparency. Examples will be presented. The software packages are not complete but they are usable and will be made available for trial use.

Matthew F. Winn is a forestry technician, **Sang-Mook Lee** is a postdoctoral fellow, and **Philip A. Araman** (presenter; paraman@fs.fed.us) is a research team leader at the Southern Research Station, USDA Forest Service, 1650 Ramble Road, Blacksburg, VA 24060, USA.